# MicroRNAs Expression and Regulation in Human Corneal Epithelium and Pterygium

TENG, Yufei

A Thesis Submitted in Partial Fulfillment

of the Requirements for the Degree of

Doctor of Philosophy

in

Ophthalmology and Visual Sciences

The Chinese University of Hong Kong

September 2013

Thesis/Assessment Committee

Professor Vishal Jhanji (Chair)

Professor Calvin Chi Pui Pang (Thesis Supervisor)

Doctor Benjamin Fuk Loi Li (Committee Member)

Professor Richard Kwong Wai Choy (Committee Member)

Professor Herman Sing-chung Cheung (External Examiner)

*Abstract of thesis entitled:*

*MicroRNAs expression and regulation in human corneal epithelium and pterygium*

*Submitted by TENG, Yufei*
*For the degree of Doctor of Philosophy*
*in Ophthalmology and Visual Sciences*
*at The Chinese University of Hong Kong in September 2013*

## Abstract

MicroRNA is a class of newly discovered epigenetic factors that transiently repress gene expression via inhibition of protein synthesis or destabilization of target mRNA. Stem cells from different lineages express a specific pattern of microRNAs, which play important regulatory roles in self-renewal, differentiation, proliferation and apoptosis. They thus contribute to maintenance of normal homeostasis, tissue regeneration and wound healing. In this study, we aim to study the expressions and biological roles of miRNA in healthy and disease states. We investigated microRNA in corneal epithelial cells (CEPCs) and differentiated corneal cells by comparing their expression pattern between limbal-periphery corneal (LPC) epithelium and central corneal epithelium in normal cornea. We characterized the regulatory roles of microRNAs in the pathogenesis of pterygium.

We obtained limbal peripheral corneal (LPC) epithelium and central corneal (CC) epithelium from cornea rim from healthy donors. Using Agilent$^{TM}$ MicroRNA Microarray (V2) and GeneSpring analysis software (v11.5), we identified 18 microRNAs which were differentially expressed between CEPC-enriched limbal-periphery corneal (LPC) and CEPC-depleted central corneal (CC) epithelium (fold changes more than 2.0, P value less than 0.05). Among them, 14 microRNAs (miR-10b, 126, 127, 139-5p, 142-3p, 142-5p, 143,

145, 146a 155, 211, 338-3p, 376a, 377) were up-regulated in LPC epithelium, and 4 microRNAs (miR-184, 193b, 149 and 575) up-regulated in CC epithelium. Results of TaqMan® quantitative microRNA assays showed predominant expressions of 8 microRNAs (miR-10b, 126, 127, 139-5p, 143, 145, 155, and 338-3p) in the LPC epithelium.

Systematic bioinformatics web-tools (DAVID, KEGG, and IPA®) were utilized to investigate the potential functions of these microRNAs by analyzing their target genes. Algorithmically, the target genes of miR-10, miR-155 and miR-126 were enriched in the annotations related to cell proliferation, migration, cytoskeleton and immune response. Based on the results from bioinformatics analysis, we focused on studying miR-10b, 126 and 155 in cornea epithelium. miRCURY LNA™ microRNA probes were used to detect the localization of the three microRNAs in human corneal epithelium. The results showed that miR-126, 10b and 155 were present in the limbal epithelium with stronger staining observed in the limbo-peripheral region as compared to the central cornea. Analysis of microRNA-gene interaction network created by Ingenuity® IPA analysis for miR-143, 145 and 155 showed their roles in the suppression oncogenes (MYC, KRAS and LAMP2) but activation of tumor suppressor genes (TNF and TP53), suggesting their potential roles in CEPC growth regulation.

Pterygium is a common ocular surface disorder characterized by corneal conjunctivalization, fibrovascular lesion, elastotic degeneration of collagen and overlying growth of corneal epithelium. It is suggested that pterygium progression is associated with the aberrant CEPCs due to damage the CEPC niche after UVB exposure. We obtained ptergium specimens and sectioned them for analysis. LPC-specific microRNAs were expressed in the pterygium. Expression of miR-143/145 and miR-184 were significantly higher in pterygium by comparing with normal human conjunctiva and limbal epithelium. In situ localization showed that miR-143 and 145 were present in both pterygial stroma and

epithelium whereas miR-10 was abundant in pterygium stroma but negative in the epithelium. In addition, miR-126 was highly detected in the blood vessels. miR-143/145 was co-localized with p53. In order to demonstrate the relationship between miR-143/145 and p53, we over-expressed miR-143/145 in primary cells derived from pterygium. Our results showed that the pterygium cells underwent apoptosis after miR-143/145 transfection. Moreover, miR-145 caused up-regulation of p53 and extensive cell death. Meanwhile, the negative regulator of p53, MDM2, was significantly down-regulated in miR-145 transfected cells, suggesting that miR-145 increased p53 accumulation in pterygium through suppressing MDM2.

In conclusion, we identified 8 LPC-specific microRNAs, which may possess regulatory functions in the self-renewal and proliferation of CEPCs. miR-143/145 and miR-184 were abnormally up-regulated in pterygium; miR-145 might be one possible cause of p53 accumulation in pterygium, which could regulate the growth of pterygium and against the tumorigenesis of corneal epithelium.

# 摘要

此摘要来自于论文
《microRNA 在人角膜上皮及翼状胬肉的表达和调节作用》
于二零一三年九月
呈交自 滕羽菲
作为 香港中文大学眼科及视觉科学哲学博士学位 所需

微小 RNA（MicroRNA）是一类内源性的、19-25 个碱基长度的小分子非编码 RNA。作为基因表达中的一类负调控因子，微小 RNA 可以通过与靶基因 mRNA 分子的 3'端非编码区互补匹配导致靶 mRNA 分子降解或抑制其合成, 从而在干细胞的自我更新，多向分化,增殖,凋亡以及生物体内环境稳态和损伤修复过程中起重要作用.本课题通过对比微小 RNA 在角膜缘上皮与中央角膜表达谱，鉴定人角膜缘干细胞特异表达的微小 RNA，并研究其在角膜再生过程中的潜在作用。

微小 RNA 芯片筛选以及实时定量 PCR 证实了 miR-10b, miR-126，miR-127,miR-139-5p,miR-143,miR-145，miR-155 以及 miR-338 在角膜缘上皮的特异表达。角膜上皮原位杂交显示 miR-10b, miR-126 在角膜缘基底层及上基底层表达较高，反映其表达与角膜缘干细胞和早期增殖细胞相关。通过生物信息学数据库分析微小 RNA 靶基因在信号通路中的关联，我们发现角膜缘干细胞特异表达的微小 RNA 的靶基因参与与干细胞增殖分化相关的信号通路，证明了其在角膜上皮干细胞增殖分化有潜在调节作用。

翼状胬肉是眼科常见病之一，是睑裂部球结膜与角膜增生的赘生组织并逐渐侵入角膜。近年研究表明翼状胬肉起源于异常发育的角膜缘干细胞以及受损的角膜缘干细胞巢。翼状胬肉的发病此，我们检测了了角膜缘干细胞特异表达的微小 RNA 在翼状胬肉上的表达。

通过与正常人结膜与角膜缘比较，翼状胬肉异常高表达 miR-143，miR-145 以及 miR-184，较高表达 miR-10b 及 miR-155.原位杂交显示 miR-143,145 在翼状胬肉上皮部和基质部均有表达，miR-10b 只在基质有表达，同时 miR－126 在上皮及微血管均有表达。结合原位杂交及免疫组化，我们发现 miR-143／145 与其正向调控分子 p53 在翼状胬肉的表达分布能够重合，说明 miR-143/145 与 p53 的表达相关.同时，miR－126 与白细胞介素 6 在翼状胬肉的表达相关。

转染 miR-145 进入翼状胬肉细胞引起了细胞凋亡，伴随着肿瘤凋亡因子 p53 的表达提高。同时， p53 的负调控因子 MDM2 的表达被 miR-145 所抑制。MDM2 是 miR45 的靶基因之一 因此，miR-145 可能通过直接抑制 MDM2 蛋白的翻译提高 p53 的表达水平，形成一个 miR-145／p53 调节通路导致细胞凋亡，从而抑制翼状胬肉的肿瘤化

本课题探索了微小 RNA 在角膜缘干细胞的表达及调控，并且证实了微小 RNA 对于翼状胬肉病理生理的调节作用，为角膜上皮细胞再生以及翼状胬肉的治疗提供了生物学基础。

## Acknowledgement

Being a PhD is an adventure to explore nature and sciences. Four years of postgraduate study is an invaluable experience to enrich my life. I am so lucky to have met so many outstanding professors, excellent colleagues and classmates in the past four years. Here I would like to express my sincere gratitude to the people who guided me, and taught me during the postgraduate study and with their support enabling me to complete this thesis.

Firstly, I would like to thank Prof. Chi-Pui Pang for designing this wonderful project for me. His continuous support in both scientific and daily life has deeply inspired me. He shows the manner and spirit as a scientist and as a gentleman, being a role model of my whole life career. I would like to thank Dr. Gary Yam for his supervision in the first three years of my study. He guided me to the scientific research through every research step; taught me all the laboratory techniques hand by hand, and patiently training me to be a qualified researcher. I would like to thank Dr. Vishal Jhanji for his constant support in supplying the clinical specimen in the past three years and giving me many enlightened ideas in pterygium research as well as the great helps in thesis writing. I am very much obliged to Prof. Benjamin Li for his help in my last year of study. Great thanks also are due to Dr. Richard Choy for his generous support in microarray the real-time PCR experiments that are key techniques in my project.

I also would like to thank our PhD graduates Dr. Sharon Lee, Dr. Gong Bo and Dr Xu Li, they shared with me the laboratory techniques and research experience at the beginning of my research career, and treated me as their younger sister. Great thanks also due to Dr. Law Kasin for his guidance in cell cycle analysis, as well as his encouragement

with his spirit and words from the Bible. I would like to thank Dr. Doreen Leung for her assistance in my experiment as well as the maintenance work of cellular lab, giving us a great working environment. Great thanks are also due to Ms Elaine To for helping me revise my thesis. I would like to thank my PhD classmates Dr. Liu Shu, Dr. Zhang Xin Dr. Yang Mingming, Ms Huang Li, Dr. Zhang Xujuan, Dr. Man Xiaofei, Ms Marco Yu, Dr. Liu ke, Dr. Yangyaping, Dr. Tan Shaoying, Dr. QinYongjie, Dr. Rong Shishong, Dr. Wang Jianghui, Mr. Biswas Sayantan, Miss Xu Guihua for their friendship. I am very much obliged to labmates and staff, Dr weiying Li, Ms Pancy Tam, Dr Kai-on Chu, Mr Kwok-ping Chan, Ms Sylvia Chiang, Dr. Yolanda Yip, Mr Jeffrey Chan, and Ms Miki Chan for their steady support.

I would like to express a sincere thankfulness to the colleagues in department of O&G. Mr. Kenneth Wong and Mr. Wilson Chong for teaching me to do the microarray analysis and real-time PCR. Besides, they supplied me generous help in my project, responded to my inquiry and helped me to solve some problems I met in my experiments. I am also grateful to Dr. Zhang Tao and Dr. Gene Wen for generously sharing with me the reagent that I urgently needed. Remarkable thanks also due to the clinicians in ShenZhen eye hospital for supplying the samples, especially the help from Dr. He Jing for arranging the specimen storage and transportation.

# Publications and academic awards

## A. Publications in peer-reviewed journals

1. Sharon Ka-Wai Lee*, **Yufei Teng***, Hoi-Kin Wong, Tsz-Kin Ng, Mingzhi Zhang, Yingpeng Liu, Lina Huang, Ping Guo, Kwong-Wai Choy, Dennis Shun-Chiu Lam, Chi-Pui Pang, Gary Hin-Fai Yam. MicroRNA-145 Regulates Human Corneal Epithelial Differentiation. PLoS One. 2011; 6:e21249. *, Co-first authors.

2. Haiqing Bai*, **Yufei Teng***, Lee Wong, Vishal Jhanji, Chi-Pui Pang, Gary Hin-Fai Yam. Proliferative and migratory aptitude in pterygium. Histochemistry and Cell Biology.2012; 134:527-535. *, Co-first authors.

3. **Yufei Teng**, Hoi-Kim Wong, Jian-Huan Chen, Kwong-Wai Choy, Dennis Shun-Chiu Lam, Chi-Pui Pang, Gary Hin-Fai Yam. Comparative microRNA expression and functions in human corneal and limbal epithelia (manuscript prepared).

4. **Yufei Teng**, Kasin Law, Benjamin Li, Gary Hin-Fai Yam, Vishal Jhanji, Chi-Pui Pang. MicroRNA expression and regulation in pterygium (manuscript in preparation).

## B. Conference presentations

1. **Yufei Teng**, Gary Hin-Fai Yam, Sharon Ka-Wai Lee, Chi-Pui Pang, Dennis Shun-Chiu Lam. MicroRNA-145 regulates human corneal epithelial differentiation. The 25th

Asia-Pacific Academy of Ophthalmology Congress 2010, Beijing, China, Sep 16 – 20, 2010. Abstract: SP-000564.

2. **Yufei Teng**, Hoi-Kin Wong, Chi-Pui Pang, Gary Hin-Fai Yam. Comparative MicroRNA Expression Profile in Human Corneal and Limbal Epithelium. ARVO 2011, Fort Lauderdale, Florida, USA, May 1-5, 2011. Abstract: 11-A-5437-ARVO

3. **Yufei Teng**, Hoi-Kin Wong, Li Huang, Richard Kwong-Wai Choy, Chi-Pui Pang, Gary Hin-Fai Yam. Comparative microRNA expression analysis in human corneal epithelium. Days of Molecular Medicine 2011, Hong Kong, Nov 10-12, 2011. Abstract: Eye Regeneration_73.

4. **Yufei Teng**, Hoi-Kin Wong, Chi-Pui Pang, Gary Hin-Fai Yam. MicroRNA profiling in human limbal epithelium. The 8th International Symposium of Ophthalmology – Hong Kong 2012, Hong Kong, Dec 14-16, 2012. Poster: SP-001566.

**Table of Content**

## List of Figures

## List of Tables

## Abbreviation

| | |
|---|---|
| **ABCG2** | ATP binding cassette transporters, G family |
| **ACAN** | Aggrecan |
| **ACTB** | Actin, beta |
| **Ago** | Argonaute |
| **Bcl-2** | B-cell CLL/lymphoma 2 |
| **bFGF** | Basic fibroblast growth factor |
| **BSA** | Bovine serum albumin |
| **CASP3** | Apoptosis-related cysteine peptidase |
| **CC** | Central cornea |
| **CD** | Cluster of differentiation |
| **CDH2** | N-Cadherin |
| **Cdk** | Cyclin-dependent kinase |
| **C/EBPB** | CCAAT/enhancer binding protein, beta |
| **CEPC** | Corneal epithelial progenitor cells |
| **CK12** | Cytokeratin 12 |
| **CK3** | Cytokeratin 3 |
| **Ct** | Cycle threshold |
| **Cx43** | Connexin 43 |
| **CXCL12** | C-X-C motif chemokine 12 |
| **CXCR** | C-X-C chemokine receptor |
| **COL2A** | Collagen, type II, alpha 1 |
| **DAPI** | 4’6’-diamidino-2-phenylindole |

| | |
|---|---|
| **DECP** | Diethylpyrocarbonate |
| **DGCR8** | Digeorge syndrome critical region 8 |
| **DKK2** | Dickkopf-related protein 2 |
| **DO** | Domain |
| **EB** | Embryonic body |
| **ECM** | Extracellular matrix |
| **EGF** | Epidermal growth factor |
| **ELF** | E74-Like Factor |
| **ESC** | Embryonic stem cell |
| **Exp-5** | Exportin-5 |
| **FACS** | Florescence activated cell sorting |
| **FGF** | Fibroblast growth factor |
| **FOXA2** | Forkhead box protein A2 |
| **GCL** | Ganglion cell layer |
| **GDNF** | Glial cell-derived neurotrophic factor |
| **GFRA** | GDNF family receptor alpha |
| **GJB1** | Gap junction beta-1 protein |
| **H&E** | Hematoxylin and eosin |
| **HGF** | Hepatocyte growth factor |
| **ICM** | Inner cell mass |
| **IGF** | Insulin-like growth factor |
| **IL-6** | Interleukin 6 |
| **IL-8** | Interleukin 8 |
| **INL** | Inner nuclear layer |
| **IPA** | Ingenuity pathways analysis |

| | |
|---|---|
| **iPSc** | Induced pluripotent stem cell |
| **ISL1** | Insulin Gene Enhancer Protein ISL-1 |
| **ITGA9** | Integrin alpha 9 |
| **ITGB8** | Integrin beta 8 |
| **IVL** | Involucrin |
| **KGF** | Keratinocyte growth factor |
| **KRAS** | Kirsten rat sarcoma viral oncogene homolog |
| **Krt 15** | Cytokeratin 15 |
| **Krt 19** | Cytokeratin 19 |
| **Krt 4/13** | Cytokeratin 4/13 |
| **LAMP2** | Lysosomal-associated membrane protein 2 |
| **LCM** | Laser capture microdissection |
| **LEC** | Limbal epithelial crypt |
| **LPC** | Limbal periphery corneal |
| **LSCD** | Limbal stem cell deficiency |
| **MAPK** | Mitogen-activated protein kinase |
| **MDM2** | Murine double minute 2 |
| **miRISC** | MicroRNA-induced silencing complex |
| **MMP** | Matrix metalloproteinase |
| **MOMP** | Mitochondrial outer membrane permeabilization |
| **Myc** | Myelocytomatosis oncogene |
| **mRNA** | Messenger RNA |
| **NCAM1** | Neural Cell Adhesion Molecule 1 |
| **NGFR** | Nerve growth factor receptor |
| **OCT** | Optimal cutting temperature |

| | |
|---|---|
| **OCT4** | Octomer 4 |
| **ONL** | Outer nuclear layer |
| **ORF** | Open reading frames |
| **PDGF** | Platelet-derived growth factor |
| **pre-miRNA** | MicroRNA precursor |
| **pri-miRNA** | Primary microRNA |
| **PT** | Pterygium |
| **RNA** | Ribonucleic acid |
| **RPE** | Retinal pigment epithelium |
| **SMAD4** | SMAD family member 4 |
| **TAC** | Transit-amplifying cells |
| **TCF4** | Transcription factor 4 |
| **TGF** | Transform growth factor |
| **TF** | Transcription factor |
| **TM** | Melting temperature |
| **TNF** | Tumor necrosis factor |
| **TRBP** | TAR RNA binding protein |
| **TrKA** | TRK1-transforming tyrosine kinase protein |
| **UTR** | Untranslated region |
| **UVB** | Ultraviolet radiation b |
| **VEGF** | Vascular endothelial growth factor |

# Chapter 1 Introduction

## 1.1 Stem cells in human cornea

### 1.1.1 Stem cells - definition, types and characterization

#### 1.1.1.1 Definition of stem cells

The classical definition of stem cells is the cells that have the capacity of self-renewal and possess the ability to generate differentiated cells. However, this broad definition is not sufficient enough to describe the genuine nature of stem cells. Robert Lanza stated the working definition of stem cells in《Essential of Stem Cells》that they are a clonal, self-renewing cell entity that are multipotent to generate differentiated cell types (Lanza, 2006).

The properties of stem cells are predominantly self-renewal, potency and clonality.

1) Self-renewal: most somatic cells have a limited life span. The number of cell doubling time is normally less than 80 times *in vitro* before senescence. In contrast, stem cells display an unlimited potential of mitotic division. One cell can divide into two daughter cells, with maintenance of undifferentiated state. For adult stem cells, it should keep the capacity of indefinite cell division throughout the lifetime. Therefore, the cells that can undergo more than 160 doublings without oncogenic transformation can be referred as having capability of self-renewal.
2) Clonality: stem cells are clonogenic entities of one single cell that can generate progenies and form cell colonies. Therefore, stem cell colony should be homogenous generating from one single cell, not a mixed population.

3) Potency: refers to the differentiation potentials of cells that can produce different cell types. The extent of potency includes totipotency, pluripotency, multipotency, oligopotency and unipotency (Mitalipov & Wolf, 2009). Totipotency refers to the cells with the capacity to give rise to all different cell types, including embryonic and extra-embryonic cell types from zygotes that can construct complete and viable organisms. Pluripotency is defined as the ability to generate all cell types of three germ layers. Embryonic stem cells derived from inner cell mass of blastocyst are pluripotent stem cells with the potential of germ-layer development. Multipotent stem cells can differentiate into multiple cell types of one germ layer or related cells within the same lineage, such as hematopoietic and mesenchymal stem cells. Oligopotency is the ability to differentiate into specialized cell types for one organ or particular cell lineage. Tissue-specific stem cells like vascular stem cells, neural stem cells and the lymphoid or myeloid stem cells are oligopotent. Adult stem cells with limited differentiation potential are also defined as progenitor cells. Unipotent stem cells only generate one single differentiated cell type, like muscle progenitor cells and corneal progenitor cells.

#### 1.1.1.2 Types of stem cells

Four stem cell types have been identified based on their origins.

**1) Embryonic stem cells**

Embryonic stem cells (ESCs) are derived from the inner cell mass (ICM) of the mammalian blastocyst or early morula (Conner, 2001). They are pluripotent and are able to differentiate into all derivatives of three primary germ layers: ectoderm, endoderm and mesoderm, and subsequently generate all cell types (Boheler et al., 2002).

The maintenance of Esc in undifferentiated state mainly relies on two mechanisms: intrinsic and extrinsic machineries. Transcription factors (including Oct4, Nanog and Sox2) are the intrinsic factors for maintaining self-renewal (Boyer et al., 2005); BMP4, LIF are the extrinsic factors in the stem cell niche to prevent cell differentiation. The signaling connection between intrinsic and extrinsic factors are through LIF/STAT3 and Wnt signaling pathways (Boyer et al., 2005; Sathananthan & Osianlis, 2010).

**2) Adult stem cells**

Adult stem cells are tissue-specific stem cells that can give rise to specialized cell types for replenishing and regenerating cell turnover in adult tissue. They are found throughout the body, especially in organs with regenerative capacity. In clinical therapy, adult stem cells are a reliable source for tissue transplantation (Barrilleaux, Phinney, Prockop, & O'Connor, 2006). The potency of adult stem cells is variable - hematopoietic stem cells that reside in bone marrow are multipotent and can give rise to all types of blood cells (Jiang et al., 2002); brain-derived neural stem cells are oligopotent that can differentiate to neurons, astrocytes and oligodendrocytes (Kennea & Mehmet, 2002), and the epidermal stem cells in skin can only generate skin epithelial cells, implying it is unipotent in nature (Lavker & Sun, 1983).

**3) Induced pluripotent stem cells**

Induced pluripotent stem cells (iPSC) are somatic cells reprogrammed to an ESC - like state through the transient expression of core pluripotent regulators like Oct4, Sox2, Klf4, and c-Myc. They gain the ESC property for self-renewal and pluripotent differentiation potential with similarly expression of ESC markers (Takahashi & Yamanaka, 2006). iPSCs are an alternative source of ESC for tissue regeneration without ethnic controversy, and can be successfully induced to commit germ layer development. The

source of iPSC can be derived from hair follicles or skin fibroblasts, as well as epithelial cells from urine. It serves as a potential for personalized medicine. The reprogramming factors for iPSC are initially four TFs: Oct4, Sox2, Klf4, and c-Myc by Yamanaka's group (Takahashi & Yamanaka, 2006), then Yu et al created the second group of four TFs: Oct4, Sox2, Nanog, and Lin28 (Yu et al., 2007). Human cord blood progenitors could be reprogrammed with Oct4 and Sox2 (Giorgetti et al., 2010); neural stem cells could be reprogrammed with only Oct4 (J. B. Kim et al., 2009). The number and identity of reprogramming molecules may depend on the factors that are initially expressed in ESC and the potency levels of the cells.

**4) Cancer stem cells**

Cancer stem cells (CSC) are special types of stem cells found in tumors or hematological cancers. They can give rise to all cell types found in particular cancer and are hence considered as the origin of tumorigenesis. CSCs continue the process of self-renewal and differentiation into multiple cell types that can generate new tumors. Therefore, CSC could serve as the target of cancer therapies (Yamada & Watanabe, 2010).

### 1.1.1.3 Characteristics of stem cells

**Symmetric and asymmetric cell divisions**

Stem cells undergo asymmetric and symmetric cells division to self-renew and generate differentiated progenies (Caussinus & Hirth, 2007). There are two types of symmetric cell division. (1) Division of one stem cell symmetrically into two daughter stem cells with the same property as the original one. This process expands the stem cell pool, which usually occurs in the early embryonic development to increase the body size, as well as in injured adult tissue to regenerate new cells. (2) Division of one into two cells with equivalent developmental potential to generate significant amount of differentiated

progenies, especially during the three germ layer development or *ex vivo* differentiation induction. Asymmetric cell division is predominant under steady-state condition, in the late stage of development or for the homeostasis of adult tissue (Caussinus & Hirth, 2007). In general, stem cell generates one morphologically identical daughter cell with the same undifferentiated state for self-renewal, and one more developmentally mature state for differentiation. During tissue development, the undifferentiated cells remain in the original stem cell pool, and the differentiated cells migrate to different positions for further lineage commitment. Therefore, stem cells transit from symmetric to asymmetric cell division in mammalian development. The mechanism of regulating stem cell division is the molecular regulators and the signaling is driven from stem cell niche or from the daughter cells.

**Cell cycle of stem cells**

The somatic cells are arrested in G1 phase for the restriction or check point on G1/S transient to prevent the initiation of S phase and DNA replication. G1/S transient restriction can be unblocked through Cdk4/6-cyclin D complex or Cdk2-cyclin E complex with activating sequential downstream factors (Lanza, 2006). The ES cells display a very short G1 phase and most cells are in S-phase. It has been found that mouse ESC contain high levels of activators of cell cycle cdk2–cyclin E/A and cdk6–cyclin D3 but lack for cell cycle inhibitors p21cip and p27Kip1(V. N. Kim, 2008). In normal conditions, adult stem cells are mitotic quiescent with prolonged G1 or G2 phase for self-maintenance of the stem cell number (Y. Wang et al., 2008).

### 1.1.2 Adult human corneal epithelial progenitor cells (CEPCs)

Corneal epithelium is the first barrier of ocular optical system to prevent external hazard entering deeper corneal layers. It is characterized as avascular and transparent tissue

with the property of immune-privileged and angiogenesis-privileged. The differentiated corneal epithelial cells have an average of 7 to 9 days without of the capacity to mitosis. The homeostatic regulation of corneal epithelium relies on the regeneration of corneal epithelial progenitor cells (CEPCs) located in the basal epithelium of limbus. Limbal epithelium or defined as limbus is a highly vascularized, pigmented and innervated annulus between the transparent cornea and opaque bulbar conjunctiva (DelMonte & Kim, 2011). CEPCs are unipotent and generate highly proliferative transit-amplifying cells (TAC) (Bhattacharyya et al.). After limited number of cell divisions, TACs terminally differentiate to epithelial cells to maintain the cell turnover in the squamous corneal epithelium.

**Location and characteristics of CEPC and TAC**

The CEPC niche is located in the "Palisades of Vogt", which is a heavily pigmented and undulated region consisting of groups of small, densely packed cells at the bottom of the limbal epithelium (Z. Chen et al., 2004a). Melanin associated pigmentation of the "palisades of Voge" protects the cells from damage caused by UV light. The vascular network uniquely underlies the limbal palisades, which supply nutrients and cytokines to CEPC growth and maintenance. Additionally, undulated basement membrane structure forms a barrier to prevent neovascularization and conjunctivalization (Daniels, Dart, Tuft, & Khaw, 2001). In recent years, some reports have defined a novel CEPC niche termed as "limbal epithelial crypt", which is a papillae-like structure arising from the undersurface of inter-palisade rete ridges of limbal palisades of Vogt and extending deeper into the limbal stroma in parallel or perpendicular to the palisade (Kulkarni et al., 2010).

CEPCs reside in limbus basal epithelium and represent less than 10% of total basal cell population (Davies & Di Girolamo, 2010). Together, they are intermingled with early and late TACs as well as post-mitotic epithelial cells. Anatomically, they may be localized

in the crypt region within the palisades. Under transmission electron microscopy, putative CEPCs are small, melanin granules - pigmented, with high nuclear to cytoplasmic ratio and indistinct nucleoli. In contrast, TACs have distinct nucleoli with vast amount of tonofilament bundles present in the cytoplasm (**Figure 1.1**) (L. Li & Xie, 2005; Schlotzer-Schrehardt & Kruse, 2005).

Functionally, CEPCs can be identified as:

1) Lowly differentiated, and absence of corneal differentiation markers, cytokeratin K3 and K12 (T. T. Sun, Tseng, & Lavker, 2010).

2) Slow cell cycle and mitotic quiescence with a retention of labeled DNA precursors for a prolonged period of time (Kruse & Tseng, 1991).

3) Highly proliferative rate in corneal injury. Limbal region shows a faster wound healing speed than the central cornea. Regeneration of CEPCs helps the reconstruction of the entire corneal epithelium in transplantation surgery (Pellegrini et al., 1997). In cell culture model, CEPC derived from limbal basal epithelium showed higher proliferative rate than cells from central corneal epithelium (Tseng, 2001) .

4) Capable of unlimited self-renewal. The clonogenic growth of CEPC can generate holoclones as other embryonic and adult stem cells (Kruse & Tseng, 1991; Tseng, Kruse, Merritt, & Li, 1996).

**Asymmetric cell division of CEPCs**

The maintenance of CEPC is through asymmetric cell division. One CEPC generates two daughter cells. One returns to the stem cell niche to maintain the stem cell pool, while the other will turn to TAC for a continuation of cell division, which will eventually terminally differentiate to become corneal epithelial cells. The progeny cells

migrate upwards and centripetally to the corneal surface to replace the dying epithelial cells in daily turnover process (**Figure 1.2**) (Daniels et al., 2001).

### 1.1.3 Gene regulation and identification of adult human CEPCs

The identification of CEPC is not definitive (Yam 2010 Book chapter). Although ABCG2 has been classified as a marker of the putative CEPC, it is also regarded as a common stem cell marker (Budak et al., 2005). Other positive markers, including p63 and integrin α9, are preferentially localized to the limbus but are not specific to CEPCs (Pajoohesh-Ganji, Ghosh, & Stepp, 2004; Pellegrini et al., 2001). Cytokeratin K3/12, RHAMM/HMMR and connexin-43 are examples of negative markers that are highly associated with corneal epithelial cell differentiation (Ahmad et al., 2008; Schermer, Galvin, & Sun, 1986).

1) Nuclear proteins

The p53 homologue, transcription factor p63, is strongly expressed in the limbal basal layer of human cornea (Mills et al., 1999). It is abundantly expressed in holoclones derived from limbus but absent in paraclones (Kawakita et al., 2009). However, the expression pattern of p63 in human corneal epithelium is inconsistent from different studies that it is not restricted to the limbal epithelia, but also present in the basal layer of central corneal and limbal periphery corneal epithelium, indicating that the expression of p63 is not CEPCs - specific (Z. Chen et al., 2004b). p63 is essential for ectodermal development and epithelial linage differentiation, p63-deficient mice displayed defects in epidermal stratification and differentiation (Mills et al., 1999). It has been found that one isoform of p63, ΔNp63 is more specific for CEPCs location that is preferentially expressed in the limbal basal layer (Hernandez Galindo, Theiss, Steuhl, & Meller, 2003). Induction of

ΔNp63 has been shown to promote the limbal epithelial outgrowth through stimulating the keratinocyte growth factor (KGF) secretion from limbal stromal fibroblast (Cheng, Wang, Kao, & Chen, 2009). In wound healing process, the expression of ΔNp63 spread from the basal cells to suprabasal cells, indicate it participate the modulation of TAc proliferation (Barbaro et al., 2007). The ΔNp63-null keratinocyte prematurely expressed terminal differentiated markers in epidermal cell lineage commitment (Romano et al., 2012). Moreover, the ΔNp63-deficient epithelia lose their components of extracellular matrix and cellular junctions, which might be caused by the suppression of Notch signaling pathway during the differentiation process (Romano et al., 2012).

Another transcription factor C/EBPδ, the CCAT enhancer-binding protein delta, was co-expressed with ΔNp63 and Bmi1，which is able to identify the mitotically quiescent CEPC in limbal basal epithelium. C/EBPδ arrested the CEPCs in G1 phase and promoted the self-renewal of holoclones (Barbaro et al., 2007).

2) Transporter molecules

ABCG2 /BCRP1 is a member of the ATP binding cassette (ABC), which is regarded as a marker of stem cells including ESC, bone marrow-derived MSC and adult stem cells from skeletal muscle and epithelium (Z. Chen et al., 2004b). In cornea, ABCG2 is positively detected in the basal and supra-basal layers of limbal epithelium but absent in central corneal epithelium. The ABCG2-positive cells derived from limbal epithelium exhibited higher colony formation and proliferation rate, indicating the cell population was enriched with CEPCs (Umemoto et al., 2005). The depletion of ABCG2 did not affect the corneal phenotype, but can increase the sensitivity of cells to phototoxicity and oxidative stress Hence ABCG2 may function to protect CEPC from external stimulus and enhances the resistance of toxic damages (Kubota et al., 2010).

3) Cytoskeletal proteins

Cytokeratins are epithelial cytoskeletal proteins that are distinctly expressed in a variety of epithelial types at different development and differentiation stages. Keratin 3 and 12 are differentiation markers, specifically present in the differentiated epithelial cells in superficial layer of corneal epithelium and limbal epithelium (Z. Chen et al., 2004a). Keratin 14 is a marker for proliferating keratinocyte and is positive in the basal layer of corneal and limbal epithelium. Keratin 15 is a human hair follicle stem cells marker that is expressed in primitive limbal basal epithelium, which is decreased during CEPC differentiation (Qi, Zheng, Yuan, Pflugfelder, & Li, 2010). Keratin 19, also a hair follicle stem cell marker, is preferentially expressed in limbal basal layer and conjunctival epithelium (Schlotzer-Schrehardt & Kruse, 2005).

4) Cell surface proteins

Cell surface proteins include cell-cell junction and cell-matrix adhesion molecules. The gap junction molecules connexin 43 (Cx43) and 50 (Cx50) are strongly expressed in corneal epithelium (Grueterich, Espana, & Tseng, 2002). Cx43 is present mainly in the basal layers whereas Cx50 is present throughout all the layers. Cx43 is regarded as a negative marker of CEPCs, which mainly affects the gap junction of differentiated corneal epithelial cells.

Corneal epithelium also contains cell adhesion molecule such as E-cadherin and N-cadherin. E-cadherin is expressed with Cx43, activating the cell-cell contact for cell proliferation and survival. Another cadherin family member, N-cadherin, is specifically expressed in the limbal basal layer (Higa et al., 2009). In vitro culture model showed that N-cadherin is solely expressed by the limbal epithelial colonies, probably by putative

progenitor cells as well as melanocytes (X. A. Huang & Lin, 2012). N-Cadherin$^{+}$ cells possess of higher proliferative ability and are co-expressing other CEPC markers such as ABSG2 and p63, suggesting N-Cadherin is a critical cell-to-cell adhesion molecule for CEPCs and stem cell niche (Hayashi et al., 2007).

5) Growth factor and receptors

The limbal and corneal epithelia express various growth factors, but most of them are not anatomically specific to CEPCs. KGF-R, TrKA and NGF are preferentially located at the limbal basal cells, whereas P75$^{NTR}$ is highly present in the superficial layers of limbal epithelium (Touhami, Grueterich, & Tseng, 2002). In cultured limbal epithelial cells, NGF and TrkA positive cells are co-localized with other putative markers like ABCG2 and p63 (Qi et al., 2008). KGF is a key growth factor for CEPCs division and differentiation. *ex vivo* study has shown that NGF signaling is crucial for CEPCs expansion (Cheng et al., 2009).

6) Novel molecules

Besides the well-known CEPC putative markers proven by immunohistochemistry, the application of large-scale microarray and transcriptome sequencing have revealed a set of novel markers that are associated with CEPCs. In 2010, Kulkarni's lab compared the gene expression profile of cells isolated from limbal epithelial crypt (LEC, presumably CEPC) with limbal and corneal epithelia. The result showed that FRZB1and RBX1 were significantly up-regulated in LEC (Kulkarni et al., 2010). Nieto-Miguel et al performed RT-PCR array on human limbal and corneal epithelia, and identified a new set of stem cell-related genes that were highly expressed in limbal epithelia, including CXCL12, ISL1, COL2A, NCAM1, ACAN, FOXA2 GJB1/Cnx32 and MSX1(Nieto-Miguel et al., 2011). Fang et al. sorted epithelial cells by adhesion time on collagen IV, and derived 3 cell populations: namely rapid adhesion cells, low adhesion cells and non-adhesion cells

through the validation on transcriptional profiling, transcription factor TCF4 and cell surface protein SPRRs were identified as potentially positive and negative markers for CEPCs, respectively (Bian et al., 2010).

### 1.1.4 CEPCs regulation

#### 1.1.4.1 The microenvironment of CEPC niche

The homeostasis of CEPCs replenishing the corneal epithelium is based on the complex interaction between epithelial and fibroblast cells of the cornea and limbus (Suzuki et al., 2009). The cytokines released by corneal epithelium act on the fibroblast of cornea, including transforming growth factor alpha (TGFα), interleukin-1β (IL-1B) and platelet-derived growth factor (PDGF) BB. In return, limbal fibroblasts produce keratinocyte growth factor (KGF) and corneal fibroblasts released hepatocyte growth factor (HGF) for corneal epithelial cell proliferation and migration. Other growth factors, like insulin-like growth factor-1 (IGF1), TGF-β1, TGF-β2 from fibroblasts can mediate both epithelial and fibroblast activities. Consequently, the corneal epithelial wound healing is relied on the autocrine and paracrine interaction of cytokines modulating the behavior of stem cells and TACs (Daniels et al., 2001). Upon injury or stress, corneal epithelial cells release IL-1β to stimulate the limbal and corneal fibroblasts to secrete KGF and HGF. Limbal fibroblasts release KGF to promote CEPCs division and corneal fibroblasts secret HGF subsequently to modulate the production and migration of TAC. In contrast, IL-1β stimulates TGF-β1, TGF-β2, which suppresses the secretion of KGF and HGF. This inhibitory pathway is a signal for repressing the CEPC division and migration to avoid the over-proliferation of CEPC (**Figure 1.3**) (D. Chen, Farwell, & Zhang, 2010; Daniels et al., 2001; L. Li & Xie, 2005).

#### 1.1.4.2 Pathway regulation of CEPC fate

Signaling pathway can regulate epithelial cell fate determination. Knockout of Notch1 in mice switched the corneal epithelium into a hyperplastic, keratinized and epidermis-like phenotype. Wnt/β-catenin signaling in CEPC serves as maintenance of stem cell self-renewal. Activation of Wnt/β-catenin signaling promotes CEPC proliferation and colony-formation with maintenance of stem cell phenotype (Nakatsu et al., 2011b). When Wnt/β-catenin pathway is suppressed by its inhibitor Dkk2, CEPC may differentiate into non-keratinizing stratified epithelium. This indicates that the corneal epithelial differentiation is initiated by the down-regulated Wnt/β-catenin signaling (Mukhopadhyay et al., 2006).

#### 1.1.4.3 Extracellular matrix of CEPCs niche environment

The limbal basement membrane provides an adherence niche to keep CEPC in close interaction with the underlying limbal stroma. By comparing the cytoskeleton molecules between limbal and corneal basal epithelia, there exist different molecular profiles of cell adhesion events:

1) limbal basement membrane preferentially expressed α9 integrin and N-cadherin but was absent for connexin 43 (Grueterich et al., 2002).

2) Collagen type IV (a3, a4, and a5) chains and laminin (a1, a3, b1, b3, g1, and g2) chains are found in central corneal basement membrane, while the limbal basement membrane contained additional collagen IV (a1 and a2) chains and laminin (α2 and β2) chains, but no collagen IV (a3, a4, and a5) chains (W. Li, Hayashida, Chen, & Tseng, 2007).

3）AE27, the anti-basement membrane component expresses intensely and continuously in the central corneal basement membrane but not in limbal basement membrane (Schlotzer-Schrehardt et al., 2007).

### 1.1.5 Limbal stem cell deficiency (LSCD)

Loss of CEPC is clinically referred as limbal stem cell deficiency (LSCD). This disorder is characterized by conjunctivalization, vascularization, chronic inflammation and persistent epithelial defects on the corneal surface, resulting in a loss of vision(Lichtinger, Pe'er, Frucht-Pery, & Solomon, 2010). Replacement with viable CEPC by either limbal grafting or cultivated limbal cell transplantation has been effective to some extent in the management of severe LSCD (Rama et al., 2010; R. J. Tsai, Li, & Chen, 2000; M. Zhou, Li, & Lavker, 2006). Permanent restoration of a transparent and intact corneal epithelium has been reported in ~76% of 112 eyes after transplantation (Rama et al., 2010). However, graft rejection poses the topmost problem to transplantation management whereas other problems include conjunctiva invasion and corneal epithelial defects. In a post hoc report, the success is associated with the amount of p63 high holoclone-forming progenitor cells in the graft (Rama et al., 2010). Hence, a better understanding of the basic biological features of these progenitor cells as well as the niche interaction will help to advance clinical technique and treatment, leading to better caring for patients. Although the clinical application of CEPC for ocular surface reconstruction has been successfully performed and is not deterred by the unknowns of genuine CEPC, the discovery of definitive CEPC markers or novel molecules involved in CEPC maintenance and regulation would enhance the isolation and expansion of these cells for better clinical applications and study of ocular stem cell biology.

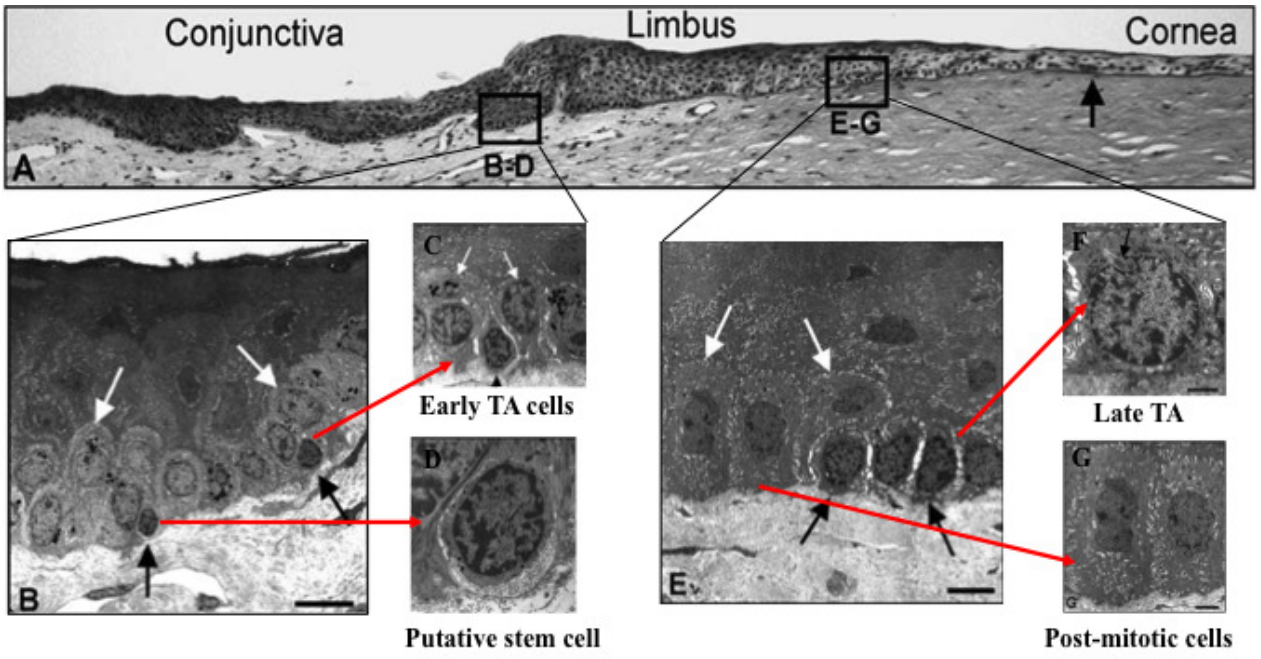


*(Schlotzer-Schrehardt & Kruse, 2005)*

**Figure 1.1 The morphology of corneal epithelial progenitor cells under transmission electron microscopy.**

(A) The morphology of human cornea and peripheral limbal epithelium, the arrow indicates termination of Bowman's membrane. (B) Putative stem cells (black arrows) and putative early progenitor or transient amplifying cells resides at the bottom of the epithelial papillae forming the palisades of Vogt. (C) Putative TA cells have distinct nucleoli prominent melanin granules and tonofilament bundles (D) Putative stem cell contain minute melanin granules, have high nuclear to cytoplasmic ratio without distinct nucleoli. (E) Cluster of putative transient amplifying cells (black arrows) close to post-mitotic basal cells (white arrows) without pigment granules. F. Putative transient amplifying cell; the arrow indicates two centrioles. G. Post-mitotic basal cells.

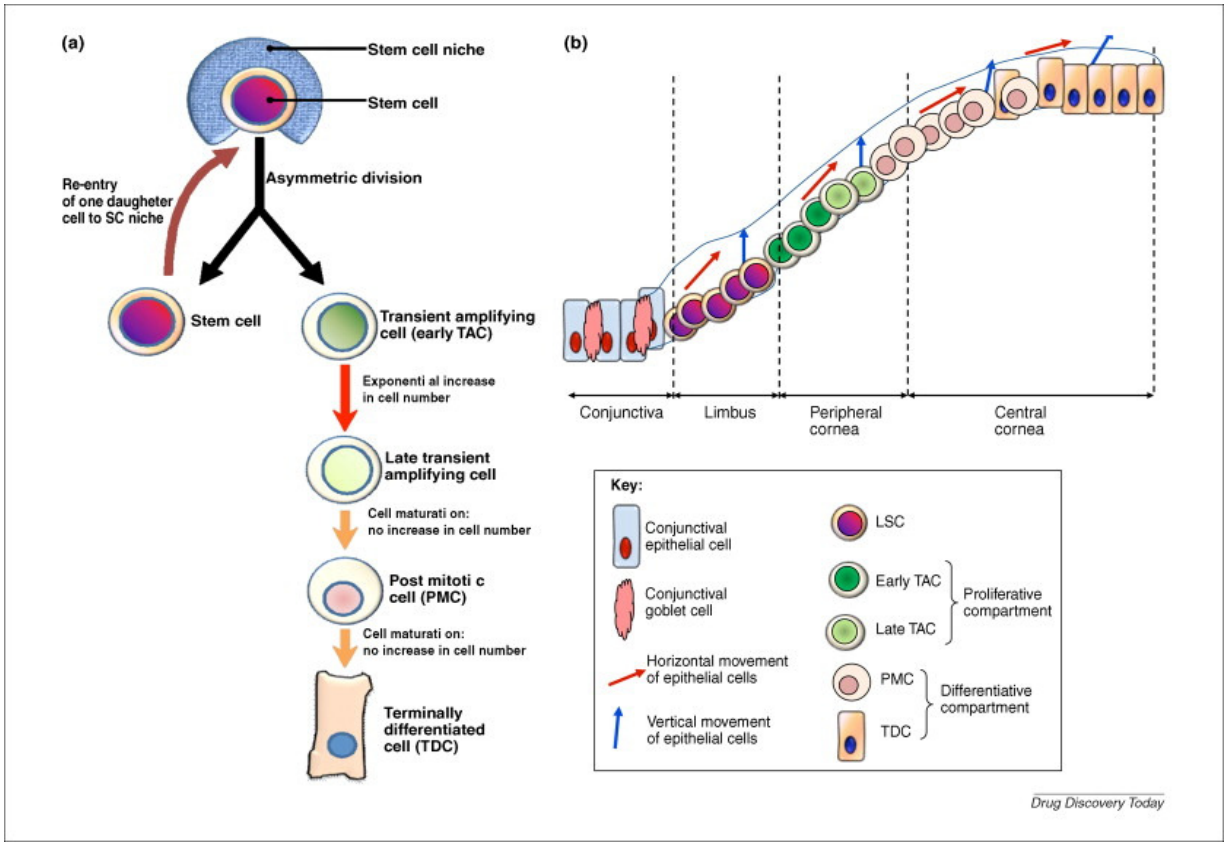


*(Ahmad, Kolli, Lako, Figueiredo, & Daniels, 2010)*

**Figure 1.2 Corneal epithelial progenitor cells division and differentiation.**

(A) One CEPC asymmetric divided into two daughter cells. One returns to the stem cell niche to maintain the stem cell pool, the other turns to TAC for increasing cell number. The cells will continue to differentiate to late TA cell, post mitotic cells (PMC) and eventually to terminally differentiated (TDC) and become corneal epithelial cells. (B) The progeny cells migrate upwards and centripetally to the corneal surface to replace the dying epithelial cells in daily turnover. During the process of differentiation, CEPCs are quiescent cells, early and late TA cells are proliferative compartment, PMCs and TDCs are differentiated compartment.

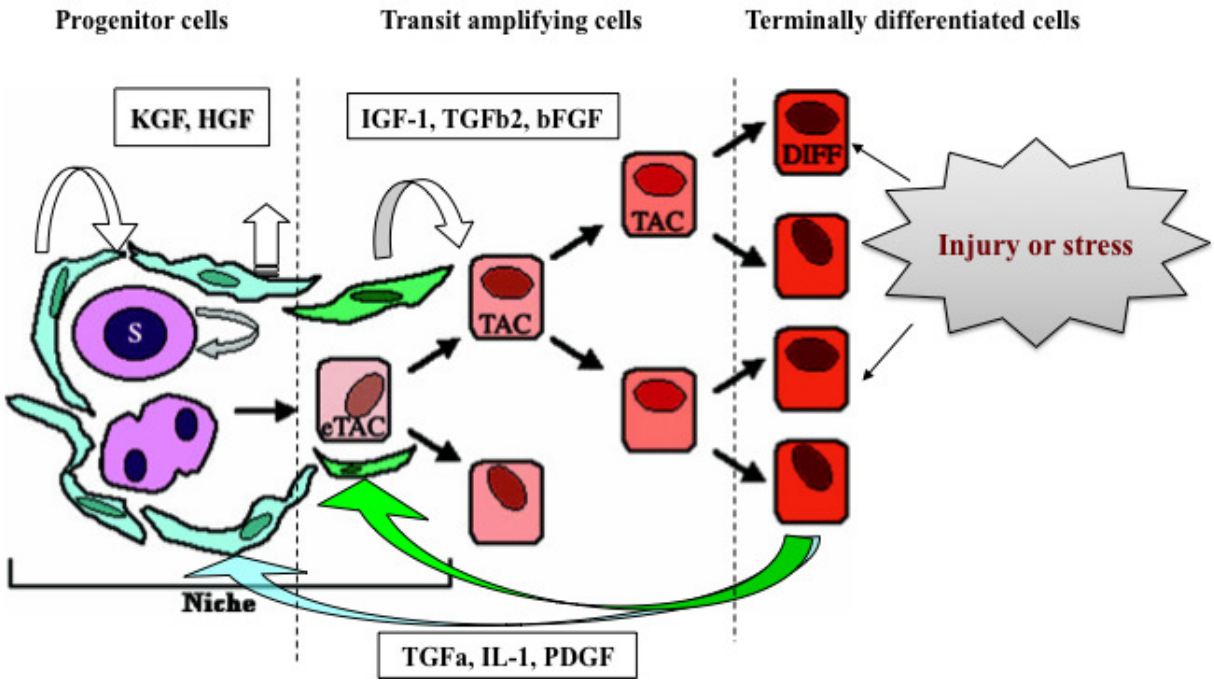


*Original picture from (Pajoohesh-Ganji & Stepp, 2005) modified by Teng Yufei 2013.*

**Figure 1.3 The microenvironment of CEPC niche**

Upon injury or stress, epithelial cells release IL-1β, TGFα, and PDGF to stimulate the limbal and corneal fibroblasts to in secreting KGF and HGF. Limbal fibroblasts release KGF to activate limbal stem cell division and differentiation, subsequently corneal fibroblasts secret HGF to modulate the production and migration of TAC. In contrast, IL-1β stimulates TGF-β1, TGF-β2, which can suppress limbal and corneal fibroblasts to secret KGF and HGF. This inhibitory pathway acts as a signal by repressing the CEPC division and migration to avoid the over-proliferation of CEPC.

## 1.2 MicroRNA

### 1.2.1 MicroRNA - definition, etiology, biosynthesis and mechanisms of action

#### 1.2.1.1 Definition of microRNA

MicroRNA is a class of newly discovered epigenetic factor that endogenously repress the gene expression at post-transcriptional stage. MicroRNAs belong to a group of small, non-coding RNAs with 19 to 25 nucleotides in length, which are believed to be ubiquitously expressed and regulate a large variety of cellular processes in worms, files, fish, plants and mammals (Bartel, 2004). The genomic origin of microRNAs is usually in intergenic region or within the intron of protein-coding genes. With the application of molecular cloning and bioinformatics prediction, over 1100 human mature microRNA sequences have been annotated and they are proposed to regulate >30% of human transcriptomes (X. Liu, Fortin, & Mourelatos, 2008). This indicates the microRNA regulation is active in a diverse spectrum of biological processes, including cell cycle, proliferation, apoptosis, differentiation, developmental timing and lineage selection, as well as in disease pathogenesis and tumorigenesis.

#### 1.2.1.2 MicroRNA biosynthesis

The biogenesis of microRNA includes two parts: (1) transcription and cleavage in nucleus. (2) Maturation and activation in the cytoplasm. MicroRNAs are initially transcribed into long primary transcripts by RNA polymerase II, named as pri-miRNA. Pri-miRNA is composed of a double-stranded stem of ~33 base pairs, a terminal loop and two flanking unstructured single-stranded segments with 5' capped and 3' polyadenylated end, which may encode one to several microRNAs. Pri-miRNA is processed to a 60-70

nucleotides hairpin-stem precursor microRNA by the nuclear microprocessor complex. The microprocessor complex comprises of RNase III endonuclease Drosha and a double-stranded RNA binding protein DiGeorge syndrome critical region 8 (DGCR8), which recognizes pri-miRNA by the minimal flanking region from the base of stem and crop. pri-miRNA asymmetrically generates one pre-miRNA that has a 5′ monophosphate and a 3′ 2-nt hydroxyl overhang as a recognition element for further microRNA processing (X. Zhang & Zeng, 2010). During the cleavage, Drosha is crucial for pre-ribosomal RNA processing. Knockdown of Drosha led to an accumulation of 12S and 32S precursor RNA (Krol & Krzyzosiak, 2004), whereas elevated Drosha alone could result in non-specific cleavage and degradation of the pri-miRNA. DGCR8 provides specificity for the expression of pre-miRNA that addition of DGCR8 resulted in the formation of a distinct pre-miRNA (Han et al., 2004; W. Zhang et al., 2011).

RanGTP and Exportin-5 (Exp-5) export pre-miRNAs to the cytoplasm in a Ran GTP-dependent manner. Exportin 5, a nuclear transport receptor, heterodimerizes with GTPase enzyme Ran, binding to the pre-miRNA to form a heterotrimeric complex. Then the complex passes through the nuclear pore, and releases the pre-RNA by Ran-GTP hydrolyzing to Ran-GDP. Exp-5 is also important for stabilizing pre-miRNAs in the nucleus (Zeng & Cullen, 2004). With the depletion of Exp-5, pre-miRNAs decreased in both cytoplasm and nucleus, suggesting that Exp-5 enhances pre-miRNA stability and promote their resistance to degradation (Zomer et al., 2010). In cytoplasm, pre-miRNA is processed to a 22 nucleotides dsRNA by Dicer complex. The Dicer protein contains one PAZ domain and two RNase III domains (Saito, Ishizuka, Siomi, & Siomi, 2005). The PAZ domain recognizes and binds to the 3` 2-nt overhang at the base region of stem loop and cut the pre-miRNA to short dsRNA structure. After the Dicer process, the microRNA duplex is unwound by helicase (Krol & Krzyzosiak, 2004). One strand of pre-miRNA is

predetermined as mature microRNA by Drosha site selection in pre-miRNA cleavage, while the complimentary strand microRNA* termed as passenger strand is degraded.

#### 1.2.1.3 Mechanism of microRNA-mediated Gene Silencing

After Dicer processes the duplex microRNA, the microRNA-mature strand is released and incorporated into RNA-induced silencing complex (RISC) to form an active RISC complex or referred as miRISC (R. I. Gregory, Chendrimada, Cooch, & Shiekhattar, 2005). Argonaute (Ago) protein family is the core component of miRISC for site-specific target recognition of mRNA. Ago protein consists of two conserved RNA binding domains: a PAZ and a PIWI domain. PAZ domain binds to the single stranded 3' end of mature microRNA and PIWI domain is structurally similar to the RNase H family that have RNA cleaving activity (Thomson & Lin, 2009). There are four Ago proteins (AGO 1- 4) in human (J. S. Yang & Lai, 2010), among them, Ago2 can directly cleave the mRNA and lead to mRNA degradation. Ago protein binds to the mature microRNA with recruiting some additional proteins like TRBP, TAR, PACT, and guiding RISC to interact with the specific site in 3' UTR of target mRNA. The perfect complementarity between microRNA and target mRNA sequence will cause degradation of target mRNA through either Ago2 induced endonucleolytic cleavage of mRNA or RISC-mediated targeting of the 3' polyA tail deadenylase action. However, microRNA and mRNA target share perfect complementarity rarely occurred. In most cases, the bound microRNA engages in imperfect complementarity with its target. This partial complementarity results in translational repression through a variety of different mechanisms. Following miRISC binding, target mRNAs may be segregated to P-bodies, in where the polyA tail of the mRNA is shorten by deadenylation, causing translation deterrence. Another mechanism of repression is Ago2 competes with the initiation factor eIF4E for binding the 5' cap of mRNA, which block ribosome assembling

to mRNA and results in the prevention of translation initiation. miRISC can also block the elongation of translation by producing secondary structure restrictions to drop-off ribosome. Finally, miRISC can directly bind to open reading frames (ORF) or 5'UTR in a manner similar to traditional 3' UTR binding. (**Figure 1.4 & Figure 1.5**) (R. I. Gregory et al., 2005; M. Li et al., 2009).

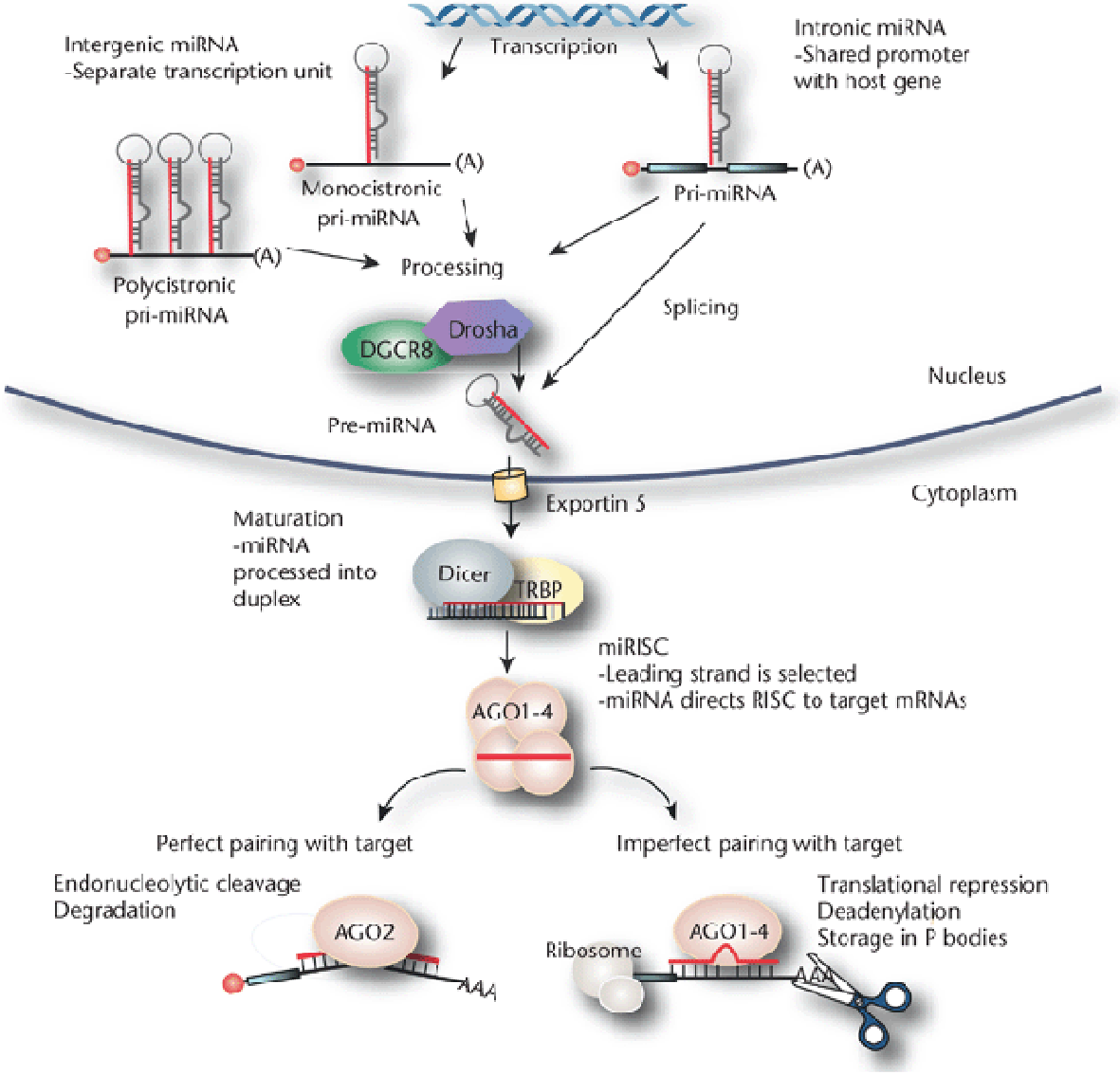


*(Chang & Mendell, 2007)*

**Figure 1.4 Biogenesis of microRNAs and the mechanism of microRNA action.**

MicroRNAs biogenesis and mechanisms of action: (1) microRNAs, originated from separate intergenic transcprtion unit or intronic region of host gene, and initially transcribed by RNA polymerase II to form a long capped and polyadenylated transcripts, termed as primary microRNAs (pri-miRNAs). (2) Pri-miRNA is processed into a 60-70 nucleotides hairpin-stem microRNA precursor (pre-miRNA) through the nuclear microprocessor complex RNase III Drosha and DGCR8. (3) Pre-miRNAs are then exported to the

cytoplasm by exportin-5 and processed into microRNA duplexes through the action of the cytoplasmic type III RNase Dicer and its partner TRBP. (4) Duplexes are then incorporated into the microRNA-induced silencing complex (miRISC), where they are processed into the mature microRNA of ~22 nt in length. (5) Ago protein guide RISC to interact with the specific site in 3' UTR of target mRNA. (6) If the bound microRNA is perfectly complementary with its target, the mRNA will be cleaved and degraded. Imperfect complementarity leads to translational repression through deadenylation.

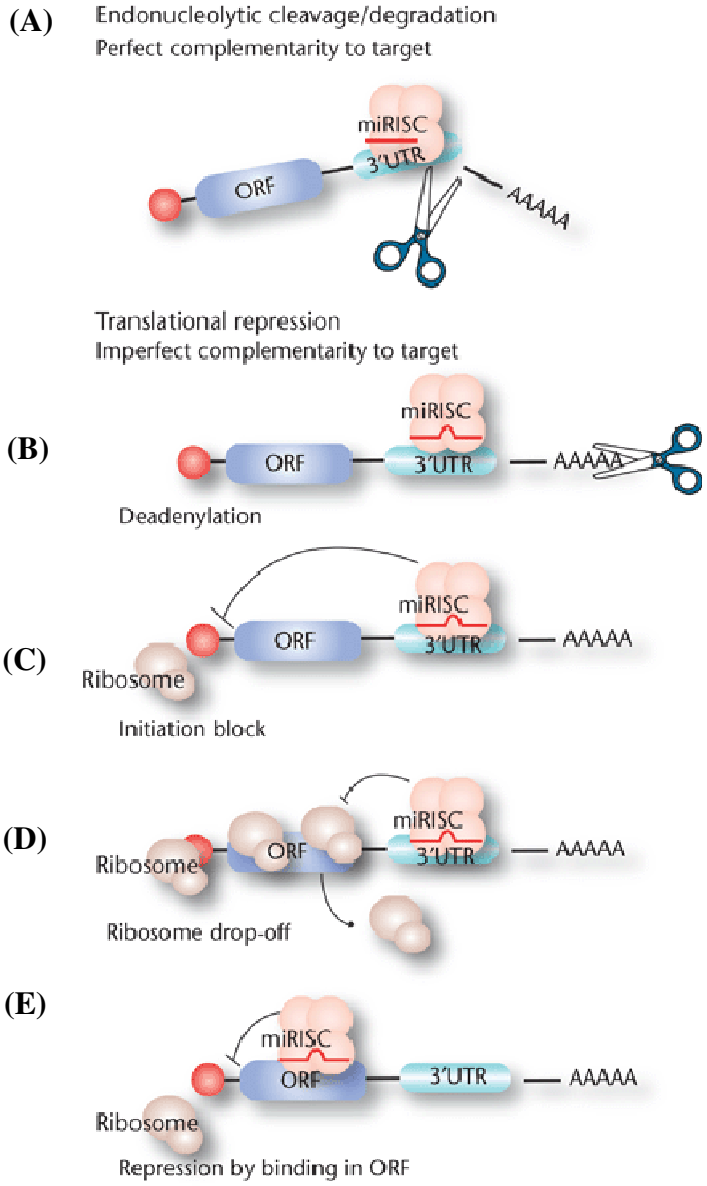


*(Chang & Mendell, 2007)*

**Figure 1.5 The mechanism of microRNA mediated gene silencing**

MicroRNAs regulate gene expression by binding to target sites in the 3'-UTR of mRNA, suppressing its translation. (A) If the microRNA and mRNA target are perfect complementary, the mRNA will be cleaved and degraded by the action of Ago2. (B) The imperfect binding will lead to translational repression. Following miRISC binding, target

mRNAs may be segregated to P-bodies, the polyA tail of the mRNA will be shortened by deadenylation. (C) miRISC preclude ribosome binding to the 5' cap, which results in a block of translation initiation. (D) miRISC block the elongation step of translation by inducing secondary structure restrictions which lead to ribosome drop-off. (E) miRISC can also directly bind to open reading frames (ORF) or 5'UTR which is similar to traditional 3' UTR binding.

### 1.2.2 MicroRNA regulation in stem cells

Dicer or Dgcr8, two key components in the microRNA biogenesis pathway, reveal the function of microRNA in ESC. The deletion of Dgcr8 and Dicer in ES cells resulted in the defects in the ability of self-renewal and differentiation. Dgcr8-deficient ES cells had an extended population doubling time due to $DGCR8^{-/-}$ cells were arrested at G1 phase. Knockdown of DGCR8 obstructed embryonic body differentiation with delay and decreased the expression of differentiation markers (Y. Wang, Medvid, Melton, Jaenisch, & Blelloch, 2007). Dicer is essential for early mouse development, as its absence results in embryonic lethality (Kanellopoulou et al., 2005). During embryonic body induction, $Dicer1^{-/-}$ cells retained the pluripotent markers and failed to express any differentiation markers in the condition of differentiated induction (Kanellopoulou et al., 2005).

ES cells exhibit a distinct microRNA signature compared to embryo body through the large-scale microRNA screening (Houbaviy, Murray, & Sharp, 2003). A set of ESC specific microRNAs has been identified, including miR-302 family, miR-17–92 cluster, C19MC microRNAs, and miR-371–373 cluster; MiR-290 family is specifically expressed in mouse ESCs (Stadler et al., 2010).

**MicroRNAs regulate ESC self-renewal**

As previously described, the short cell cycle of ES cells is relied on the cyclin E-cdk2 pathway to promote G1-S transition. Inhibition of ESC-related microRNAs could lead to G1 phase arrest (Y. Wang & Blelloch, 2009). The members of miR-290 (in mouse) and miR-302 (in human) target on cyclin E-Cdk2 upstream inhibitors (including CDKN1A, CDC2L6, retinoblastoma-like 2 protein, and Lats2); MiR-372 and miR-92b target on another two inhibitors of G1/S progression p21Cip (Cdkn1a) and p57 (CDKNIC),

respectively (Sengupta et al., 2009). Increasing cyclin E-Cdk2 activity could promote the G1/S progression (Y. Wang & Blelloch, 2009). Therefore, miR-290, miR-302, and miR-17–92 clusters are termed as ES-specific cell cycle-regulating microRNAs (ESCC-miRs) which can recuse the growth defect of DGCR8-/- cells by down-regulating these inhibitors and results in ESC rapid proliferation (Y. Wang et al., 2008).

The sequence of pluripotent factors Oct4, Sox2 and Nanog bind to the promoter region of miR-302 to initiate the transcription of miR-302 cluster. The miR-302 cluster expression requires the promotion of Oct4/Sox2 in human ESCs, therefore the expression level of miR-302 cluster is correlated with Oct4/Sox2 during embryogenesis (Card et al., 2008).

**MicroRNA regulate ESC differentiation**

Xu et al. had reported that miR-145 was significantly up-regulated upon hESC differentiation. Ectopic expression of miR-145 inhibited ESC self-renewal and promoted the differentiation through direct targeting on Oct4, Sox2 and Klf4. In contrast, Oct4 repressed the miR-145 promoter transcription prior to differentiation, which formed a double negative feedback loop to transient human ESC from self-renewal to differentiation (N. Xu, Papagiannakopoulos, Pan, Thomson, & Kosik, 2009). In mouse ESC, Oct4 and Sox2 were suppressed by miR-134, miR-296 and miR-470. Sox2 and Klf4 were negatively modulated by miR-200c, miR-203, and miR-183 (Tay, Zhang, Thomson, Lim, & Rigoutsos, 2008).

Let-7 is broadly expressed in differentiated cell types and adult organs. Transfection of let-7 into DGCR8-/- cells rescued the differentiation defect by repressing the pluripotent factor expression. Let-7 was completely absent in ESC and was gradually up-regulated

during differentiation. Lin28, a protein co-expressed with Oct4/Sox2/ Nanog/Tcf3 in ES cells, directly suppresses the maturation of Let-7 (Zhong et al., 2010). ESCC microRNAs and let-7 family members exhibited opposite functions in ESC through modulating c-Myc (Melton, Judson, & Blelloch, 2010). As a target gene of let-7, c-Myc was elevated by ESCC microRNAs in ESC. Additionally, ESCC microRNAs synergistically improved the expression of Lin 28 (Judson, Babiarz, Venere, & Blelloch, 2009).

In ESC, ESCC microRNA expression is controlled by the pluripotent factors Oct4, Sox2, Nanog, Tcf3, and c-Myc. ESCC microRNAs indirectly up-regulated cMyc to form a positive feedback loop which may reinforce their own expression. At undifferentiated stage, Lin28 is increased by Oct4/Sox2/Nanog, then its negative regulator let-7 is suppressed by ESCC microRNAs (Qiu, Ma, Wang, Peng, & Huang, 2010). As ESCs differentiate, Oct4, Sox2 and Nanog were decreased coupled with the down-regulation of ESCC microRNAs and Lin28. With the loss of suppression from Lin28, let-7 functionally matures to target on c-Myc and other pluripotent genes as well as Lin28 to reinforce its own expression (Newman & Hammond, 2010). Therefore, core ES cell transcription factors and the microRNAs coordinate to form a regulatory circuitry switching the ES cells between self-renewal and differentiation.

Small molecules have been investigated for iPSC reprogramming. Based on the different reports, microRNAs could not independently switch the somatic cell phenotype (Wilson et al., 2009). However, ESCC microRNAs could cooperatively enhance Oct4, Sox2 and Klf4 transfection efficiency (Lin et al., 2008). Since ESCC microRNA is an activator of c-Myc, probably as a replacement of c-Myc in iPSC reprogramming. Additionally microRNA could promote the iPSC generation efficiency by epigenetic regulation. The

suppression of miR-302 on AOF caused DNMT1 deficiency and promoted DNA demethylation of somatic cell reprogramming (Kuo, Deng, Deng, & Ying, 2012).

### 1.2.3 MicroRNA regulation in human eyes

#### 1.2.3.1 MicroRNA expression pattern

Through the comparison between different tissues and cell populations, microRNAs display a tissue/stage-specific manner. In mammalian retina, a distinct atlas of microRNA expression was profiled. Microarray analysis identified 78 microRNAs highly expressed in adult mouse retina. Among them, 21 were potentially retina-specific when compared with other adult tissues (Sundermeier & Palczewski, 2012). Next-generation sequencing has dramatically expanded the known number of retinal microRNAs to more than 250 (Sundermeier & Palczewski, 2012). MicroRNAs such as miR-124a, -182, -183, 96, 204, 9, 181a, 29c, and let-7d were prone to be specific to adult mouse retina versus other tissues (such as brain and heart) (S. Xu, 2009).

The microRNA spatial distribution in retina can be detected by laser captured micro-dissection (LCM) and in situ hybridization approaches. MicroRNA real-time PCR analysis has been performed on total RNA collected from the ganglion cell layer (GCL), inner and outer nuclear layers (ONL) of adult mouse retina cutting by LCM. The results showed that both miR-204 and miR-211 were highly expressed in inner nuclear layer (INL) and miR-210 was detected in all three layers, but less in INL (Hackler, Wan, Swaroop, Qian, & Zack, 2010).

By in situ hybridization, miR-183/96/182 cluster was expressed limitedly in all photoreceptors, as well as interneuron in INL and ONL but not in ganglion cell layer (Karali,

Peluso, Marigo, & Banfi, 2007). The expression pattern of miR-182 was co-localized with rhodopsin in the OS of rod photoreceptors. MiR-204 was intensively expressed in GCL and the innermost part of INL where amacrine cell are located (Deo, Yu, Chung, Tippens, & Turner, 2006). It is also abundantly found in adult mouse and human fatal RPE (F. E. Wang et al., 2010b). MiR-204 is co-expressed with its host gene Trpm3 in RPE, INL, and GCL of neural retina in adult and in the choroid plexus of the lateral ventricles of embryonic eyes (Deo et al., 2006; Karali et al., 2007). Besides the retina, miR-204 was strongly expressed by the epithelium of lens and ciliary body (Conte et al., 2010). MiR-29c is present in photoreceptors and the outermost part of the INL. MiR-181a is expressed in both amacrine and GCL and the innermost part of INL (Sundermeier & Palczewski, 2012).

MicroRNA expression pattern during retinal development was also profiled, with the comparison of microRNA expression in different development stages. Expression of miR-124a was strongly expressed in the eye at E14.5, in the innermost cell layer where progenitors started differentiating into ganglion cells (Karali et al., 2007). In adult retina, miR-124a was expressed in all layers with intensive staining in the outer (OS) and the inner segment (IS) of the photoreceptors, but not glial cells. Hence, miR-124a is specifically expressed in differentiated neurons of retina (Hackler et al., 2010). MiR-9 was strongly expressed in all cells of mouse retina at E14.5, but at postnatal stage, it is restricted to the central region of INL where Müller cells reside, indicating that miR-9 maybe expressed in neural progenitors and Müller cells (La Torre, Georgi, & Reh, 2013; S. Xu, 2009). Human fatal choroid (16 to 20 week of gestation) highly expressed miR-126, 146a, 142-3p, 199b and 214 compared to human fatal RPE (F. E. Wang et al., 2010b).

In the anterior segment, miR-184 was highly expressed in the epithelium of mouse lens and mouse central cornea (Ryan, Oliveira-Fernandes, & Lavker, 2006b). The

expression of miR-124 and miR-204 were uniformly expressed in all lens epithelial cells; and miR-205 was expressed throughout the corneal epithelium (Karali et al., 2010).

#### 1.2.3.2 Function of microRNAs in eyes

MicroRNA expression is essential for optic cup development and mature retinal neuronal survival and function (Davis, Mor, & Ashery-Padan, 2011). The conditional knockout of Dicer in mice abrogated retinal neurogenesis, iris and corneal morphogenesis (Y. Li & Piatigorsky, 2009). Inhibition of Dicer in mouse retina led to morphological defects of the photoreceptor rosettes, progressive retinal cells degeneration and disorganization during retinogenesis, followed by decreased electroretinogram (ERG) responses (Damiani et al., 2008). *In vitro* study showed that the Dicer1-deficient retinal progenitor cells were prone to apoptosis, and failed to differentiate to other retinal neuronal subtypes (Georgi & Reh, 2010).

MiR-183/96/182 cluster is sensory organ-specific microRNAs. They are abundantly expressed in sensory neurons like retinal photoreceptors, taste buds of olfactory epithelium and lingual epithelium, as well as dorsal root ganglia (S. Xu, Witmer, Lumayag, Kovacs, & Valle, 2007). Expression of miR-183/96/182 cluster was dramatically decreased in human retinitis pigmentosa model (Loscher et al., 2007). MiR-183/96/182 cluster and miR-204/211 exhibited diurnal variant that were down-regulated during dark adaptation and up-regulated in light-adapted mouse retinas (Krol et al., 2010). Diurnal variation in expression was directly caused by the exposure to light but not circadian rhythm. Deletion of miR-183 cluster in a transgenic mice model (Sponge Transgenic Mouse) increased the sensitivity of light-induced retinal degeneration. *Casp2* as a direct target of the miR-183 cluster, was increased in response to light exposure (Zhu et al., 2011). Accordingly, miR-183 functions

as a preventive measure of photoreceptors from the light stress by silencing apoptosis related genes.

MiR-204 contributes to lens differentiation and optic cup dorsoventral polarization. In early medaka fish eye development, loss of miR-204 resulted in lens abnormalities, microphthalmia, and eye coloboma. MiR-204 targets on transcription factor Meis2 and the knockdown of miR-204 elevated Meis2 and subsequently activate the Pax6 transcriptional pathway (Conte et al., 2010). In retinal pigment epithelium, miR-204/211 maintained the phenotype of epithelium by preventing epithelial-mesenchymal transit (EMT). TGF-β signaling is the key effector in EMT process that induces epithelium transit to mesenchymal phenotype. MiR-204 targeted on two genes belonging to TGF-β signaling pathway, namely TGF-beta receptor 2 (TGF-betaR2) and SMAD (SNAIL2). The suppression of miR-204 on EMT hence is crucial for the blood-retina epithelial barrier of RPE (F. E. Wang et al., 2010b).

For the neuron abundant microRNA, gain or loss of miR-124a did not affect neuronal determination (Cao, Pfaff, & Gage, 2007) but it could regulate the neuronal maturation and maintenance during development. MiR-124a was required to prevent the death of newly differentiated cone photoreceptors (K. Liu et al., 2011b). This was evident by overexpression of miR-124a promoted the neural cell proliferation and enhanced the cell survival through reducing the expression of homeobox transcription factor Lhx2 (Sanuki et al., 2011).

In Xenopus, miR-24a was present in the neural retina throughout xenopus eye development. Inhibition of miR-24a resulted in increased apoptosis of retinal precursors and the appearance of small eye size. MiR-24a could target on pro-apoptotic factors, including caspase-9 and apoptosis protease-activating factor 1 (apaf1), and its suppression of

apoptosis-related genes would be essential for promoting neural progenitor survival (Walker & Harland, 2009).

### 1.2.4 MicroRNA regulation in adult human CEPC

In adult mouse corneas, the expression of miR-184 was enriched in the central basal epithelium but negligible in the limbal and conjunctival epithelia; whereas miR-205 was expressed throughout the entire corneal, limbal and conjunctival epithelia. miR-205 is also expressed strongly in the epidermis, hence it is regarded as a keratinocyte specific microRNA (J. Li et al., 2010). MiR-205 suppressed the keratinocyte adhesion and enhanced the migration and proliferation of corneal keratinocyte through the activation of Akt signaling pathway via targeting on SHIP2. Meanwhile corneal enriched miR-184 was found to antagonize the suppression of miR-205 on SHIP2 levels, leading to the keratinocyte apoptosis and cell death (Yu et al., 2008b). Hence, miR-205 and miR-184 function to balance and maintain the corneal epithelial cell growth. MiR-184 was also found to be expressed in early eye development. It was increased during the corneal epithelial differentiation of iPSCs. Knockdown of miR-184 resulted in a decrease in Pax6 and Krt3, suggesting its potential roles in determination of corneal-epithelial lineage commitment during eye development (Shalom-Feuerstein et al., 2012).

MiR-31 was found to be preferential expressed by human central corneal epithelium. It was higher in the primary cultured corneal epithelium derived keratinocyte than limbal epithelial derived keratinocyte. MiR-31 directly target on FIH-1, on one hand affecting glycogen metabolism in corneal epithelium (Peng, Hamanaka, et al., 2012), on the other hand promoting corneal epithelial cell differentiation through activation of Notch signaling. The expression pattern of FIH-1 was opposite with miR-31 which was abundant in LPC epithelium but absent in CC epithelium. FIH-1 antagonized miR-31 to impair keratinocyte

differentiation by attenuating Notch signaling, which formed a balance in regulation of corneal epithelium differentiation (Peng, Kaplan, et al., 2012).

In our previous work, global screening using microRNA microarray followed by qPCR validation had identified 9 specific microRNAs differentially expressed in human limbo-peripheral corneal epithelium (containing CEPC) versus central corneal epithelium (without CEPC) (Lee et al., 2011). Two microRNAs, hsa-miR-143 and hsa-miR-145, were significantly up-regulated in limbal epithelium. By in situ hybridization using lock nucleic acid-modified oligonucleotide probe on frozen human cornea section, both microRNAs were specifically localized in the limbal epithelia, but not in corneal epithelia. However, the expression was predominant in the winged-cell and parabasal layers, with signal decreasing towards the superficial layers. The basal epithelium where CEPC reside had low expression of these microRNAs. *in vitro* studies have demonstrated that miR-145 promoted the early differentiation of CEPC with higher expression of cytokeratin 3/12 and connexin-43, and affected epithelium formation and integrity, via direct targeting on integrin beta 8 (Lee et al., 2011).

**Table 1.1 Summary of reported microRNAs distribution and functions in retina.**

| MicroRNA | Retina | | | | | | Target | Function | Reference |
|---|---|---|---|---|---|---|---|---|---|
| | RPE | ONL | INL-bipolar | INL-amacrine | INL-muller | GCL | | | |
| miR-124a | | + | + | + | − | + | NeuroD1<br>Lhx2 | Neuronal maturation and maintenance | (Sanuki et al., 2011)<br>(K. Liu et al., 2011b) |
| miR-182 | − | + | + | + | | + | Adey6 | Prevent photoreceptors from light stress | (Jin et al., 2009) |
| miR-183 | − | + | + | + | | + | Mitf | | (S. Xu, 2009) |
| miR-96 | − | + | + | + | | + | | | |
| miR-204 | + | | | + | | | Meis2 | Maintains the phenotype of epithelium | (Conte et al., 2010) |
| miR-9 | Retinal precursors | | | | + | | | Retinal progenitors developmental transition | (La Torre et al., 2013) |
| miR-181a | | | | + | | | | | (S. Xu, 2009) |
| miR-29c | | + | + | | | | | | (S. Xu, 2009) |
| let-7d | | | + | + | | | | | (S. Xu, 2009) |
| miR-24a | Retinal precursors | | | | | | Apaf1 | Promoting neural progenitor survival | (Walker & Harland, 2009) |

**Table 1.2 Summary of reported microRNAs distribution and functions in anterior segment**

| microRNA | Corneal epithelium | | Lens | Trabecular meshwork | Target | Function | Reference |
|---|---|---|---|---|---|---|---|
| | Limbal epi | Central epi | | | | | |
| miR-184 | - | + | + | | | Promote corneal-epithelial differentiation | (Shalom-Feuerstein et al., 2012) |
| miR-205 | + | + | | | *Ship2* | Enhance cell proliferation and migration | (Yu et al., 2008b) |
| miR-204 | | | + | | *Meis2* | | (Conte et al., 2010) |
| miR-124 | | | + | | *Bmp1* | | (Luna, Li, Qiu, |
| miR-29b | | | | | *Adaml2* | Suppress ECM related genes under chronic | Epstein, & Gonzalez, |
| | | | | + | *Nkiras2* | oxidative stress conditions | 2009) |
| miR-31 | - | + | | | *Fih-1* | Promote corneal epithelial differentiation | (Peng, Kaplan, et al., 2012) |

## 1.3 Pterygium

### 1.3.1 The pathogenesis of pterygium

A pterygium is an abnormally growing tissue invading from corneoscleral limbus onto clear cornea, characterized by corneal surface conjunctivalization, chronic fibrovascular lesion, extensive inflammation, and connective tissue remodeling. Pterygium pathogenesis was occurred in two stages：1) the progressive damage of limbal corneal-conjunctival epithelial barrier ; 2) the invasion of conjunctiva cells to cornea followed with epidermal proliferation, angiogenesis, inflammatory infiltration, fibroblasts activation and extracellular matrix changes(such as accumulation of elastin, glycosaminoglycans, and elastotic degeneration of collagen) (Coroneo, Di Girolamo, & Wakefield, 1999; Di Girolamo, Chui, Coroneo, & Wakefield, 2004).

The original of pterygium has been proved to be limbal epithelium rather than conjunctival epithelium. The immunohistological evidences showed that the leading edge of the pterygium head contained altered vimentin-expressing CEPCs (Dushku & Reid, 1994), additionally the stem cell markers p63 was found to be expressed in basal layers of pterygium head. Therefore, the hypothetic theory of pterygium pathogenesis is that the initial pterygial cells are actually abnormal corneal epithelial progenitor cells (Dushku, John, Schultz, & Reid, 2001). Pterygial epithelial cells broken down the limbal barrier and centripetally migrated to the cornea. The leading edge of the pterygium dissolved the Bowman's layer, followed with the adjacent conjunctiva epithelial cells and non-transparent stromal fibroblast overlying cover of cornea surface, forming a wing-like appearance (Figure 1.6) (Coroneo et al., 1999). Hence, the leading edge of pterygium facing cornea termed as pterygium head and the following section adjunct to conjunctiva termed as pterygium body. Pterygium will increase in size and obscure vision without surgically

removal (Y. Y. Tsai, Chang, et al., 2005). The epidemiologic evidence revealed that the exposure of ultraviolet (UV) is an important risk factor for the development of pterygium (Lucas, 2011). The UV radiation can trigger corneal epithelial progenitor cells failure, causing DNA damage, oxidative stress and gene expression alter. UV radiation may induce chemokine and cytokines secretion in keratinocytes and affect actin cytoskeleton assembly as well as down-regulates adhesion molecules. The molecular pathways were activated in response to acute UVB including the induction of P38 mitogen-activated protein (MAP) kinases and the down-stream activation of transcription factors c-Jun, c-Fos and AP-1(Di Girolamo et al., 2004; Hong et al., 2001). This UV activating response is believed to be a protective effect in resisting cell apoptosis (Chaturvedi, Qin, Stennett, Choubey, & Nickoloff, 2004).

### 1.3.2 Histological and immunohistochemical aspects of Pterygium

(1) Stem cell markers

Pterygium is originated from the aberrant corneal progenitor cells which maintain the expression of some stem cell markers. cDNA library identified that both conjunctiva marker Krt13 and corneal epithelium marker Krt12 were abundant in pterygium. Immunofluorescence localization showed the leading edge pterygium was mixed up staining of Krt12 and Krt13, suggesting the pterygium epithelium contains corneal-, limbal- and conjunctival-like cells (Jaworski et al., 2009). In addition, the limbal epithelium markers Krt15 and Krt19 were also detected in pterygium, consistent with the hypothesis that a pterygium is the result of an abnormal limbal epithelial basal stem cell that moves onto the corneal basement membrane over Bowman's layer (Reid & Dushku, 2010).

Pterygium was also positive for the bone marrow stem cells markers. immunoreactivity of AC133, cell marker for the primitive haematopoietic progenitors was detected in the epithelial and stromal cells. CD34, marker for the haematopoietic progenitor cells and endothelium was observed in the endothelial cells of vascular cells. haematopoietic and stromal progenitor cells marker c-Kit was expressed mainly in the basal epithelium of the pterygium head, and some spindle-shaped stromal cells. pterygium stroma was positive for STRO-1，a differentiation antigen present on bone marrow fibroblast cells and on various nonhaematopoietic progenitor cells The expression of bone marrow stem cells markers in the pterygium stroma implying bone marrow stem cells might migrate through peripheral blood to the corneal limbal area, which may lead to epithelium-mesenchymal transformation, elastotic degeneration, angiogenesis and inflammatory infiltration in pterygium (Ye, Song, Kang, Yao, & Kim, 2004).

Previous report from our lab proved that cells derived from pterygium head showed a higher colony formation efficiency and migratory aptitude than pterygium body. CEPCs marker P63 was strongly expressed in the basal layer of pterygium head and decreased towards the superficial cell layers, Pax6 was present predominantly in the full thickness epithelium of pterygium head and restrict to the upper layer of pterygium body (Bai et al., 2010), suggesting the pterygium head maintained the stem cell features with higher migratory and proliferative capacity.

(2) Cytokines and growth factors

Growth factors, such as basic fibroblast growth factor (bFGF), platelet-derived growth factor (PDGF), transforming growth factor-β (TGF-β), and tumor necrosis factor-α (TNF-α), have been shown in both resident and inflammatory cells in pterygium tissue. UVB and other pterygium risk factors trigger the secretion of pro-inflammatory mediators

such as interleukins (IL-1, IL-6, IL-8), TNF-α and TGF-β (Kennedy et al., 1997). IL-1 is constitutively expressed in corneal epithelium and released upon epithelial injury, and act as a key mediator in pterygium development. In response to the UV radiation, IL-1 and IL-1 receptor were activated primarily and stimulated the secretion of other cytokines like IL6, IL8, TNF-a, subsequently evoke MAP kinase pathways with up-regulation of downstream c-jun and c-Jun, c-Fos and AP-1. With the stimulation of IL-1and P38 MAPK pathway, IL-6 and IL-8 was produced from the whole cornea and expressed in the superficial layers of pterygium epithelium (Di Girolamo, Wakefield, & Coroneo, 2006). IL-8 can induce corneal neovascularization and act as a mitogen and activator for vascular endothelial cells; IL-6 was abundant in inflamed corneas, which can promote the corneal epithelial cell proliferation through altering the extracellular matrix composition. TNF-a has been reported to be expressed in pterygium epithelium and stroma followed with the induction of IL-1 and UVB. TNF-α can mediate the release of a number of cytokines and chemokines such as VEGF, b-FGF to induce inflammation and angiogenesis. EGFR induced by UVB were present solely in the epithelium of pterygium. EGFR was also expressed in normal corneal epithelium with the higher intensity in basal limbal epithelium, which is involved in corneal epithelium wound healing. UV radiation induced EGFR expression was observed within 15 mins of exposure, which subsequently activated MAP kinases (ERK, JNK and p38). The interaction and cross-link between EGFR, IL1, IL-8 and TNF-a can coordinately stimulate corneal keratinocyte and stroma to release matrix metalloproteinase proteins, which is a key factor in the formation and development of pterygium.

(3) Matrix Metalloproteinase family (MMP)

Matrix Metalloproteinase family (MMPs) was abundant in pterygium, immunochemistry detection showed that the MMPs was consistently up-regulated in the head of pterygium, the invading region contains altered corneal progenitor cells. Most of

MMPs are capable to degrade extracellular matrix (ECM), so as to promote tissue remolding, healing and tumor invasion. Increased production of various MMPs is observed in both epithelial and stroma of pterygium, which is released by various cell components of the pterygium. Among them, MMP-1 (categorized as collagenases), MMP-2, and MMP-9 (categorized as gelatinases), are probably the main MMPs responsible for the dissolution of Bowman's layer. MMP-1 was the most abundant protease in pterygium that was present in both epithelium and fibroblast nearest to the Bowman's layer (Dushku et al., 2001). MMP-2 and MMP-9 were intensive in the basal epithelium corresponded with regions of denatured Bowman's membrane. By comparison between normal tissue and pterygium, MMP-2 was constitutively expressed by corneal fibroblasts and dramatically increased in pterygium; MMP-9 was only responded to corneal damage (such as pterygium) for cell migration and remolding, but was absent in normal conjunctiva and cornea (Y. Y. Tsai, Chiang, Yeh, Lee, & Cheng, 2010). Besides, MMP-1 and MMP-9 were dominantly expressed in the leading edge of a pterygium, suggesting their key roles in the migration and invasion of pterygial cells through degrading collagen IV in the basal membrane of corneal epithelial cells (Y. Y. Tsai et al., 2010). The expression level and activities of MM-2 and MMP-9 were variable with the progression of pterygium. The early stage of pterygium (edge of the pterygium did not pass the midline between the limbus and pupillary margin) only expressed latent MMP-2 but not the activated form, whereas pterygium in advanced stage (the pterygium invading over the pupil) contains both activated MMP-2 and MMP-9 (S. F. Yang et al., 2009). Moreover, the fibroblast of pterygium head produced more MMP-1 and MMP-3 than pterygium body (An, Wu, & Lin, 2011).

The abnormal expression of MMPs was due to the UVB radiation and cytokines stimulation. MMP-1 was the initial MMPs that were increased following UVB exposure. As described previously, pro-inflammatory cytokines such as TNF-a, IL-1, IL- 6, and IL-8 were

also induced by UVB exposure, which subsequently stimulated MMP-2, MMP-3 and MMP-9 and other MMPs (Kennedy et al., 1997; S. F. Yang et al., 2009). The excessive expression of MMPs coordinately dissolved the Bowman's membrane and ECM. MMP-1 act as collagenase and can cut the intact collagens into pieces, and then the collagen fragment was completely cleaved by gelatinases (MMP-2 and MMP-9). Gelatinases can also release growth factors such as VEGF and bFGF for angiogenesis and the proliferation of pterygium (Y. Y. Tsai et al., 2010).

(4) Tumor markers

Tumor suppressor p53, the key TF in maintenance of genomic stability, has been identified abnormally expressed in pterygium. p53 protein is involved in several aspects of cell cycle arrest, apoptosis, control of genome integrity, and DNA repair. The wild type p53 is undetectable in normal cells due to its short half-life (6-20 mins); but the mutation in p53 gene increases the stability of protein, which is accumulated in the cells and verified by antibodies. To data, over 20 studies have observed p53 protein expression in pterygium by immunochemistry analysis, but the results in different groups was inconsistent that the prevalence of p53 positive staining pterygium varied from 7.9% to 100% (Y. Y. Tsai, Chang, et al., 2005). The abnormal expression of p53 protein in the pterygium is considered to be a result of uncontrolled cellular proliferation like p53 mutation in tumorigenesis, however, whether p53 gene was mutated in pterygium was still controversy. The only positive report on p53 mutation is just 15.7% prevalence rate, which is inconsistent with the observation on immunochemistry (Y. Y. Tsai, Cheng, et al., 2005). Therefore, the mechanism of p53 regulation in pterygium may not be the same as in tumor.

**Table 1.3 Stem cell marker, growth factors and cytokines in pterygium**

| Stem cell marker | Epithelium head | Epithelium body | Fibroblasts | Vascular endothelium | References |
|---|---|---|---|---|---|
| **Krt 19** | Present | | | | (Jaworski et al., 2009) |
| **Krt 15** | Present | Basal layer | | | (Jaworski et al., 2009) |
| **Krt 4/13** | Present | | | | (Jaworski et al., 2009) |
| **P63** | Present all layers | Basal layer | Absent | Present | (Bai et al., 2010) |
| **ABCG2** | Weak | Basal layer | | | (Bai et al., 2010) |
| **Pax6** | Present all layers | Upper layer | | | (Bai et al., 2010) |
| **AC133** | Present | | Present | | (Ye et al., 2004) |
| **CD43** | | | | Present | (Ye et al., 2004) |
| **c-Kit** | Absent | Basal layer | Present | | (Ye et al., 2004) |
| **STRO-1** | | | Present | | (Ye et al., 2004) |
| **Cytokine/growth factor** | **Epithelium** | | **Fibroblasts** | **Vascular endothelium** | **References** |
| **bFGF** | Present | | Present in Pterygium fibroblast culture supernatant | Present | (Kria, Ohira, & Amemiya, 1996) |
| **CTGF** | Present | | Present | Present | van Setten et al. (2003) |

| | | | | |
|---|---|---|---|---|
| **EGF receptor** | Present | Absent | Present | (Wan, Wang, Voorhees, & Fisher, 2001) |
| **IL-6** | Present in epithelium absent in basal cells | Not described | Present | (Di Girolamo, Kumar, Coroneo, & Wakefield, 2002) |
| **IL-8** | Present in epithelium<br>Absent in basal cells | Not described | Present | Di Girolamo et al. (2002) |
| **PDGF** | Present | Tissues and pterygium fibroblast cultures | Present | (Kria et al., 1996) |
| **TNF-α** | Present | Present | No details reported | (Kria et al., 1996) |
| **TGF-β** | Present | Tissues and cultured cells | Present | (Kria et al., 1996) |
| **VEGF** | Present | Present | Present | (Detorakis, Zaravinos, & Spandidos, 2010) |
| **IGF-2** | Pterygium basal epithelium and conjunctival goblet cell | Pterygium fibroblast culture supernatants | Not described | (Solomon et al. 2003) |
| **Stem cell factor** | Non-specific staining | Present and strongest at the cap | No staining | (Nakagami et al. 2000) |

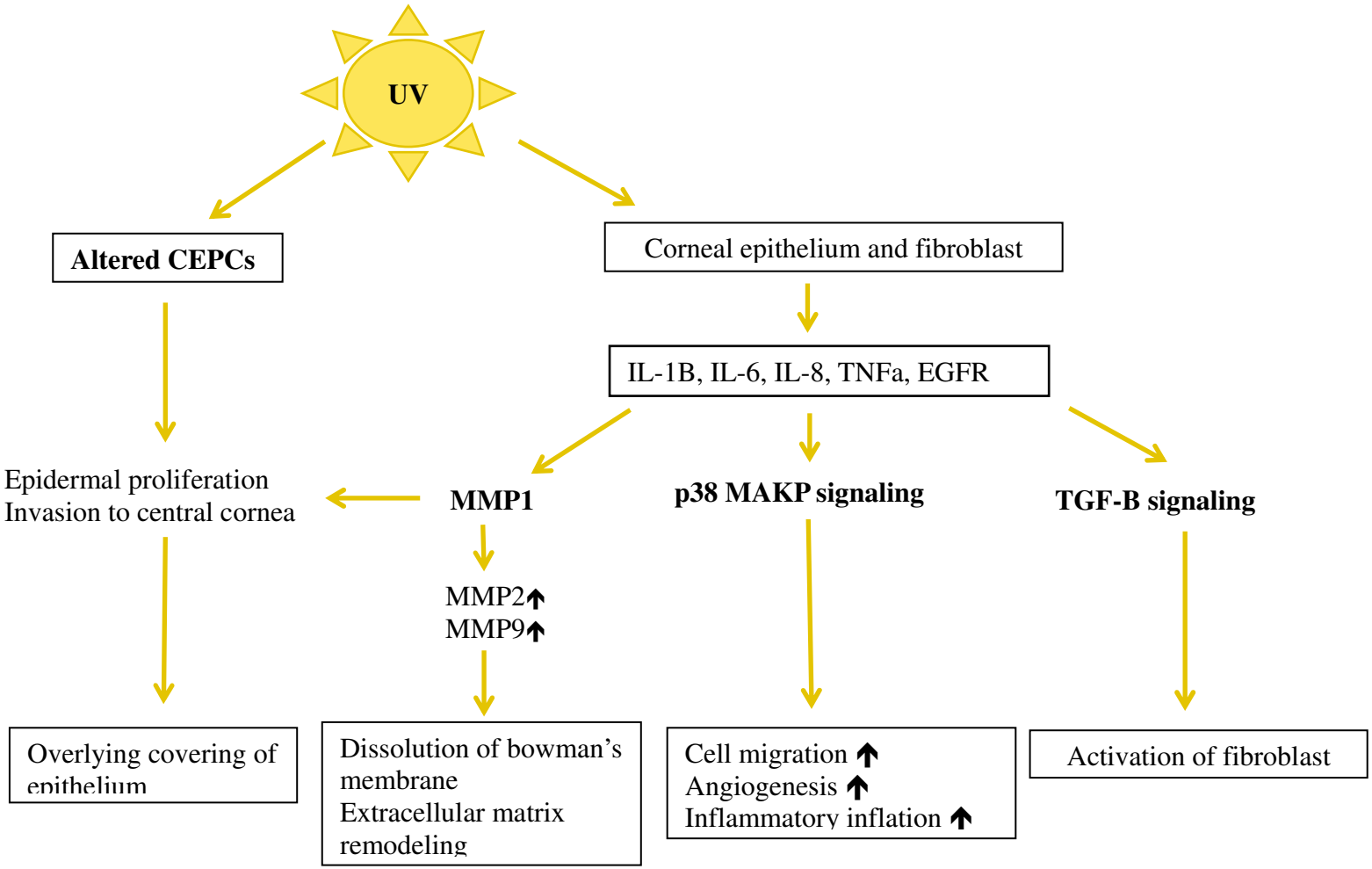


**Figure 1.6 Pathogenesis of pterygium**

# Chapter 2 Hypothesis and objectives

## 2.1 Identification of limbal-specific microRNAs and the potential role in corneal homeostasis

From the literature review and current reports, we found that limbal epithelium displayed progenitor cell enriched manner with an identification of stem cell markers. MicroRNAs are crucial for stem cell regulation and eye morphogenesis. In clinical aspect, corneal epithelium graft rejection poses the topmost problem in cornea transplantation management; a better understanding of the basic biological features of these progenitor cells as well as the niche interaction will help to advance clinical technique and treatment, leading to better caring for patients. Therefore, we hypothesized that microRNAs can regulate corneal epithelial progenitor cells and modulate the homeostasis of corneal epithelium. Our previous study has confirmed two microRNAs (miR-143 and 145) were significantly highly expressed in the limbal epithelium compared to the central corneal epithelium. The functional analysis showed that these two microRNAs were related to CEPC differentiation. My study continued to investigate the microRNA expression pattern in LPC and CC epithelia, to confirm the expression level of all 18 microRNAs detected by the microRNA microarray comparison analysis, and explored the potential functions of the confirmed microRNAs in corneal epithelium by using a series of bioinformatics analysis. With the correlation and the reported markers for CEPCs and key regulators for corneal epithelium, a regulatory network between microRNAs, proteins and core pathway has been drawn. We therefore confirmed the microRNA expression pattern in corneal epithelium and characterized the interactions between microRNAs and corneal epithelium-associated proteins.

## 2.2 Identification of microRNA expression in pterygium

Pterygium is an ocular surface disease that is characterized by corneal conjuntivalization. It is caused by the damage of CEPCs in the limbal epithelium. A number of proteins including tumor suppressors, growth factors and receptors, as well cell matrix molecules were related to the pathogeneses of pterygium. However, the expression and functions of microRNA in pterygium remains unknown. Pterygium is a tumor like tissue with high recurrent rate, abnormal expression of p53, and ability of invasion. Since normal stem cell and tumor cells share the similar ability of self-renewal and differentiation, many pathways that are associated with stem cells may also regulate cancer development, such as Wnt, Notch MAPK signaling. For example, haematopoietic stem cells have shown the possibility to undergo leukaemic transformation. The progenitor cells with restricted differentiation ability are also the target of transforming mutation and causes dysregulated self-renewal (Reya, Morrison, Clarke, & Weissman, 2001). However, the mechanism of transformation from stem cells to cancer cells is not fully revealed. In this study, we hypnotized the pathological CEPCs in pterygium gain of some tumor cell features such as over-proliferation, invasion and ECM remodeling, used it as a novel model for investigating the epigenetic regulation in transformation between progenitor cells and solid tumor cells. Therefore, we aim to examine if there exists any aberrant expression in pterygium by detecting the expression level of limbal-specific microRNAs in pterygium when compared with normal LPC epithelium and normal conjunctiva.

## 2.3 Investigation of the functions of microRNA in pterygium

In tumorigenesis, microRNAs have been proven to function as both tumor suppressor and activator. Pterygium is known to display similar features as tumor such as its recurrence and hyperplasticity, the function of microRNAs in pterygium may also be similar as those expressing in tumors. Once the limbal barrier is disrupted, microRNAs may function as an activator to enhance cell migration and proliferation, or as a suppressor to inhibit cell growth. The investigation of microRNA function in pterygium may better demonstrate the molecular regulation of microRNAs and protein in the pathogenesis of pterygium, subsequently may be recruited as a potential therapeutic target in the treatment of pterygium. With the aim of exploring the regulatory functions of microRNA in pterygium, we correlated microRNA expression pattern with pterygium-associated proteins and identified the target genes of the microRNAs in pterygial cells, to investigate the possible mechanism of pterygium progression.

# Chapter 3 Materials and Methodology

## 3.1 MicroRNA expression in adult human corneas and pterygium

### 3.1.1 Human cornea and pterygium specimen collection

The human corneas and pterygium samples were originated from the Chinese population. The research followed the principle of the Declaration of Helsinki, which was approved by the Ethics Committee on Human Research of the Chinese University of Hong Kong. Human corneal rims were collected from ShenZhen Eye Hospital and Hong Kong Lions Eye Bank. The corneal rims were preserved in Optisol-GS medium (Bausch and Lomb, Irvine, CA, U.S.A.) after transplantation surgery and transferred to the laboratory immediately. The donor information was listed in **Table 3.1**. Pterygium was collected from Prince of Wales hospital. Surgery removed pterygium was preserved in ice cold 1x PBS and transferred immediately to the lab. The patient information was listed in **Table 3.2**

### 3.1.2 Human cornea and pterygium sample preparation.

The corneal rim was rinsed with sterile 1x PBS (0.01 M, Invitrogen) three times. The ciliary body and endothelium of cornea were removed by gentle scrapping with a surgical blade. The corneal rims were cut into small pieces 50 x 50 mm2 with a surgical blade. The conjunctiva was isolated and preserved in Trizol reagent (Invitrogen) for RNA extraction. The small pieces of corneal rim were then separated into limbal peripheral corneal (LPC) epithelium and central corneal (CC) epithelium. With the removal of the stoma, samples were stored in Trizol® reagent (Invitrogen) at -80 $^{o}$C until RNA extraction.

Pterygium was rinsed with sterile 1x PBS twice to remove the blood the surface of pterygium. For RNA extraction, pterygium was lysed in 200 ul to 300 ul Trizol® reagent (Invitrogen) and stored at -80 $^{o}$C. For cryosection, the pterygium was slightly unfolded by blade scraping under dissection microscopy and was adjusted to correct orientation for embedding.

**Cryosection**

The small piece of corneal rim and full-length of pterygium were embedded in optimal cutting temperature (OCT) tissue freezing medium (Tissue-Tek) and quickly cooled down in liquid nitrogen. Frozen blocking was stored at -80 $^{o}$C until sectioning. For proceeding cryosection, the frozen blocking was transferred to cryostat and equilibrated to the sectioning temperature at -20 $^{o}$C for at least 30 min. The samples were placed in appropriate orientation for slicing the sagittal plane containing both epithelium and stroma. The cryosections were sliced at 6 μm of thickness and picked up with Superfrost PLUS glass slides (Superfrost+, Thermo Scientific). The slides were air-dried at room temperature for at least 30 min and fixed with 4% PFA for 10 min, followed with PBS washing and stored at -20 $^{o}$C.

**Haematoxylin and Eosin Staining**

Slides with sections were stained in haematoxylin for 2 min at room temperature. The nucleus were then differentiated by immersing slides in acid alcohol for 30 secs, followed by the bluing up process using Scott's tap water for another 1 mins. The cytoplasm was further stained by eosin for 2 min. The slides were then washed and dehydrated in 50, 70, 80, 90 and 100 % alcohol, each for 5 min, and mounted with Fluoromount-G Mounting medium (Southern Biotech) and examined under light microscopy.

### 3.1.1.2 Laser capture micro-dissection

Frozen sections mounted on PEN-membrane glass slide (Leica 11505158) was fixed in ice-cold 75% ethanol, 100% ethanol and washed with DECP-$H_2O$ for 1 min. The slide was air-dried at room temperature for at least 40 min and stored in 50ml centrifuge tube with silica on the bottom. The tube was sealed and stored in -80 $^oC$ freezer until dissection. Micro-dissection was performed using Laser Microdissection Systems LMD7000 according to the standard protocol. Briefly, membrane slides with sections were placed in the holder of microscopy. The eppendorff tubes with 20 ul Trizol® reagent (Invitrogen) on the cap were set up to the collector tray. The real-time captured image was displayed in the software. After customizing the device and adjusting the focus to appropriate magnification, the section of interest was defined by drawing the lines. Laser beam was steered by optics along the cut line (laser power: 19-25uJ, pulse frequency: 200-300 HZ, wavelength: 1nm-3nm). The detached specimen was dropped to the cap of eppendorff tubes by gravity and lysed in Trizol® reagent.

### 3.1.1.3 RNA extraction from tissue

Freshly collected tissues were rinsed briefly with 1x PBS and added 1 mL Trizol® reagent (Invitrogen) per 50-100 mg for RNA isolation. The tissues were homogenized by pipetting up and down until fully lysed. The homogenized samples were incubated for 5 mins at room temperature. Added 140 mL chloroform per 700 ml homoegenate. The mixture was shaken vigorously for 15 seconds and incubated for 3 mins for phase separation. The samples were then centrifuged for 15 min at 12,000 x g at 4°C. The upper aqueous phase was collected and transferred to a new collection tube. Added absolute ethanol (1.5x volume) to the tube and mixed thoroughly. miRNeasy kit (QIAGEN) was used to purify the total RNA including microRNA, according to the purification protocol.

Briefly, samples were transferred into RNAeasy Mini spin column, centrifuged at ≥8000 x g (≥10,000 rpm) for 15 s at room temperature. 700 ul buffer RWT was added to the column and centrifuged at ≥8000 x g for 15 s. The column was washed twice with 500 ul buffer RPE and centrifuged at ≥8000. RNase free water was added into the column to elute the RNA. RNA concentration was measured by absorbance (A260/A280) using the NanoDrop Spectrophotometer ND-1000 (NanoDrop).

### 3.1.2 MicroRNA profiling and GeneSpring analysis

#### 3.1.2.1 MicroRNA expression profiling

100 ng RNA was dephosphorylated and labeled by microRNA Complete Labeling and Hyb Kit (Agilent) according to the manufacturer's instructions. The dried and labeled microRNA sample was re-suspended in 18 ul nuclease-free water, 4.5 ul 10X GE Blocking Agent (Agilent) and 22.5 ul 2X Hi-RPM hybridization buffer (Agilent), followed by heating at 100°C for 5 mins. Upon cooling in ice water bath for 5 min, the mixture was hybridized to Human microRNA Microarray V2 which screened for the expression of 723 human microRNAs (Sanger database v.10.1) for 20 hours at 55°C in a rotating Agilent hybridization oven. After hybridization, microarrays were washed 5 mins at room temperature with GE Wash Buffer 1 (Agilent) and 5 min with 37°C GE Wash buffer 2 (Agilent). Slides were scanned immediately after washing on the Agilent DNA Microarray Scanner (G2505B) using one color scan setting for 8x15k array slides (Scan Area 61x21.6 mm, Scan resolution 5um, Dye channel is set to Green and Green PMT is set to 100%). The scanned images were analyzed with Feature Extraction Software 9.5.3.1 (Agilent) using default parameters (protocol miRNA-v1_95_May07 and Grid: 016436_F_D_20091031) to obtain background subtracted and spatially detrended Processed Signal intensities. Features flagged in Feature Extraction as Feature Non-uniform outliers were excluded.

#### 3.1.2.2 Data normalization and analysis

The scanned images were analyzed with Feature Extraction Software 9.5.3.1 (Agilent) using default parameters to obtain background subtracted and spatially de-trended Processed Signal intensities. The processed data were imported to GeneSpring GX 11.5 (Agilent) for further analysis. The data normalization was followed GeneSpring software standard procedure, briefly, the data set were transformed by log2 and summarized the repeated spots with cutting -off the measurements less than 0.01, the expression intensity was normalized to 75th percentile to standardize each chip and each gene for cross – array comparison. Differentially expressed microRNAs or genes were identified using unpaired Student's t test with P-values cut-off by 0.01 and fold change more than 2.0.

### 3.1.3 Validations of microRNA expression on corneal epithelium

#### 3.1.3.1 Taqman® microRNA assay

Total RNA was reverse transcribed to cDNA using TaqMan® MicroRNA Reverse Transcription Kit (Applied Biosystems, Foster City, CA, USA). In brief, 10 ug total RNA was reverse transcribed by miR-specific primer with a tail sequence recognized by the universal primer. The reaction cocktail contained 5x reverse transcription buffer, 100nMdNTP mix, recombinant RNase inhibitor, Multiscribe reverse transcriptase, 5xTaqman microRNA specific primer and RNA sample. The reaction was at 16°C for 30 mins, at 42°C for 30 mins and at 85°C for 5 mins. The product of RT reaction was diluted 1:3 (vol:vol) with RNANase-free water and amplified by Taqman Real-time microRNA assay using Taqman 2X Universal PCR Master Mix and MicroRNA Assay Primers on PRISM 7900HT Sequence Detection System (Applied Biosystems) following the manufacturer's protocol. Briefly, a reaction cocktail containing 0.25µl 20x TaqMan

microRNA assay, 1.4 µl diluted cDNA, 2.5µl TaqMan 2x Universal PCR Master Mix and nuclease-free water (0.85 µl) was incubated in the following conditions: 10 min at 95°C, 40 cycles each of 15 s at 95°C and 1 min at 60°C. Real-time PCR reactions were performed at least duplicate and were assayed in an optical 96-well plates using ABI PRISM® 7900HT Sequence Detection System (ABI). The fluorescence signal was converted into numerical values by SDS 2.1 software (Applied Biosystems). The relative quantification was performed utilizing the comparative Ct method ($\mathbf{2}^{(\Delta Ct\ miR\ LPC-\ \Delta Ct\ miR\ CC)}$) after normalization with housekeeping U6. The statistically significant difference was determined using non-parametric paired Student's t-test with p value < 0.5 considered to be significant.

### 3.1.3.2 LNA-based microRNA in situ hybridization

Cryosections (6 µm thick) of tissue were fixed in 4% neutral-buffered paraformaldehyde (Sigma), and washed in diethyldicarbonate (DEPC)-treated PBS. The samples were acetylated with 0.6% acetic anhydride (Sigma-Aldrich), 1.34% triethanolamine (Sigma-Aldrich), 60 mM HCl. (Riedel) for 10 mins and then treated with 5 ug/ml proteinase K (Sigma, St Louis, MI) at 37 °C for another 10 min, followed with DEPC-treated PBS washing for three times. The slides were placed horizontally in the hybridization chamber and pre-hybridized at hybridization temperature (55 °C) for 2 hours in hybridization solution containing 50% formamide (Riedel), 5x SSC, 200 µg/mL yeast tRNA (Sigma-Aldrich), 1x Denhardt's solution (Sigma-Aldrich), 500 µg/mL salmon sperm DNA (Sigma-Aldrich) and 0.4g Roche blocking reagent (Roche). Locked nucleic acid-based miRCURY LNA™ Detection probes, 5' digoxigenin (DIG) labeled (Exiqon, Vedbæk,Denmark) used in our study were listed in **Table 3.3**. Prior hybridization, added 0.1 ul probes per 100ul denaturing hybridization solution containing 50% formamide (Riedel), 5x SSC, 200 µg/mL yeast tRNA (Sigma-Aldrich), 1x Denhardt's solution (Sigma-Aldrich),

500 µg/mL salmon sperm DNA (Sigma-Aldrich), 0.4 g Roche blocking reagent (Roche) 10% CHAPS (Sigma-Aldrich) and 20% Tween (Fluka) at final concentration 1 pmol and denatured at 80 °C for 5 min. After pre-hybridization, the sections were incubated with denaturing hybridization solution containing specific microRNAs or scrambled probes (3 pmol) and hybridized overnight at 55 °C. The slides and hybridization chamber were sealed with Parafilm® to maintain their humidity. After post-hybridization, the slides were placed in 5x SSC to remove the parafilm® and then washed in 0.2x SSC at 55°C for 1 hour. Next, 100ul blocking solution (0.1 M Tris pH 7.5, 0.15 M NaCl, 10% FBS) was added to each section and incubated for 1 hour at room temperature. The probe localization was detected by anti-DIG-alkaline phosphatase conjugate antibody (Roche, Basel, Switzerland) with 1:1000 dilution and incubated overnight at 4 °C. The slides were washed three times for 5 mins in B1 solution (0.1 M Tris pH 7.5, 0.15 M NaCl) at room temperature. Followed by the development reaction with nitroblue tetrazolium/ 5-bromo-4-chloro-3-indolyl phosphate (NBT/BCIP, Roche) or Fast Red Tablet (Roche 11496549001). For NBT/BCIP detection of hybridization signals, 100 mg/ml NBT (Roche, 1383213) and 50 mg/ml, BCIP (Roche, cat no. 1383221), 24 mg/ml levamisol and 10% Tween 20 were diluted in developer solution (0.1 M Tris pH 9.5, 0.1 M NaCl, and 50 mM $MgCl_2$). Slides were placed in a humidified chamber and 150 ul developer NBT/BCIP developer solution was added for each slides, developed at room temperature in the dark for 1-4 days. The slides were washed in PBST (1 x PBS, 1% Tween 20), followed by counterstaining with nuclear fast red (Sigma-Aldrich). The slides were mounted by Fluoromount-G Mounting medium (Southern Biotech) and examined under light microscopy (DMRB, Leica, Vertrieb, Germany). For Fast Red reaction, one Fast Red tablet was dissolved in 2 ml 0.1M Tris–HCl, pH 8.2 and shaken for 1 to 3 mins. 100 ul solution was added for one section and developed at room temperature in

the dark for 30 mins to 5 hours. The slides were mounted by Fluoromount-G Mounting medium (Southern Biotech) and examined under fluorescence microscopy Cy3 tunnel.

For double staining in conjunction with detection of proteins, after anti-DIG-AP antibody incubation the slides were washed three times with B1 solution (0.1 M Tris pH 7.5, 0.15 M NaCl). Primary antibody was added in blocking solution and incubated for 2 hours at room temperature. The slides were washed three times and incubated for another 2 hours at room temperature in the dark with an appropriate green fluorescent secondary antibody Alexa 488 (mouse, rabbit or goat) diluted 1:500 in blocking solution. The slides were mounted by Fluoromount-G Mounting medium (Southern Biotech) and examined under fluorescence microscopy.

## 3.2 MicroRNA bioinformatics analyses

### 3.2.1 Corneal epithelial gene correlation assay

Significantly expressed microRNAs were subject to TargetScan Human 6.0 (http://www.targetscan.org (Garcia et al., 2011)), miRDB (http://mirdb.org/miRDB) and PicTar (http://pictar.mdc-berlin.de) algorithms to identify potential target genes. The gene list was cross-matched with the corneal epithelial gene expression profile GSE-5543 deposited in NCBI Gene Expression Omnibus 23. Differentially expressed genes regulated by candidate microRNAs were imported to DAVID Functional Annotation Bioinformatics Microarray Analysis v6.7 (http://david.abcc.ncifcrf.gov) provided in the public domain by National Institute of Allergy and Infectious Disease (NIAID, NIH). We examined the functional gene clusters of the differentially expressed genes and/or to identify biological and molecular events that were regulated by these genes in corneal epithelium. The

likelihood of event presentation in the Gene Ontology Consortium annotation categories (GO biological process, GO cell component, GO molecular functions) was examined.

### 3.2.2 Gene pathway analysis

The predicted gene targets of microRNA candidates were inputted to web-based DIANA LAB (DNA Intelligent Analysis) DIANA-mirPath (http://diana.cslab.ece.ntua.gr/pathways) (Papadopoulos, Alexiou, Maragkakis, Reczko, & Hatzigeorgiou, 2009)) for microRNA target gene pathway analysis. Enrichment analysis of multiple microRNA targets was done by comparing each set of microRNA targets to all known KEGG pathways database. Pathway significance was calculated by Fisher's Exact test. Enrichment analysis on individual microRNA predicted targets were executed and ranked by enrichment score.

### 3.2.3 Gene-microRNA interaction

The association of validated microRNAs and targets or functions was examined by Ingenuity Pathway Analysis®-microRNA analysis (Ingenuity Systems, Mountain View, CA, USA; http://www.ingenuity.com ) using the Ingenuity® Knowledge Base, a database derived from known functions and interactions of genes published from literature. Direct and indirect suppression and activation was presented in network graphics integrating and interconnecting the functional annotations between genes, proteins and microRNAs.

## 3.3 Functional regulation of microRNAs

### 3.3.1 Culture of primary pterygium-derived cells

Freshly collected primary pterygium was rinsed twice with sterile PBS followed with removal of blood vessel by a surgical blade. The full-length pterygium was dissected into head and body parts according to the sharp, and each was incubated separately in 50 ug/ml dispase II (Invitrogen) and 100 mM D-sorbitol (Sigma) in DMEM/F12 medium (Invitrogen) for 60 min at 37°C. The loosened epithelium was further dissociated into single cells by 0.15% trypsin for 5 min at 37°C. Single cells were cultured in DMEM/F12 medium supplemented with 10% heat-denatured fetal bovine serum (Invitrogen) and antibiotics (penicillin–streptomycin, Invitrogen) for 21 days with fresh medium replenished every 3 days.

### 3.3.2 The structure and expansion of lentivector - based microRNA precursor constructs

MicroRNA precursor constructs pMIR-143 and pMIRNA-145 and scrambled negative control synthesized by system biosciences (SBI, CA, USA) were used in our study. The microRNA precursor sequences from microRNA database Sanger's miRBase (http://www.mirbase.org) were inserted into SBI's microRNA Precursor Constructs. Each construct consisted of the stem loop structure and 300-500 base pairs of upstream and downstream flanking genomic sequence, which ensured the microRNAs expressed from SBI's Clones act as naturally as possible. The microRNA precursor molecules were cloned in a lentiviral-based vector as a ready-to-infect lentiviral plasmid. The structure pMIRNA vector (Figure 3.1) contained CMV-driven transcript, ampicillin resistance gene, copGFP,

SV40 origin, SV40 polyadenylation, genetic elements (cPPT, GAG, LTRs) pUC origin and ampicillin resistance gene.

1ul of microRNA precursor constructs was mixed with 25 ul E.coli competent cells (DH5α™, Invitrogen) and incubated on ice for 30 mins, followed by heat shocked at 45 $^{o}$C for 45 sec, then quickly placed on ice for another 2 mins. SOC medium (Invitrogen) was added and incubated at 37 $^{o}$C for 30 mins with vigorous shaking at 250 rpm. The bacterial suspension was plated on ampicillin (100ug/ml, Invitrogen) supplemented LB Agar plates (Invitrogen) and incubated at 37 $^{o}$C overnight. The bacterial clones from LB Agar plates were picked and resuspended in 4 ml LB broth (Invitrogen) containing ampicillin, and incubated at 37 $^{o}$C for 6-8 hours with sharking. Plasmid DNA was extracted using QIAGEN Plasmid mini Kit (QIAGEN) according to the standard protocol. Briefly, Bacteria cells were harvested by centrifugation at 6000x g for 15 mins at 4 $^{o}$C. Pellet was resuspended in 4 ml Buffer P1 supplemented with RNase A, then added with 4 ml Buffer P2. After incubation at room temperature for 5 mins, 4 ml Buffer P3 was mixed up to the solution. The mixture was poured in to the barrel of QIAfilter Cartridge (QIAGEN) and incubated at room temperature for 10 mins, with removal of the precipitate floating on the top. The plunger was then inserted in QIAfilter Cartridge to filter plasmid DNA solution. The plasmid DNA was bound to the pre-equilibrated QIAGEN-tip 100 and washed with 10 ml Bufer QC, followed by adding 5 ml Buffer QF to elute the plasmid DNA. The plasmid DNA was precipitated with 3.5 ml isopropanol and centrifuged at 13000 rpm, 4 $^{o}$C for 30 mins and then washed with 70% ethanol. The DNA pellet was air-dried for 5-10 mins and then re-dissolved in DECP-water. The plasmid DNA concentration was measured by absorbance (A260) using the NanoDrop Spectrophotometer ND-1000.

### 3.3.3 Chemical transfection

SBI's microRNA precursor vectors with pre-mir-143 and pre-mir-145 sequence were used for microRNA overexpression and vector with scrambled sequence was used as negative control. Transfection efficiency was determined by the ratio of DNA plamid and lipofectamin. The optimization of transfection ratio was performed to obtain best the best transfection efficiency and minimum cell death caused by lipofectamine®. Cos7 cells were seeded at 1x $10^5$ in 6-well plate, each well was transfected with 4 ug DNA construct and 6 ul lipofectamine® (2:3), 2 ug DNA construct with 6 ul lipofectamine® (1:3) and 3 ug DNA construct with 6 ul lipofectamine® (1:2), respectively. After 48 hours of incubation, the green fluorescence conjugated with pre-microRNA construct was detected under phase contrast microscopy with fluorescence filter. As shown in Figure 3.2, the cells expressed green fluoresce indicating that the DNA construct was successfully integrated into the genomic DNA of the cells and correctly translated. The transfected ratio at 2:3 showed the highest transfection efficiency.

Primary cultured pterygial cells were seeded in 6-well plate (Corning Life Sciences, Lowell, MA) one day before transfection.4 ug of microRNA precursor constructs or scrambled control was mixed with 6 ul transfection reagent (Lipofectamine®2000, Invitrogen) in 500 ul Opti-MEM I Reduced Serum Media (Life technologies) and incubated for 15 mins at room temperature. The cells were washed with pre-warmed 1xPBS for 2 times and added 500 ul Opti-MEM I Reduced Serum Media for each well. The mixture of microRNA constructs and lipofectamine® was added to the cells and incubated for 24 hours. 1 to 2 ml culture medium was added to the cells and further intubate for 24 hours. 48 hours after transfection, the cells were harvest for subsequent experiments. The microRNA overexpression level was detected by TaqMan® real-time PCR.

## 3.4 Characterization of microRNA over-expressing cells

### 3.4.1 Immunochemistry

Sections on slides were post-fixed in 4% paraformaldehyde, rinsed with PBS and placed in ice-cold freshly prepared 50 mM ammonium chloride (Sigma) in PBS at -20 $^{o}$C for 10 min to quench free aldehyde and retrieve antigens. Samples were blocked in 1% bovine serum albumin (BSA, fraction V, Sigma), 0.15% saponin (Sigma) and 0.01% Triton X-100 in PBS for 20 mins. They were placed in primary antibodies diluted in PBS added with 1% BSA, 0.425% saponin, 0.0015% Triton X-100 and Tween 20 (Sigma) for 2 hrs at room temperature or 4 $^{o}$C overnight. After PBS washes, appropriate fluorescein (Alexa 488 or RedX)-conjugated secondary IgG antibody and 4', 6'-diamidino-2-phenyindole (DAPI) diluted in PBS containing 1% BSA were added for an hour at room temperature, followed by PBS washes. Sections without primary antibody incubation were the negative controls. The sections were mounted in Fluormount-G (Sigma) for examination under fluorescence microscopy.

### 3.4.2 Western blotting

Cell lysate was prepared using RIPA Buffer with protease inhibitors and quantified using protein assay. Protein (20 μg) was loaded onto a 10% SDS–PAGE gel then transferred onto nitrocellulose and incubated with mouse monoclonal antibody at 4 °C overnight in blocker (1% non-fat dry milk in TTBS), followed by incubation with HRP-conjugated secondary anti mouse. Blots were then developed using ECL Substrate (Amersham) following manufacturer's instructions. HRP-conjugated GAPDH was incubated further for normalization. The blots were again developed using ECL substrate.

### 3.4.3 Cell cycle analysis and fluorescence activated cell sorting

The cells were harvested 48 hours after transfection, and washed twice with ice-cold 1x PBS. The cell pellets were re-suspended and fixed in ice-cold 75 % ethanol in 1.7 ml Eppendorf tube and stored in -20 $^{o}$C. On the day of experiment, 75 % ethanol was removed by centrifuge and the cells were washed twice with ice-cold PBS. For cell cycle analysis, propidium iodide (50 µg/ml) and RNase A (0.1 mg/mL) diluted in cold PBS were added to the cells and incubated with 1 hour at room temperature. Excess staining was removed by centrifugation at 1500 rpm for 5 min. The cells were resuspended in 500 µl PBS for flow cytometric analysis using BD FACS Caliber (LSR Fortessa flow cytometer; BD Biosciences). Data were analyzed using FACSDiva$^{TM}$ software (BD Biosciences). The data was normalized with the total number in order to calculate the percentage. For cell sorting, after fixation, the cells were washed twice with ice-cold PBS and incubated in rabbit anti-p53 CM1 antibody and mouse anti-MDM2 antibody individually at 1:100 dilution for 2 hrs at room temperature. After removal of the primary antibody, appropriated secondary antibody (Alexa Fluro 488 rabbit IgG or Rhodamin Red-X anti –mouse IgG) were added to the cells and incubated for 1 hour at room temperature. The stained cells were analyzed by flow cytometer BD FACS Caliber (LSR Fortessa flow cytometer; BD Biosciences). Data were analyzed using FACSDiva$^{TM}$ software (BD Biosciences).

### 3.4.4 Reverse transcription and quantitative real-time PCR analysis

Total RNA extracted from cells was reverse transcribed to cDNA by using PrimeScript First Strand cDNA Synthesis Kit (TaKaRa) following the manufacturer's protocol. Briefly, a cocktail containing 200 ng of template RNA, 1 ul dNTP (10mM), and1 ul random 6 mer (50 µM) were mixed up to total volume of 10 µl by RNase-free water. The mixture was heated to 65 $^{o}$C for 5 mins and then was cooled immediately on ice for at least 1 min. 4µl 5x

PrimeScript Buffer, 0.5 µl RNase Inhibitor (40U/µl) and 1µl PrimerScript RTase and RNase-free water were added to the mixture for total volume of 20 µl. The mixture was assayed in thermal cycler at 30 °C for 10 min, 42°C for 60 min, 70°C for 15 min and stores the cDNA at -20 °C. cDNA products were then quantitated by real-time PCR using Roche FastStart Universal SYBR Green on Roche LightCycler® 480 Real-Time PCR System according to the manufacturer's protocol. Briefly, a reaction cocktail containing 5µl FastStart Universal SYBR Green, 0.5 µl forward primer (10 nM), 0.5 µl reverse primer (10 nM), 2 ul cDNA and nuclease-free water mixed up for a total volume of 10 µl. PCR reactions was performed at least triplicate and quantified using Roche LightCycler® 480 Real-Time PCR System. The relative quantification was performed utilizing the comparative Ct method after normalization with housekeeping GAPDH.

**Table 3.1 Information of cornea donors**

| Donor code | Sex/Age | Eye | Cause of death | Days from harvest to tissue processing |
|---|---|---|---|---|
| SZ52 | F/52y | OD | Traffic accident | 7 |
| SZ55 | M/50y | OD | Primary pulmonary hypertension | 7 |
| SZ59 | M/37y | OS | Traffic accident | 5 |
| SZ64 | F/68y | OS | Heart disease | 5 |
| SZ65 | F/68y | OD | Heart disease | 5 |
| SZ66 | M/60y | OS | Heart disease | 4 |
| SZ67 | M/60y | OD | Heart disease | 6 |
| SZ70 | M/28y | OS | Traffic accident | 3 |
| SZ71 | M/28y | OD | Traffic accident | 4 |

**Table 3.2 The sex and age of pterygium patients.**

| Patient code | Sex / age | Type | |
|---|---|---|---|
| PT40 | M/66y | Right pterygium | RNA |
| PT41 | F/60y | Left pterygium | RNA |
| PT42 | F/64y | | RNA |
| PT44 | F/65y | | RNA |
| PT45 | F/45y | | RNA |
| PT48 | F/74y | | RNA |
| PT50 | M/80y | | RNA |
| PT51 | F/67y | Right pterygium | RNA |
| PT53 | M/48y | | Cytosection |
| PT56 | M/58y | Left pterygium | Primary culture |
| PT57 | F/62y | Right pterygium | Primary culture |
| PT58 | F/70y | Right pterygium | Primary culture |
| PT59 | M/75y | Left pterygium | Primary culture |
| PT62 | F/54y | | LCM |
| PT63 | F/68y | | LCM |
| PT64 | F/84y | | Cytosection |
| PT66 | F/54y | Right pterygium | Cytosection |

**Table 3.3 The sequence of TaqMan® MicroRNA Assays used in this study.**

| Assay Name | ABI Assay ID | Mature microRNA Sequence |
|---|---|---|
| hsa-miR-126 | 002228 | UCGUACCGUGAGUAAUAAUGCG |
| hsa-miR-142-3p | 000464 | UGUAGUGUUUCCUACUUUAUGGA |
| hsa-miR-142-5p | 002248 | CAUAAAGUAGAAAGCACUACU |
| hsa-miR-143 | 002249 | UGAGAUGAAGCACUGUAGCUC |
| hsa-miR-145 | 000467 | GUCCAGUUUUCCCAGGAAUCCCU |
| hsa-miR-146a | 000468 | UGAGAACUGAAUUCCAUGGGUU |
| hsa-miR-149 | 002255 | UCUGGCUCCGUGUCUUCACUCCC |
| hsa-miR-155 | 002623 | UUAAUGCUAAUCGUGAUAGGGGU |
| hsa-miR-193b | 002367 | AACUGGCCCUCAAAGUCCCGCU |
| hsa-miR-211 | 000514 | UUCCCUUUGUCAUCCUUCGCCU |
| hsa-miR-377 | 000566 | AUCACACAAAGGCAACUUUUGU |
| hsa-miR-575 | 001617 | GAGCCAGUUGGACAGGAGC |
| hsa-miR-10b | 002218 | UACCCUGUAGAACCGAAUUUGUG |
| hsa-miR-338-3p | 002252 | UCCAGCAUCAGUGAUUUUGUUG |
| hsa-miR-184 | 000485 | UGGACGGAGAACUGAUAAGGGU |
| hsa-miR-139-5p | 002289 | UCUACAGUGCACGUGUCUCCAG |
| has-miR-127 | 000452 | UCGGAUCCGUCUGAGCUUGGCU |
| hsa-miR-376a | 000565 | AUCAUAGAGGAAAAUCCACGU |
| U6 snRNA | 001973 | GTGCTCGCTTCGGCAGCACATATACTAA<br>AATTGGAACGATACAGAGAAGATTAGC<br>ATGGCCCCTGCGCAAGGATGACACGCA<br>AATTCGTGAAGCGTTCCATATTTT |

**Table 3.4 5' digoxigenin (DIG) labeled miRCURY LNA™ Detection probes used in this study.**

| microRNA Probe | Product no. | Description | Tm | Sequences |
|---|---|---|---|---|
| hsa-miR-10b | 38850-01 | 5`-DIG labeled | 84 °C | ATTCCCCTAGAATCGA ATCTGT |
| hsa-miR-126 | 38024-01 | 5`-DIG labeled | 72 °C | CGCGTACCAAAAGTA ATAATG |
| hsa-miR-143 | 38887-01 | 5`-DIG labeled | 89 °C | ACCAGAGATGCAGCA CTGCACC |
| hsa-miR-145 | 38889-01 | 5`-DIG labeled | 83 °C | AGAACAGTATTTCCA GGAATCC |
| hsa-miR-155 | 38935-01 | 5`-DIG labeled | 78 °C | TGTTAATGCTAATATG TAGGAG |
| U6. hsa/mmu/rno | 99002-01 | Positive Control, 5`-DIG labeled | 84 °C | CACGAATTTGCGTGTC ATCCTT |
| Scramble-miR | 99004-01 | Negative Control, 5`-DIG labeled | 87 °C | GTGTAACACGTCTATA CGCCCA |

**Table 3.5 List of antibody used in this study**

| Antibody | Company | Cat No. | Source |
|---|---|---|---|
| IL-6 (H-183) pAb | Santa Cruz | | Rabbit |
| DIG-AP, Fab fragment | Roche | 1093274 | |
| p53-NCL-CM1, pAb | Novocastra | S1826 | Rabbit |
| MDM2 (SMP14), mAb | Santa Cruz | sc-965 | Mouse |
| Alexa Fluro 488 goat anti-rabbit IgG conjugate | Invitrogen | A11008 | |
| Rhodamin Red-X- goat anti –mouse IgG conjugate | Invitrogen | R6394 | |

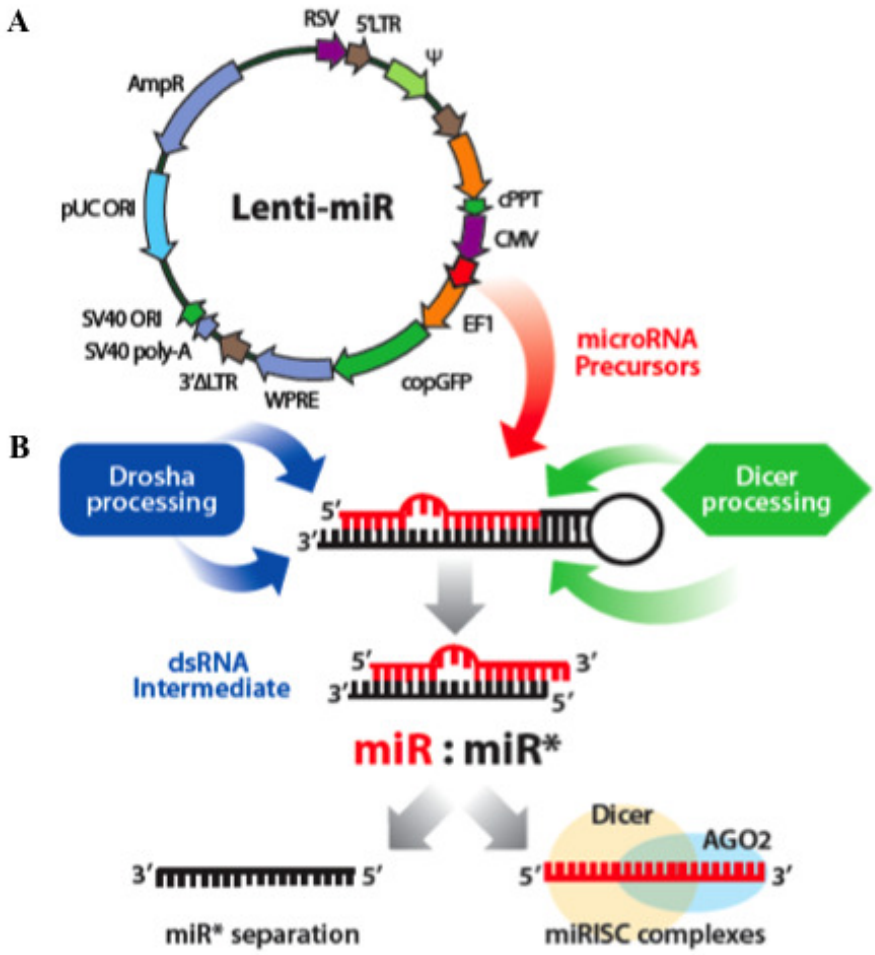


**Figure 3.1 The structure of pre-miR-microRNA vector and mechanism of microRNA overexpression.**

(A) The structure of pre-miR-microRNA vector: 1. SV40 polyadenylation signal enables efficient termination of transcription and processing of recombinant transcripts. 2. Hybrid RSV-5'LTR promoter provides a high level of expression of the full-length viral transcript. 3. Genetic elements (cPPT, GAG, LTRs) were necessary for stably integrating the viral expression construct into genomic DNA. 4. SV40 origin is for stable propagation of the pMIRNA1 plasmid in mammalian cells. 5. pUC origin for high copy replication and maintenance of the plasmid in E.coli cells. 6. Ampicillin resistance gene for selection in

E.coli cells. 7. copGFP fluorescent marker to visualize transfection efficiency. (B) The microRNAs expressed from SBI's constructs were correctly processed in the cell into mature microRNAs through interaction with endogenous RNA processing machinery and regulatory partners, leading to properly cleaved microRNAs, which ensured the mature microRNAs act as naturally as possible.

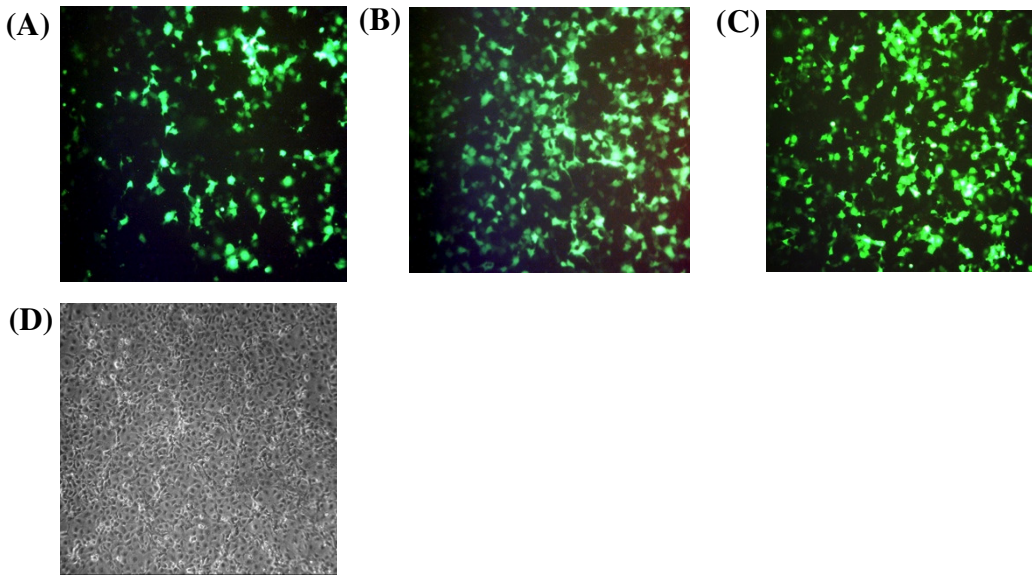


**Figure 3.2 Transfection efficiency of scrambled control construct with expression of GFP.**

Cos7 cells were transfected with pre-miR-scrambled construct, 48 hours after transfection, the GFP was detected under fluorescence microscopy. The transfection efficiency was shown by the expression of GFP in the cells with different ratio of DNA plasma / transfection reagent: (A) 2 ug DNA plasma in 6 ul transfection reagent (1:3); (B) 3 ug DNA plasma in 6 ul transfection reagent (1:2); (C) 4 ug DNA plasma in 6 ul transfection reagent (2:3). (D) The transfected cells under phase contrast microscopy.

**Table 3.6 List of primers used in polymerase chain reaction**

| Gene | Orientation | Sequence | Tm | Product (bp) |
|---|---|---|---|---|
| MDM2 | Forward | CATTGTCCATGGCAAAACAG | 56 $^{o}$C | 80 |
| | Reverse | GGCAGGGCTTATTCCTTTTC | 56 $^{o}$C | 80 |
| GAPDH | Forward | GAAGGTGAAGGTCGGAGT | 57 $^{o}$C | 226 |
| | Reverse | GAAGATGGTGATGGGATTTC | 57 $^{o}$C | 226 |

# Chapter 4 Results

## 4.1 MicroRNA microarray and GeneSpring analysis

### 4.1.1 Identification of human corneal CC and LPC epithelia

To isolate and enrich the CEPC cell population for microRNA analysis, our previous study compared the reported protocols including single cell isolation and colony-formation, florescence activated cell sorting (FACS) with CEPC markers, laser capture microdissection (LCM), and manual microdissection. Corneal cell isolation might change the CEPC phenotype under culture condition. Using cell sorting and LCM, the RNA yield was too low such that it was not sufficient for microRNA expression analysis. Moreover, the longtime of manipulation in cell sorting and LCM could cause nucleic acid degeneration and contamination, which might lead to a false result in microRNA identification. Therefore, manual microdissection was used for preserving the natural nucleic acid profile. The fresh human corneal rims were separated into central corneal and limbo-peripheral corneal (LPC) epithelia after removing stroma. We cut LPC epithelia from the side closed to conjunctiva, and kept 1 mm distance to isolate CC epithelia. CEPC putative markers ABCG2 and P63 were used to identify the cell population of the corneal CC and LPC epithelia using real-time PCR and western blotting. The result showed that LPC epithelium solely expressed ABCG2 and contained higher P63 protein than CC epithelia (**Figure 4.1**). Therefore, although LPC epithelia were not homogenous CEPC population, it was highly enriched with CEPCs compared to CC epithelia.

### 4.1.2 MicroRNA profiling in human corneal epithelium

To identify the microRNA expression profile in human corneal epithelium, we performed a global screening of microRNA expression on human CC and LPC epithelia using Agilent® microRNA microarray platform V2. The sample quality was evaluated by keratinocyte-specific microRNA miR-205 which was has been found to be expressed by mouse corneal, limbal and conjunctival epithelia. With miR-205 as criteria, 4 of 6 pairs human CC and LPC epithelia were selected based on constitutive expression of miR-205 for further analysis. (**Table 4.1**)

By cluster analysis that classified the entities with similar expression intensity as one cluster, we found thirty-seven microRNAs were enriched in human corneal epithelia (including LPC and CC regions) with mean normalized signal greater than 4.0 (**Figure 4.2 & Table 4.2**). Ranking the gTotal gene signal (representing the actual hybridization signal to the chip), miR-184 was the highest microRNA (mean gTotal gene signal = 5161.7) expressed in corneal epithelium, which was about 3 folds more than the second enriched microRNA (miR-638: mean gTotal gene signal = 1828.4), followed with miR-768-5p (mean gTotal gene signal = 544.4). The most abundant microRNA family was let-7 family (let-7a = 80.1; let-7b = 518.7; let-7c = 81.6; let-7e = 63.3; let7f = 14.7). The next were miR-125 (miR-125a = 26.7 & miR-125b=57.5) and miR-29 families (miR-29a = 34.7; miR-29c = 18.0). The miR-23b/24/27b cluster was also highly expressed (miR-23b = 86.2; miR-24 = 392.5; miR-27b = 7.2). To investigate the potential roles of these microRNAs in corneal epithelium, we compared the microRNAs list with previously reported microRNA expression pattern for mouse corneal epithelium, mouse retina, human retinal pigment epithelia and skin keratinocytes (**Table 4.2**). Among these enriched microRNAs, 15 were conserved to express in mouse corneal epithelium, namely let-7b & f, 23a, 27a, 29a, 125a & b, 130a, 184, 200c, 205, 320 and 23b/24/27b cluster. Besides, 9 microRNAs were also

conserved in adult mouse retina (let-7b, 24, 92, 184, 130a, 193b, 200c, 205 and 320). Taken together with the reported microRNAs in human retinal pigment epithelia, 6 microRNAs were found constitutively expressed in corneal epithelia and RPE, namely miR-24, 130a, 184, 205, 320 and let-7b. There were also 19 microRNAs expressed in both human corneal epithelium and skin epithelial keratinocytes (miR-22, 27a, 29a & c, 101, 125a & b, 130a, 193b, 195, 200c, 23b/24/27b cluster and let-7 family). miR-638, 768-5p, 572, 370, 768-3p, 663, 565 and 107 were solely enriched in human corneal epithelia, may be the result of miR-638, 768-5p, 572, 768-3p, 663 and 565 were relatively novel microRNAs that were not annotated at that time of these studies. Interestingly, human and mouse corneal epithelium, Human RPE and skin keratinocytes were all highly expressed miR-23b, 200c, 125a, 27a&b and let-7f, suggesting their potential roles in maintenance of epithelium phenotype. Notably, miR-24 and miR-130a were expressed in all the four sections.

### 4.1.3 MicroRNA profiling and expression in human LPC and CC epithelia

The raw hybridization signal intensity of microRNA Chip was normalized by GeneSpring GX v11.5 software. The repeated probes of each microRNA were summarized, all the raw values were log2 transformed to minimize the biological noise; the expression intensity were normalized to 75$^{th}$ percentile for data analysis. By cutting-off at 2-fold difference of normalized intensity ($log_2$ transformed) and $P$ value < 0.05 (unpaired Student's t-test), 18 microRNAs were identified to be differentially expressed between human LPC and CC epithelia. the normalized intensity was listed in **Table 4.4** and heat map represent each expression value was shown in **Figure 4.3**. 14 microRNAs (miR-10b, 126, 127, 139, 142-3p, 142-5p, 146a, 155, 211, 338, 376a, 377 and 143/145 cluster) were up-regulated in LPC, compared to CC samples (**Figure 4.3 and Table 4.3**). The highest up-regulated microRNAs in LPC epithelia were miR-143/145 (miR-143: fold change = 28.8; $P$

= 0.0006 and miR-145: fold change = 23.9; $P = 0.0003$), followed with miR-10b (mean fold change = 17; $P = 0.0127$), miR-126 (mean fold change = 19.1; $P = 0.025$) and miR-388 (mean fold change = 11.5; $P = 0.0132$). In contrast, 4 microRNAs were down-regulated in LPC epithelia **Table 4.3**). They were miR-184 (mean fold change = 4.9, $P = 0.00005$); miR-149 (mean fold change = 2.6, $P = 0.031$); miR-193b (mean fold change = 2.6; $P = 0.0024$) and miR-575 (mean fold change = 3.4; $P = 0.043$).

**(A)**

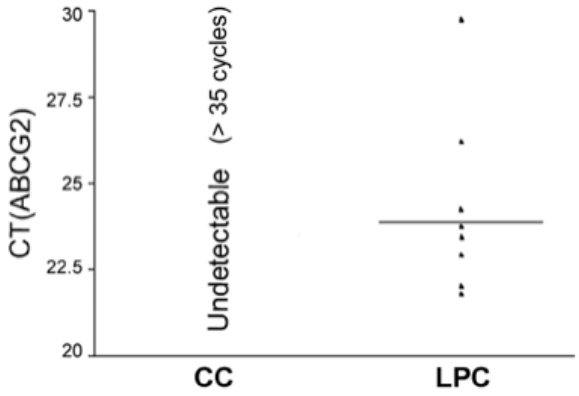


**(B)**

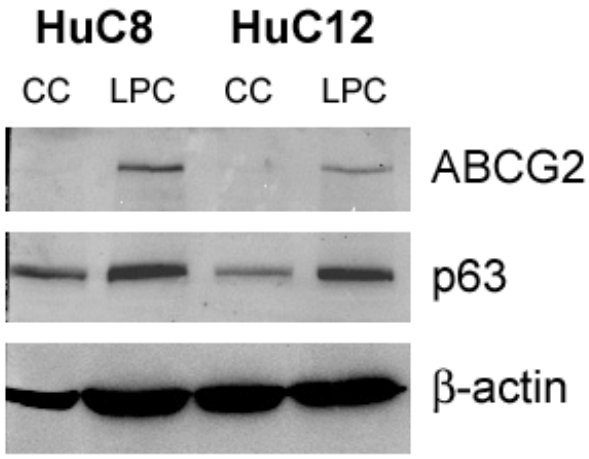


**Figure 4.1 Real-time PCR and western blotting identified the CEPCs enrichment in CC and LPC epithelia.**

The expression level of stem cell markers ABCG2 and P63 was examined in our samples. (A) Quantitative real-time PCR confirmed ABSCG was not detectable in CC epithelia (Ct value more than 35). (B) Western bolting identified ABCG2 and P63 were enriched in LPC epithelia.

**Table 4.1 The selection of CC and LPC samples based on miR-205 expression signal intensity for microarray analysis.**

| Sample code | Normalized intensity (log scale) | Raw intensity | Flag | Tissue |
|---|---|---|---|---|
| 3902C | 5.8111095 | 94.38289 | Present | Cornea |
| 3902L | 5.7720556 | 113.04199 | Present | Limbal |
| 3911C | 5.5232797 | 226.44197 | Present | Cornea |
| 3911L | 5.1286793 | 886.9467 | Present | Limbal |
| 3917C | 0 | 1 | Absent | Cornea |
| 3917L | 0 | 1 | Absent | Limbal |
| 3925C | 2.8497512 | 7.2087607 | Present | Cornea |
| 3925L | 0 | 1 | Absent | Limbal |
| 3933C | 7.0114965 | 5309.882 | Present | Cornea |
| 3933L | 8.749537 | 8564.524 | Present | Limbal |
| 3846C | 8.39562 | 8894.284 | Present | Cornea |
| 3846L | 6.469433 | 3269.6492 | Present | Limbal |

Six pairs of human CC and LPC samples (Code: 3902C/L, 3911C/L, 3917C/L, 3925C/L, 3933C/L, 3846C/L) were performed in microRNA microarray. The GeneView data showed the miR-205 signal intensity of each sample from the microarray. The raw intensity was directly obtained from the scanner reading, the normalized intensity was standardized based on 75 percentile of the raw intensity and transformed with log2 scale. The normalized intensity = 0 indicated no expression signal was flagged as absent. Therefore, two pairs of samples with normalized intensity =0 was excluded in our analysis.

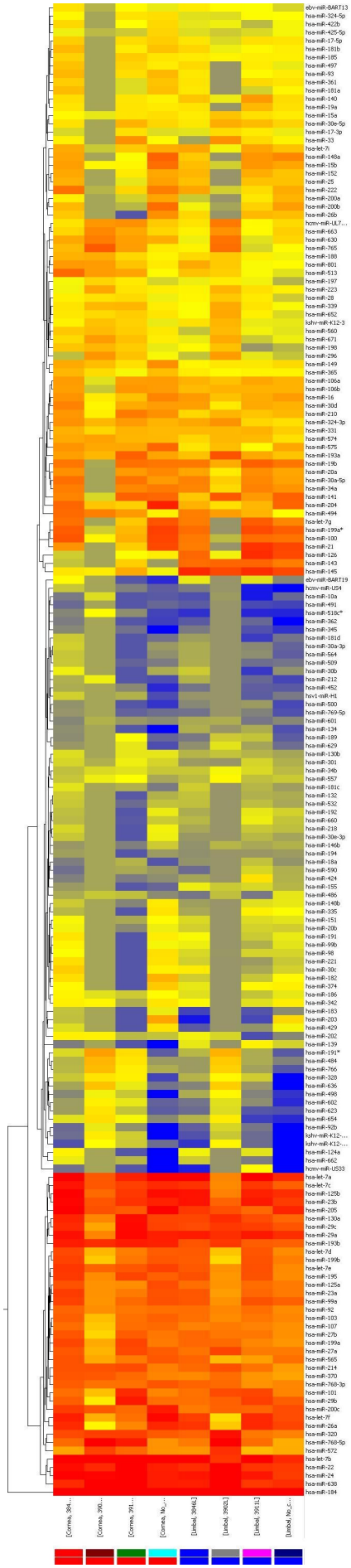

**Figure 4.2 MicroRNA expression profile in 4 pairs of human CC and LPC epithelia.**

Cluster analysis showed the expression profile of all samples by classifying the similarity of expression intensity of all entireties. It identified the enriched microRNA expressed in human corneal epithelium (both CC and LPC epithelia).

**Table 4.2 MicroRNAs enriched in human corneal epithelium.**

| Corneal epithelium | | | Reported expression | | | |
|---|---|---|---|---|---|---|
| **Rank** | **Enriched microRNAs** | **Mean gTotal gene signal** | **Mouse corneal epithelium** | **Mouse retina** | **Human RPE** | **Human skin keratinocytes** |
| 1 | miR-184 | 5161.7 | + | + | + | - |
| 2 | miR-638 | 1828.4 | - | - | - | - |
| 3 | miR-768-5p | 544.4 | - | - | - | - |
| 4 | let-7b | 518.7 | + | + | + | + |
| 5 | miR-24 | 392.5 | + | + | + | + |
| 6 | miR-22 | 197.8 | - | - | - | + |
| 7 | miR-193b | 183.2 | - | + | - | + |
| 8 | miR-320 | 129.6 | + | + | + | - |
| 9 | miR-572 | 123.9 | - | - | - | - |
| 10 | miR-205 | 94.4 | + | + | + | - |
| 11 | miR-214 | 88.1 | - | - | + | - |
| 12 | miR-23b | 86.2 | + | - | + | + |
| 13 | miR-200c | 81.8 | + | + | - | + |
| 14 | let-7c | 81.6 | - | - | - | + |
| 15 | let-7a | 80.1 | - | - | + | + |
| 16 | miR-370 | 78.9 | - | - | - | - |
| 17 | miR-765 | 76.6 | - | - | - | - |
| 18 | let-7e | 63.3 | - | - | + | + |
| 19 | miR-125b | 57.5 | + | - | + | + |
| 20 | miR-768-3p | 48.3 | - | - | - | - |
| 21 | miR-29a | 34.7 | + | - | - | + |
| 22 | miR-130a | 33.5 | + | + | + | + |
| 23 | miR-663 | 31.8 | - | - | - | - |
| 24 | miR-195 | 29 | - | - | - | + |

| | | | | | | |
|---|---|---|---|---|---|---|
| 25 | miR-92 | 28.6 | - | + | - | - |
| 26 | miR-125a | 26.7 | + | - | + | + |
| 27 | miR-23a | 26.1 | + | - | + | - |
| 28 | miR-99a | 25.3 | - | - | + | - |
| 29 | miR-29c | 18 | - | - | + | + |
| 30 | miR-565 | 17.1 | - | - | - | - |
| 31 | miR-199a | 16.8 | - | - | + | - |
| 32 | let-7f | 14.7 | + | - | + | + |
| 33 | miR-27a | 13.3 | + | - | + | + |
| 34 | miR-103 | 11.3 | - | - | + | - |
| 35 | miR-101 | 10.9 | - | - | - | + |
| 36 | miR-107 | 9.3 | - | - | - | - |
| 37 | miR-27b | 7.2 | + | - | + | + |

Thirty-seven microRNAs were detected and ranked according to gTotal gene signal (representing the actual hybridization signal). Their existence was compared to previously reported list for mouse corneal epithelium and neural retina, human retinal pigment epithelia and skin keratinocytes.

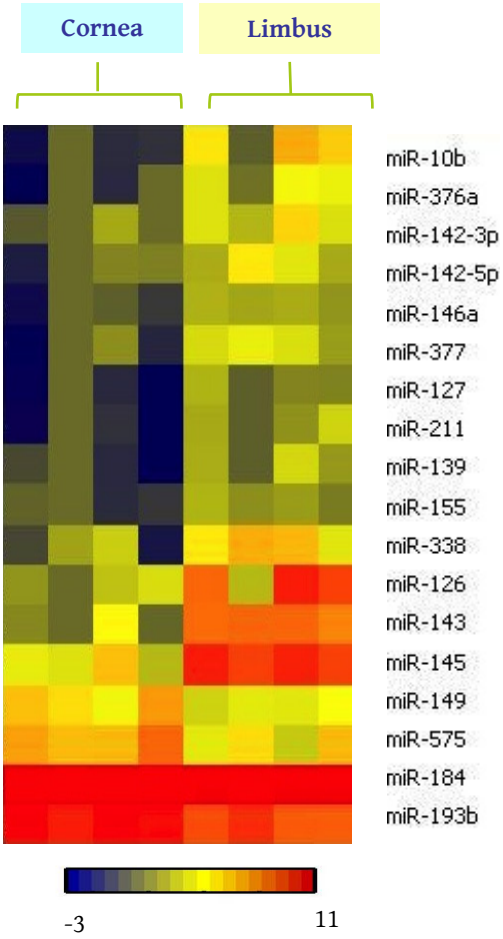


**Figure 4.3 Heat map of differentially expressed microRNAs in human CC and LPC epithelia analyzed GeneSpring V11.5.**

18 microRNAs were identified to be differentially expressed in human CC and LPC epithelia, with cut-off fold change more than 2.0, p-value less than 0.05, unpaired student T test.

**Table 4.3 The fold change and p-value of 18 differentially expressed microRNAs**

| ***Up-regulated in LPC vs CC*** | **P-Value** | **Fold Change** | **CC Mean intensity (Log Scale)** | **LPC Mean intensity (Log Scale)** | **CC SD** | **LPC SD** |
|---|---|---|---|---|---|---|
| hsa-miR-145 | 0.00029 | 23.93 | 1.806 | 6.386 | 1.082 | 0.446 |
| hsa-miR-143 | 0.0006 | 28.84 | 0.116 | 4.966 | 1.446 | 0.313 |
| hsa-miR-146a | 0.0078 | 4.23 | -1.676 | 0.404 | 1.034 | 0.245 |
| hsa-miR-142-3p | 0.0088 | 4.54 | -0.547 | 1.635 | 0.693 | 0.910 |
| hsa-miR-155 | 0.0102 | 3.00 | -1.474 | 0.111 | 0.733 | 0.450 |
| hsa-miR-10b | 0.0126 | 16.97 | -2.019 | 2.066 | 0.949 | 2.127 |
| hsa-miR-338 | 0.0132 | 11.47 | -0.707 | 2.813 | 1.782 | 0.966 |
| hsa-miR-377 | 0.0168 | 7.46 | -1.701 | 1.197 | 1.639 | 0.663 |
| hsa-miR-376a | 0.0178 | 8.21 | -1.907 | 1.130 | 1.461 | 1.181 |
| hsa-miR-142-5p | 0.0210 | 4.79 | -0.979 | 1.282 | 1.089 | 0.969 |
| hsa-miR-211 | 0.0220 | 6.80 | -2.593 | 0.172 | 1.529 | 0.954 |
| hsa-miR-126 | 0.0250 | 19.10 | 0.409 | 4.665 | 0.955 | 2.707 |
| hsa-miR-127 | 0.0269 | 5.46 | -2.687 | -0.240 | 1.532 | 0.693 |
| hsa-miR-139 | 0.0364 | 5.47 | -2.214 | 0.239 | 1.537 | 0.992 |
| ***Down-regulated in LPC vs CC*** | **P-Value** | **Fold Change** | **CC Mean intensity (Log Scale)** | **LPC Mean intensity (Log Scale)** | **CC SD** | **LPC SD** |
| hsa-miR-184 | 0.00005 | 0.1989 | 11.696 | 9.366 | 0.301 | 0.340 |
| hsa-miR-193b | 0.0024 | 0.3885 | 7.084 | 5.720 | 0.221 | 0.498 |
| hsa-miR-149 | 0.031 | 0.3779 | 2.998 | 1.594 | 0.951 | 0.314 |
| hsa-miR-575 | 0.043 | 0.2976 | 3.964 | 2.215 | 0.849 | 1.080 |

The normalized expression intensity, fold change and P value of 18 differential expressed microRNAs, signal intensity was transformed by Log 2 scale, student's unpaired T test.

**Table 4.4 The normalized signal intensities of corneal samples from Agilent® microRNA microarray profiling.**

| ID_REF | 3846C | 3846L | 3902C | 3902L | 3911C | 3911L | 3933C | 3933L |
|---|---|---|---|---|---|---|---|---|
| **hsa-miR-10b** | -3.044 | 2.548 | -0.749 | -1.048 | -2.195 | 3.678 | -2.089 | 3.085 |
| **hsa-miR-126** | 0.0498 | 5.113 | -0.7493 | 0.735 | 0.930 | 6.787 | 1.406 | 6.022 |
| **hsa-miR-127** | -3.386 | 0.646 | -0.750 | -1.048 | -2.300 | -0.257 | -4.314 | -0.298 |
| **hsa-miR-139** | -1.491 | 0.535 | -0.749 | -1.049 | -2.300 | 1.331 | -4.315 | 0.138 |
| **hsa-miR-142-3p** | -1.144 | 1.486 | -0.749 | 0.703 | 0.454 | 2.886 | -0.750 | 1.466 |
| **hsa-miR-142-5p** | -2.578 | 0.539 | -0.749 | 2.524 | -0.235 | 1.578 | -0.353 | 0.485 |
| **hsa-miR-143** | -0.149 | 5.036 | -0.749 | 5.161 | 2.234 | 5.164 | -0.869 | 4.505 |
| **hsa-miR-145** | 1.658 | 6.818 | 1.476 | 6.003 | 3.322 | 6.724 | 0.766 | 5.999 |
| **hsa-miR-146a** | -3.050 | 0.626 | -0.749 | 0.418 | -1.026 | 0.512 | -1.878 | 0.060 |
| **hsa-miR-149** | 3.314 | 1.212 | 2.748 | 1.604 | 1.836 | 1.577 | 4.093 | 1.981 |
| **hsa-miR-155** | -0.952 | 0.652 | -0.749 | -0.034 | -2.235 | 0.242 | -1.960 | -0.414 |
| **hsa-miR-193b** | 7.225 | 5.681 | 6.768 | 6.436 | 7.247 | 5.398 | 7.097 | 5.366 |
| **hsa-miR-211** | -3.221 | 0.501 | -0.749 | -1.049 | -2.087 | 0.010 | -4.315 | 1.224 |
| **hsa-miR-184** | 11.934 | 9.632 | 11.584 | 9.647 | 11.322 | 8.939 | 11.946 | 9.246 |
| **hsa-miR-338** | -1.562 | 2.523 | 0.344 | 3.671 | 1.155 | 3.480 | -2.763 | 1.575 |
| **hsa-miR-575** | 3.915 | 1.625 | 3.354 | 2.764 | 3.408 | 1.042 | 5.179 | 3.430 |
| **hsa-miR-376a** | -3.809 | 1.503 | -0.749 | -0.625 | -2.299 | 1.884 | -0.771 | 1.760 |
| **hsa-miR-377** | -3.668 | 1.374 | -0.749 | 1.724 | -0.018 | 1.463 | -2.369 | 0.228 |

## 4.2 Confirmation of limbal epithelium specific MicroRNAs

### 4.2.1 Validation of microRNA expression on human LPC and CC epithelium

We then validated the expression of candidate microRNAs on nine pairs of human LPC and CC epithelia using Taqman® real-time PCR analysis. The raw cycle threshold (Ct) value was normalized with housekeeping snRNA U6, which has been proved to be the most stable housekeeping across different tissues (Biosystems). The data was analyzed by relative fold change method with statistical analysis using Wilcoxon matched-pairs signed rank test. The relative expression intensity was transformed by $\log_2$ scale.

Two reported microRNAs miR-205 and 184, which were present in mouse corneal epithelia, were firstly validated in our study. As Ryan's report, miR-205 was expressed throughout the mouse corneal epithelium and miR-184 was solely expressed in the central corneal epithelium (Ryan et al., 2006b). Taqman® real-time PCR result confirmed this similar pattern in human corneal epithelium. As shown in **figure 4.4**, miR-205 was expressed strongly in both CC and LPC epithelia without significant difference ($P$ = 0.8077), with the relative expression intensity of 7.977±2.028 and 7.753±3.042 in CC and LPC, respectively. In contrast, miR-184 was highly expressed in CC (relative intensity = 4.929±1.254) than LPC (relative intensity = 2.937±1.236). The difference was statistical significant ($P$ = 0.0005).

The pervious study in our lab confirmed the miR-143/145 cluster was significantly up-regulated in LPC epithelia. In my study, miR-143 and miR-145 were included as a parameter to evaluate the sample quality. After U6 normalization, miR-143 and 145 were the most significantly up-regulated in LPC epithelia in all samples (miR-143, $P$=0.0001 and miR-145, $P$=0.0004) (**Figure 4.5**).

6 microRNAs were also validated to be significantly up-regulated in LPC epithelia. They were miR-10b ($P$ = 0.0391; relative intensity CC = 0.5661±2.006, LPC = 3.464±2.131), miR-126 ($P$ = 0.0039; relative intensity CC = 6.98±2.06; LPC = 11.54± 2.87), miR-127 ($P$ = 0.0313; relative intensity CC = -4.827±1.752, LPC = -1.351±1.681), miR-139 ($P$ = 0.0313; relative intensity CC = -5.523±3.255, LPC = -1.600±2.978), miR-155 ($P$ = 0.0391, relative intensity CC = 2.758±1.389, LPC = 4.850±2.229) and miR-338 ($P$ = 0.0313, relative intensity CC = -9.770±2.108, LPC = -6.059±1.741) (**Figure 4.6**). The remaining 7 microRNAs (miR-142-5p, 146a, 149, 193b, 211 and 376a) had marginal difference ($P$ > 0.05) (**Figure 4.7**).

Out of 18 microRNAs, 16 were expressed consistently in all samples but miR-377 and 575 were not detected. A total of nine microRNAs were differentially expressed between LPC and CC epithelia (9 higher in LPC and 1 higher in CC).

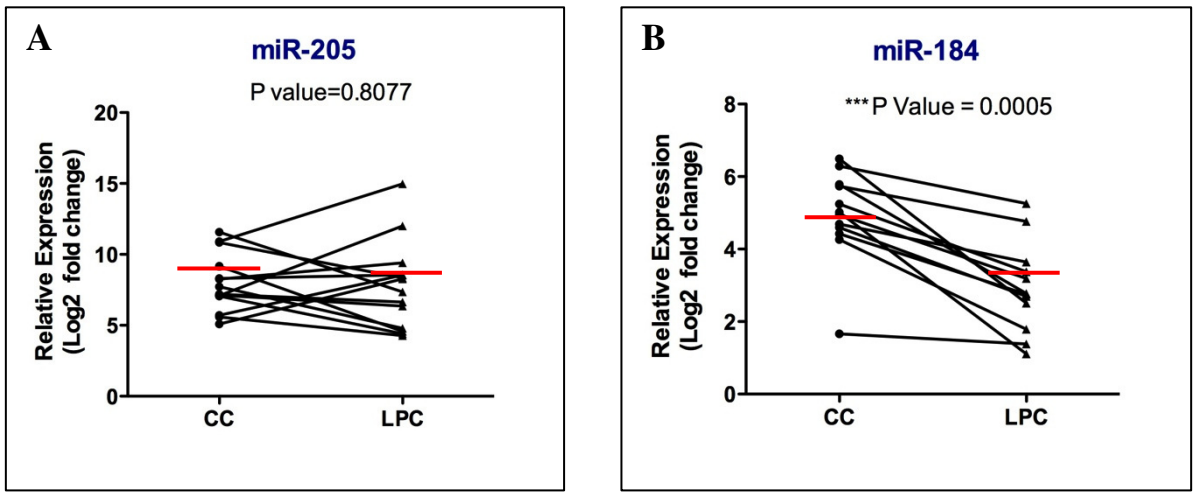


**Figure 4.4 Expression analysis of miR-205 and 184 in human CC and LPC epithelia.**

TaqMan® real-time PCR quantified the expression level of miR-205 and miR-184 in CC and LPC. miR-205 had no statistically significant difference in CC and LPC. miR-184 were significantly up-regulated in CC epithelia, compared to CC. (n=9, normalization with housekeeping U6, Fold change transformed to log2 scale, Wilcoxon matched-pairs signed rank test, P value < 0.05 considered statistical significant). Red bar indicated the mean value of relative intensity.

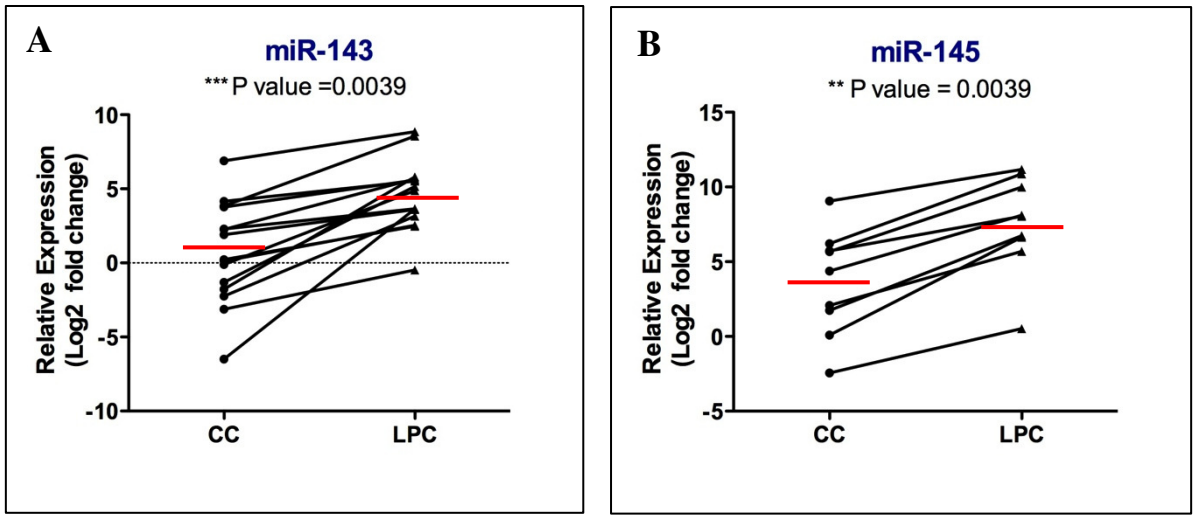


**Figure 4.5 Expression analysis of miR-143 and 145 in human CC and LPC epithelia**

MiR-143 and 145 were significantly up-regulated in LPC epithelia as compared to CC (n=9, data normalization with housekeeping U6, fold change transformed to $\log_2$ scale, statistical significance was calculated by Wilcoxon matched-pairs signed rank test, $P < 0.05$ was considered statistical significant). Red bar indicated the mean value of relative intensity.

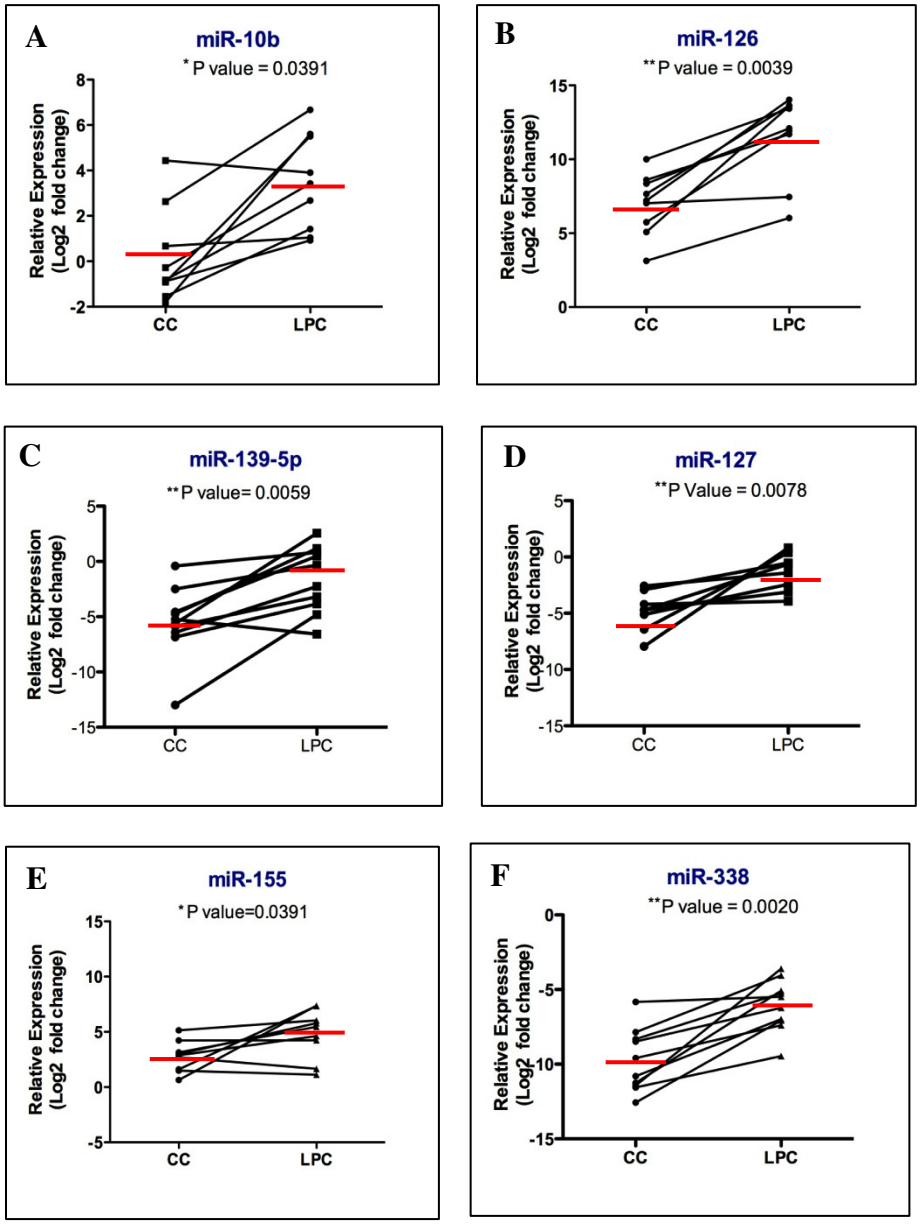


**Figure 4.6 Six microRNAs (miR-10b, miR-126 miR-139-5p, miR-127, miR-338-3p miR-155) were limbal-specific.**

TaqMan® real-time PCR confirmed 6 microRNAs were significantly up-regulated in LPC epithelia as compared to CC (n=9). Data normalized with housekeeping U6, fold change transformed to $\log_2$ scale, statistical significance was calculated by Wilcoxon matched-pairs signed rank test, $P < 0.05$ was considered statistical significant. Red bar indicated the mean value of relative intensity.

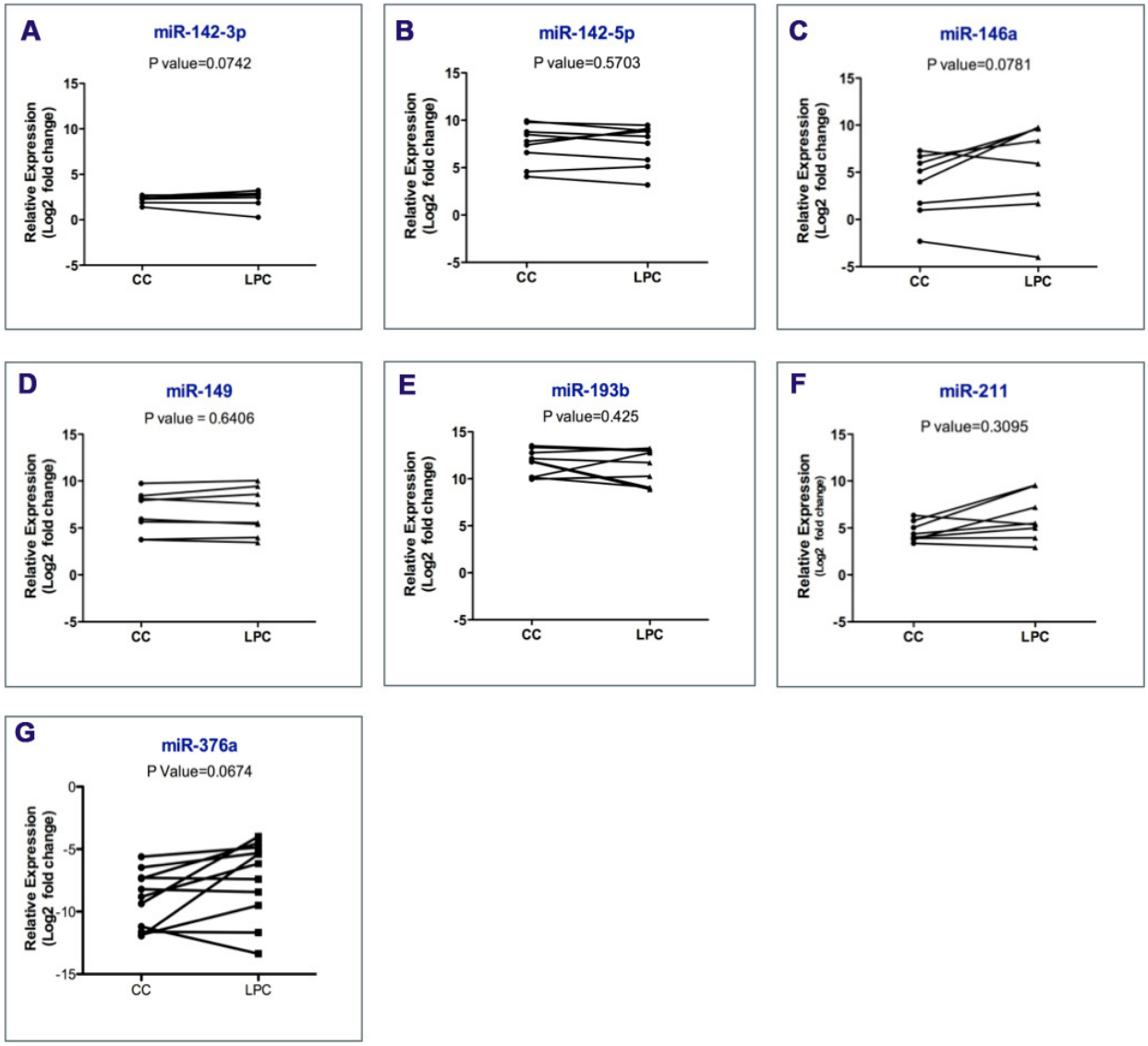


**Figure 4.7 Seven microRNAs (miR-142-3p, miR-142-5p, miR-146a, miR-149, miR-193b, miR-211 and miR-376a) were not limbal-specific.**

TaqMan® real-time PCR validated 7 microRNAs present in LPC epithelia, and CC epithelium, but no significant difference in LPC and CC epithelia (n=9, normalization with U6, fold change transformed to $\log_2$ scale, Wilcoxon matched-pairs signed rank test, $P < 0.05$ considered statistical significant).

### 4.2.2 Limbal specific MicroRNAs visualization

MicroRNA localization was detected by locked nucleic acid (LNA)-based *in situ* hybridization. Fresh corneal cryosections were hybridized with denatured DIG-labeled LNA-miRCURY™ oligo probes for miR-10b, 126 and 155, scrambled negative control and snU6 positive control. For the LNA-miRCURY™ oligo probes to specially target the mature microRNAs; the blue or purple signal in cell cytoplasm was regarded as positive result. To obtain a better localization pattern, nuclear fast red was used for counterstaining as a red signal in the cell nucleus. NTP/BCIP substrate was used for developing the reaction color, however, one drawback of NTP/BCIP was that it might cause non-specific signal in the edge of tissue, therefore the high, non-structure staining in the outer layer of epithelium was regarded as a false positive signal.

#### 4.2.2.1 *in situ* expression of microRNAs in human limbal and corneal epithelia

MiR-126, 10b and 155 were visualized on human cornea cryosections (thickness=6 μm). As shown in **Figure 4.8**, all of the three microRNAs were differentially expressed, with a more intensive signal detected in the limbal epithelium, contrasted by a patchy expression in the central corneal epithelium. MiR-126 was predominantly expressed in all layers of limbal epithelium, but little signal was detected in the central corneal epithelium (**Figure 4.8A**). Moreover, miR-126 was also strongly expressed in the blood vessels underlying the limbal epithelium. A strong signal for miR-10b was observed in all layers of limbal epithelium, and gradually decreased towards the central corneal epithelium (**Figure 4.8B**). The hybridization signal for miR-155 was weak in both limbal and corneal epithelium, which was in concordant with its low expression level in the microarray and qPCR findings. Higher magnification showed miR-155 was intense in the suprabasal layers of limbal region but less in basal layers (**Figure 4.8C**). Negligible staining was found for

sections hybridized with scrambled sequences. Similar results were found in 3 separate experiments.

#### 4.2.2.2 *in situ* expression of microRNAs in mouse limbal and corneal epithelia

For the long-term of human cornea preservation and transportation after harvested from donors, the integrity and quality of microRNA in human corneal epithelium cannot be guaranteed, which may cause false negative results in hybridizing intensity. Thus, mouse corneal epithelia were used as an alternative to confirm the spatial distribution of microRNA candidates. Differed from human, mouse cornea had a thinner limbal epithelium with one cell layer and thicker central corneal epithelium containing 4 to 6 layers (**Figure 4.9**). This may give a subtle staining of microRNA localization in CEPCs enriched limbal region. Fresh eyeballs harvested from 6 to 8 weeks BALB/c mice were fixed and sectioned for hybridizing miR-126, 155 and 10b probes, respectively. miR-10b and 126 displayed a higher intensity in mouse limbal epithelium than in central cornea (**Figure 4.10 A&B**). . MiR-126 was preferentially expressed in the basal cells of limbal epithelium, and continuously extended to the basal layer of central cornea, but were completely negative in superficial layers (**Figure 4.10A**). The expression pattern for miR-10b was most intense in the basal layer of limbal epithelium, but little signal was detected in the central region (**Figure 4.10B**). MiR-155 was relatively weakly expressed in all the layers of limbal and central epithelia (**Figure 4.10C**). Negligible staining was found for sections hybridized with scrambled sequences.

In summary, together with the previous report from our laboratory, in situ hybridization cornea revealed the spatial distribution miR-10b, 126, 155, 143 and 145 in corneal epithelium, and confirmed their preferential location in limbal epithelium (**Table 4.4**). The expression pattern of microRNA in human corneal epithelium was indistinct,

which did not display a cell-specific manner. However, in the mouse corneal epithelium, the signal of miR-126 and 10b were restricted to the basal layer of limbal epithelium in where the CEPCs and eTAc reside, but absent in the superficial layer. This observation indicated miR-126 and 10b were mainly expressed in the undifferentiated cells in mouse corneal epithelium and was absent in terminal differentiated epithelium cells.

Therefore, the presence of these microRNAs in limbal region suggests its crucial roles in regulation of genes related with CEPC proliferation and differentiation, which was further investigated in section 4.3.

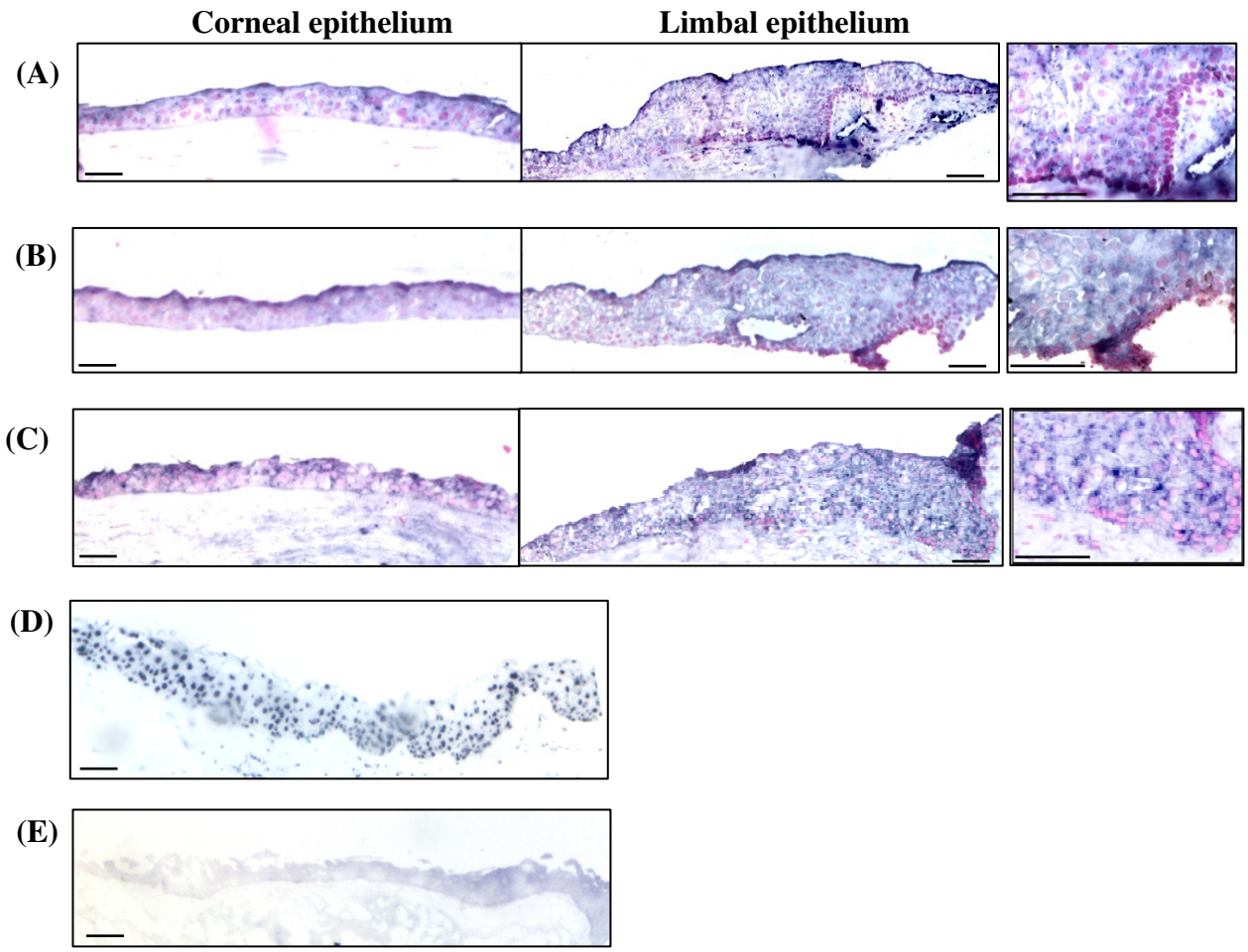


**Figure 4.8** ***in situ*** **hybridization of miR-126, miR-10b and miR-155 in human corneal epithelia.**

Spatial distribution of miR-126, 10b and 155 in the cross section of human corneal epithelium using in situ hybridization: (A) miR-10b, (B) miR-126, (C) miR-155, (D) U6 positive control, (E) scrambled negative control.

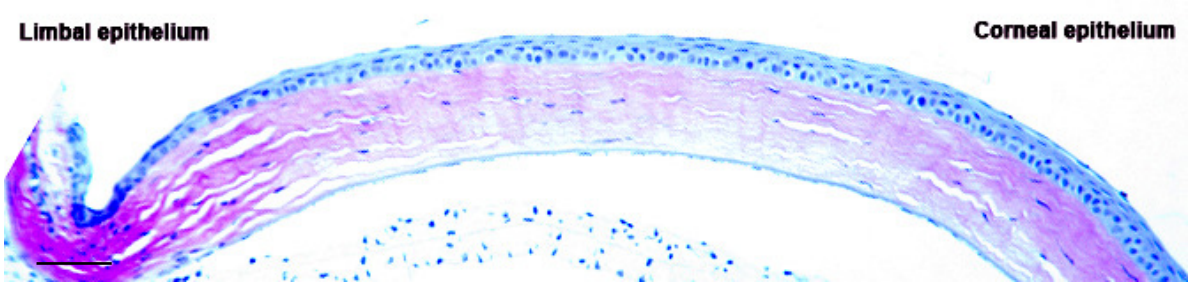


**Figure 4.9 H&E staining on Balb/c mouse corneal epithelium.**

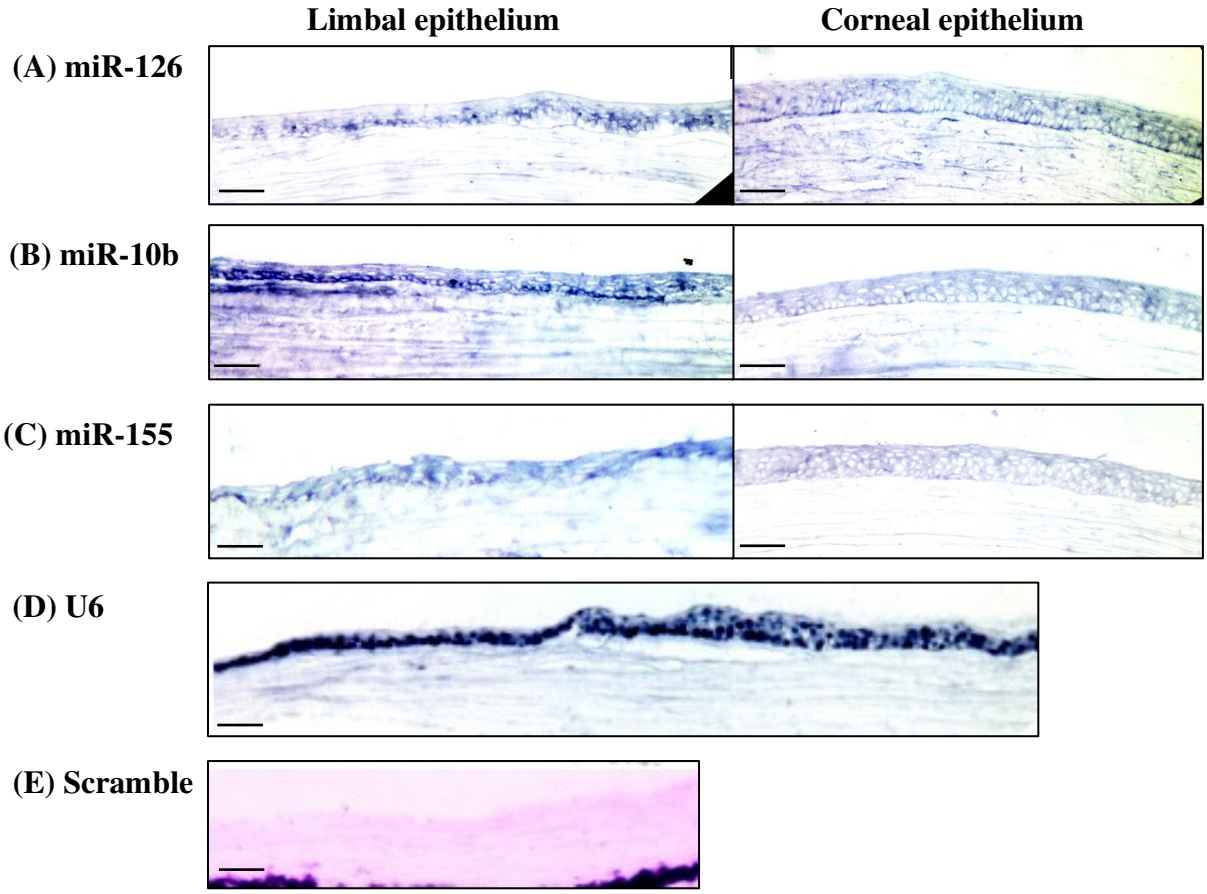


**Figure 4.10** ***in situ*** **hybridization of miR-126, miR-10b and miR-155 in mouse corneal epithelium.**

Spatial distribution of miR-126, 10b and 155 in the cross section of mouse corneal epithelium using in situ hybridization: (A) miR-10b, (B) miR-126, (C) miR-155, (D)U6 positive control, (E) scrambled negative control.

**Table 4.5 Summary of microRNAs expression in corneal epithelium**

| miRNA probe | Human | | | Mouse | |
|---|---|---|---|---|---|
| | Corneal Epithelium Basal | Limbal Epithelium Basal | Limbal Epithelium Supra Basal | Corneal Epithelium Basal | Limbal Epithelium Basal |
| miR-126 | +/- | ++ | ++ | + | +++ |
| miR-155 | +/- | + | ++ | +/- | ++ |
| miR-10b | - | ++ | ++ | +/- | +++ |
| miR-143 | + | ++ | +++ | + | +++ |
| miR-145 | + | ++ | +++ | + | +++ |

- : Negative
+ : Weak expression
++ : Moderate expression
+++: Strong expression

## 4.3 Bioinformatics of human CEPC-associated microRNAs

### 4.3.1 Gene Ontology analysis

As indicated by the importance of microRNA regulation in different biological systems, microRNAs may also be associated with corneal epithelium activities. We hypothesized that the 16 validated microRNAs could participate in corneal epithelium formation and maintenance. The target genes predicted by TargetScan were correlated with the reported cornea epithelial gene profile (Turner, Budak, Akinci, & Wolosin, 2007) (GEO Series accession number: GSE5543). The sorted gene list was overlapped with DAVID database to calculate the enrichment score for GO annotation so as to reveal the potential biological functions and processes influenced by these microRNAs.

In GSE5543 gene profile, the down-regulated genes in human corneal epithelium (compared to conjunctiva) that were predictively targeted by our microRNA set were found to participate in several major processes: (1) immune response, cellular and tissue protection, including inflammatory response ($P = 3.59\text{x}10^{-6}$), lymphocyte activation ($P = 1.07\text{x}10^{-4}$), response to oxidative stress ($P = 1.99\text{x}10^{-3}$) and external stimuli ($P = 1.84\text{x}10^{-2}$), and MHC protein complex ($P = 4.73\text{x}10^{-2}$); (2) cell survival and growth, including cytokine receptor activity ($P = 3.19\text{x}10^{-5}$), regulation of programmed cell death ($P = 3.32\text{x}10^{-3}$) and cell division ($P = 1.37\text{x}10^{-2}$) as well as (3) cell movement and interaction, including cell localization ($P = 3.03\text{x}10^{-3}$) and gap junction ($P = 4.93\text{x}10^{-2}$). Conversely, the up-regulated genes in corneal epithelium potentially affected by microRNAs were involved in cell processes: (1) cell survival, which was cell death regulation ($P = 8.05\text{x}10^{-5}$), caspase activation ($P = 1.38\text{x}10^{-2}$); (2) cell growth, including EGF-like activity ($P = 9.08\text{x}10^{-4}$), growth factor binding ($P = 7.62\text{x}10^{-3}$), cell cycle regulation ($P = 2.33\text{x}10^{-2}$) and cell development ($P = 2.33\text{x}10^{-2}$); as well as (3) cell movement and interaction, including

extracellular matrix ($P$ = 2.8x10$^{-3}$), cell-matrix adhesion ($P$ = 3.47x10$^{-3}$) and cell-cell adhesion ($P$ = 3.08x10$^{-2}$). Interestingly, vascular and neuronal development was also highlighted in association with our microRNA set which was more expressed in the limbal epithelium: blood coagulation ($P$ = 5.46x10$^{-3}$) and blood vessel development ($P$ = 1.56x10$^{-2}$), and neuron differentiation ($P$ = 9.6x10$^{-3}$). The specific microRNAs and associated target genes involved in various pathways were listed in **Table 4.5.**

### 4.3.2 Significant pathway analysis

With the analysis of DIANA-mirPath bioinformatics web-tool, the predicted target genes of limbal specific microRNAs were associated with several major limbal epithelial cell events and individual involvement of each micoRNA in the pathway entities were ranked with an enrichment score (enrichment score = -ln ($P$), significant cut-off = 3) (**Figure 4.11 and Table 4.6**). They were (1) stem cell regulation, with particular significance on Wnt signaling ($P$ = 8x10$^{-6}$) with the highest involved microRNAs miR-10b (score = 13.3) and miR-145 (score = 7.8). Mitogen-activated protein kinase (MAPK, $P$ = 2x10$^{-5}$), with the highest involved microRNA miR-155 (score = 9.8). (2) Intercellular junctions and cell motility, with significant relationship with pathway of adheres junction ($P$ = 5x10$^{-6}$) affected by miR-145 (score = 11.3) and miR-10 (score = 6.1). Besides, other three pathways include the regulation of actin cytoskeleton ($P$ = 7x10$^{-6}$), focal adhesion ($P$ = 0.0004) and tight junctions ($P$ = 0.0038) with the similar genes significantly associated with miR-143 (scores = 7.31, 8.84 and 7.41, respectively). (3) Immune response, with significance on affecting T-cell receptor signaling ($P$ = 0.0015) and B cell signaling ($P$ = 0.025) which were mainly influenced by miR-155 (score = 26.23 and 13.1, respectively). (4) Growth factor effect, with high significance on TGFβ signaling ($P$ = 7x10$^{-5}$) related with

miR-145 (score = 13.6) and miR-155 (score = 7.7); and ErbB signaling pathway ($P$ = 0.0002) associated with miR-143 (score = 5.77).

### 4.3.3 MicroRNA-mRNA interaction analyses

Ingenuity® Pathways Analysis platform was conducted to analyze the validated interaction between microRNAs and targets. A global molecular network was generated based on the direct or indirect suppression and activation in different tissues from experimental observation collected by Ingenuity Knowledgebase®. The molecules were filtered by corneal epithelium gene expression profile, which might give a hint for the potential interactions associated with limbal epithelial cell events.

**IPA® analysis of miR-143, 145 and 155 target gene interaction**

TP53 and MYC were the major genes directly and indirectly influenced by the 3 microRNAs: miR-143, 145 and 155 (**Figure 4.12A**). IPA analysis showed both miR-143 and 145 suppressed *MYC*, *KRAS* and *LAMP2* in cell growth regulation (blue arrow). Meanwhile, miR-155 regulated tumor necrosis factor (*TNF*) to stimulate *TP53*, which in return up-regulated miR-155 (red arrow). TNF might also transactivate apoptosis-related genes *DARK1* and *BIK* (grey highlight), and might suppress oncogenes, *MYC* and *DLEU1*. Moreover, miR-155 could induce apoptosis through caspase-3 activation (**Figure 4.12C blue arrow**). IL1B and IL8 were the key stimulators to corneal cell growth and could be up-regulated by miR-155, forming a loop to induce inflammatory response through KRAS regulation (**Figure. 4.12B red arrow**). Alternatively, it could affect CEBPB, a limbal stem cell marker, via a direct suppressive interaction or through IL6 activity ((**Figure. 4.12C red arrow**).

**IPA® analysis of miR-127-3p, miR-184 and miR-338-3p**

IPA analysis revealed the interaction of miR-127-3p, 184 and 338-3p with growth factors in cornea. As shown in **Figure 4.13**, TGFB1 could up-regulate XBP1 as the target of miR-127-3p and NFATC2 as the target of miR-184. In the corneal epithelium, TGFB1 regulates both limbal and corneal epithelial cells to suppress the expression of hepatocyte growth factor and keratinocyte growth factor, subsequently inhibiting the overgrowth of corneal epithelial cells. TGFB1 might activate the targets of miR-127-3p and 184, suggesting a potential role on corneal epithelial regulation. Vimentin and epidermal growth factor receptor were proven to be expressed in the corneal epithelium. IPA network also showed that miR-338-3p and epidermal growth factor receptor might collaborate to suppress vimentin gene expression.

**Table 4.5 Gene ontology analyisis on cornea genes associated with candidate microRNAs**

**(A) Down-regulated cornea genes associated with candidate microRNAs**

| Rank | **Pathways** | **Enrichment score** | **P-value** | **microRNA targeted genes** |
|---|---|---|---|---|
| 1 | Inflammatory response | 5.53 | 3.59E-06 | 10b (CXCR2, CXCR4, IL8, ITGB2, LYZ); 139-3p (ELF3); 139-5p (CD46, CD302); 142-3p (CD302, LYZ, SGMS1); 143 (CD46, IL10RB, LYZ); 145 (CD40, CXCR2, CYBA); 146a (CCL5, CFH, CXCR4, IL6, LY75); 149 (AIF1, C1RL, CCR3, CYP4F11, IL6, IL10RB); 155 (CYP4F11, F3, IGF2); 205 (LY75, LYZ); 211 (AIF1); 338-3p (ALOX5, CD55, MECOM); 376a (LY75, SGMS1) |
| 2 | Cytokine receptor activity | 2.83 | 3.19E-05 | 10b (CXCR2); 142-3p (IL6ST); 143 (CSF2RA, IL10RB); 145 (CXCR2); 149 (IL10RB); 184 (IL15RA); 205 (IL4R); 211 (IL1R1, IL7R, IL13RA1); 338-3p (IL4R) |
| 3 | Positive regulation of lymphocyte activation | 1.76 | 1.07E-04 | 142-3p (IL6ST, TGFBR2); 145 (CD40, CD47, TGFBR2); 146a (CD83, IL6, ITPKB); 149 (CD47, IL6); 155 (CD38, CD47, TGFBR2); 205 (IL4R); 211 (IL7R, IL13RA1, TGFBR2); 338-3p (IL4R); 376a (CD47, ITPKB) |
| 4 | Response to oxidative stress | 1.46 | 1.99E-03 | 10b (PTPRK); 142-3p (SLC11A2); 145 (SLC11A2); 146a (CCL5, GPX3, PDLIM1, SLC11A2, STAT1); 146b-5p (SLC11A2); 149 (DUOX2, PTPRK, SLC11A2); 155 (CD38, SLC11A2, STAT1); 211 (DHCR24, PML, SLC11A2, TXNIP, UCP2) |
| 5 | Localization of cell | 1.89 | 3.03E-03 | 10b (CXCR2, IL8, ITGB2, MET, PTPRK); 139-5p (CDH2, CXCR4, NR4A2); 142-3p (ARID5B); 143 (ARID5B); 145 (CDH2, CXCR2, NR4A2, SIX1); 146a (CCL5, CEACAM1, IL6, SDCBP); 149 (FOXC1, IL6, PTPRK, TNS1); 155 (SDCBP, SIX1); 211 (CDH2, CXCR4, FOXC1, NR4A2, SIX1); 338-3p (CEACAM1, CXCR4); 376a (SORD) |
| 6 | Programmed cell death | 2.47 | 3.32E-03 | 10b (CXCR2, ITGB2, SRGN, UNC5B); 139-5p (CXCR4, DAPK1, DYRK2, ZC3H12A); 142-3p (BID, SGMS1, SLC11A2); 143 (BAG1, STEAP3, TP53AIP1, XAF1); 145 (CXCR2, MCF2L, SLC11A2); 146a (DOCK1, IL6, SLC11A2, STAT1, TNFAIP8); 149 (IL6, SLC11A2, STK17A); 155 (BAG1, DOCK1, DYRK2, F3, GPR65, SLC11A2, STAT1, TNFAIP8); 205 (RNF130, TNFAIP8); 211 (CXCR4, DHCR24, PML, SLC11A2); 338-3p (CXCR4, DOCK1, |

| | | | | |
|---|---|---|---|---|
| | | | | DYRK2, TNFAIP8, TP53AIP1); 376a (DYRK2, SGMS1, TP53AIP1, XAF1) |
| 7 | Positive regulation of cell division | 1.57 | 1.37E-02 | 145 (PDGFD); 146a (PPBP); 149 (PDGFC); 155 (IGF2); 205 (VEGFA); 376a (PDGFC) |
| 8 | Response to external stimulus | 1.53 | 1.84E-02 | 10b (IL8); 142-3p (IL6ST); 146a (CCL5, IL6); 149 (IL6); 155 (F3); 205 (VEGFA) |
| 9 | Regulation of apoptosis | 1.57 | 3.01E-02 | 139-5p (DYRK2, PLAGL1, RAB27A); 142-3p (BID); 143 (DAPK1, IGFBP3, RAB27A); 145 (ALDH1A3, MCF2L, PLAGL1, RAB27A, RUNX3); 146a (NOTCH2, PLAGL1, RARB, STAT1); 149 (NOTCH2, PTGIS, STK17A); 155 (CD38, DYRK2, STAT1); 184 (NOTCH2); 205 (MX1, NOTCH2, RAB27A); 211 (MX1, NOTCH2, PML, TXNIP); 338-3p (DAPK1, DYRK2, PTGIS); 376a (DYRK2, NOTCH2, PLAGL1, RAB27A) |
| 10 | Leukocyte activation | 1.07 | 3.14E-02 | 10b (CXCR2, IL8); 139-5p (CXCR4, LCP1, RAB27A); 142-3p (TGFBR2); 143 (RAB27A); 145 (CD40, CXCR2, LCP1, RAB27A, TGFBR2); 146a (ITPKB); 149 (CSF1); 155 (IGF2, TGFBR2); 184 (BST2); 205 (RAB27A); 211 (CXCR4, IL7R, TGFBR2); 338-3p (CXCR4, LCP1); 376a (ITPKB, RAB27A) |
| 11 | Positive regulation of acute inflammatory response | 0.99 | 3.22E-02 | 142-3p (IL6ST); 146a (CCL5, IL6); 149 (IL6) |
| 12 | MHC protein complex | 1.67 | 4.73E-02 | 10b (HLA-DPB1, HLA-E); 139-5p (AZGP1); 143 (AZGP1, HLA-DPB1, HLA-E); 146a (HLA-C); 149 (HLA-E); 205 (HFE); 376a (HFE, HLA-C) |
| 13 | Gap junction | 0.9 | 4.93E-02 | 142-3p (ADCY9, GNA11); 145 (PDGFD); 149 (PDGFC); 155 (PLCB1); 205 (PLCB1); 211 (LPAR1, PRKACB); 376a (PDGFC) |

**(B) Up-regulated cornea genes associated with candidate microRNAs**

| Rank | Pathways | Enrichment score | P-value | MicroRNA (miR) targeted genes |
|---|---|---|---|---|
| 1 | Regulation of cell death | 3.12 | 8.05E-05 | 10b (CADM1, CD24, GAS1, TIAM1, VDR); 139-3p (GSPT1, JUN, RASGRF1, THBS1); 142-3p (PRUNE2); 143 (CD44, FOXO1, GPR109B, NQO1, NTF3, TIAM1); 145 (CD44, FOXO1, PMAIP1, RASGRF1, SMAD3, TGFB2, VDR); 146a (ARHGEF4, CADM1, PMAIP1, PTGS2); 146b-5p (ARHGEF4, CARD10); 149 (BCL2L13, CEBPG, TGFB2); 155 (CARD10, CD24); 205 (ADRB2, BCL2L13, CADM1, CD24, CEBPG, MOAP1, NQO1, PRUNE2); 211 (CD44, CLU, FOXO1, GPR109B, GSPT1, PROC); 338-5p (ADRB2, ARHGEF3, CADM1, CARD10, PRNP, PRUNE2); 376a (TIAM1) |
| 2 | EGF-like activity | 1.84 | 9.08E-04 | 10b (LTBP1); 139-3p (TEK, THBD, THBS1); 143 (PLAU); 145 (CELSR1); 146a (PTGS2); 149 (CNTNAP2, PLAU); 205 (CNTNAP2); 211 (CNTNAP2, LTBP1, ODZ4, PROC); 338-5p (CNTNAP2); 376a (MATN2) |
| 3 | Extracellular matrix | 2.32 | 2.80E-03 | 10b (LTBP1, SPOCK1); 139-3p (SPOCK1, THBS1); 143 (CD44, COL4A5, COL5A3, FLRT2, SPOCK1); 145 (CD44, TGFB2); 146a (LAMB3, WNT3); 149 (GPC1, TGFB2); 155 (SPARC, SPOCK1); 205 (SPARC); 211 (CD44, COL5A3, COL17A1, FLRT2, LTBP1); 376a (MATN2) |
| 4 | Cell-matrix adhesion | 2.27 | 3.47E-03 | 10b (CADM1, CD24, CLEC7A, SPOCK1); 139-3p (DSC2, DSG1, PTPRS, SPOCK1, TEK, THBS1); 143 (CD44, COL5A3, FLRT2, SPOCK1); 145 (CD44, CELSR1, CYR61); 146a (CADM1, LAMB3); 149 (CNTNAP2, DSC3); 155 (CD24, CYR61, SPOCK1); 205 (CADM1, CD24, CNTNAP2); 211 (CD44, CDH4, CLCA2, CNTNAP2, COL5A3, COL17A1, DSC2, DSG1, FLRT2); 338-5p (CADM1, CNTNAP2, DSC3); 376a (CLCA2, DSC3, NLGN4X, RHOB) |
| 5 | Blood coagulation | 1.06 | 5.46E-03 | 10b (ANXA8, ANXA8L2, SERPINE1); 139-3p (THBD); 143 (SERPINE1, PLAU); 145 (SERPINE1); 149 (PLAU); 155 (F2RL2); 211 (PROC) |
| 6 | Growth factor binding | 1.53 | 7.62E-03 | 10b (LTBP1); 139-3p (CRIM1, THBS1); 143 (NTF3); 145 (CRIM1, CYR61); 149 (HTRA1, NTRK2); 155 (CYR61); 211 (LTBP1, NTRK2); 338-3p (NTRK2) |

| | | | | |
|---|---|---|---|---|
| 7 | Neuron differentiation | 0.53 | 9.60E-03 | 10b (CD24, GAS1, RORA); 139-3p (EMX2, RASGRF1); 142-3p (DRD1, NRL); 143 (CD44, MYO6, NTF3); 145 (CD44, MYO6, RASGRF1, TGFB2); 149 (CNTNAP2, NTRK2, TGFB2); 155 (CD24, DRD1); 205 (CD24, CNTNAP2); 211 (CD44, CDH4, CNTNAP2, DRD1, NTF3, NTRK2); 338-5p (CNTNAP2, NRL, NTRK2) |
| 8 | Positive regulation of caspase activity | 1.45 | 1.38E-02 | 139-3p (GSPT1); 145 (PMAIP1, SMAD3); 146a (PMAIP1); 146b-5p (PMAIP1); 149 (BCL2L13); 205 (BCL2L13, MOAP1); 211 (GSPT1) |
| 9 | Positive regulation of cell adhesion | 0.78 | 1.47E-02 | 10b (CD24); 139-3p (THBS1); 145 (CYR61, SMAD3, TGFB2); 149 (TGFB2); 155 (CD24, CYR61); 205 (CD24) |
| 10 | Blood vessel development | 1.48 | 1.56E-02 | 139-3p (JUN, THBS1); 143 (CD44, FOXO1, MYO1E, PLAU); 145 (CD44, CYR61, FOXO1, TGFB2); 149 (NTRK2, PLAU, TGFB2); 155 (CYR61); 211 (CD44, FOXO1, NTRK2); 338-5p (NTRK2); 376a (RHOB) |
| 11 | Cell cycle arrest | 0.88 | 2.33E-02 | 10b (GAS1); 139-3p (THBS1); 142-3p (KAT2B); 143 (RB1); 145 (SMAD3, TGFB2); 149 (TGFB2); 205 (KAT2B) |
| 12 | Positive regulation of cell development | 0.82 | 2.33E-02 | 10b (TIAM1); 143 (NTF3, TIAM1); 145 (SMAD3, TGFB2); 149 (TGFB2); 211 (CDH4); 376a (TIAM1) |
| 13 | Cell-cell adhesion | 1.15 | 3.08E-02 | 10b (CADM1, CD24, CLEC7A); 139-3p (DSC2, DSG1, TEK); 143 (CD44); 145 (CD44, CELSR1); 146a (CADM1); 149 (DSC3); 155 (CD24); 205 (CADM1, CD24); 211 (CD44, CDH4, DSC2, DSG1); 338-5p (CADM1, DSC3); 376a (DSC3) |

Significant pathways and biological functions potentially affected by the differentially expressed microRNAs in corneal epithelium. Potential target genes predicted by TargetScan were overlapped with the reported cornea epithelial gene profile GSE5543. The sorted gene list was then inputted to KEGG pathway analysis and gene annotation and enrichment for the potential biological functions and processes influenced by these microRNAs.

**Table 4.6 KEGG pathway analysis on the target genes of 6 limbal-specific microRNAs**

| KEGG pathway | P value | MicroRNAs | Target genes associated |
|---|---|---|---|
| ***(1) Stem cell regulation*** | | | |
| Wnt signaling | $8x10^{-6}$ | miR-10b, 126, 139-5p, 143, 145, 155, 338-3p | *APC, BTRC, CAMK2D, CAMK2G, CCND1, CCND2, CTNNBIP1, FZD4, FZD5, FZD7, FZD9, LRP6, MAP3K7, NFAT5, NFATC1, PPP3CA, RAC1, ROCK1, SENP2, SMAD2, SMAD3, SMAD4, TBL1X, VANGL1* |
| MAPK signaling | $2x10^{-5}$ | miR-126, 139-5p, 143, 145, 155, 338-3p | *ACVR1B, ARRB2, BDNF, CACNB2, CRK, CRKL, DUSP6, ELK4, FGF1, FGF5, FGF7, FLNB, FOS, KRAS, MAPK1, MAP2K4, MAP3K3, MAP3K7IP2, MAP3K7, MAP3K10, MAP3K14, MAP4K2, MAP4K4, MAPK7, PDGFRA, PPP3CA, RAC1, RAP1B, RASA1, RASA2, RPS6KA3, SOS1, TAOK1, TAOK2, TGFBR1, TGFBR2* |
| ***(2) Cell motility and skeleton*** | | | |
| Adherens junction | $5x10^{-6}$ | miR-139-5p, 143, 145, 155 | *ACTB, ACTG1, ACVR1B, IGF1R, MAPK1, MAP3K7, PVRL1, RAC1, SMAD4, SMAD2, SMAD3, SSX2IP, TGFBR1, TGFBR2, WASL, YES1* |
| Regulation of actin cytoskeleton | $7x10^{-6}$ | miR-10b, 126, 139-5p, 143, 145, 155, 338-3p | *ACTA1, ACTB, ACTG1, APC, ARPC5, CFL2, CRK, CRKL, FGF1, FGF5, FGF7, GIT1, ITGA6, ITGAV, ITGB8, KRAS, LIMK1, LIMK2, MAPK1, MYH9, MYH10, MYLK, PDGFRA, PIK3CA, PIK3R1, RAC1, ROCK1, SOS1, SSH2, TIAM1, VAV3, WASL* |
| Focal adhesion | 0.0004 | miR-126, 139-5p, 143, 145, 155, 338-3p | *ACTB, ACTG1, BCL2, CAV2, CCND1, CCND2, COL1A1, COL5A1, COL5A2, CRK, CRKL, FLNB, IGF1R, ITGA6, ITGAV, ITGB8, MAPK1, MYLK, PDGFD, PDGFRA, PIK3CA, PIK3R1, RAP1B, RAC1, ROCK1, SOS1, VAV3* |
| Tight junction | 0.0038 | miR-10b, 139-5p, 143, 145, 155 | *ACTB, ACTG1, AMOTL1, ASH1L, CLDN1, CTTN, EPB41, INADL, KRAS, LLGL2, MAGI2, MPP5, MYH9, MYH10, PARD6B, PPP2R3A, PRKCE, VAPA, YES1* |

| | | | |
|---|---|---|---|
| ***(3) Immune-response*** | | | |
| T cell receptor signaling | 0.0015 | miR-10b, 139-5p, 143, 145, 155 | CARD11, CBL, CD28, FOS, ITK, KRAS, MAP3K14, NFAT5, NFATC1, PIK3CA, PIK3R1, PPP3CA, SOS1, SPNS1, VAV3 |
| B cell receptor signaling | 0.025 | miR-10b, 139-5p,143, 145, 155 | PIK3CA, FOS, KRAS, PIK3R1, CARD11, VAV3, NFATC1, PPP3CA, NFAT5, JUN |
| ***(4) Growth Factors*** | | | |
| TGFβ signaling | $7x10^{-5}$ | miR-10b, 139-5p, 143, 145, 155 | *ACVR1B, ACVR2A, ACVR2B, GDF6, INHBB, MAPK1, ROCK1, RPS6KB1, SMAD1-5, SP1, TGFBR1, TGFBR2, ZFYVE9* |
| ErbB signaling pathway | 0.0002 | miR-126 139-5p, 143, 145, 155, 338-3p | *ABL2, CAMK2D, CAMK2G, CBL, CRK, CRKL, ERBB3, ERBB4, GAB1, KRAS, MAPK1, MAP2K4, PIK3CA, PIK3R1, RPS6KB1, SOS1* |

Significant pathways affected by LPC-enriched microRNA and target genes. The target genes of LPC-enriched microRNAs were correlated with KEGG pathway database to unfold their potential effect on limbal epithelium events.

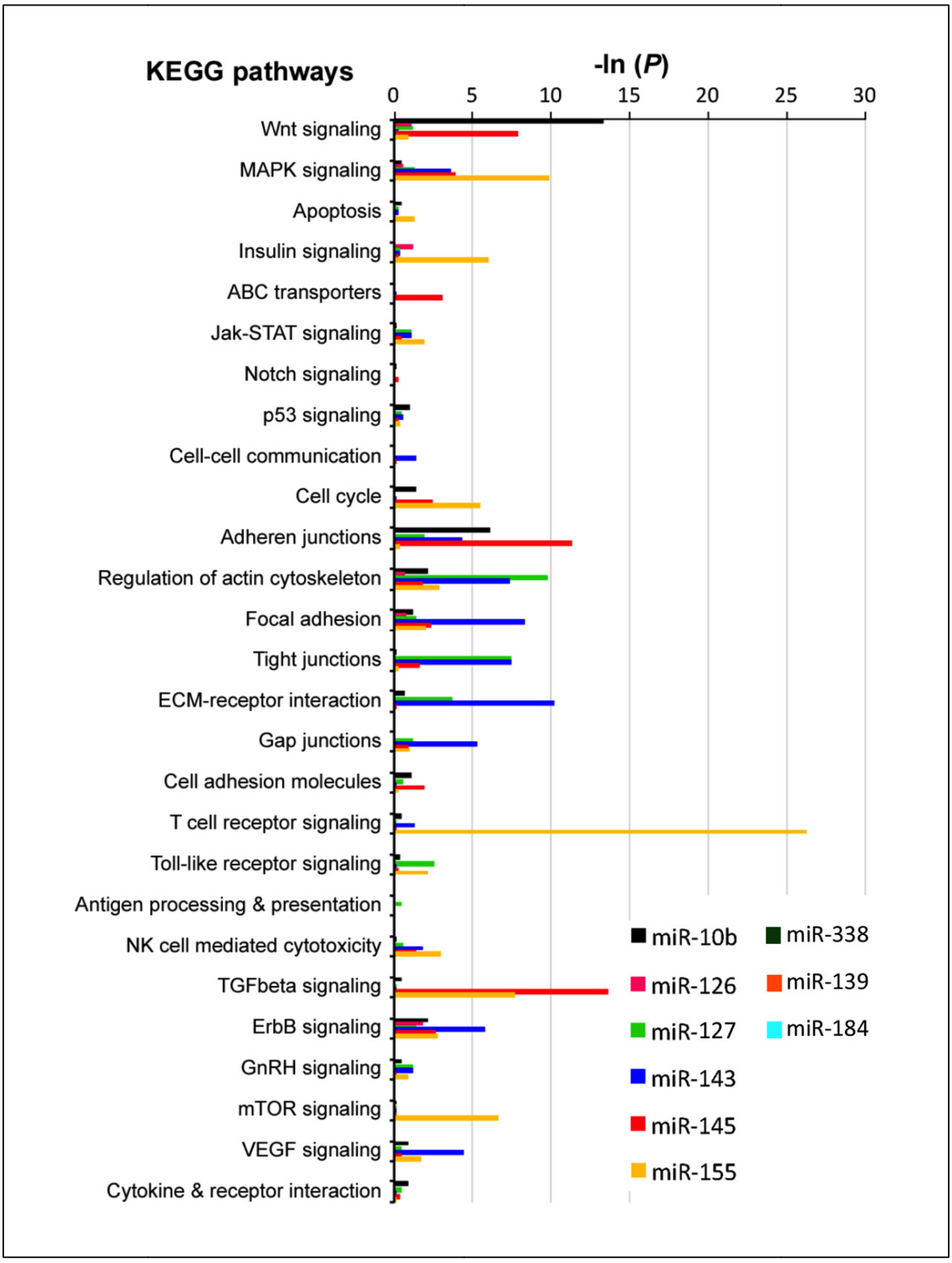
KEGG pathways
-ln (P)
0
5
10
15
20
25
30
Wnt signaling
MAPK signaling
Apoptosis
Insulin signaling
ABC transporters
Jak-STAT signaling
Notch signaling
p53 signaling
Cell-cell communication
Cell cycle
Adheren junctions
Regulation of actin cytoskeleton
Focal adhesion
Tight junctions
ECM-receptor interaction
Gap junctions
Cell adhesion molecules
T cell receptor signaling
Toll-like receptor signaling
Antigen processing & presentation
NK cell mediated cytotoxicity
TGFbeta signaling
ErbB signaling
GnRH signaling
mTOR signaling
VEGF signaling
Cytokine & receptor interaction
miR-10b
miR-126
miR-127
miR-143
miR-145
miR-155
miR-338
miR-139
miR-184

**Figure 4.11 the correlation analysis of each microRNA associated with KEGG pathway terms.**

The correlation analysis on the target genes of 6 limbal specific microRNAs overlapping with the KEGG pathway terms, calculated using Fisher exact test. The *P* value was transformed to -ln, the higher score the less *P* value, which represented more genes associated with that KEGG term. The significant value is 3.0 [-ln (0.05)].

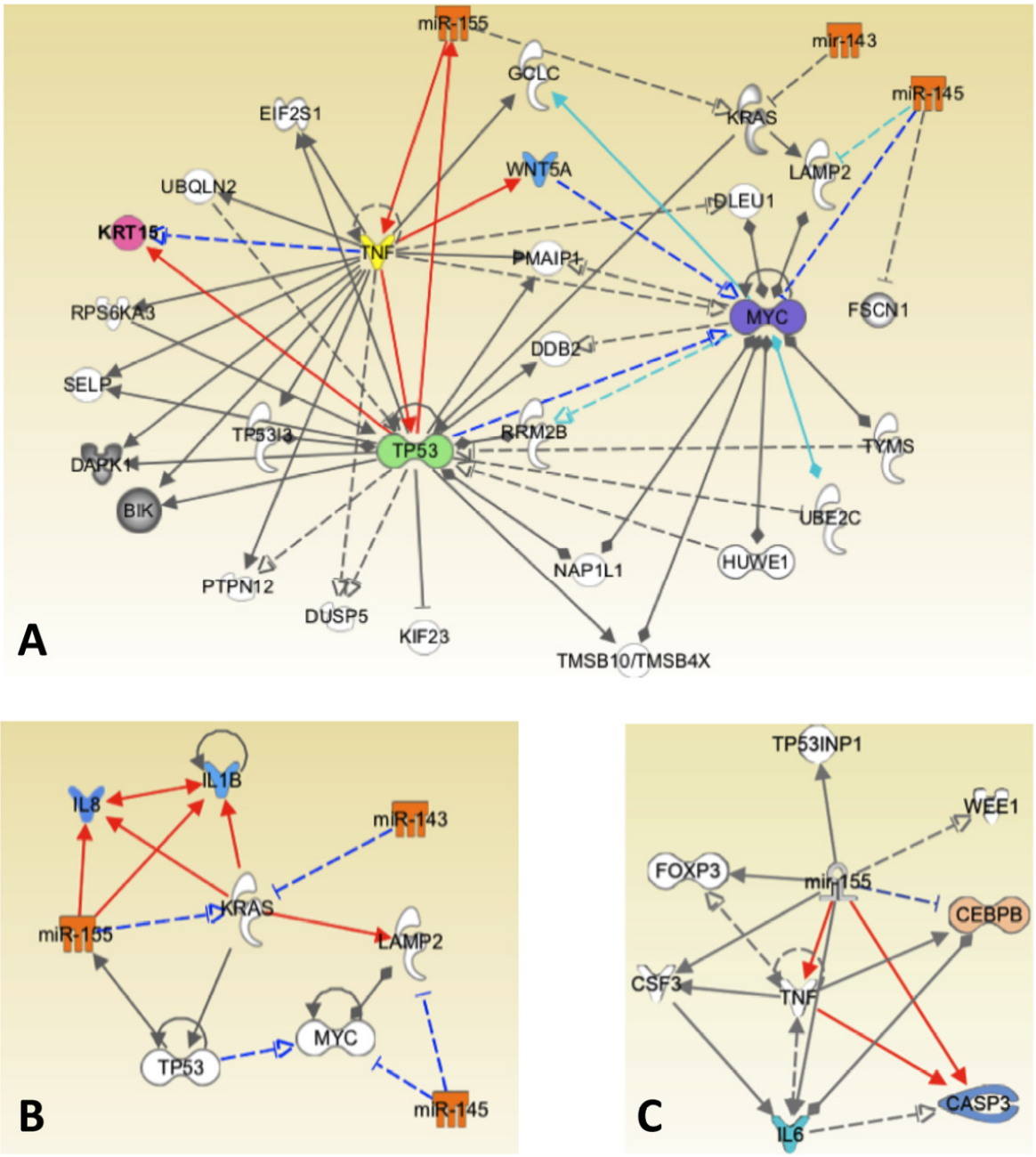


**Figure 4.12 IPA® analysis of miR-143/145 and miR-155**

Regulatory network formed by miR-143, 145 and 155 and protein interaction illustrating their potential roles on limbal stem cell regulation. The image was created using the Ingenuity Pathways Analysis® (IPA®) platform by overlapping experimental observed interaction onto a global molecular network from the Ingenuity® knowledgebase. Highlighted icon: arrows indicate activation, dotted arrows for gene

direct/indirect suppression, dotted lines for microRNA direct inhibition. (**A**) TP53/Myc network formed by the concerted action of miR-143, 145 and 155. (**B**) IL8/IL1B feedback loop regulated by miR-155. (**C**) Inhibitory effect of miR-155 on CEBPB and activation of CASP3.

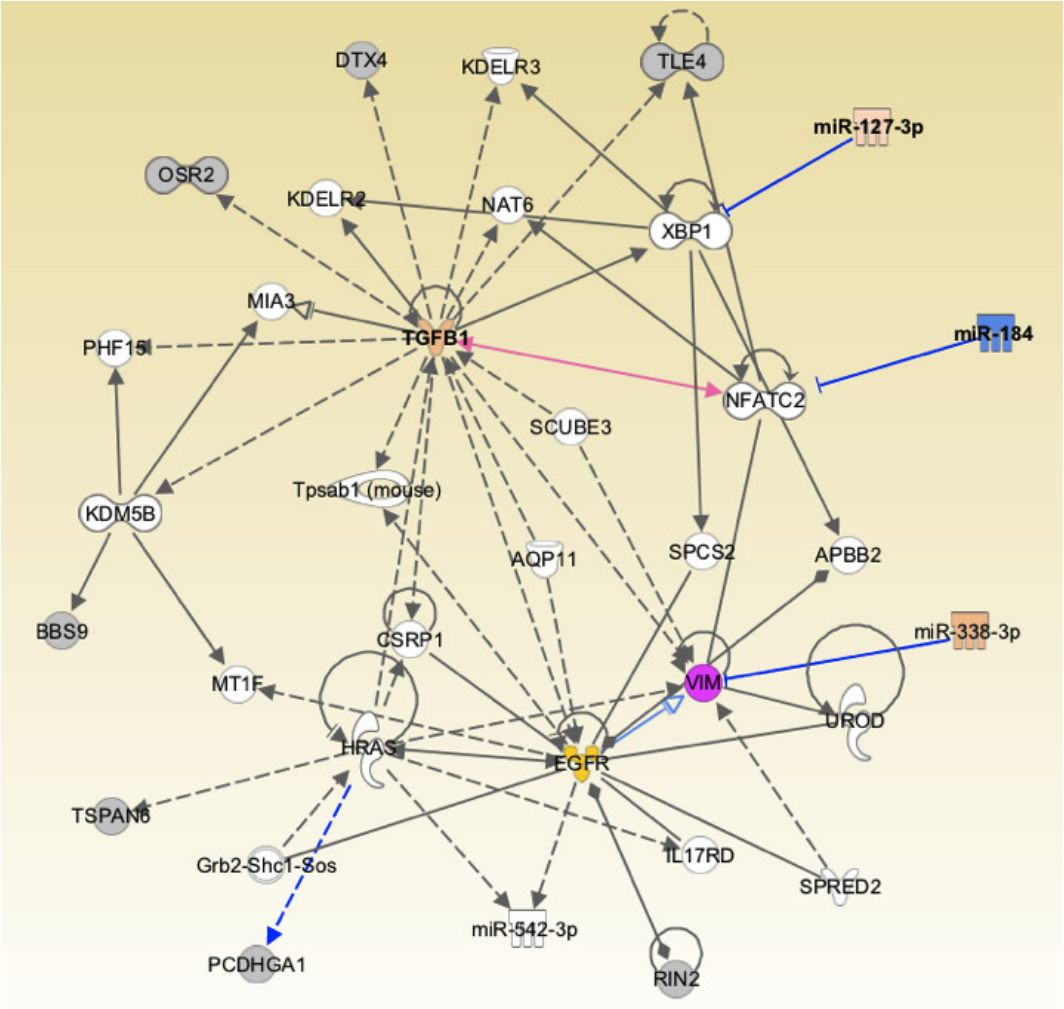


**Figure 4.13 IPA® analysis of miR-127-3p, miR-184 and miR-338-3p**

Regulatory network formed by miR-127-3p, miR-184 and miR-338-3p and protein interaction illustrating their potential roles on limbal stem cell regulation. The image was created using the Ingenuity Pathways Analysis® (IPA®) platform by overlapping experimental observed interaction onto a global molecular network from the Ingenuity® knowledgebase. Highlighted icon: arrows indicate activation, dotted arrows for gene direct/indirect suppression, dotted lines for microRNA direct inhibition.

## 4.4 CEPC-associated microRNAs and pathologic corneas

### 4.4.1 Pathologic corneas — pterygium

Pterygium is a result of destruction of limbal stem cells (CEPC) by UV radiation, followed by invasion of conjunctiva cells on corneal basement membrane. As a hyperplasic disorder, the occurrence of pterygium showed similarities with tumorigenesis. Hence, we used pterygium as a CEPC disease model to explore the potential microRNA functions in aberrant CEPCs and ocular surface tumorigenesis. All pterygium samples obtained from Hong Kong Chinese patients, collected from Hong Kong Eye Hospital and Prince of Wales Hospital after an informed consent was obtained. One donated cornea specimen with pterygium supplied by Hong Kong Lions Eye Bank was recruited to show the morphology of pterygium in cornea.

The histochemistry of pterygium by hematoxylin and eosin (H&E) staining showed the morphology of pterygium at early stage (the pterygium did not pass limbal region). Pterygial epithelial cells crossed the limbal barrier and centripetally migrated to the cornea (**Figure 4.14A**). Squamous metaplasia was observed in the leading edge of pterygium (**Figure 4.14B**). The Bowman's membrane underlying pterygium was dissolved, followed with the adjacent conjunctiva epithelial cells and non-transparent stromal fibroblast overlying the cornea surface. (**Figure 4.14 C&D).** In conjunctiva segment, the stromal fibroblasts were activated, accompanied by inflammatory cells infiltration, fibrovascular proliferation, ECM remodeling as well as extensive elastotic degeneration (**Figure 4.14E).** Interestingly, pterygial limbal epithelium exhibit less cell layers than the normal cornea, and the structure of CEPCs niche “Palisades of Vogt” was absent, implying the normal CEPCs was damaged (**Figure 4.14D).**

### 4.4.2 Taqman® Real time PCR analysis on pterygium

#### 4.4.2.1 MicroRNA expression analysis of primary pterygium compared with human LPC epithelia and conjunctiva.

Total RNA from seven full-length of primary pterygium was extracted and reverse transcribed by TaqMan® microRNA reverse transcription kit. Four pairs of healthy human LPC epithelia and conjunctiva epithelia were used as calibrators to detect microRNA expression pattern in pterygium. MiR-205, 184, 143.145, 10b, 126 and 155 were quantified by TaqMan® microRNA assay. With the normalization of housekeeping U6, the results showed that miR-184, mir-143 and 145 were significantly up-regulated in pterygium compared to normal conjunctiva and LPC epithelia (miR-184: *p value* = 0.0155; relative intensity: pterygium = 3.137 ± 1.517, LPC = -0.5221 ± 2.587, Conjunctiva = 2.061 ± 0.3044; miR-143: *p value* = 0.0171, relative intensity: pterygium = 3.202 ± 1.290, LPC =0.2041 ± 1.436; conjunctiva = 1.042 ± 2.354; miR-145: *p value* = 0.0276, relative intensity: pterygium = 3.654 ± 1.475, LPC =0.6580 ± 0.9308; conjunctiva = 2.028 ± 2.105; one way ANOVA) (**Figure 4.15&4.16**). Interestingly, with the comparison between pterygium and LPC by Mann Whitney test, miR-10b and miR-155 were highly expressed in pterygium with significant difference (miR-10b; *p value* = 0.0424, relative intensity: pterygium = -0.2544 ± 1.414, LPC =-2.410 ±1.760; miR-155: *p value* = 0.0424, relative intensity: pterygium = -2.385 ± 1.546, LPC =-4.960 ±1.417). The expression level of miR-126 in pterygium was highest in all the detected microRNAs but was not pterygium-specific (p value =0.5334, relative intensity: pterygium = 4.885 ± 2.005; LPC=3.144 ± 1.827, conjunctiva=4.853 ± 2.570) (**Figure 4.16).** Accordingly, as summarized in **Table 4.7,** the expression level of miR-143/145

was CC < LPC< Coj < pterygium; miR-184 was CC > LPC < Coj < pterygium; miR-10b and 155 were CC < LPC = Coj < pterygium.

#### 4.4.2.2 MicroRNA expression analysis in pterygium epithelium and stroma

Pterygium consists of epithelium and stroma, which exhibited different cell features. Pterygium epithelium is the leading edge to invade corneal epithelium, which is characterized by epidermal proliferation with the expression of some stem cell markers. Pterygium fibroblasts from stroma display characteristics of transformed cells, including loss of heterozygosity and microsatellite instability.

To compare the differential expression of microRNA in pterygium epithelium and stroma, the epithelium and stroma of pterygium was separated using laser capture micro-dissection. The cryosection at 15 μm were mounted onto PEN membrane slides and processed for LCM. The laser cut along the contour of the target region on the section and the underlying membrane, followed with collected samples in individual sterile eppendorf tubes (500 ul in volume) containing Trizol® reagent (**Figure 4.17**). TaqMan® real-time microRNA analysis identified the relative expression ratio of pterygium epithelium compared with stroma (using stroma as calibrator). The result showed that miR-10b, 126 143, and 145 was up-regulated in pterygium stroma at 11.29 fold, 6.25 fold, 4.51 fold and 12.58 fold change higher than epithelium. Conversely, miR-184 was up-regulated in epithelium at 2.54 fold changes higher than stroma respectively. Fold change of miR-155 and 205 were less than 2.0 (fold change was 1.73 and 1.84, respectively), which were considered as sample variation.

### 4.4.3 The spatial distribution of microRNA in pterygium

To detect the localization of microRNAs in pterygium, in situ hybridization with LNA-based microRNA probes was performed on pterygium cryosections (6 μm in thickness). The probe with scramble sequence was used as negative control, while small nuclear RNA U6 probe was used as a positive control. For a better detection of microRNA expression, both NBT/BCIP and fast red substrate were used for color reaction. NBT/BCIP is blue-purple (depending on the pH of solution); it is sensitive but is easy to produce non-specific signals. Fast red substrate can be detected by red florescence, which is less sensitive but more specific.

Pterygium displayed a strong signal of miR-143 and 145 in epithelium and stroma (**Figure 4.20 A&D**). MiR-143/145 was present in the pterygial epithelium with more intensive signal in the basal and suprabasal layers (**Figure 4.20 B&E**). In the stromal compartment, miR-143/145 was specifically positive in the fibrovascular and some fibroblasts (**Figure 4.20 C&F**). The hybridization intensity of miR-145 in stroma was stronger than miR-143, which was consistent as real-time result (miR-145 in pterygium stroma was 12.58 fold higher than epithelium; whereas miR-143 in pterygium stroma was 6.35 fold higher than epithelium).

However, the NBT/BCIP staining (**Figure 4.19**) showed inconsistent results compared to the fast red. The stronger blue signal in the epithelium compared to stroma may be because of NBT/BCIP accumulating in the cells after long incubation time. To avoid this interference, fast red substrate was used in the later study to reveal the microRNA signals.

MiR-126 was abundant in the pterygial epithelium compartment with a strong signal detected in all layers of epithelium (**Figure 4.21A&B**). The specific localization of miR-126 was also detected in the fibrovascular stroma (**Figure 4.21C**). In contrast, a strong signal of miR-10 was observed in pterygial stroma but negative in epithelium, the expression of miR-10 was intense in the collagen of fibroblast cells ((**Figure 4.21D&E**). This observation was consistent as the result from real-time PCR that miR-10b was dramatically up-regulated in pterygial stroma at 11.29 fold change than epithelium. MiR-155 was moderately expressed in the basal layer of pterygial epithelium and stroma with a weak signal (**Figure 4.21C**). U6 was used as positive control and stained in the nuclear region (**Figure 4.20C**). Negligible staining was found for sections hybridized with scrambled sequences ((**Figure 4.20D**).

In summary as shown in **Table 4.7**, the in situ hybridization localized the microRNA expression in pterygium, miR-126, 143, and 145 were intensively detected in both pterygium epithelium and stroma. This observation supported the result from microRNA quantitative analysis in comparison between pterygium， LPC, and conjunctiva. However, the pterygial epithelium contained more intensity of miR-126, 143, 145 than stroma in ISH, which was inconsistent with microRNAs analysis on LCM-isolated epithelium and stroma. This may be because of the pterygial stroma has high level of inflammation and angiogenesis with more expression of growth factors and cytokines. The miR-126, 143, 145 may be up-regulated by these growth factors and were enriched in the fibrovasular and inflammatory cells in stroma.

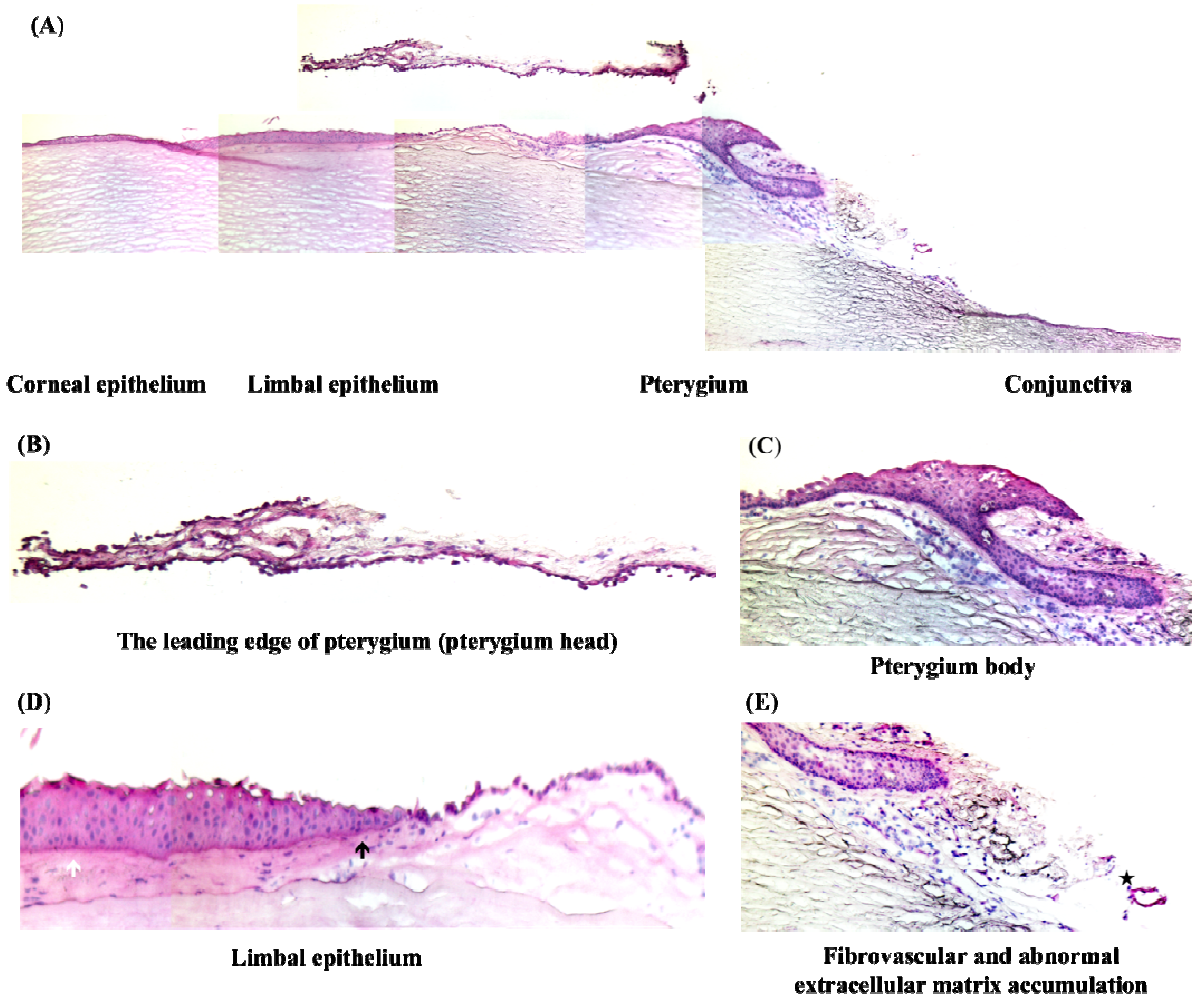


**Figure 4.14 The histochemistry of pterygium specimen by hematoxylin and eosin (H&E) staining**

Whole cornea with pterygium were sectioned and stained with hematoxylin and eosin. (A) The morphology of pterygium growth from limbal epithelium. (B) The pterygium epithelium that centripetally invades the cornea display squamous metaplasia and goblet cell hyperplasia. (C) The epidermal proliferation and fibroblasts activation in pterygium body. (D) The absence of Bowman's membrane in regions adjacent to the proliferating epithelium (black arrow). Bowman's layer is intact approaching the central cornea (white arrow). (E) The fibrovascular, inflammatory infiltration and extensive elastotic degeneration in the conjunctival segment.

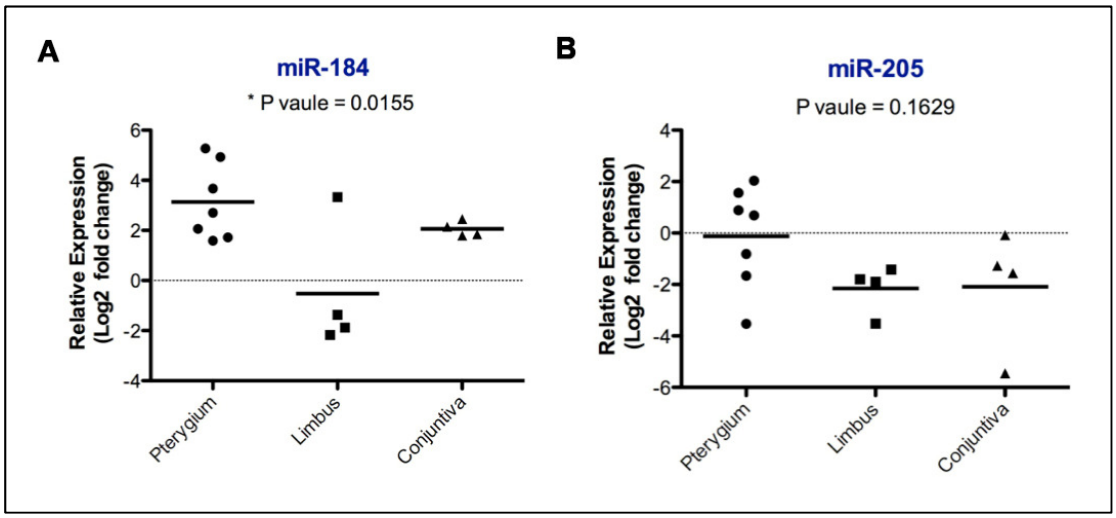


**Figure 4.15 Expression analysis of mR-184 and miR-205 in primary pterygia, compared to normal conjunctiva and LPC epithelia**

TaqMan® real time PCR quantified the expression level of miR-205 and miR-184 in LPC, conjunctiva and pterygium. MiR-205 had no statistically significant difference between pterygium, conjunctiva and LPC epithelium. MiR-184 was significantly up-regulated in pterygium as compared to LPC and conjunctiva. The data were normalized with housekeeping U6, the fold change were transformed to log2 scale. Significance was calculated by One way ANOVA with $P < 0.05$ considered to be statistical significant.

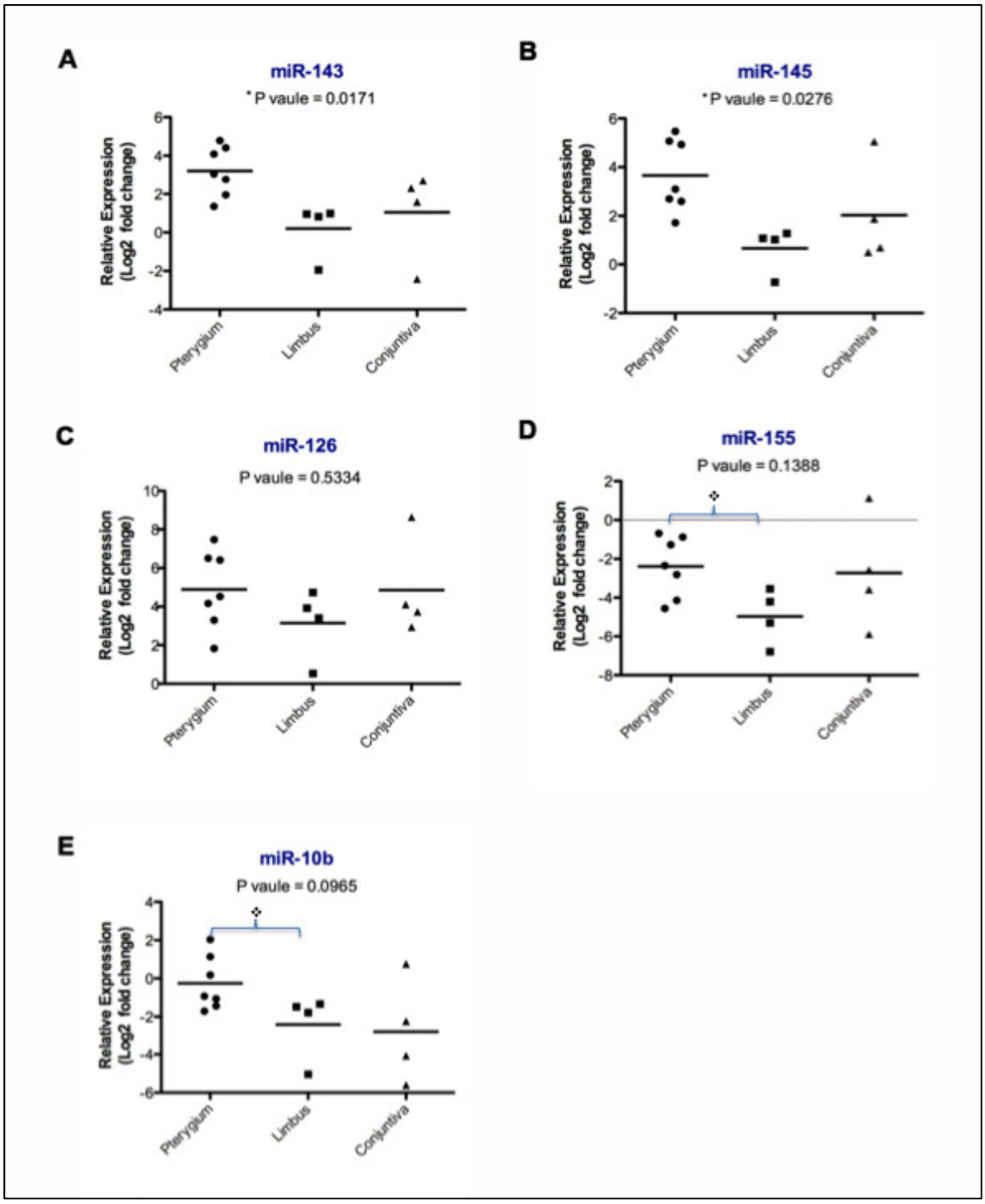


**Figure 4.16 MicroRNA expression analysis in primary pterygium**

Using TaqMan® real-time PCR, the expression level of miR-143/145 and miR-126, 10b, and 155 in primary pterygium, normal LPC epithelium and conjunctiva was

quantified and compared. miR-143 and 145 were significantly up-regulated in pterygium as compared to LPC and conjunctiva ($P$ = 0.0171 and 0.0276, respectively; One way ANOVA). Comparing between LPC epithelium and pterygium, miR-10b and 155 were significantly up-regulated in pterygium ($P$ = 0.0424 and 0.0310, respectively; Mann Whitney U-test). The data were normalized with housekeeping U6; the fold changes were transformed to $\log_2$ scale; $P < 0.05$ was considered statistical significant.

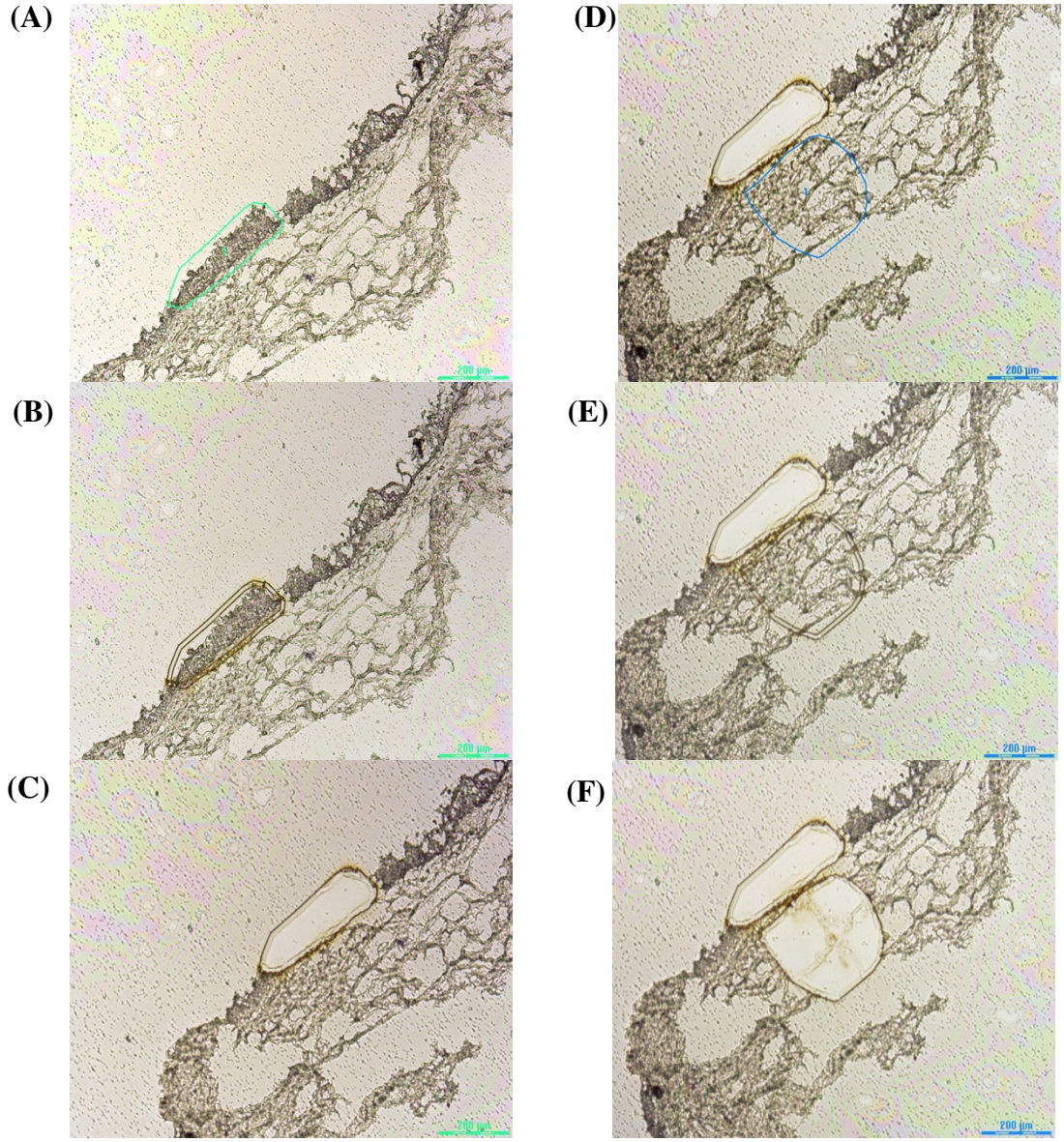


**Figure 4.17 Laser capture micro-dissection of a pterygium**

Procedure of LCM on pterygium: (A) A line drawn to define the region of epithelium. (B) The membrane was cut by real-time laser along the track. (C) Epithelium specimen was collected into an Eppendorf tube by gravity. (D) A line drawn to define the region of stroma. (E) The membrane was cut by real-time laser along the track. (E) Stroma specimen was collected into an Eppendorf tube by gravity.

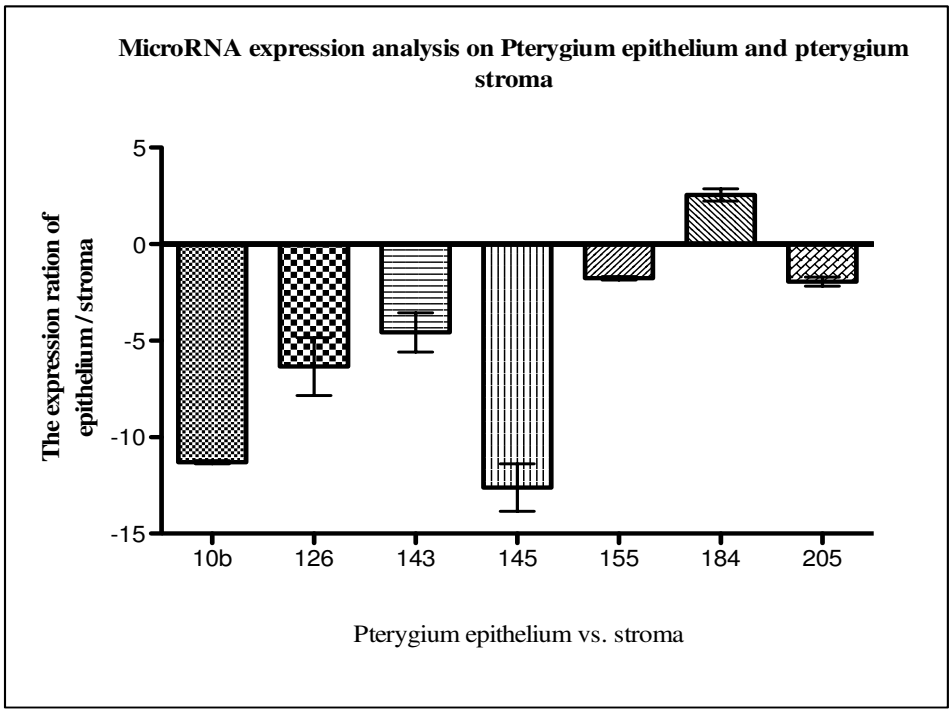


**Figure 4.18 MicroRNA expression analysis in pterygium epithelium and stroma.**

TaqMan® real-time PCR quantified the expression level of microRNAs in pterygial epithelium and stroma. The expression ratio between epithelium and stroma was calculated by ΔCt value. The data were normalized with housekeeping U6.

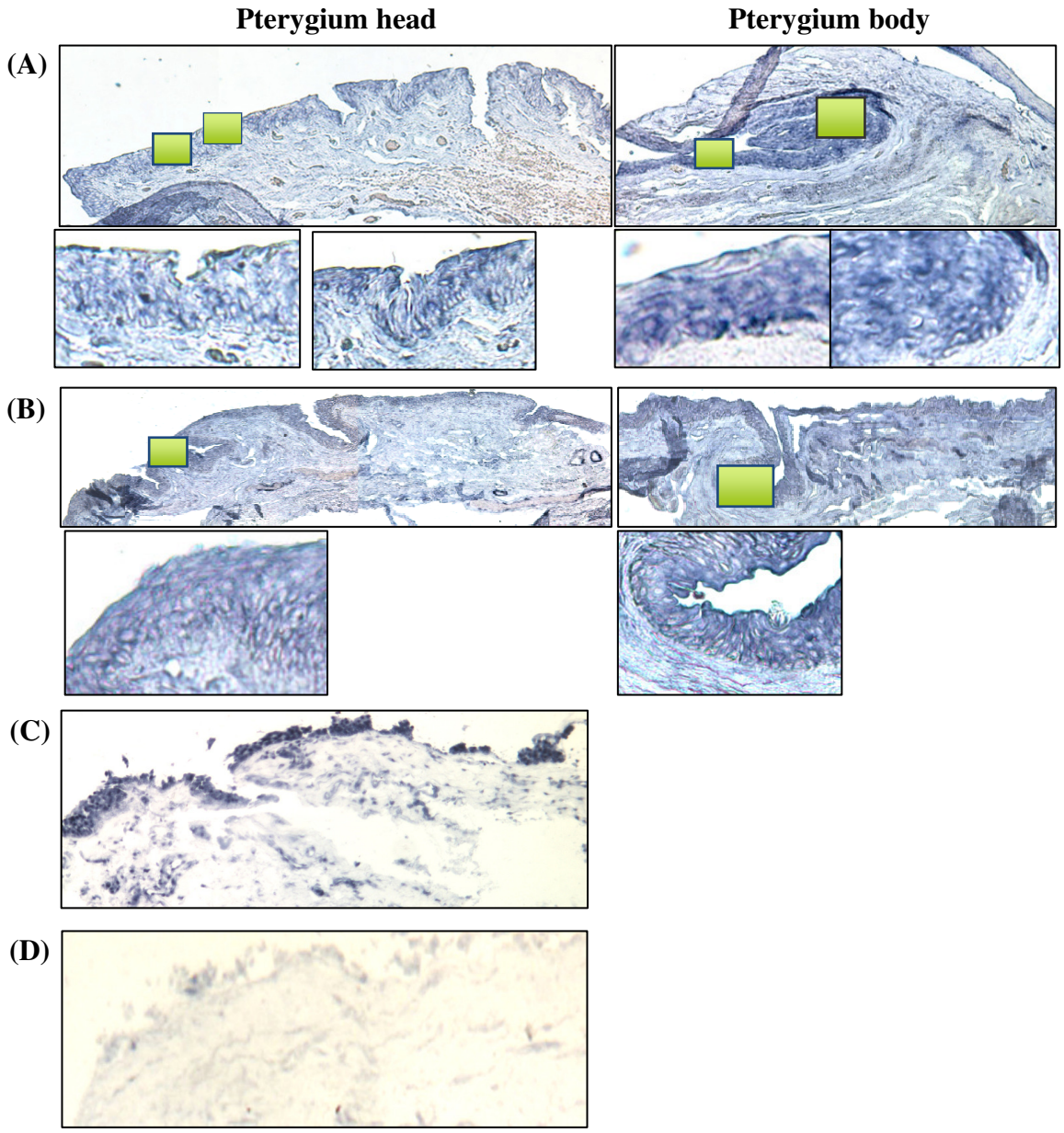


**Figure 4.19 Localization of miR-143 and miR-145 in pterygium (NBT/BCIP reduction method)**

Spatial distribution of miR-143 and miR-145 in the cross section of pterygium head and body by in situ hybridization High magnification of the areas was indicated by square. (A) miR-143, (B) miR-145, (C) U6 positive control, (D) scrambled negative control.

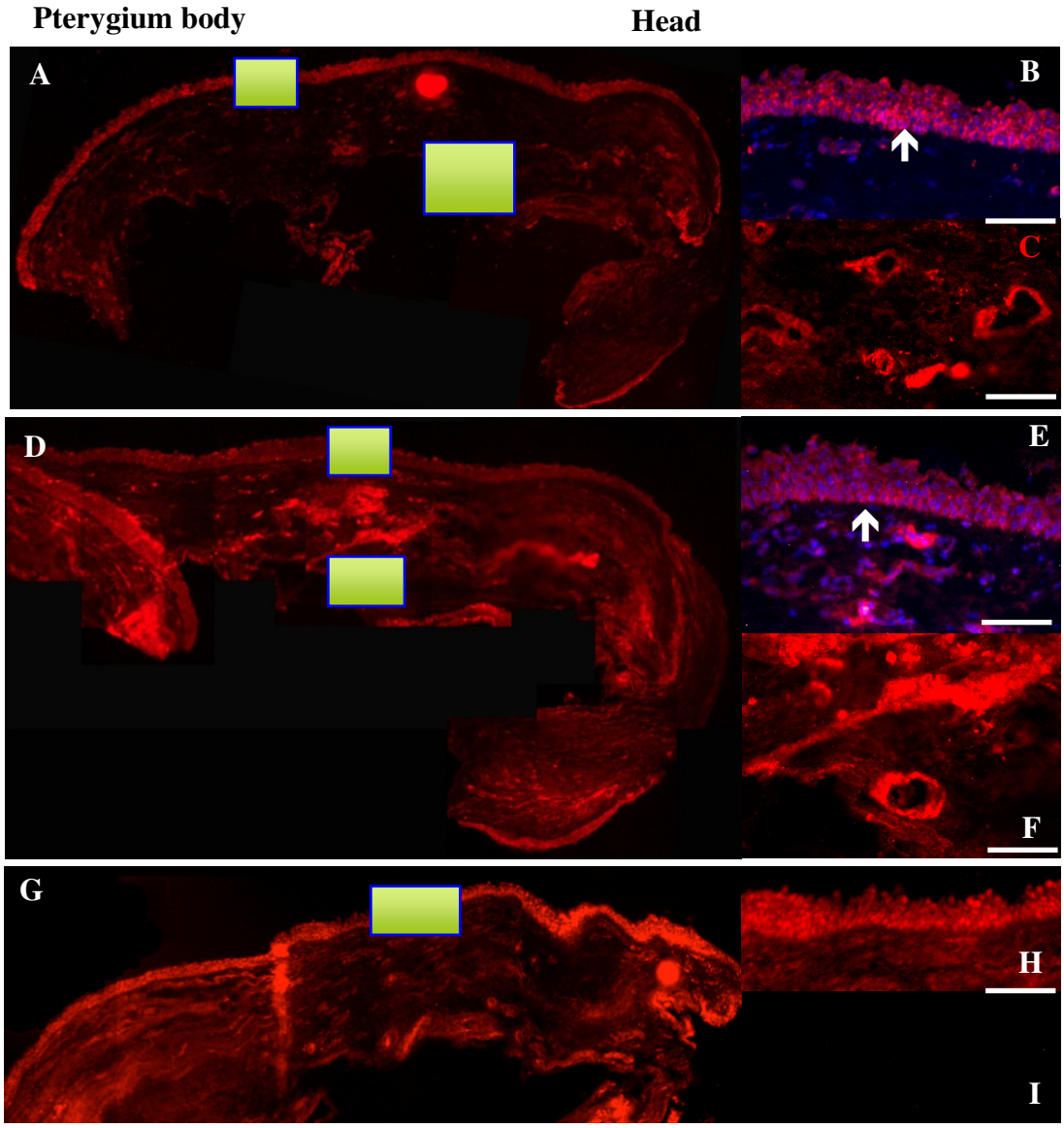


**Figure 4.20 Localization of miR-143/miR-145 in pterygia (fast red method)**

Spatial distribution of miR-143 and miR-145 in pterygial head and body region by in situ hybridization with signal developed by fast red method. Nuclear was stained blue with DAPI. High magnifications of the areas were indicated by square. (A) The distribution of miR-143 in stroma and epithelium of pteryglium. (B&D) Strong signal of

miR-143 was detected in the basal layer of epithelium (white arrow) and fibrovascular. (D) The distribution of miR-145 in stroma and epithelium of pterygium. (E&F) higher magnification disclosed the miR-145 was more intensive in the basal layer (white arrow) and fibrovascular. (G&H) U6 as positive control was positive in nuclear. (I) scrambled negative control, no fluorescence detected. Scale Bar: 100 um.

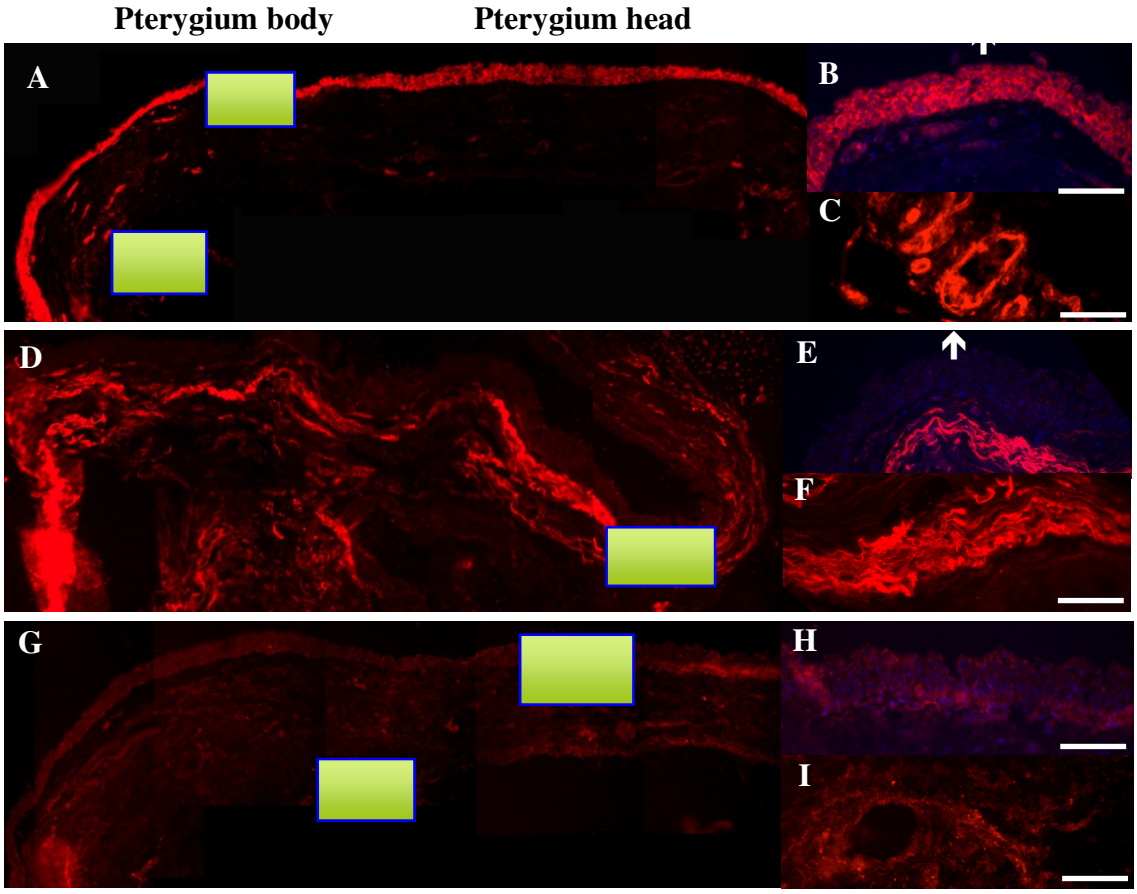


**Figure 4.21 Localization of miR-126, 155 and 10b in pterygium (fast Red)**

Spatial distribution of miR-126, 10b, 155 in the cross-section of pterygial head and body regions by in situ hybridization with signal revealed by fast red method. Nuclei are stained blue with DAPI. High magnification of the areas was indicated by square. (A-C) miR-126 was abundant in epithelium, and fibrovasular. (D-F) miR-10b was enriched in pterygial stroma, but negative in pterigial epithelium (white arrow). (G-I) miR-155 was weakly expressed in both pterygial epithelium and stroma. U6 positive control and scrambled negative control were as same as miR-143/145. Scale bar: 100 um.

### 4.4.4 Correlated localization of microRNAs with pterygium related molecules

To explore the correlation between specific microRNA and its protein in pterygium, a protocol for combination of microRNA in situ hybridization and immunohistochemistry was performed on the same section of pterygium, to reveal the correlation between microRNA and pterygium related molecules.

#### 4.4.4.1 Correlation of microRNAs with p53 in pterygium

Tumor suppressor p53, as the positive regulator of miR-143/145, has been identified to be abnormally expressed in pterygium. Transcriptional activity of miR-143 and 145 can be enhanced by p53 in tumor cells (Boominathan, 2010). In this study, we correlated the expression of p53 with miR-143/145 by the combination staining of in situ hybridization and immunohistochemistry. In addition, IPA® network disclosed that p53 can up-regulate miR-155 with the activation of TNF-α, to verify this network, miR-155 was parallel stained with P53.

**Immunohistochemistrical staining for P53 in primary pterygium**

Prior to parallel staining, immunohistochemistrical staining for p53 was performed to confirm the expression pattern using anti-p53-CM1 antibody in 5 primary pterygia. One donated cornea with pterygium was recruited to compare the expression of p53 in cornea, pterygium and conjunctiva from same specimen. Spatially restricted expression of p53 was observed in cornea with pterygium that p53 was present in pterygium but not negative in conjunctiva and cornea (**Figure 4.22**). Unexpectedly, as opposed to the reported p53 nuclear – positive pattern, our result showed that p53 was located in both nuclear and cytoplasm of the epithelial cells (**Figure 4.23 A&B**). In particular, specific nuclei staining were found in the epithelium of pterygium head

(**Figure 4.23C&D**), whereas cytoplasmic localization of p53 was observed in pterygium body within the same sample (**Figure 4.23E&F**).

Interestingly, this was the first observation on cytoplasmic p53 in pterygium. Up to date more than 20 reports have identified p53 expression in pterygium, but the prevalence of p53 positive staining pterygium varied from 7.9% to 100% (Y. Y. Tsai, Chang, et al., 2005). One factor causing this variation in different studies might be the different p53 antibody used in immunohistochemistry. In our study, we used anti - p53 CM1 antibody to recognize the whole segment of p53 protein in both the nucleus and the cytoplasm, while DO7 or DO1 can just bind shorter segments of p53 protein (**Figure 4.23H)**. In parallel experiment, both CM1 and DO1 antibody was used to stain the same sample, only CM1 group showed the positive result (**Figure 4.23G**). p53 antibody used in other studies was either DO7 or DO1, which may be the cause for the inconsistent findings in different groups. From the prognostic evaluation for cancer patients, CM1 was proved to be the most sensitive antibody in detection of p53 (H. Zhang, 1999). Consequently, our immunohistochemistry results revealed the cytoplasmic localization of p53 in primary pterygium. The cytoplasmic localization of p53 was induced by cellular stress signals, which mainly function on triggering apoptosis via mitochondrial outer membrane permeabilization (MOMP) and inhibits autophagy (Green & Kroemer, 2009).

**Double staining of miR-143, 145 with P53**

To detect the correlation between p53 and miR-143/145 cluster in pterygium, we combined the in situ hybridization of microRNA probes with immunohistochemistry of p53 in the same pterygium section. By parallel staining in pterygium, the distribution of miR-143/145 can be overlapped with P53 in both epithelium and stroma (**Figure 4.24**

**A&B**). The higher magnification illustrated the co-localized of miR-143 and 145 in the epithelium, suggesting the correlated expression of the p53 and miR-143/145.

**Double staining of miR-155 with P53**

Parallel staining of miR-155 and p53 in pterygium showed the expression level of p53 was much stronger than miR-155. Staining of miR-155 was weak in both epithelium and stroma. The higher magnification illustrated miR-155 was more intensive in the basal epithelium, whereas p53 was present in all layer of epithelium, suggesting the miR-155 expression was not correlated with p53 (**Figure 4.24**).

### 4.4.4.2 Co-localization of miR-126 and IL6 in pterygium

IL-6 produced from corneal epithelium fibroblast and endothelium is abundant in the inflamed cornea, and functions to promote the corneal epithelial cells growth. IL-6 can be induced by UVB in pathogenesis of pterygium, which may induce inflammation and angiogenesis (Di Girolamo et al., 2002).

IL-6 was correlated with miR-126, the endothelium-enriched microRNAs. The parallel staining showed miR-126 and IL-6 were co-localized in the epithelium and the blood vessel of the stroma **(Figure 4.25).** However, strong signal of IL-6 was also detected in the superficial layer of pterygial epithelium, but the hybridization intensity of miR-126 was weaker in outer layer. This observation may be due to the fact that IL-6 was a secreted cytokine that was primarily expressed in the epithelial surface.

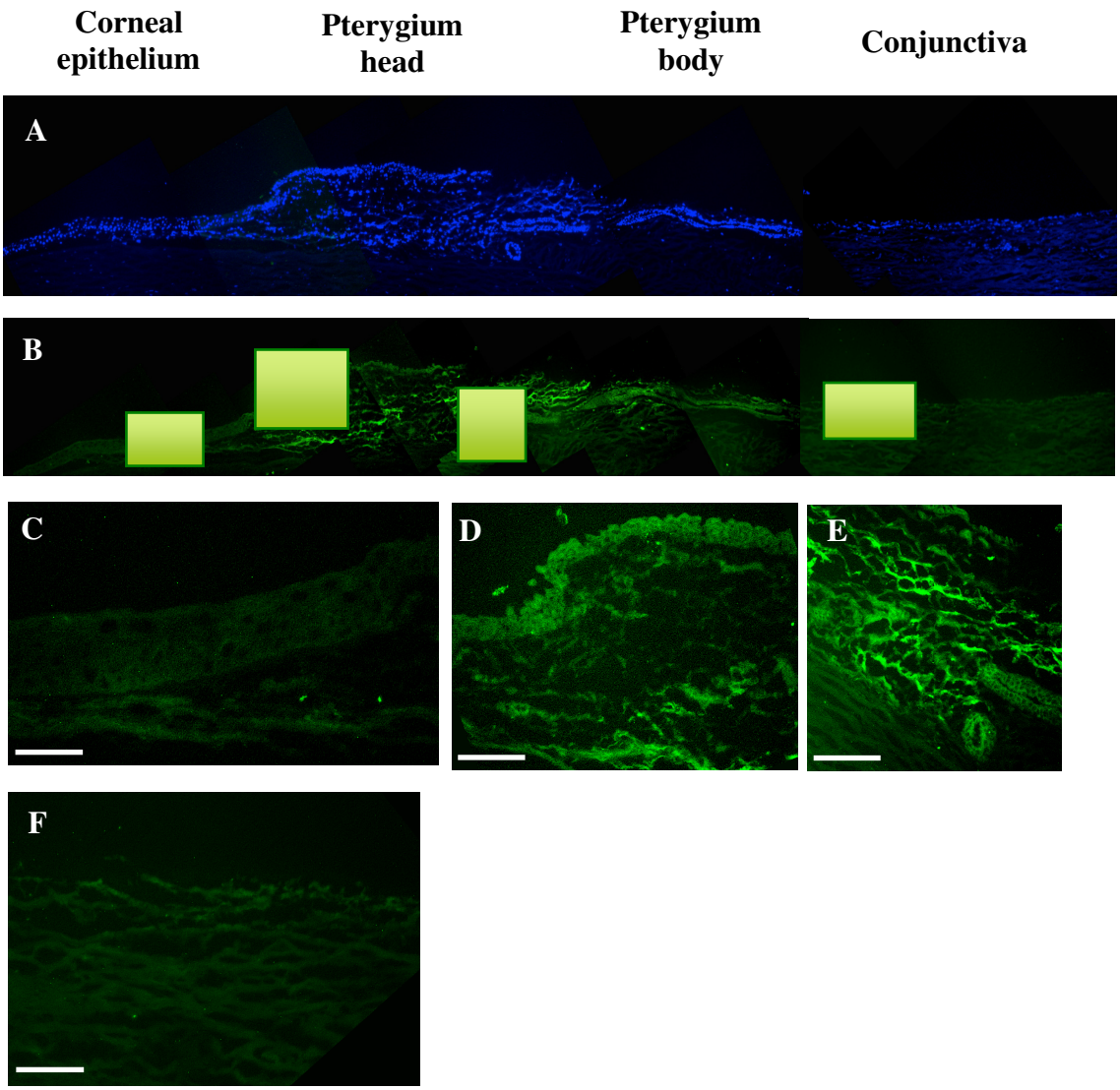


**Figure 4.22 Expression of p53 in a donated cornea with pterygium.**

(A) Whole specimen was counterstained with DAPI to distinguish the cell nuclei (blue). (B) Immunohistochemistry staining of p53 on cornea, pterygium and conjunctiva. (C) Expression of p53 was negative in corneal epithelium. (D, E) p53 was strongly expressed in pterygium head and body. (F) Expression of p53 was absent in conjunctiva.

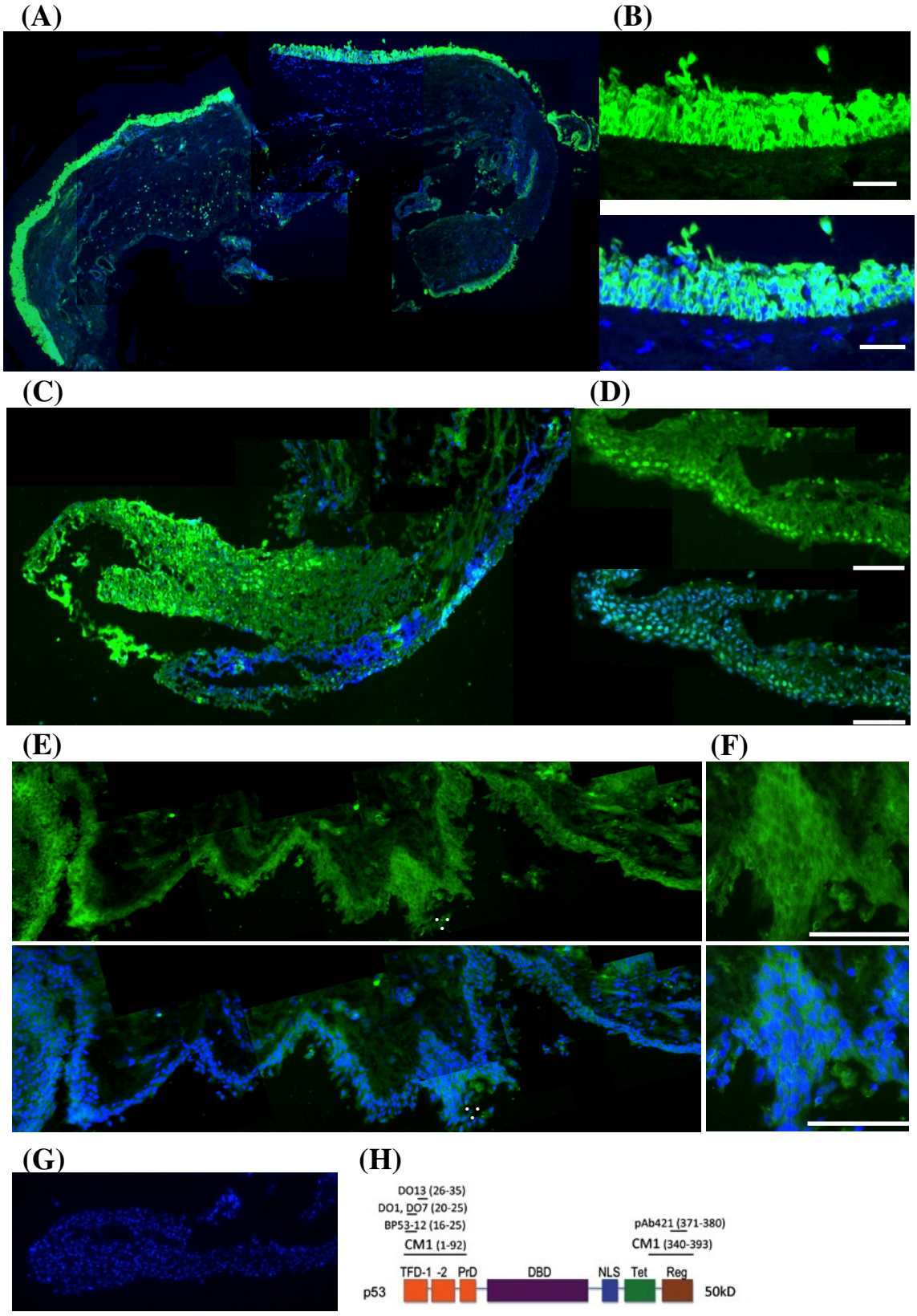
(A)
(B)
(C)
(D)
(E)
(F)
(G)
(H)
DO13 (26-35)
DO1, DO7 (20-25)
BP53-12 (16-25)
CM1 (1-92)
pAb421 (371-380)
CM1 (340-393)
TFD-1 -2 PrD
DBD
NLS
Tet
Reg
p53
50kD

**Figure 4.23 Nucleus and cytoplasmic distribution of p53 in primary pterygium**

Localization of p53 in pterygium, nuclei are stained blue with DAPI (A) p53 was strongly positive in all layers of pteryglial epithelium . (B) Higher magnification (20x) showed the p53 was stained in both nucleus and cytoplasm. (C) p53 was expressed in the epithelium of pterygium head . (D) Higher magnification (20x) showed the nucleus staining of p53. (E) p53 was expressed in the epithelium of pterygium body in. (F) Higher magnification (40x) showed the cytoplasmic localization of p53. (G) immunostaining with anti - p53 DO1 antibody on PT54 showed a negative signal of p53. (H) Different anti-body for p53 immunohistochemistry detection. Scale bar: 100 um.

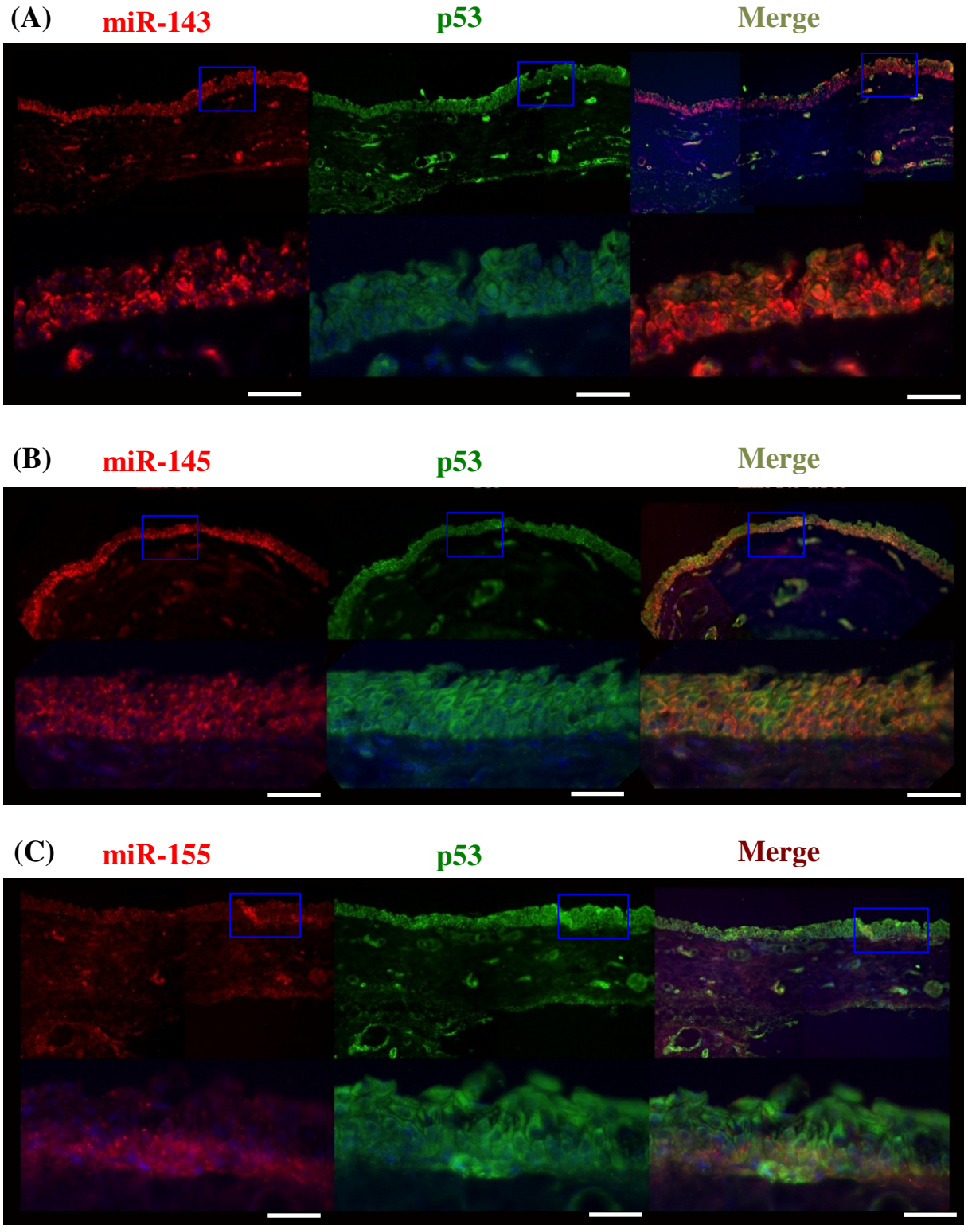
(A)
miR-143
p53
Merge
(B)
miR-145
p53
Merge
(C)
miR-155
p53
Merge

**Figure 4.24 Double staining of miR-143, 145, 155 with p53**

**Double** staining of miR-143, 145, and 155 with p53 by combination of in situ hybridization (red fluorescence) and immunohistochemistry (green fluorescence) using microRNA specific probes and anti-p53 CM1 antibody. Nuclei are stained blue with DAPI. High magnifications of the areas indicated by an asterisk. (A) Localization of miR-143 (red) and p53 (green) in pterygium epithelium and stroma. MiR-143 overlapping with p53 (orange) exhibited a co-localized expression pattern. Higher magnification (40x) showed the clear co-localization of miR-143 with p53 in cytoplasm. (B) Localization of miR-145 (red) and p53 (green) pterygium epithelium and stroma. MiR-145 overlapping with p53 (yellow) exhibited a co-localized expression pattern. Higher magnification (40x) showed the clear co-localization of miR-143 with p53 in cytoplasm. (C) Localization of miR-155 (red) and p53 (green) pterygium epithelium and stroma. The expression of miR-155 in pterygium was weak and cannot be overlapped with p53. Higher magnification (40x) showed miR-155 was intensive in the basal layer and p53 was present in all layers of epithelium. Scale bar: 100 um.

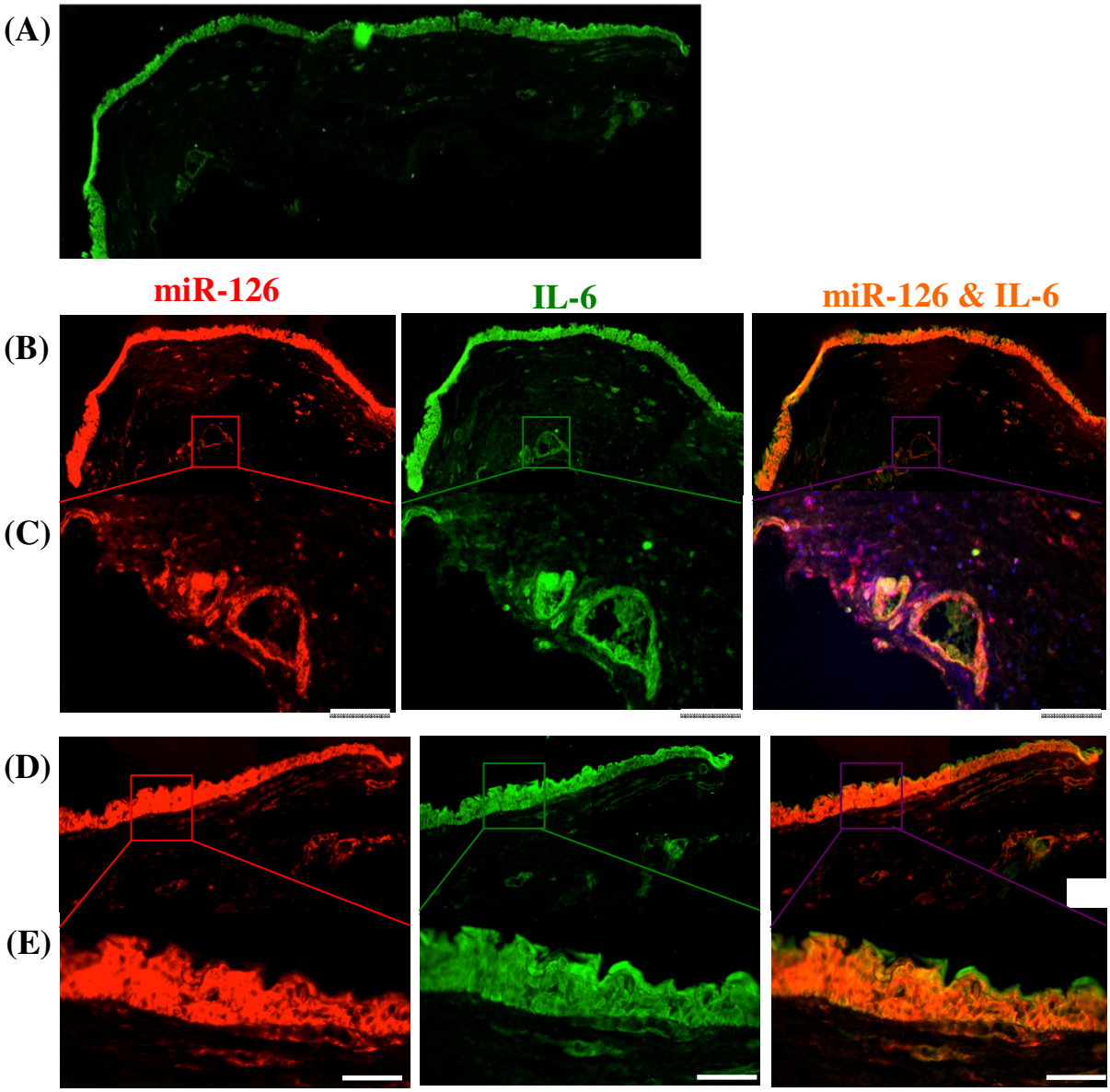


**Figure 4.25 Double staining of miR-126 and IL-6 pterygium**

Double staining miR-126 and IL-6 by combination of in situ hybridization (red fluorescence) and immunohistochemistry (green fluorescence) using miR-126 specific probes and anti- IL-6 antibody. Nuclei are stained blue with DAPI. High magnification of the areas was indicated by square. (A) IL-6 expression was positive in pterygium epithelium and fibrovascular, and weakly stained in stroma. (B). Localization of miR-

126 (red) and IL-6 (green) in epithelium and stroma of pterygium body. MiR-126 overlapping with IL-6 (orange) exhibited a co-localized expression pattern. (C) Co-localization of miR-126 and IL-6 in vascular (D) Double staining of IL-6 and miR-126 in the head of pterygium. (E) Overlapping IL-6 with miR-126 in the epithelium of pterygium showed IL6 was more intensive in the outer layer. Scale bar: 100 um.

## 4.5 Function analysis of miR-143/145 transfected pterygial cells

### 4.5.1 Overexpression of miR-143/145 in primary cultured pterygium cells

48 hours after transfection, the cells were harvested for RNA extraction. The overexpression level of miR-143/145 was validated by Taqman® real-time PCR, miR-143 and 145 was elevated by 36.37 fold and 285.03 fold respectively as compared to scrambled control – transfected cells (**Figure 4.26**).

### 4.5.2 Cell cycle and gene expression analysis of miR-143/145 transfected cells

48 hours after transfection, the pterygial cells with miR-143 and miR-145 transfection was dramatically decreased as compared with scrambled control (**Figure 4.26A**), indicating that the overexpression of miR-143 and miR-145 in pterygial cells can induce cell death. To confirm the microRNA-induced cell apoptosis, cell cycle analysis was performed on the miR-143/145 or scrambled sequences transfected pterygial cells by fixing the cells and treating with propidium iodide (PI, 5 ug/ml) to bind the nuclear chromatin. The dye was measured by FASC to quantitatively assess DNA content. Meanwhile, to evaluate the immuno-activity of p53 in this microRNA-induced cell death, the transfected pterygial cells were incubated in parallel with anti-p53 CM1 antibody followed by adding appropriated secondary antibody, the immune-intensity was measured by FASC as well. The florescence intensity was transformed with log2 unit, and the cells events were normalized with the percentage. Thus, the highest events (peak) represent the highest percentage of the cells, X-axis of the peak indicate the expression intensity of the majority of cells. Here, the expression level of each group was determined by comparing the intensity of each cell peak.

The cell cycle in scrambled control group consisted of 7.32% sub-G0 (DNA less than one copy, cleavage), 74.03% G0/G1 (quiescent cells with one DNA copy), 3.46% cells were in S phase (cells undergoing DNA replication), and 15.19% G2/M (mitotic cells). The overexpression of miR-143 and 145 increased the cells in sub-G1 phase were 26.88%, and 40.9% respectively, indicating cell death and DNA cleavage (**Figure 4.27)**. Furthermore, miR-145 transfected cells with highest apoptosis percentage exhibited an increased normalized staining intensity of p53 with the peak of intensity shift right, as compared with scrambled**.** But no difference was observed in miR-143 transfected cells when compared to scrambled control. Thus, our results suggested that miR-143 and 145 trigger the cell death in pterygium, at the same time, miR-145 could enhance the expression of p53 (**Figure 4.28**).

One negative regulator of p53, MDM2 was the predicted target of miR-145. TargetScan database (Human V6.2) showed miR-145 the 3' UTR of MDM2 mRNA partially complementary with miR-145 at 8mer seed match, which implicated a high probability of direct binding. To detect the machinery of miR-145 up-regulation on p53, we detected MDM2 expression level by real-time PCR and FASC on the miR-145 transfected cells. 48 hours after transfection, cells were harvested for RNA extraction or ethanol fixation. Real-time PCR quantified the expression level of MDM2 in miR-143/145 transfected cells when using scrambled group as calibrator. As compared with scrambled negative control, the expression level of MDM2 in miR-145 transfected cells was significantly down-regulated. This result indicated that the expression level of MDM2 was decreased by 2 fold with the elevation of miR-145 compared to scrambled cells **(Figure 4.29A)**. To confirm the protein expression of MDM2 after miR-145 transfection, cells were fixed and stained with MDM2 antibody; the immune-intensity

was detected using FASC. As shown in **Figure 4.29B**, MDM2 signal intensity of the peak was left-shift in miR-145 transfected cells when compared to scrambled control, which indicated the expression intensity was decreased with miR-145 ectopic expression. Therefore, our result confirmed that the expression of MDM2 was suppressed by miR-145, which may be a direct target of miR-145 in regulation of pterygium.

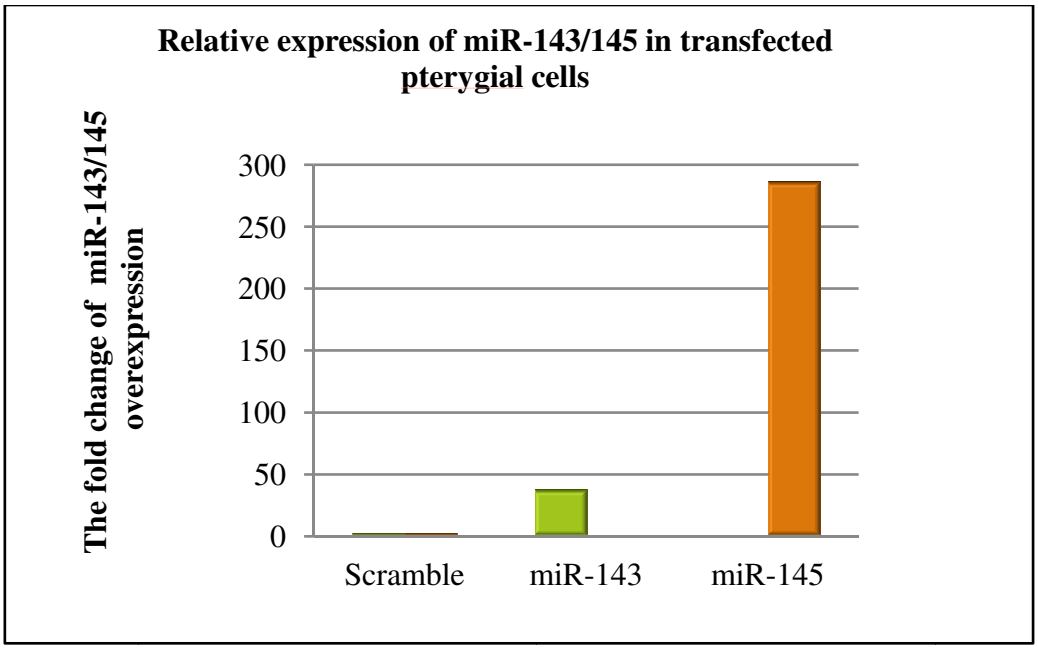


**Figure 4.26 miR-143 and 145 overexression in pterygium cells**

The expression level of miR-143 and 145 was validated by quantitative real-time PCR after transfection. The relative expression level of miR-143 and 145 was elevated by 36.37 fold and 285.03 fold respectively compared to scrambled control.

**(A) Transfected cells**

**(B) Cell cycle analysis (PI)**

**Scrambled**

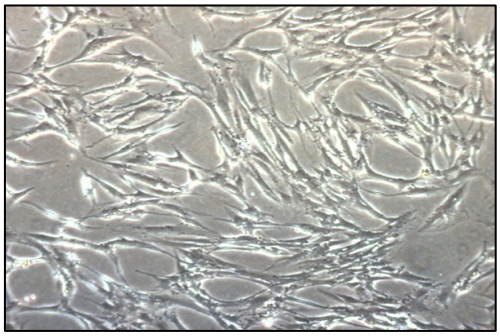

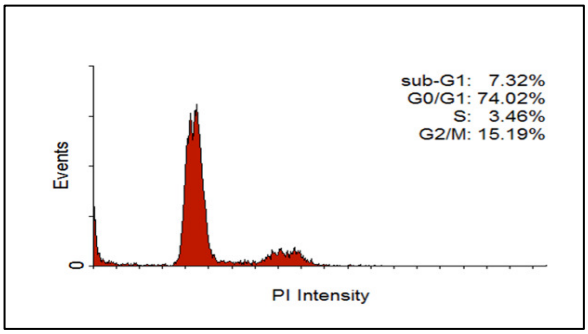


**miR-143**

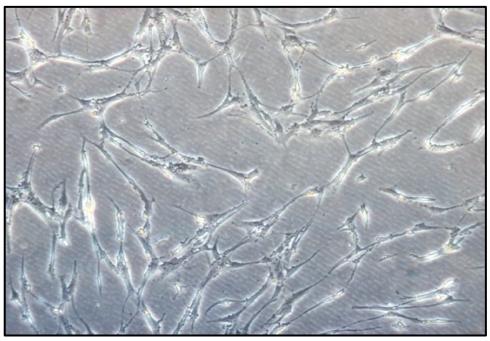

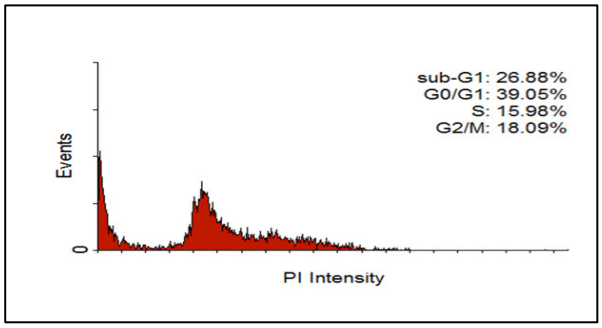


**miR-145**

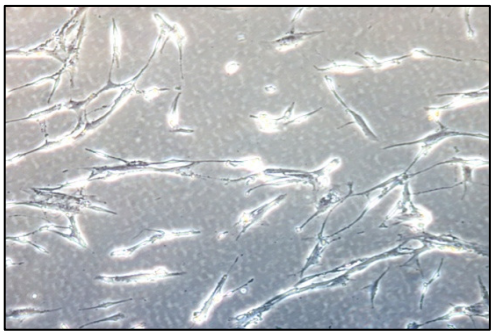

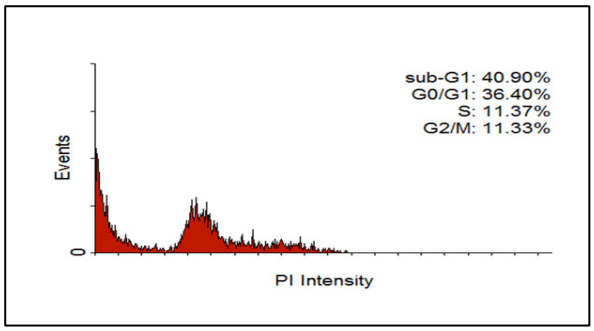

**Figure 4.27 Cell cycle analysis of pterygial cells transfected with miR-143/145**

(A) 48 hours after transfection, pterygial cells were dramatically decreased compared with scrambled. (B) Flow cytometry histogram analysis showing the cell cycle after miR-143/145 transfection in primary cultured pterygiual cells (passage = 3), the sub G1 phase is 7.32% in scrambled, 26.85% in miR-143 transfected and 40.9% in miR-145 transfected cells.

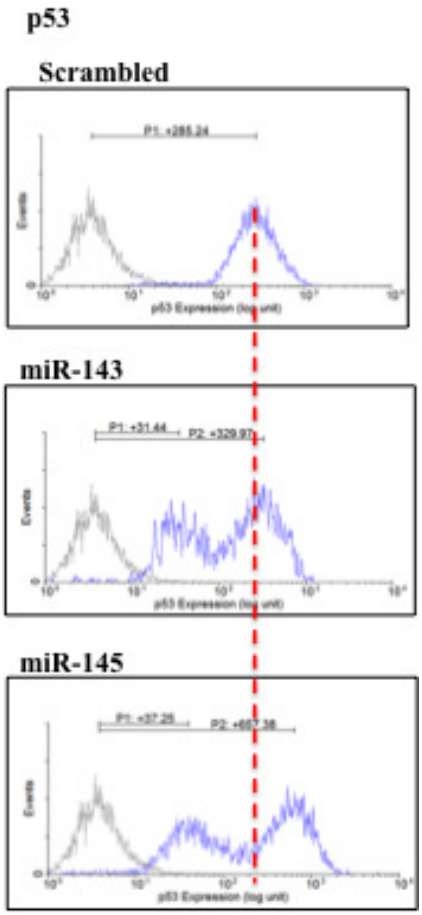


**Figure 4.28 p53 expression in pterygial cells transfected with miR-143/145.**

p53 expression in miR-143 and miR-145 transfected cells, p53 expression was increased in miR-145 transfected cells (peak right-shift ) compared to scrambled, but no change on miR-143 transfected cells.

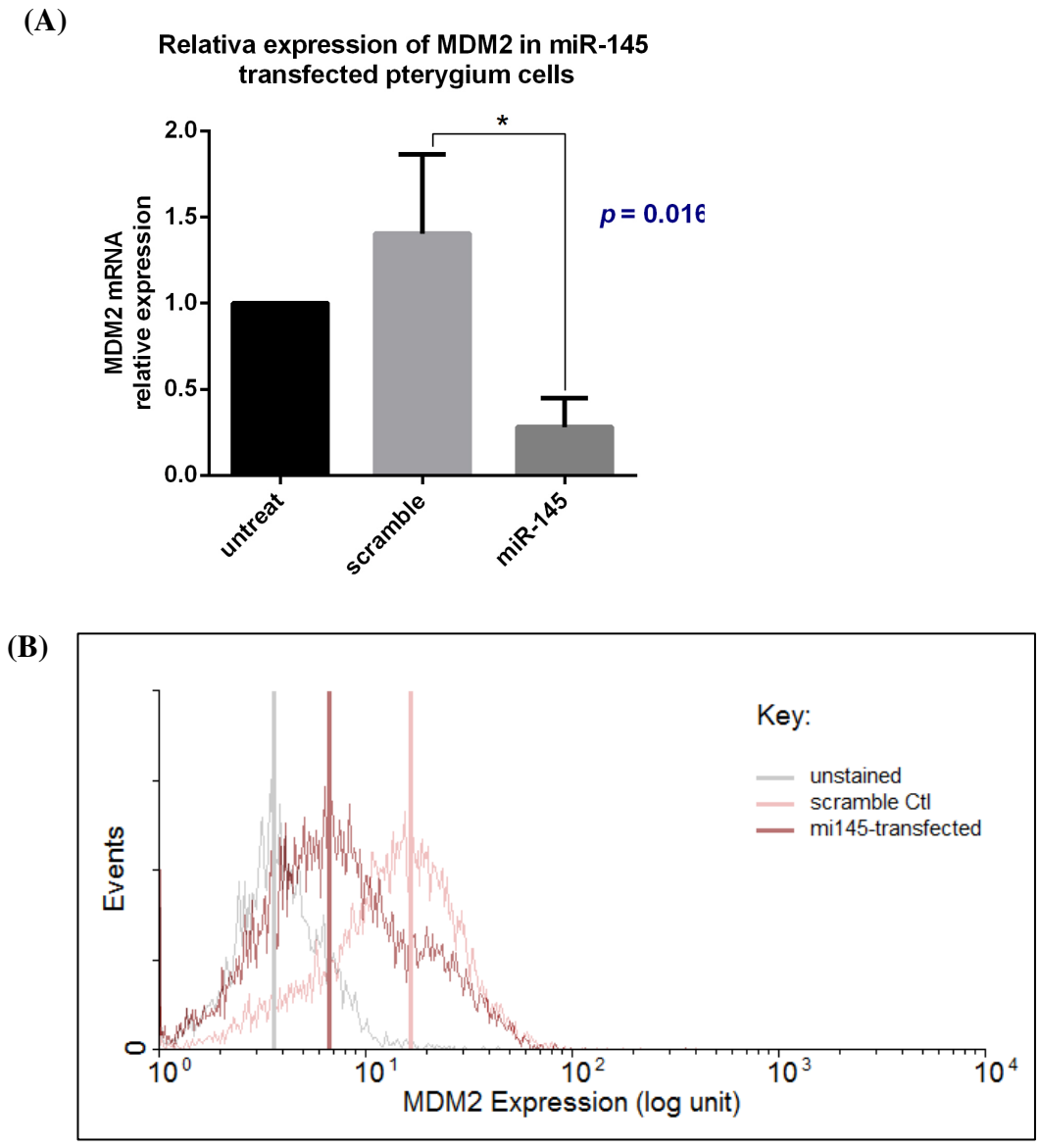


**Figure 4.29 miR-145 suppress the expression of MDM2 expression in pterygium cells**

(A) Quantitative real-time PCR identified the expression of MDM2 in scrambled, miR-143 and 145 transfected cells. The expression of MDM2 was reduced 2 folds in miR-145 transfected cells compared with scrambled control. (B) Flow cytometry

histogram analysis showing MDM2 expression in pterygial cells transfected with miR-145, the peak of MDM2 intensity in miR-145 transfected cell was left shift as compared to scrambled control.

# Chapter 5 Discussion

## 5.1 Human corneal – epithelia enriched microRNAs

Our study elucidated the role of microRNAs in human corneal epithelium homeostasis. From microarray study, 37 microRNAs were found to be enriched in human corneal epithelium. The expression profile was closer to human skin keratinocytes and RPE than to the neuronal retina, indicating these microRNAs were associated with the regulation of epithelial cell property. Among them, some are known to be crucial for the epithelium growth and maintenance. For example, miR-184 and 205 were reported to be abundantly expressed in mouse corneal epithelium (Ryan, Oliveira-Fernandes, & Lavker, 2006a). MiR-205 was constitutively expressed in both limbal and corneal epithelia, whereas miR-184 was specifically present in the basal and suprabasal layers of corneal epithelium but not in the limbal epithelium. They acted antagonistically on regulating SHIP2 level in the epithelial cell proliferation (Yu et al., 2008a). As miR-184 is also reported as a tumor suppressor, its expression in cornea could be related to arrest corneal cell overgrowth and regulating apoptosis for a homeostatic control between the differentiated epithelial cells and less differentiated progenitor cells. Moreover, miR-200c and 205 were down-regulated during the epithelial to mesenchymal transition (EMT) induced by transforming growth factor beta (TGFβ) (P. A. Gregory, Bert, et al., 2008). In contrast, their over-expression prevented EMT or altered the morphological change from mesenchymal to epithelial transition (P. A. Gregory, Bert, et al., 2008; P. A. Gregory, Bracken, Bert, & Goodall, 2008). MiR-200c and 205 targeting to the transcription repressors (ZEB1 and ZEB2), regulated E-cadherin-associated cellular adhesion and migration and cytoskeletal changes during

epithelial maintenance (Hurteau, Carlson, Roos, & Brock, 2009). Stem cell antigen-1 (Sca-1) in mouse mammary epithelial cells also induced miR-205 expression and promoted cell proliferation (Greene, Gunaratne, Hammond, & Rosen, 2010). Unlike in retinal cells, the sensory organ-specific cluster miR-182/183/96 (S. Xu et al., 2007) was weakly expressed in human corneal epithelium (gTotal Gene Signal for miR-96 was -0.651, miR-182 was -0.862, and miR-183 was -0.612). Also, the retinal terminal neuron-expressing miR-124a (K. Liu et al., 2011a) had negligible expression (total gene signal was -3.574). Interestingly, miR-24, 125b and 214 that were enriched in human corneal epithelium had been reported to be associated with retinal development of *Xenopus* (Decembrini et al., 2009) and miR-214 was also expressed in choroids (F. E. Wang et al., 2010a).

## 5.2 The coreanl epithelium expressed miRNAs

MicroRNA microarray identified 18 microRNAs differentially expressed in CC and LPC epithelim, TaqMan® real-time PCR vaildated miR-142-3p, 142-5p, 146a, 149, 193b, 211, and miR-376a were expressed in human corneal epithelia but they were not limbal specific. The target genes of these microRNAs were correlated with the reported CEPCs related markers or growth factors in modulating corneal epithelium homeostasis to explore the potential roles (**Table 5.1A&B**). Many Stem cell makers were targeted by these microRNAs; p63 was targeted by miR-10b, 211,149 and 184; Integrin α9 was targeted by miR-142-5p; ABCG2 was the pridicted target of miR-142-3p, miR-145 and miR-146a.

The CC epithelium abundant microRNA miR-193b predict target on the current reported corneal epithelium expressing molecus TCF4 and SPRR. MiR-193b and miR-

149 have been reported to be increased upon calcium-induced keratinocyte differentiation and terminally differentiated keratinocytes, meanwhile, miR-376a was reduced by more than 2 fold change in the undifferentiated keratinocyte; exhibited a similar trend as CC epithelia and LPC epithelia in same differentiation status (Hildebrand et al., 2011). MiR-193b functions as promoting brown adipocyte abiogenesis by blocking myogenesis in brown fat (L. Sun, Xie, et al., 2011), as well as a tumor suppressor (Leivonen et al., 2011). Hence its roles may sever the same as miR-184 that repressed cell proliferation in central corneal epithelium. MiR-142–3p and 146a were identified highly expressed in human fetal choroid (16-20 wk). Mir-211 was identified to be expressed in fetal human retinal pigment epithelium (RPE) together with miR-204, function as maintaining epithelial phenotype of human RPE (Tang, Sun, Wang, Du, & Liu, 2010; F. E. Wang et al., 2010b). miR-142-3p and 142-5p were enriched in peripheral blood mononuclear cells. 142-3p was essential for hematopoiesis (Nishiyama et al., 2012) . Moreover, miR-142-3p can target on ABCG2 in colon cancer cells (Shen, Zeng, Zhu, & Fu, 2013).

**Table 5.1A Corneal epithelium expressed microRNAs predicted target on CEPCs markers.**

| Gene | Protein | microRNA entities | |
|---|---|---|---|
| | | **Limbal epithelium** | **Corneal epithelium** |
| *Transcription factors* | | | |
| *TP63* | P63 | miR-10b, miR-211 | miR-149, miR-184 |
| *TCF4* | TCF4 | miR-142-5p, miR-145, miR-146a, miR-155, miR-211 | miR-193b |
| *CEBPB* | C/EBPδ | miR-155 | |
| *HIF1AN* | HIF1AN | miR-211 | miR-184 |
| *Transporter molecules* | | | |
| *ABCG2* | ABCG2 | miR-142-3p, miR-145, miR-146a | |
| *Glycolytic enzymes* | | | |
| *ENO1* | α-enolase | miR-143 | |
| *Intercellular signaling molecule* | | | |
| *NOTCH1* | Notch1 | | miR-149 |
| *Cell matrix interaction molecules* | | | |
| *ITGA9* | Integrin α9 | miR-142-5p | |
| *CDH2* | N-Cadherin | miR-145, miR-211 | |
| *Cytoskeletal protein* | | | |
| *KRT3* | *CK3/12* | miR-142-3p | |
| *Keratinocytes cross-linked envelope* | | | |
| *SPRR* | *SPRR family* | | miR-193b |
| *IVL* | Involucrin | miR-211 | |

**Table 5.1B Corneal epithelium expressed microRNAs predicted target on corneal related growth factors.**

| Gene | Protein | microRNA entities | |
|---|---|---|---|
| | | **Limbal epithelium** | **Corneal epithelium** |
| ***Growth factor and receptor*** | | | |
| ***EGFR*** | EGFR | miR-155 | |
| ***NGFR*** | NGFR (p75) | miR-143 | miR-149 |
| ***GDNF*** | GDNF | miR-142-5p, miR-143, miR-145, miR-211 | |
| ***GFRA1*** | GFRa-1 | miR-142-5p, miR-145, miR-155, miR-211 | |
| ***TGFB1*** | TGFB1 | miR-142-3p | |
| ***TGFBR1*** | TGFBR1 | miR-142-5p, miR-145, miR-211 | |
| ***HGF*** | HGF | miR-142-5p | |

## 5.3 8 limbal-sepcific microRNAs

By quantitative PCR analysis on additional 9 pairs of corneal samples, we have validated 8 microRNAs (miR-10b, 126, 127, 139-5p, 143, 145, 155 and 338) were significantly enriched in limbal peripheral corneal epithelium compared to central corneal epithelium. Conversely, miR-184 was significantly up-regulated in central corneal epithelium.

From literature search, miR-127 and miR-139-5p were biomarkers that were up-regulated in many tumor cells, such as hepatocellular carcinoma, colorectal cancer and breast cancer (Mosakhani et al., 2012; M. Yang et al., 2013). miR-338-3p was a oligodendrocyte-specific miRNAs in brain and spinal cord, functions as promoting neuronal differentiation via silencing the negative regulators of its host gene (Barik, 2008). For the functions of miR-127, 139-5p and 338 were not related with CEPCs, we excluded these three microRNAs and mainly focused on the expression of miR-10b, 126 and 155.

*In situ* hybridization analysis using LNA-modified oligo probes demonstrated miR-10b, 126 and 155 were strongly express in limbal epithelium, but weaker in central corneal epithelium. The expression pattern of miR-10b and 126 was restricted to the basal cells of mouse corneal epithelium but were indistinct in human cornea. The mouse corneal epithelium was regenerated by CEPCs in the limbal basal layer, which produces TA cells to migrate centrally to the outer layers. The positive staining of miR-10b and 126 was detected in the CEPCs enriched region, suggesting miR-10b and 126 were preferential expressed by CEPCs and early TA cells in mouse corneal epithelium.

The inconsistent expression pattern of microRNAs in human and mouse corneal epithelium may be due to the structure of human limbal epithelium being more complicated that was heterogeneous with CEPCs and their differentiated progenies early TAc and late TAc, the distribution of cells was gradually differentiated without displaying a distinct cell identity. Thus, the expression pattern of microRNAs in human limbal epithelium did not display a clear boundary in different layers and region.

Our previous study proved that miR-145 reduced epithelial cell proliferation by blocking the S-phase entry and induced cell apoptosis. On the other hand, it promoted epithelial cell differentiation by up-regulating CK3/12 and connexin-43 expression. Its action on corneal epithelial differentiation could be mediated through its direct targeting on integrin beta 8 (ITGB8) (Lee et al., 2011).

LPC-enriched microRNAs might participate in various cell events. miR-126 is a novel microRNA found in the limbal epithelium. From literatures, it has been shown as an angiogenesis-related microRNA regulating vascular integrity and angiogenesis (S. Wang et al., 2008). During vascular formation, miR-126 enhanced the action of vascular endothelial growth factor (VEGF) and basic fibroblast growth factor (bFGF) by repressing the negative regulators of angiogenesis signaling molecules, *Spred-1* and *PIK3R2*. However, a different role of miR-126 was observed in breast carcinogenesis and retinal neovascularization that pro-angiogenic factors (VEGF and IGF-2) were reduced by an ectopic expression of miR-126 (Q. Zhou et al., 2011). Additionally, KEGG pathway analysis showed that miR-126 predictedly target on *IRS1*, *PIK3R2,* and *VEGFA*, which were involved in insulin, VEGF and mTOR signaling (**Figure 5.2**). *In situ* hybridization on human fetal choroid confirmed the specificity of miR-126 in the choroidal endothelial cells (F. E. Wang et al., 2010a). As the origin of corneal

neovascularization or inflammation, the limbal epithelium is highly vascularized. The presence of miR-126 in limbal epithelium may regulate corneal angiogenesis.

MiR-10b is an onco-miR de-regulated in various human cancer tissues and cell lines with its function to promote tumor cell migration and invasion (Lund, 2010). It has been shown to regulate ribosome biogenesis in corporation with *Myc* oncogene in cancer cells, thereby affecting cellular transformation (Ladeiro et al., 2008). MiR-10b is encoded by Hox cluster, which is a key transcription factor and modulator of embryonic development by determining the segment structures (Negrini & Calin, 2008). Meanwhile, it directly targets on *HoxD10* in glioma to induce cell invasion (L. Sun, Yan, et al., 2011a). miR-10b was also expressed in myogenic progenitor cells with a regulatory role in cell proliferation and differentiation in muscle regeneration *in vitro* and *in vivo* (Y. Chen, Gelfond, McManus, & Shireman, 2011). Although the relationship of miR-10b and *Hox* in normal tissues is still unconfirmed, it might be possible that miR-10b contributes to adult stem cell proliferation. In corneal epithelium, it was predominantly expressed in the limbal basal and suprabasal layers, which are enriched with progenitor cells, early and late transit amplifying cells. This implies a potential function of miR-10b in cell proliferation, mitosis as well as migration. From the pathway analysis, miR-10b might target on several genes of Wnt/β-catenin signaling pathway (*GSK3B, CSNK2A2, ROCK2, PPP3CC, CAMK2B, CXXC4, and MAP3K7*). Among them, *CXXC4, $GSK_3B$, $CSNK_2A_2$* and $MAP_3K_7$ are the negative regulators of Wnt/β-catenin and Notch1 signaling (Katoh, 2009) (**Figure 5.3**). From the literature, these pathways are involved in self-renewal and differentiation of corneal progenitor cells (Nakatsu et al., 2011a). Therefore, we hypnotized that miR-10b could promote cell

cycle and proliferation via its suppression on the negative regulators of Wnt/β-catenin or Notch1 signaling pathway.

MiR-155 affects B-cell maturation and immunoglobulin production in response to antigen (Yin, Wang, McBride, Fewell, & Flemington, 2008). It and its primary transcript, B-cell integration cluster (BIC), were up-regulated by various immune stimuli, including Toll-like receptor (TLR) ligands, tumor necrosis factor-α (TNFα), interferon-β and B-cell receptor (BCR) (Tsitsiou & Lindsay, 2009). In human RPE, miR-155 was induced during inflammatory response after an exposure to inflammatory cytokine mix (IFNδ, TNFα and IL-1β) or activation of JAK/STAT pathway (Kutty et al., 2010). Meanwhile, the cell quiescence-related transcription factor CEBPB was identified as the target of miR-155 in herpes virus (Skalsky et al., 2007). From TargetScan prediction, miR-155 might target *TCF4* and different growth factors (namely *EGFR* and *GFRa-1*), implying that it might regulate the inflammatory secretion process in the corneal epithelium. The other predicted targets were genes involved in MAPK, insulin and mTOR signaling, suggesting the potential suppressive effect on cell proliferation, differentiation and migration. Moreover, from gene interaction analysis, miR-155 was also shown to be apoptosis-related. In my microarray and qPCR experiments, the differential expression of miR-155 was moderate (signal intensity = 17.7 in microarray; $P = 0.039$ in qPCR). Likewise, the ISH experiment showed that miR-155 was not strongly expressed in the limbal epithelium, when compared to the corneal epithelium. Therefore, miR-155 might be moderately expressed in normal corneal epithelium; however it could be stimulated by the cytokine and ligand exposure upon wounding and healing process of which the immune response is taking place.

## 5.4 Gene Ontology and pathway analysis

To explore the regulatory roles of the 9 LPC-enriched microRNAs, I performed a series of bioinformatics analysis to identify the target genes, significant pathways and gene networks. The data set of cornea-expressing genes compared to conjunctiva was selected to correlate with target genes of the microRNAs from microarray. This screening of microRNA-mRNA pathway analysis would detect their potential roles in CEPC and corneal epithelium.

### Gene ontology

For the down-regulated genes, the candidate microRNAs may affect the genes related with inflammatory response and cytokine receptor activity, like LYZ (regulated by miR-10, 142-3p, 143 and 205), CXCR2 (by miR-10b and 146a), and CD46 (by miR-139-5p and 143). The up-regulated cornea genes were correlated with microRNAs significantly associated with regulation of cell death and cell adhesion-like molecules, such as CADM1 (by miR-10b, 146a, 205 and 338-5p), CNTNAP2 (by miR-149, 205, 211 and 338-3p), and PRUNE2 (by miR-142-3p, 205 and 338-3p).

### KEGG pathway

***(A) Corneal epithelial progenitor cell regulation***

Wnt and MAPK signaling pathways were crucial in stem cell regulation. Some participating genes were the predicted targets annotated by these LPC-enriched microRNAs. Notably, miR-10b could target GSK3B, CSNK2A2, ROCK2, PPP3CC, CAMK2B, CXXC4, and MAP3K7 in the Wnt pathway. Among them, CXXC4, GSK3B, CSNK2A2 and MAP3K7 were known as the negative regulators of Wnt and Notch signaling, hence potentially affecting cell proliferation (**Figure 5.4**). Besides, miR-155

could modulate FOS, PTPRQ, PAK2, DUSP14, CACNB4, MAP4K3, TAB2, KRAS, BDNF, TAOK1, RAPGEF2, SOS1, FGF9, RPS6KA3, MAP3K2, RELA, FGF7, RAP1B, and MAPK10 expression in MAPK pathway (Figure 5.4). In addition, the key molecules FOS, JUN, KRAS and MAPK family in the MAPK signaling were regulated by miR-139-5p, 143 and 155. The coordinated activity of miR-145 and 338-5p on DUSP6, EVI1 and RASA1/2 could also negatively regulate MAPK signaling, affecting CEPC differentiation.

***(B) Intercellular junctions and cell motility***

Adherens junction and regulation of actin cytoskeleton were the two significant pathways involved in cell motility and communication influenced by LPC-enriched microRNAs. Regulation of focal adhesion and tight junctions were also significantly affected. Over 20 annotated corneal genes targeted by miR-143 and 145 were associated with cell motility and cell skeleton, including focal adhesion, formation of cell junction (adherens, tight and gap junctions) and extracellular matrix composition. ACTG1, MAP3K7, SMAD2 and SSX2IP targeted by miR-10b were genes participating in focal adhesion activity (Walsh et al., 2008). Besides, ITGA6 and ITGB8 targeted by miR-139-5p were also involved in focal adhesion, ECM-receptor interaction and cytoskeletal regulation. IGF targeted by miR-338-3p and SOS1 by miR-155 was linked with focal adhesion and gap junction (Casamassima & Rozengurt, 1998).

***(C) Immune response***

The cornea is immune privileged with a lack of blood vessels and antigen presenting cells. MicroRNAs might assist to maintain a balance between pro- and anti-inflammation. From our analysis, genes for T cell and B cell receptor signaling and for natural killer cell-mediated cytotoxicity, such as *FOS*, *KRAS*, *NFAT5* and *VAV3* were

targets of miR-155. This is consistent with the previous report that miR-155 is a mediator of immune response (Lindsay, 2008). Besides, Toll-like receptor signaling, which is a key pathway in corneal epithelium inflammation, could be affected by miR-155 through predictive targeting on *FOS*, *IKBKE*, *MAP3K7IP2* and *PIK3R1*. MHC1 encoded protein *CANX,* which is a component of antigen processing and presentation, was also a target of miR-139-5p.

***(D) Growth factors***

Cell turnover and wound healing of corneal epithelium is affected by various growth factors and cytokines, including IGF, basic FGF and EGF. They participate in stimulating cell growth, division and migration. LPC-enriched microRNAs were found significantly associated with TGFβ, ErbB and insulin pathways. TGFβ signaling was affected by miR-155 through targeting on ACVR2B, GDF6, SMAD1/2, SP and TGFBR2 as well as by miR-145, which targets on ACVR1B, ACVR2A, INHBB, ROCK1, RPS6KB1, SMAD3/4/5, SP1, TGFBR2 and ZFYVE9. MiR-139-5p might regulate TGFβ signaling by targeting on its repressor THBS1, which may act as an implicit activator of TGF secretion. The insulin signaling could be affected by miR-155 with targets of CBL, KRAS, PIK3R1, PRKAR1A, RHEB, SOCS1 and SOS1, of which SOS1 and RHEB were the pathway suppressor (Hulsmans, De Keyzer, & Holvoet, 2011). The two targets of miR-126 (CRK and LRP6) could be associated with ErbB and insulin signaling for cell survival. Besides, predictive targets of miR-155 (CAB39, PIK3R1, RHEB and RPS6KA3) might be linked to mTOR signaling, which subsequently suppresses VEGF effect and cell growth (Trinh et al., 2009).

**IPA® analysis**

IPA® analysis based on the reported interaction between microRNA and protein showed the network of microRNAs coordinate regulation on genes. MiR-143, 145 and 155 might antagonize transcription factors to regulate cell proliferation and hence maintain a balance between cell growth and apoptosis. MiR-143 and 145 could suppress oncogenes including *KRAS* and *MYC* to inhibit cell overgrowth (Kent et al., 2010; Sachdeva et al., 2009). From the IPA Network, *TNF* was stimulated by miR-155 through *TP53* action (Nakatsu et al., 2011b), which trans-activated *TP53* to form a positive feedback loop. TNF is a key mediator of cytokines in the corneal epithelium with the activation on apoptosis-related genes (*BIK* and *DAPK1*) (J. Y. Kim, Kim, Lee, & Park, 2011; Yoo et al., 2012), and repression on oncogene *MYC (Nakashima, Kumakura, Mishima, Ishikura, & Kobayashi, 2005)*. Therefore, TNF up-regulation by miR-155 might induce cell apoptosis. *KRT15* and *Wnt5* are highly expressed in limbal basal epithelium containing progenitors and proliferating TA cells (Nakatsu et al., 2011b). From literatures, TNF repressed *KRT15* in epidermal stem cells (Werner & Munz, 2000) and activated *Wnt5a* in human mesenchymal stem cells (Briolay et al., 2013), indicating it is a potential factor to initiate cell proliferation and differentiation. MiR-155 could, on the other hand, increase the translation level of TNF (Bala et al., 2011), subsequently activating NFγB and MAPK pathways (Mohan, Mohan, Kim, & Wilson, 2000). In addition, it could directly stimulate *IL1B* and *IL8* (Bhattacharyya et al., 2011), forming a loop to promote the corneal cell growth and induce inflammatory response. The limbal quiescent stem cell marker *CEBPB* was repressed by miR-155 (He, Xu, Ding, Kuang, & Zheng, 2009), which could directly activate CASP3 and/or, through stimulating TNF, to induce apoptosis (H. Q. Wang et al., 2011). Hence, up-regulation of miR-155 might result in immune response and cell death.

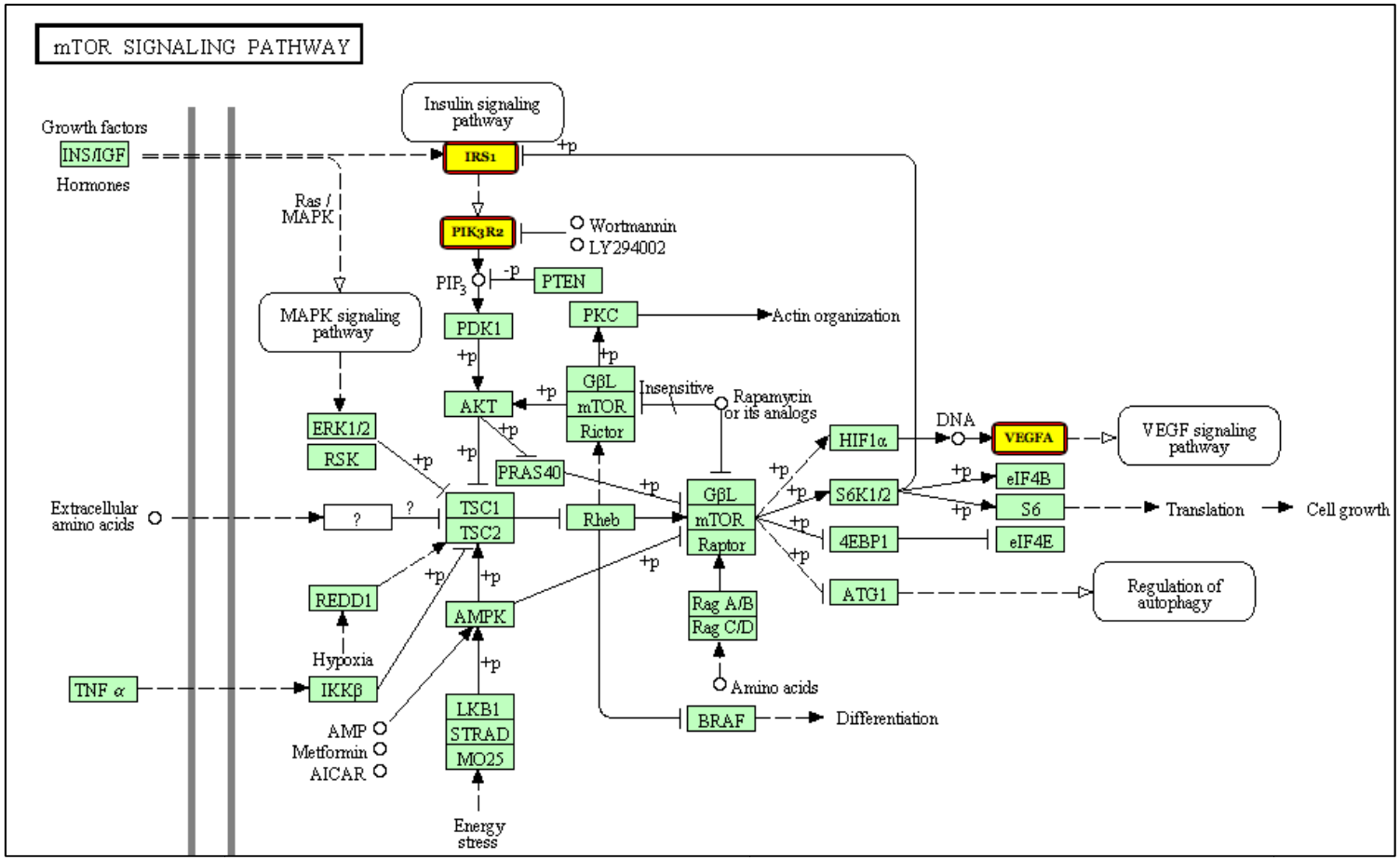


**Figure 5.2 Target genes of miR-126 in mTOR signaling pathway**

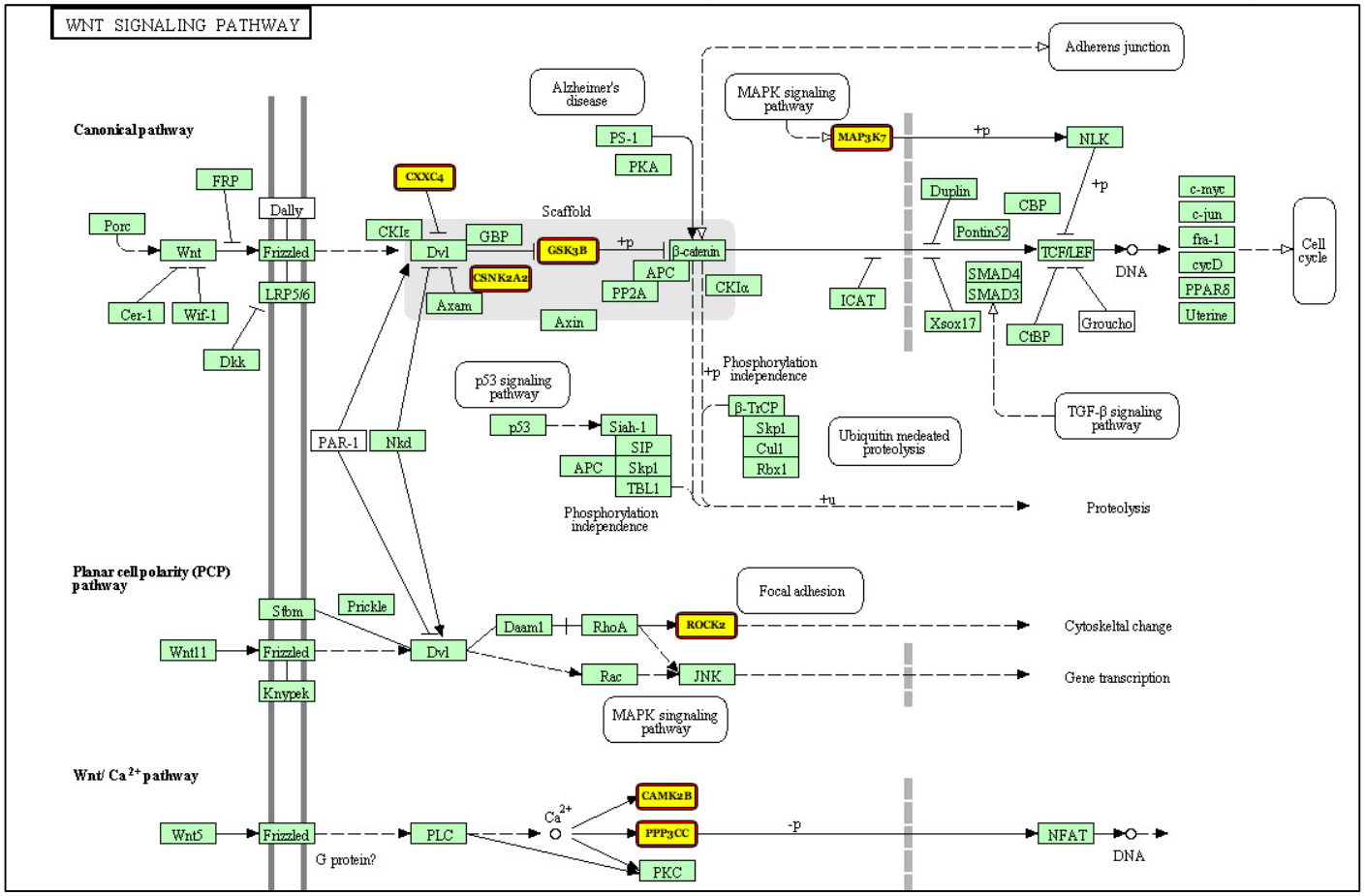


**Figure 5.3 Target genes of miR-10b in Wnt signaling pathway**

MiR-10b algorithmically target on the negative regulator of Wnt signaling pathway CXXC4, $GSK_3B$, $CSNK_2A_2$, and $MAP_3K_7$.

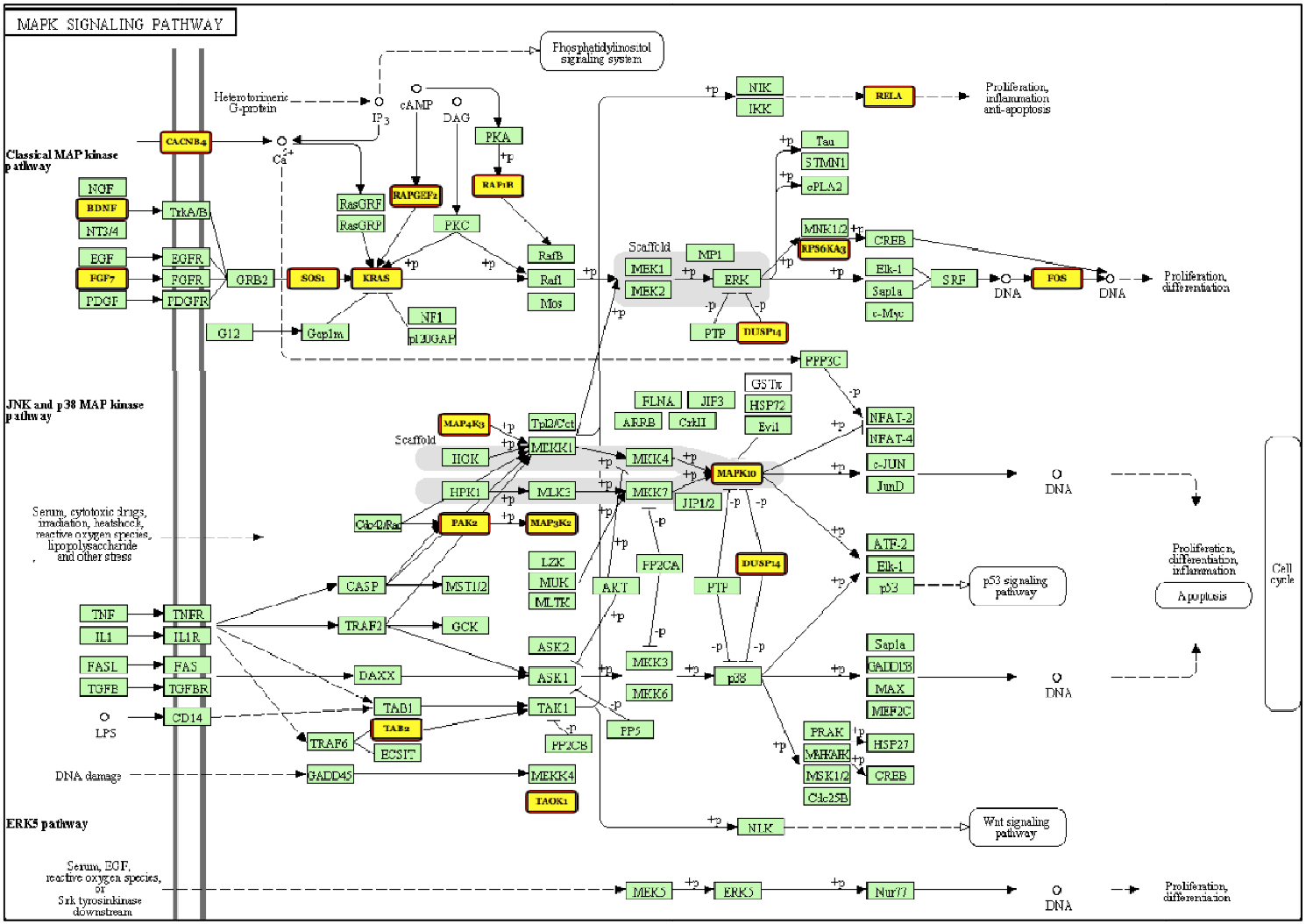


**Figure 5.4 Target genes of miR-155 in MAPK signaling pathway**

## 5.5 microRNAs expression in pterygium

From microRNA quantitative analysis on pterygia, LPC, and conjunctiva, miR-143, 145 and 184 were found to be significantly up-regulated in pterygium. By comparing the expression level on pterygium epithelium and stroma, miR-143/145 was down-regulated in epithelium while miR-184 was up-regulated in epithelium. TaqMan® real-time PCR also confirmed that the expression of miR-155 and miR-10b in pterygium was significantly higher than normal LPC epithelia. The expression of miR-10b was intense in pterygium stroma but negative in epithelium, specifically positive in the fibroblast and collagen of pterygium stroma.

As mentioned, the occurrence of pterygium possesses similar features with tumorigenesis, the microRNA expression in pterygium may relate with this function. MiR-184 was a biomarker that is up-regulated in squamous cells carcinoma of tongue and oesophageal squamous cell carcinoma, which indicated its preferential expression in tissue with squamous metaplasia (Hsu et al., 2012; Komatsu et al., 2011). In normal cornea, miR-184 was a key regulator for promoting corneal development and differentiation by maintenance of the expression of Pax6 and CK3. Interestingly, our previous study also found Pax6 and CK3 were present in pterygial epithelium (Bai et al., 2010). Thus, the accumulation of miR-184 in pterygium epithelium may be related to the epidermal proliferation of pterygium (**Figure 5.5**).

miR-10b was abundant in the over-proliferative fibroblast of pterygium. As an onco-miR, miR-10b was over-expressed in many tumors compared with the normal tissues; and functions as a promoter of the cancer cells invasion (Dong et al., 2012). MiR-10b contributes to the migration and invasion of cancer cells by up-regulating

migration/invasion-associated molecules. In human glioblastoma cells, miR-10b can increase MMP-14 expression via miR-10b/HOXD10/MMP-14/uPAR signaling pathway (L. Sun, Yan, et al., 2011b). Accordingly, the function of miR-10b in pterygium may act as inducting pterygial cell migration by activating MMPs (**Figure 5.5**). Furthermore, the expression of miR-10b and p53 was reciprocal in pterygium that miR-10b was solely positive in stroma whereas p53 was abundant in epithelium compartment, suggesting a suppressive potential of miR-10b on p53.

The signal intensity of miR-155 was weak in both pterygium and LPC epithelium, but was significantly up-regulated in pterygium. As a key modulator in inflammation, miR-155 can regulate many signaling pathways, such as (TGF)-β signaling, p38 MAPK signaling and ERK signaling and might activate many cytokines like TNF-α, TGFB1, TGFB2, and EGFR to promote cells invasion and migration. Meanwhile, the expression of miR-155 can be up-regulated by TGF beta signaling, so as to promote the EMT and tight junction dissolution in breast cancer (Kong et al., 2008). Therefore, the presence of miR-155 in pterygium may be related to the inflammation inflated and cell migration (**Figure 5.5**). The expression of miR-155 can be up-regulated by mutant p53 in breast tumors, but in our study the expression pattern of miR-155 did not correlated with p53, suggesting the p53 expressed in pterygium was wild-type rather than mutation.

Immunohistochemistry detection of IL-6 in our pterygium samples demonstrated that it was present in all layers of whole pterygium epithelium and was also positive in the some collagen as well as blood vessels. miR-126 displayed the same location as IL-6 staining in epithelium, stroma and fibrovascular of pterygium. The pro-inflammatory

cytokine IL-6 was abundant in inflamed corneas, promoting the corneal epithelial cell proliferation through altering the extracellular matrix composition. In pterygium pathogenesis, IL-6 stimulated MAP kinase pathways to increase the downstream genes c-Jun, c-Fos and AP-1. Meanwhile, p38 MAPK pathway can promote the cornea to secrete IL-6 for cell migration and angiogenesis. miR-126, the endothelial cell-specific microRNA, has been reported to promote the differentiation of mesenchymal stem cells into endothelial-like cells with increased release of VEGF and bFGF, through the activation of MAPK/ERK pathways (F. Huang et al., 2013). Accordingly, miR-126 in pterygium may serve as an activator of p38 MAPK pathways to induce the secretion of IL-6, so as to promote angiogenesis by transforming the fibroblast cells to endothelial cells (**Figure 5.5**).

## 5.6 The expression and function of P53 in pterygium

The immunohistochemistry of p53 (**Figure 4.22**) showed an intensive signal in pterygium epithelium, blood vessel and mild staining in fibroblast. The expression of p53 in pterygium is a common phenomenon reported by many studies (Y. Y. Tsai, Chang, et al., 2005), but the mechanism of p53 accumulation in pterygium is still unknown. The wild type p53 was instable and cannot be detected in normal tissue, while this protein was stabilized by the p53 mutation and accumulated in the cells; therefore, the p53 expression level is an important prognostic factor of many cancers. One hypothesis on p53 abnormal expression in pterygium was that p53 gene was mutated by the UV radiation, causing a damaged p53-dependent programmed cell death mechanism, which activates the p53-Rb-TGF-β pathway to excessively product TGF-β. TGF-β acts as a key modulator for leading to angiogenesis, collagen accumulation, and Bowman's layer dissolution. However, whether p53 was mutated in pterygium is still controversial.

DNA from pterygial epithelial cells was examined by sequencing; two reports from Schneider and Shimmura's groups proved there were no mutation detected in exons 5-8 of the point mutations of TP53 gene (Schneider, John-Aryankalayil, Rowsey, Dushku, & Reid, 2006), conversely, Tsai Yi-Yu's group detected p53 gene mutations exon 4-8 with the prevalence of 15.7% (Y. Y. Tsai, Cheng, et al., 2005). These inconsistent findings of P53 mutation cannot explain the high expression level of p53 in pterygium. Another supposition of p53 stabilization in pterygium is virus infection, the HPV infection was detected in pterygium, but still, the results were inconsistent in different teams: Guthoff R et al and Nicholas Dushku et al reported that HPV was negative in both pterygium and limbal tumors (Dushku, Hatcher, Albert, & Reid, 1999); the only one positive report from Tsai Yi-Yu et al demonstrated that 31 of 129 pterygium tissues were HPV positive. Thus, a widely accepted explanation of p53 accumulation in pterygium is due to the response to UV exposure with the evidence that wild type p53 was increased upon exposed to UV in keratinocytes and declined after 3-4 days (Chouinard, Valerie, Rouabhia, & Huot, 2002).

Cytoplasmic distribution of p53 displayed an UVB-dependent manner in normal human keratinocytes. 8 hours after exposure of keratinocytes to UVB irradiation leads to cytoplasmic accumulation of p53 due to the activation of p38 MAPK pathway that induce the post-transcriptional modification of p53 through protein acetylation and phosphorylation. Consequently the half-life of wild type p53 is stabilized and exported from nucleus, localized and accumulated to cytoplasm (Di Girolamo et al., 2004). Blocking cellular export receptor CRM1 (exportin-1)-dependent nuclear export does not affect the cytoplasmic distribution of p53 in irradiated cells, suggesting p53 was primarily expressed in cytoplasm (Chaturvedi et al., 2004; Chouinard et al., 2002).

UVB-induced activation of p38 pathway may provide a protective effect to enhance resistance of normal human keratinocytes to UV stress by cytoplasmic sequestration (Chouinard et al., 2002). Accordingly, in pterygium p53-induced cell cycle arrest may be related to the cell protective effect to against the apoptosis or alter gene expression caused by UV (Chaturvedi et al., 2004). However, the function of p53 in cytoplasm of normal cells is not fully understood. Cytoplasmic localization of p53 mainly affected mitochondria, triggering the release of pro-apoptotic factors from the mitochondrial intermembrane space via induction of MOMP. p53 induced by cellular stress was accumulated in the cytoplasm and interacted with pro-apoptotic Bcl2 family members Bax, act as a pro-apoptotic effect (Green & Kroemer, 2009). Moreover, Bax were present in pterygium epithelium. Consequently, p53 trans-localized to the cytoplasm in pterygium epithelium may function as pro-apoptosis.

### 5.7 p53 and miR-143/145

From microRNA TaqMan® real-time PCR analysis, miR-143 and 145 were identified to be significantly higher in pterygium compared with normal conjunctiva and LPC epithelia, the LCM and in situ hybridization results confirmed the localization of these two microRNAs was strongly expressed in both pterygium stoma and epithelium. By the combination of in situ hybridization and immunohistochemistry, miR-143/145 and p53 was stained in the same section. The co-location of the two molecules was observed that the expression pattern was overlapped in pterygium epithelium and stroma (**Figure 4.23**). The upstream of pre-miR-143/ 145 sequence contained 2 putative p53 response elements, suggesting that transcription factor p53 act as a positive regulator of miR-143/145 by binding to its promoter (Boominathan, 2010). MiR-143 and 145 were significantly up-regulated in a p53-mediated DNA damage response that

the production of pre-miR-143/145 and mature miR-143/145 were increased by induction of p53. Conversely, knockdown of p53 attenuated the expression of pre-miRNAs and mature microRNA of this cluster, suggesting the up-regulation of miR143/145 had a p53-dependent manner. The elevation of both pre-miRNAs and mature microRNAs indicated that the promotion occurred in transcriptional and post-transcriptional stage. p53 post-transcriptional regulation on miR-143/145 cluster occurs through facilitation Drosha-mediated processing of primary microRNAs to precursor microRNAs (Suzuki et al., 2009).

MiR-143 and 145 was found to be down-regulated in many cancers such as colorectal cancer (Ng et al., 2009), bladder cancer (Takagi et al., 2009), breast cancer (S. Wang et al., 2009) and esophageal squamous cell carcinoma (Kano et al., 2010) , which may due to the inactive p53 mutants in these cancer disturb the production and maturation of miR-143/145. Upon human ESCs differentiation, miR-145 was also up-regulated at a p53-dependent manner, p53 promote the ESC differentiation by promoting the expression of miR-145, subsequently result in the inhibitory effect of miR-145 on targeting pluripotent factors Oct4, Sox2 and Klf4 (Jain et al., 2012). Therefore, the co-localization of miR-143/145 and p53 might be the result of p53 promoting the expression of miR-143/145 at transcriptional and post-transcriptional stage to enhance the production of mature miR-143 and miR-145 in pterygium.

Our data revealed that the expression level of p53 was increased with overexpression of miR-145. In cancers cells, the p53 protein was degenerated by the interaction with murine double minute 2 (MDM2), which diminished the p53-induced cell apoptosis and caused the over-proliferation of tumor cells. Moreover, MDM2 has been verified to be the direct target of miR-145 that the expression of MDM can be

attenuated by ectopic expression of miR-145 in tumors (J. Zhang et al., 2013). Our results also proved the suppressive effect of miR-145 on MDM2 expression in pterygial cells. Therefore, the correlated regulation of miR-145 and p53 on pterygium may act through the miR-145 dependent MDM2 turnover to elevate p53 in response to UV-caused DNA damage stress; likewise, p53 can enhance the expression of miR-145, forming a double positive feedback loop to suppress cellular growth and therefore triggering the apoptosis of pterygium cells (**Figure 5.4**). Accordingly, this miR-145 - p53 regulatory feedback loop restricts the proliferative ability of pterygium cells; function as self-protective machinery for corneal epithelium through the equilibrium of p53 to prevent tumorigenesis of pterygium.

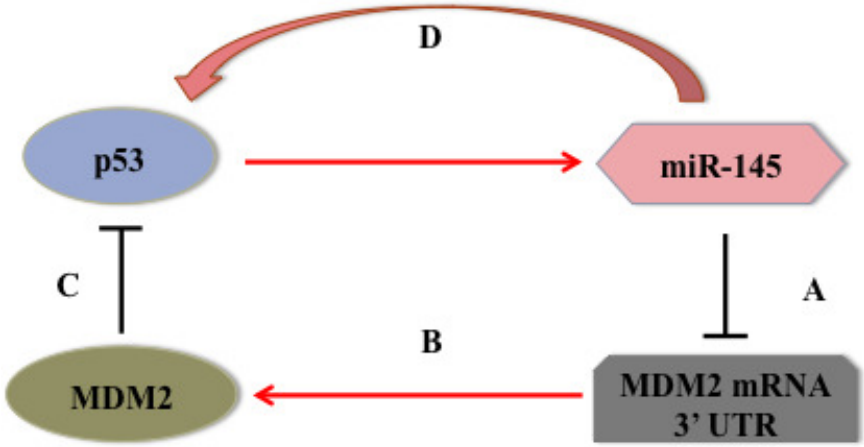


**Figure 5.4 The regulatory circuitry of p53 and miR-145.**

(A) miR-145 is post-transcriptionally activated by up-regulated p53. (B) miR-145 bind to 3'UTR of MDM2 mRNA to negatively regulate its expression. (C) MDM2 can degenerate p53 protein. (D) miR-145 may increase the expression of p53 through suppressing MDM2.

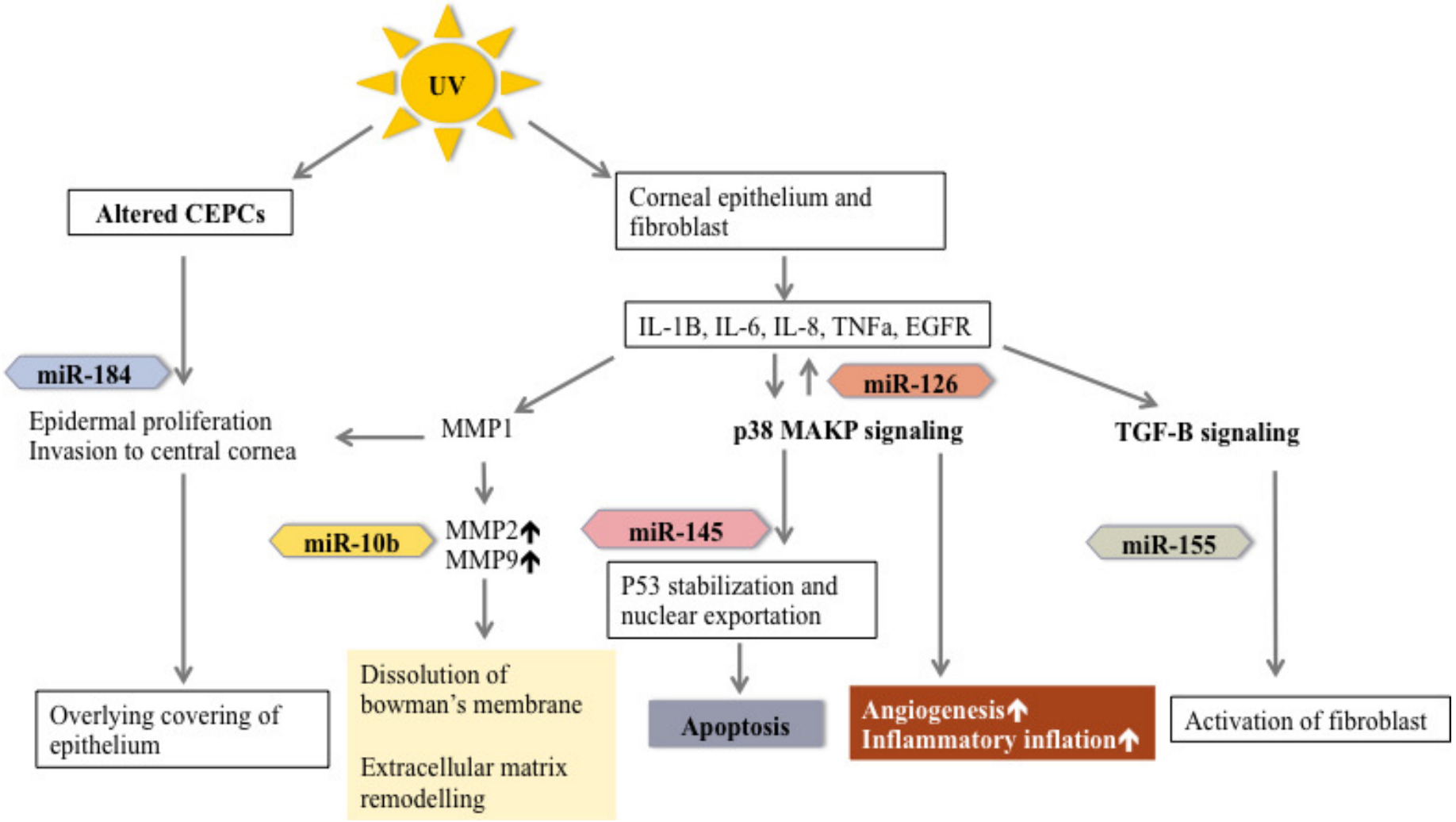


**Figure 5.5 The hypothetical microRNAs and proteins regulatory mechanism in pathogenesis of pterygium.**

# Chapter 6 Conclusions and suggestion for further work

Our study identified the microRNA expression profile in CEPCs-enriched population from human LPC epithelium by the comparison with differentiated cells -enriched population from CC epithelium. A distinct set of microRNAs has been confirmed to be specific to human limbal epithelium, including miR-10b, 126, 127, 139-5p, 155 and 338-3p. Bioinformatics analysis revealed that these microRNAs potentially regulate epithelial differentiation and phenotype maintenance, as well as self-renewal of progenitor cells, cell migration, immune response and angiogenesis. Moreover, a network linking-up the interaction between microRNAs and cornea related molecules suggested that microRNAs formed a balance between oncogenes and tumor suppressors, as well as the regulatory roles in cytokines and growth factor. This interaction suggested a novel insight in the epigenetic regulation of human corneal epithelium. Further studies could investigate the biological role of microRNAs in the corneal epithelium according to this network by detecting the protein expression changed with related microRNAs.

The second part of the thesis, for the first time, identified a novel set of microRNAs; miR-143/145 and miR-184 were significantly up-regulated in pterygium as compared to the normal limbal epithelium and conjunctiva. Moreover, miR-143/145 was co-localized with p53 in pterygium, implying a positive correlation between miR-143/145 cluster and p53. miR-145 caused an up-regulation of p53 and induced apoptosis in pterygial cells through targeting on the negative regulator of p53, MDM2.

Therefore, miR-145 might be the main cause of p53 accumulation in pterygium and also serve as protective factor for cornea epithelium to against UV-induced DNA damage.

More experimental evidences are needed to prove the miR-145 and p53 positive regulatory loop found in this study. Further studies could aim at verifying the double positive interaction between miR-145 and p53 through induction of p53 siRNA or suppressing p53 expression in pterygium cells to define which is the primarily molecule in pathogenesis of pterygium. Also validation of the direct suppression of miR-145 on down-regulation of MDM2 is necessary for a complete regulatory pathway.

Our study specified a disease model for understanding the microRNA expression alteration in progenitor cells and tumor-like cells. Additionally, the parallel localization of microRNAs with the proteins related with pterygium disclosed the regulation of microRNAs in pathogenesis of pterygium. The finding in this study proved that miR-145 can up-regulate p53 expression to induce apoptosis of pterygial cells, suggesting miR-145 might be a therapeutic molecule to resistant the UV-induced DNA damage and the tumorigenesis. Pterygium can be effectively removed surgically, but recurrence is not uncommon. Therefore, more investigation should be focused on the exploration of miR-145 in recurrent pterygium through comparing its expression level in primary and recurrent pterygium, to identify the correlation between miR-145 and pterygium recurrence. The detection of miR-145 in ocular surface tumor is necessary to prove that miR-145 may act as a tumor suppressor in cornea. Hence the novel epigenetic regulatory mechanism found in pterygium may serve as a new treatment target for the therapy of aberrant CPECs like pterygium or corneal tumor.

# Chapter 7 Reference


Ahmad, S., Kolli, S., Lako, M., Figueiredo, F., & Daniels, J. T. (2010). Stem cell therapies for ocular surface disease. *Drug Discov Today, 15*(7-8), 306-313. doi: 10.1016/j.drudis.2010.02.001

Ahmad, S., Kolli, S., Li, D. Q., de Paiva, C. S., Pryzborski, S., Dimmick, I., . . . Lako, M. (2008). A putative role for RHAMM/HMMR as a negative marker of stem cell-containing population of human limbal epithelial cells. *Stem cells, 26*(6), 1609-1619. doi: 10.1634/stemcells.2007-0782

An, M. X., Wu, K. L., & Lin, S. C. (2011). Detection and comparison of matrix metalloproteinase in primary and recurrent pterygium fibroblasts. *Int J Ophthalmol, 4*(4), 353-356. doi: 10.3980/j.issn.2222-3959.2011.04.05

Bai, H., Teng, Y., Wong, L., Jhanji, V., Pang, C. P., & Yam, G. H. (2010). Proliferative and migratory aptitude in pterygium. *Histochem Cell Biol, 134*(5), 527-535. doi: 10.1007/s00418-010-0751-5

Bala, S., Marcos, M., Kodys, K., Csak, T., Catalano, D., Mandrekar, P., & Szabo, G. (2011). Up-regulation of microRNA-155 in macrophages contributes to increased tumor necrosis factor {alpha} (TNF{alpha}) production via increased mRNA half-life in alcoholic liver disease. *J Biol Chem, 286*(2), 1436-1444. doi: 10.1074/jbc.M110.145870

Barbaro, V., Testa, A., Di Iorio, E., Mavilio, F., Pellegrini, G., & De Luca, M. (2007). C/EBPdelta regulates cell cycle and self-renewal of human limbal stem cells. *J Cell Biol, 177*(6), 1037-1049. doi: jcb.200703003 [pii]10.1083/jcb.200703003

Barik, S. (2008). An intronic microRNA silences genes that are functionally antagonistic to its host gene. *Nucleic Acids Res, 36*(16), 5232-5241. doi: 10.1093/nar/gkn513

Barrilleaux, B., Phinney, D. G., Prockop, D. J., & O'Connor, K. C. (2006). Review: ex vivo engineering of living tissues with adult stem cells. *Tissue Eng, 12*(11), 3007-3019. doi: 10.1089/ten.2006.12.3007

Bartel, D. P. (2004). MicroRNAs: genomics, biogenesis, mechanism, and function. *Cell, 116*(2), 281-297. doi: S0092867404000455 [pii]

Bhattacharyya, S., Balakathiresan, N. S., Dalgard, C., Gutti, U., Armistead, D., Jozwik, C., . . . Biswas, R. (2011). Elevated miR-155 promotes inflammation in cystic fibrosis by driving hyperexpression of interleukin-8. *J Biol Chem, 286*(13), 11604-11615. doi: 10.1074/jbc.M110.198390

Bian, F., Liu, W., Yoon, K. C., Lu, R., Zhou, N., Ma, P., . . . Li, D. Q. (2010). Molecular signatures and biological pathway profiles of human corneal epithelial

progenitor cells. *Int J Biochem Cell Biol, 42*(7), 1142-1153. doi: S1357-2725(10)00133-0 [pii]10.1016/j.biocel.2010.03.022

Biosystems, Applied. Endogenous Controls for Real-Time Quantitation of miRNA Using TaqMan® MicroRNA Assays. *Applied Biosystems*.

Boheler, K. R., Czyz, J., Tweedie, D., Yang, H. T., Anisimov, S. V., & Wobus, A. M. (2002). Differentiation of pluripotent embryonic stem cells into cardiomyocytes. *Circ Res, 91*(3), 189-201.

Boominathan, L. (2010). The tumor suppressors p53, p63, and p73 are regulators of microRNA processing complex. *PLoS One, 5*(5), e10615. doi: 10.1371/journal.pone.0010615

Boyer, L. A., Lee, T. I., Cole, M. F., Johnstone, S. E., Levine, S. S., Zucker, J. P., . . . Young, R. A. (2005). Core transcriptional regulatory circuitry in human embryonic stem cells. *Cell, 122*(6), 947-956. doi: S0092-8674(05)00825-1 [pii]10.1016/j.cell.2005.08.020

Briolay, A., Lencel, P., Bessueille, L., Caverzasio, J., Buchet, R., & Magne, D. (2013). Autocrine stimulation of osteoblast activity by Wnt5a in response to TNF-alpha in human mesenchymal stem cells. *Biochem Biophys Res Commun, 430*(3), 1072-1077. doi: 10.1016/j.bbrc.2012.12.036

Budak, M. T., Alpdogan, O. S., Zhou, M., Lavker, R. M., Akinci, M. A., & Wolosin, J. M. (2005). Ocular surface epithelia contain ABCG2-dependent side population cells exhibiting features associated with stem cells. *Journal of cell science, 118*(Pt 8), 1715-1724. doi: 10.1242/jcs.02279

Cao, X., Pfaff, S. L., & Gage, F. H. (2007). A functional study of miR-124 in the developing neural tube. *Genes Dev, 21*(5), 531-536. doi: 10.1101/gad.1519207

Card, D. A., Hebbar, P. B., Li, L., Trotter, K. W., Komatsu, Y., Mishina, Y., & Archer, T. K. (2008). Oct4/Sox2-regulated miR-302 targets cyclin D1 in human embryonic stem cells. *Mol Cell Biol, 28*(20), 6426-6438. doi: MCB.00359-08 [pii]10.1128/MCB.00359-08

Casamassima, A., & Rozengurt, E. (1998). Insulin-like growth factor I stimulates tyrosine phosphorylation of p130(Cas), focal adhesion kinase, and paxillin. Role of phosphatidylinositol 3'-kinase and formation of a p130(Cas).Crk complex. *The Journal of biological chemistry, 273*(40), 26149-26156.

Caussinus, E., & Hirth, F. (2007). Asymmetric stem cell division in development and cancer. *Prog Mol Subcell Biol, 45*, 205-225.

Chang, T. C., & Mendell, J. T. (2007). microRNAs in vertebrate physiology and human disease. *Annu Rev Genomics Hum Genet, 8*, 215-239. doi: 10.1146/annurev.genom.8.080706.092351

Chaturvedi, V., Qin, J. Z., Stennett, L., Choubey, D., & Nickoloff, B. J. (2004). Resistance to UV-induced apoptosis in human keratinocytes during accelerated senescence is associated with functional inactivation of p53. *J Cell Physiol, 198*(1), 100-109. doi: 10.1002/jcp.10392

Chen, D., Farwell, M. A., & Zhang, B. (2010). MicroRNA as a new player in the cell cycle. *J Cell Physiol, 225*(2), 296-301. doi: 10.1002/jcp.22234

Chen, Y., Gelfond, J., McManus, L. M., & Shireman, P. K. (2011). Temporal microRNA expression during in vitro myogenic progenitor cell proliferation and differentiation: regulation of proliferation by miR-682. *Physiol Genomics, 43*(10), 621-630. doi: 10.1152/physiolgenomics.00136.2010

Chen, Z., de Paiva, C. S., Luo, L., Kretzer, F. L., Pflugfelder, S. C., & Li, D. Q. (2004a). Characterization of in human limbal epithelia. *Stem Cells, 22*(3), 355-366. doi: 10.1634/stemcells.22-3-355

Chen, Z., de Paiva, C. S., Luo, L., Kretzer, F. L., Pflugfelder, S. C., & Li, D. Q. (2004b). Characterization of putative stem cell phenotype in human limbal epithelia. *Stem Cells, 22*(3), 355-366. doi: 10.1634/stemcells.22-3-355

Cheng, C. C., Wang, D. Y., Kao, M. H., & Chen, J. K. (2009). The growth-promoting effect of KGF on limbal epithelial cells is mediated by upregulation of DeltaNp63alpha through the p38 pathway. *J Cell Sci, 122*(Pt 24), 4473-4480. doi: 10.1242/jcs.054791

Chouinard, N., Valerie, K., Rouabhia, M., & Huot, J. (2002). UVB-mediated activation of p38 mitogen-activated protein kinase enhances resistance of normal human keratinocytes to apoptosis by stabilizing cytoplasmic p53. *Biochem J, 365*(Pt 1), 133-145. doi: 10.1042/BJ20020072

Conner, D. A. (2001). Mouse embryonic stem (ES) cell culture. *Curr Protoc Mol Biol, Chapter 23*, Unit 23 23. doi: 10.1002/0471142727.mb2303s51

Conte, I., Carrella, S., Avellino, R., Karali, M., Marco-Ferreres, R., Bovolenta, P., & Banfi, S. (2010). miR-204 is required for lens and retinal development via Meis2 targeting. *Proc Natl Acad Sci U S A, 107*(35), 15491-15496. doi: 0914785107 [pii]10.1073/pnas.0914785107

Coroneo, M. T., Di Girolamo, N., & Wakefield, D. (1999). The pathogenesis of pterygia. *Curr Opin Ophthalmol, 10*(4), 282-288.

Damiani, D., Alexander, J. J., O'Rourke, J. R., McManus, M., Jadhav, A. P., Cepko, C. L., . . . Strettoi, E. (2008). Dicer inactivation leads to progressive functional and structural degeneration of the mouse retina. *J Neurosci, 28*(19), 4878-4887. doi: 10.1523/JNEUROSCI.0828-08.2008

Daniels, J. T., Dart, J. K., Tuft, S. J., & Khaw, P. T. (2001). Corneal stem cells in review. *Wound Repair Regen, 9*(6), 483-494. doi: 483 [pii]

Davies, S. B., & Di Girolamo, N. (2010). Corneal stem cells and their origins: significance in developmental biology. *Stem Cells Dev, 19*(11), 1651-1662. doi: 10.1089/scd.2010.0201

Davis, N., Mor, E., & Ashery-Padan, R. (2011). Roles for Dicer1 in the patterning and differentiation of the optic cup neuroepithelium. *Development, 138*(1), 127-138. doi: 138/1/127 [pii]10.1242/dev.053637

Decembrini, S., Bressan, D., Vignali, R., Pitto, L., Mariotti, S., Rainaldi, G., . . . Cremisi, F. (2009). MicroRNAs couple cell fate and developmental timing in retina. *Proc Natl Acad Sci U S A, 106*(50), 21179-21184. doi: 0909167106 [pii]10.1073/pnas.0909167106

DelMonte, D. W., & Kim, T. (2011). Anatomy and physiology of the cornea. *J Cataract Refract Surg, 37*(3), 588-598. doi: S0886-3350(10)01924-3 [pii]10.1016/j.jcrs.2010.12.037

Deo, M., Yu, J. Y., Chung, K. H., Tippens, M., & Turner, D. L. (2006). Detection of mammalian microRNA expression by in situ hybridization with RNA oligonucleotides. *Dev Dyn, 235*(9), 2538-2548. doi: 10.1002/dvdy.20847

Detorakis, E. T., Zaravinos, A., & Spandidos, D. A. (2010). Growth factor expression in ophthalmic pterygia and normal conjunctiva. *Int J Mol Med, 25*(4), 513-516.

Di Girolamo, N., Chui, J., Coroneo, M. T., & Wakefield, D. (2004). Pathogenesis of pterygia: role of cytokines, growth factors, and matrix metalloproteinases. *Prog Retin Eye Res, 23*(2), 195-228. doi: 10.1016/j.preteyeres.2004.02.002

Di Girolamo, N., Kumar, R. K., Coroneo, M. T., & Wakefield, D. (2002). UVB-mediated induction of interleukin-6 and -8 in pterygia and cultured human pterygium epithelial cells. *Invest Ophthalmol Vis Sci, 43*(11), 3430-3437.

Di Girolamo, N., Wakefield, D., & Coroneo, M. T. (2006). UVB-mediated induction of cytokines and growth factors in pterygium epithelial cells involves cell surface receptors and intracellular signaling. *Invest Ophthalmol Vis Sci, 47*(6), 2430-2437. doi: 10.1167/iovs.05-1130

Dong, C. G., Wu, W. K., Feng, S. Y., Wang, X. J., Shao, J. F., & Qiao, J. (2012). Co-inhibition of microRNA-10b and microRNA-21 exerts synergistic inhibition on the proliferation and invasion of human glioma cells. *Int J Oncol, 41*(3), 1005-1012. doi: 10.3892/ijo.2012.1542

Dushku, N., Hatcher, S. L., Albert, D. M., & Reid, T. W. (1999). p53 expression and relation to human papillomavirus infection in pingueculae, pterygia, and limbal tumors. *Arch Ophthalmol, 117*(12), 1593-1599.

Dushku, N., John, M. K., Schultz, G. S., & Reid, T. W. (2001). Pterygia pathogenesis: corneal invasion by matrix metalloproteinase expressing altered limbal epithelial basal cells. *Arch Ophthalmol, 119*(5), 695-706.

Dushku, N., & Reid, T. W. (1994). Immunohistochemical evidence that human pterygia originate from an invasion of vimentin-expressing altered limbal epithelial basal cells. *Curr Eye Res, 13*(7), 473-481.

Garcia, D. M., Baek, D., Shin, C., Bell, G. W., Grimson, A., & Bartel, D. P. (2011). Weak seed-pairing stability and high target-site abundance decrease the proficiency of lsy-6 and other microRNAs. *Nat Struct Mol Biol, 18*(10), 1139-1146. doi: 10.1038/nsmb.2115

Georgi, S. A., & Reh, T. A. (2010). Dicer is required for the transition from early to late progenitor state in the developing mouse retina. *J Neurosci, 30*(11), 4048-4061. doi: 10.1523/JNEUROSCI.4982-09.2010

Giorgetti, A., Montserrat, N., Rodriguez-Piza, I., Azqueta, C., Veiga, A., & Izpisua Belmonte, J. C. (2010). Generation of induced pluripotent stem cells from human cord blood cells with only two factors: Oct4 and Sox2. *Nat Protoc, 5*(4), 811-820. doi: 10.1038/nprot.2010.16

Green, D. R., & Kroemer, G. (2009). Cytoplasmic functions of the tumour suppressor p53. *Nature, 458*(7242), 1127-1130. doi: 10.1038/nature07986

Greene, S. B., Gunaratne, P. H., Hammond, S. M., & Rosen, J. M. (2010). A putative role for microRNA-205 in mammary epithelial cell progenitors. *J Cell Sci, 123*(Pt 4), 606-618. doi: 10.1242/jcs.056812

Gregory, P. A., Bert, A. G., Paterson, E. L., Barry, S. C., Tsykin, A., Farshid, G., . . . Goodall, G. J. (2008). The miR-200 family and miR-205 regulate epithelial to mesenchymal transition by targeting ZEB1 and SIP1. *Nat Cell Biol, 10*(5), 593-601. doi: ncb1722 [pii] 10.1038/ncb1722

Gregory, P. A., Bracken, C. P., Bert, A. G., & Goodall, G. J. (2008). MicroRNAs as regulators of epithelial-mesenchymal transition. *Cell Cycle, 7*(20), 3112-3118. doi: 6851 [pii]

Gregory, R. I., Chendrimada, T. P., Cooch, N., & Shiekhattar, R. (2005). Human RISC couples microRNA biogenesis and posttranscriptional gene silencing. *Cell, 123*(4), 631-640. doi: S0092-8674(05)01109-8 [pii]10.1016/j.cell.2005.10.022

Grueterich, M., Espana, E., & Tseng, S. C. (2002). Connexin 43 expression and proliferation of human limbal epithelium on intact and denuded amniotic membrane. *Invest Ophthalmol Vis Sci, 43*(1), 63-71.

Hackler, L., Jr., Wan, J., Swaroop, A., Qian, J., & Zack, D. J. (2010). MicroRNA profile of the developing mouse retina. *Invest Ophthalmol Vis Sci, 51*(4), 1823-1831. doi: 10.1167/iovs.09-4657

Han, J., Lee, Y., Yeom, K. H., Kim, Y. K., Jin, H., & Kim, V. N. (2004). The Drosha-DGCR8 complex in primary microRNA processing. *Genes Dev, 18*(24), 3016-3027. doi: gad.1262504 [pii] 10.1101/gad.1262504

Hayashi, R., Yamato, M., Sugiyama, H., Sumide, T., Yang, J., Okano, T., . . . Nishida, K. (2007). N-Cadherin is expressed by putative stem/progenitor cells and melanocytes in the human limbal epithelial stem cell niche. *Stem Cells, 25*(2), 289-296. doi: 2006-0167 [pii] 10.1634/stemcells.2006-0167

He, M., Xu, Z., Ding, T., Kuang, D. M., & Zheng, L. (2009). MicroRNA-155 regulates inflammatory cytokine production in tumor-associated macrophages via targeting C/EBPbeta. *Cell Mol Immunol, 6*(5), 343-352. doi: 10.1038/cmi.2009.45

Hernandez Galindo, E. E., Theiss, C., Steuhl, K. P., & Meller, D. (2003). Expression of Delta Np63 in response to phorbol ester in human limbal epithelial cells expanded on intact human amniotic membrane. *Invest Ophthalmol Vis Sci, 44*(7), 2959-2965.

Higa, K., Shimmura, S., Miyashita, H., Kato, N., Ogawa, Y., Kawakita, T., . . . Tsubota, K. (2009). N-cadherin in the maintenance of human corneal limbal epithelial progenitor cells in vitro. *Invest Ophthalmol Vis Sci, 50*(10), 4640-4645. doi: iovs.09-3503 [pii]10.1167/iovs.09-3503

Hildebrand, J., Rutze, M., Walz, N., Gallinat, S., Wenck, H., Deppert, W., . . . Knott, A. (2011). A comprehensive analysis of microRNA expression during human keratinocyte differentiation in vitro and in vivo. *J Invest Dermatol, 131*(1), 20-29. doi: jid2010268 [pii] 10.1038/jid.2010.268

Hong, J. W., Liu, J. J., Lee, J. S., Mohan, R. R., Mohan, R. R., Woods, D. J., . . . Wilson, S. E. (2001). Proinflammatory chemokine induction in keratocytes and inflammatory cell infiltration into the cornea. *Invest Ophthalmol Vis Sci, 42*(12), 2795-2803.

Houbaviy, H. B., Murray, M. F., & Sharp, P. A. (2003). Embryonic stem cell-specific MicroRNAs. *Dev Cell, 5*(2), 351-358. doi: S1534580703002272 [pii]

Hsu, C. M., Lin, P. M., Wang, Y. M., Chen, Z. J., Lin, S. F., & Yang, M. Y. (2012). Circulating miRNA is a novel marker for head and neck squamous cell carcinoma. *Tumour Biol, 33*(6), 1933-1942. doi: 10.1007/s13277-012-0454-8

Huang, F., Fang, Z. F., Hu, X. Q., Tang, L., Zhou, S. H., & Huang, J. P. (2013). Overexpression of mir-126 promotes the differentiation of mesenchymal stem cells toward endothelial cells via activation of pi3k/akt and mapk/erk pathways and release of paracrine factors. *Biol Chem*. doi: 10.1515/hsz-2013-0107

Huang, X. A., & Lin, H. (2012). The miRNA Regulation of Stem Cells. *Wiley Interdiscip Rev Membr Transp Signal, 1*(1), 83-95. doi: 10.1002/wdev.5

Hulsmans, M., De Keyzer, D., & Holvoet, P. (2011). MicroRNAs regulating oxidative stress and inflammation in relation to obesity and atherosclerosis. *FASEB journal : official publication of the Federation of American Societies for Experimental Biology, 25*(8), 2515-2527. doi: 10.1096/fj.11-181149

Hurteau, G. J., Carlson, J. A., Roos, E., & Brock, G. J. (2009). Stable expression of miR-200c alone is sufficient to regulate TCF8 (ZEB1) and restore E-cadherin expression. *Cell Cycle, 8*(13), 2064-2069. doi: 8883 [pii]

Jain, A. K., Allton, K., Iacovino, M., Mahen, E., Milczarek, R. J., Zwaka, T. P., . . . Barton, M. C. (2012). p53 regulates cell cycle and microRNAs to promote differentiation of human embryonic stem cells. *PLoS Biol, 10*(2), e1001268. doi: 10.1371/journal.pbio.1001268

Jaworski, C. J., Aryankalayil-John, M., Campos, M. M., Fariss, R. N., Rowsey, J., Agarwalla, N., . . . Wistow, G. (2009). Expression analysis of human pterygium shows a predominance of conjunctival and limbal markers and genes associated with cell migration. *Mol Vis, 15*, 2421-2434.

Jiang, Y., Jahagirdar, B. N., Reinhardt, R. L., Schwartz, R. E., Keene, C. D., Ortiz-Gonzalez, X. R., . . . Verfaillie, C. M. (2002). Pluripotency of mesenchymal stem cells derived from adult marrow. *Nature, 418*(6893), 41-49. doi: 10.1038/nature00870

Jin, Z. B., Hirokawa, G., Gui, L., Takahashi, R., Osakada, F., Hiura, Y., . . . Iwai, N. (2009). Targeted deletion of miR-182, an abundant retinal microRNA. *Mol Vis, 15*, 523-533.

Judson, R. L., Babiarz, J. E., Venere, M., & Blelloch, R. (2009). Embryonic stem cell-specific microRNAs promote induced pluripotency. *Nat Biotechnol, 27*(5), 459-461. doi: nbt.1535 [pii]10.1038/nbt.1535

Kanellopoulou, C., Muljo, S. A., Kung, A. L., Ganesan, S., Drapkin, R., Jenuwein, T., . . . Rajewsky, K. (2005). Dicer-deficient mouse embryonic stem cells are defective in differentiation and centromeric silencing. *Genes Dev, 19*(4), 489-501. doi: 19/4/489 [pii]10.1101/gad.1248505

Kano, M., Seki, N., Kikkawa, N., Fujimura, L., Hoshino, I., Akutsu, Y., . . . Matsubara, H. (2010). miR-145, miR-133a and miR-133b: Tumor suppressive miRNAs target FSCN1 in esophageal squamous cell carcinoma. *Int J Cancer*. doi: 10.1002/ijc.25284

Karali, M., Peluso, I., Gennarino, V. A., Bilio, M., Verde, R., Lago, G., . . . Banfi, S. (2010). miRNeye: a microRNA expression atlas of the mouse eye. *BMC Genomics, 11*, 715. doi: 1471-2164-11-715 [pii]10.1186/1471-2164-11-715

Karali, M., Peluso, I., Marigo, V., & Banfi, S. (2007). Identification and characterization of microRNAs expressed in the mouse eye. *Invest Ophthalmol Vis Sci, 48*(2), 509-515. doi: 48/2/509 [pii]10.1167/iovs.06-0866

Katoh, M. (2009). Transcriptional mechanisms of WNT5A based on NF-kappaB, Hedgehog, TGFbeta, and Notch signaling cascades. *International journal of molecular medicine, 23*(6), 763-769.

Kawakita, T., Shimmura, S., Higa, K., Espana, E. M., He, H., Shimazaki, J., . . . Tseng, S. C. (2009). Greater growth potential of p63-positive epithelial cell clusters maintained in human limbal epithelial sheets. *Invest Ophthalmol Vis Sci, 50*(10), 4611-4617. doi: iovs.08-2586 [pii]10.1167/iovs.08-2586

Kennea, N. L., & Mehmet, H. (2002). Neural stem cells. *J Pathol, 197*(4), 536-550. doi: 10.1002/path.1189

Kennedy, M., Kim, K. H., Harten, B., Brown, J., Planck, S., Meshul, C., . . . Ansel, J. C. (1997). Ultraviolet irradiation induces the production of multiple cytokines by human corneal cells. *Invest Ophthalmol Vis Sci, 38*(12), 2483-2491.

Kent, O. A., Chivukula, R. R., Mullendore, M., Wentzel, E. A., Feldmann, G., Lee, K. H., . . . Mendell, J. T. (2010). Repression of the miR-143/145 cluster by oncogenic Ras initiates a tumor-promoting feed-forward pathway. *Genes Dev, 24*(24), 2754-2759. doi: 10.1101/gad.1950610

Kim, J. B., Greber, B., Arauzo-Bravo, M. J., Meyer, J., Park, K. I., Zaehres, H., & Scholer, H. R. (2009). Direct reprogramming of human neural stem cells by OCT4. *Nature, 461*(7264), 649-643. doi: 10.1038/nature08436

Kim, J. Y., Kim, Y. J., Lee, S., & Park, J. H. (2011). BNip3 is a mediator of TNF-induced necrotic cell death. *Apoptosis, 16*(2), 114-126. doi: 10.1007/s10495-010-0550-4

Kim, V. N. (2008). Cell cycle micromanagement in embryonic stem cells. *Nat Genet, 40*(12), 1391-1392. doi: ng1208-1391 [pii]10.1038/ng1208-1391

Komatsu, S., Ichikawa, D., Takeshita, H., Tsujiura, M., Morimura, R., Nagata, H., . . . Otsuji, E. (2011). Circulating microRNAs in plasma of patients with oesophageal squamous cell carcinoma. *Br J Cancer, 105*(1), 104-111. doi: 10.1038/bjc.2011.198

Kong, W., Yang, H., He, L., Zhao, J. J., Coppola, D., Dalton, W. S., & Cheng, J. Q. (2008). MicroRNA-155 is regulated by the transforming growth factor beta/Smad pathway and contributes to epithelial cell plasticity by targeting RhoA. *Mol Cell Biol, 28*(22), 6773-6784. doi: 10.1128/MCB.00941-08

Kria, L., Ohira, A., & Amemiya, T. (1996). Immunohistochemical localization of basic fibroblast growth factor, platelet derived growth factor, transforming growth factor-beta and tumor necrosis factor-alpha in the pterygium. *Acta Histochem, 98*(2), 195-201.

Krol, J., Busskamp, V., Markiewicz, I., Stadler, M. B., Ribi, S., Richter, J., . . . Filipowicz, W. (2010). Characterizing light-regulated retinal microRNAs reveals rapid turnover as a common property of neuronal microRNAs. *Cell, 141*(4), 618-631. doi: S0092-8674(10)00357-0 [pii]10.1016/j.cell.2010.03.039

Krol, J., & Krzyzosiak, W. J. (2004). Structural aspects of microRNA biogenesis. *IUBMB Life, 56*(2), 95-100. doi: 10.1080/15216540410001670142

Kruse, F. E., & Tseng, S. C. (1991). A serum-free clonal growth assay for limbal, peripheral, and central corneal epithelium. *Invest Ophthalmol Vis Sci, 32*(7), 2086-2095.

Kubota, M., Shimmura, S., Miyashita, H., Kawashima, M., Kawakita, T., & Tsubota, K. (2010). The anti-oxidative role of ABCG2 in corneal epithelial cells. *Invest Ophthalmol Vis Sci, 51*(11), 5617-5622. doi: iovs.10-5463 [pii]10.1167/iovs.10-5463

Kulkarni, B. B., Tighe, P. J., Mohammed, I., Yeung, A. M., Powe, D. G., Hopkinson, A., . . . Dua, H. S. (2010). Comparative transcriptional profiling of the limbal epithelial crypt demonstrates its putative stem cell niche characteristics. *BMC Genomics, 11*, 526. doi: 1471-2164-11-526 [pii]10.1186/1471-2164-11-526

Kuo, C. H., Deng, J. H., Deng, Q., & Ying, S. Y. (2012). A novel role of miR-302/367 in reprogramming. *Biochem Biophys Res Commun, 417*(1), 11-16. doi: 10.1016/j.bbrc.2011.11.058

Kutty, R. K., Nagineni, C. N., Samuel, W., Vijayasarathy, C., Hooks, J. J., & Redmond, T. M. (2010). Inflammatory cytokines regulate microRNA-155 expression in human retinal pigment epithelial cells by activating JAK/STAT pathway. *Biochemical and biophysical research communications, 402*(2), 390-395. doi: 10.1016/j.bbrc.2010.10.042

La Torre, A., Georgi, S., & Reh, T. A. (2013). Conserved microRNA pathway regulates developmental timing of retinal neurogenesis. *Proc Natl Acad Sci U S A, 110*(26), E2362-E2370. doi: 10.1073/pnas.1301837110

Ladeiro, Y., Couchy, G., Balabaud, C., Bioulac-Sage, P., Pelletier, L., Rebouissou, S., & Zucman-Rossi, J. (2008). MicroRNA profiling in hepatocellular tumors is associated with clinical features and oncogene/tumor suppressor gene mutations. *Hepatology, 47*(6), 1955-1963. doi: 10.1002/hep.22256

Lanza, R. P. (2006). *Essentials of stem cell biology*. Amsterdam ; Boston: Elsevier/Academic Press.

Lavker, R. M., & Sun, T. T. (1983). Epidermal stem cells. *J Invest Dermatol, 81*(1 Suppl), 121s-127s.

Lee, S. K., Teng, Y., Wong, H. K., Ng, T. K., Huang, L., Lei, P., . . . Pang, C. P. (2011). MicroRNA-145 Regulates Human Corneal Epithelial Differentiation. *PLoS One, 6*(6), e21249. doi: 10.1371/journal.pone.0021249

PONE-D-10-05042 [pii]

Leivonen, S. K., Rokka, A., Ostling, P., Kohonen, P., Corthals, G. L., Kallioniemi, O., & Perala, M. (2011). Identification of miR-193b Targets in Breast Cancer Cells and Systems Biological Analysis of Their Functional Impact. *Mol Cell Proteomics, 10*(7), M110 005322. doi: M110.005322 [pii]10.1074/mcp.M110.005322

Li, J., Bai, H., Zhu, Y., Wang, X. Y., Wang, F., Zhang, J. W., . . . Yu, J. (2010). Antagomir dependent microRNA-205 reduction enhances adhesion ability of human corneal epithelial keratinocytes. *Chin Med Sci J, 25*(2), 65-70. doi: 2481 [pii]

Li, L., & Xie, T. (2005). Stem cell niche: structure and function. *Annu Rev Cell Dev Biol, 21*, 605-631. doi: 10.1146/annurev.cellbio.21.012704.131525

Li, M., Marin-Muller, C., Bharadwaj, U., Chow, K. H., Yao, Q., & Chen, C. (2009). MicroRNAs: control and loss of control in human physiology and disease. *World J Surg, 33*(4), 667-684. doi: 10.1007/s00268-008-9836-x

Li, W., Hayashida, Y., Chen, Y. T., & Tseng, S. C. (2007). Niche regulation of corneal epithelial stem cells at the limbus. *Cell Res, 17*(1), 26-36. doi: 7310137 [pii]10.1038/sj.cr.7310137

Li, Y., & Piatigorsky, J. (2009). Targeted deletion of Dicer disrupts lens morphogenesis, corneal epithelium stratification, and whole eye development. *Dev Dyn, 238*(9), 2388-2400. doi: 10.1002/dvdy.22056

Lichtinger, A., Pe'er, J., Frucht-Pery, J., & Solomon, A. (2010). Limbal stem cell deficiency after topical mitomycin C therapy for primary acquired melanosis with atypia. *Ophthalmology, 117*(3), 431-437. doi: S0161-6420(09)00841-0 [pii]10.1016/j.ophtha.2009.07.032

Lin, S. L., Chang, D. C., Chang-Lin, S., Lin, C. H., Wu, D. T., Chen, D. T., & Ying, S. Y. (2008). Mir-302 reprograms human skin cancer cells into a pluripotent ES-cell-like state. *RNA, 14*(10), 2115-2124. doi: rna.1162708 [pii]10.1261/rna.1162708

Lindsay, M. A. (2008). microRNAs and the immune response. *Trends in immunology, 29*(7), 343-351. doi: 10.1016/j.it.2008.04.004

Liu, K., Liu, Y., Mo, W., Qiu, R., Wang, X., Wu, J. Y., & He, R. (2011a). MiR-124 regulates early neurogenesis in the optic vesicle and forebrain, targeting NeuroD1. *Nucleic acids research, 39*(7), 2869-2879. doi: 10.1093/nar/gkq904

Liu, K., Liu, Y., Mo, W., Qiu, R., Wang, X., Wu, J. Y., & He, R. (2011b). MiR-124 regulates early neurogenesis in the optic vesicle and forebrain, targeting NeuroD1. *Nucleic Acids Res, 39*(7), 2869-2879. doi: gkq904 [pii]10.1093/nar/gkq904

Liu, X., Fortin, K., & Mourelatos, Z. (2008). MicroRNAs: biogenesis and molecular functions. *Brain Pathol, 18*(1), 113-121. doi: BPA121 [pii]10.1111/j.1750-3639.2007.00121.x

Loscher, C. J., Hokamp, K., Kenna, P. F., Ivens, A. C., Humphries, P., Palfi, A., & Farrar, G. J. (2007). Altered retinal microRNA expression profile in a mouse model of retinitis pigmentosa. *Genome Biol, 8*(11), R248. doi: gb-2007-8-11-r248 [pii]10.1186/gb-2007-8-11-r248

Lucas, R. M. (2011). An epidemiological perspective of ultraviolet exposure--public health concerns. *Eye Contact Lens, 37*(4), 168-175. doi: 10.1097/ICL.0b013e31821cb0cf

Luna, C., Li, G., Qiu, J., Epstein, D. L., & Gonzalez, P. (2009). Role of miR-29b on the regulation of the extracellular matrix in human trabecular meshwork cells under chronic oxidative stress. *Mol Vis, 15*, 2488-2497.

Lund, A. H. (2010). miR-10 in development and cancer. *Cell death and differentiation, 17*(2), 209-214. doi: 10.1038/cdd.2009.58

Melton, C., Judson, R. L., & Blelloch, R. (2010). Opposing microRNA families regulate self-renewal in mouse embryonic stem cells. *Nature, 463*(7281), 621-626. doi: nature08725 [pii]10.1038/nature08725

Mills, A. A., Zheng, B., Wang, X. J., Vogel, H., Roop, D. R., & Bradley, A. (1999). p63 is a p53 homologue required for limb and epidermal morphogenesis. *Nature, 398*(6729), 708-713. doi: 10.1038/19531

Mitalipov, S., & Wolf, D. (2009). Totipotency, pluripotency and nuclear reprogramming. *Adv Biochem Eng Biotechnol, 114*, 185-199. doi: 10.1007/10_2008_45

Mohan, R. R., Mohan, R. R., Kim, W. J., & Wilson, S. E. (2000). Modulation of TNF-alpha-induced apoptosis in corneal fibroblasts by transcription factor NF-kappaB. *Investigative ophthalmology & visual science, 41*(6), 1327-1336.

Mosakhani, N., Sarhadi, V. K., Borze, I., Karjalainen-Lindsberg, M. L., Sundstrom, J., Ristamaki, R., . . . Knuutila, S. (2012). MicroRNA profiling differentiates colorectal cancer according to KRAS status. *Genes Chromosomes Cancer, 51*(1), 1-9. doi: 10.1002/gcc.20925

Mukhopadhyay, M., Gorivodsky, M., Shtrom, S., Grinberg, A., Niehrs, C., Morasso, M. I., & Westphal, H. (2006). Dkk2 plays an essential role in the corneal fate of the ocular surface epithelium. *Development, 133*(11), 2149-2154. doi: dev.02381 [pii]10.1242/dev.02381

Nakashima, A., Kumakura, S., Mishima, S., Ishikura, H., & Kobayashi, S. (2005). IFN-alpha enhances TNF-alpha-induced apoptosis through down-regulation of c-Myc protein expression in HL-60 cells. *J Exp Clin Cancer Res, 24*(3), 447-456.

Nakatsu, M. N., Ding, Z., Ng, M. Y., Truong, T. T., Yu, F., & Deng, S. X. (2011a). Wnt/beta-catenin signaling regulates proliferation of human cornea epithelial stem/progenitor cells. *Investigative ophthalmology & visual science, 52*(7), 4734-4741. doi: 10.1167/iovs.10-6486

Nakatsu, M. N., Ding, Z., Ng, M. Y., Truong, T. T., Yu, F., & Deng, S. X. (2011b). Wnt/beta-catenin signaling regulates proliferation of human cornea epithelial stem/progenitor cells. *Investigative ophthalmology & visual science, 52*(7), 4734-4741. doi: 10.1167/iovs.10-6486

Negrini, M., & Calin, G. A. (2008). Breast cancer metastasis: a microRNA story. *Breast Cancer Res, 10*(2), 203. doi: bcr1867 [pii]10.1186/bcr1867

Newman, M. A., & Hammond, S. M. (2010). Lin-28: an early embryonic sentinel that blocks Let-7 biogenesis. *Int J Biochem Cell Biol, 42*(8), 1330-1333. doi: S1357-2725(09)00093-4 [pii]10.1016/j.biocel.2009.02.023

Ng, E. K., Tsang, W. P., Ng, S. S., Jin, H. C., Yu, J., Li, J. J., . . . Sung, J. J. (2009). MicroRNA-143 targets DNA methyltransferases 3A in colorectal cancer. *Br J Cancer, 101*(4), 699-706. doi: 6605195 [pii]10.1038/sj.bjc.6605195

Nieto-Miguel, T., Calonge, M., de la Mata, A., Lopez-Paniagua, M., Galindo, S., de la Paz, M. F., & Corrales, R. M. (2011). A comparison of stem cell-related gene expression in the progenitor-rich limbal epithelium and the differentiating central corneal epithelium. *Mol Vis, 17*, 2102-2117.

Nishiyama, T., Kaneda, R., Ono, T., Tohyama, S., Hashimoto, H., Endo, J., . . . Fukuda, K. (2012). miR-142-3p is essential for hematopoiesis and affects cardiac cell fate in zebrafish. *Biochem Biophys Res Commun, 425*(4), 755-761. doi: 10.1016/j.bbrc.2012.07.148

Pajoohesh-Ganji, A., Ghosh, S. P., & Stepp, M. A. (2004). Regional distribution of alpha9beta1 integrin within the limbus of the mouse ocular surface. *Developmental dynamics : an official publication of the American Association of Anatomists, 230*(3), 518-528. doi: 10.1002/dvdy.20050

Papadopoulos, G. L., Alexiou, P., Maragkakis, M., Reczko, M., & Hatzigeorgiou, A. G. (2009). DIANA-mirPath: Integrating human and mouse microRNAs in pathways. *Bioinformatics, 25*(15), 1991-1993. doi: 10.1093/bioinformatics/btp299

Pellegrini, G., Dellambra, E., Golisano, O., Martinelli, E., Fantozzi, I., Bondanza, S., . . . De Luca, M. (2001). p63 identifies keratinocyte stem cells. *Proceedings of the National Academy of Sciences of the United States of America, 98*(6), 3156-3161. doi: 10.1073/pnas.061032098

Pellegrini, G., Traverso, C. E., Franzi, A. T., Zingirian, M., Cancedda, R., & De Luca, M. (1997). Long-term restoration of damaged corneal surfaces with autologous cultivated corneal epithelium. *Lancet, 349*(9057), 990-993. doi: S0140-6736(96)11188-0 [pii]10.1016/S0140-6736(96)11188-0

Peng, H., Hamanaka, R. B., Katsnelson, J., Hao, L. L., Yang, W., Chandel, N. S., & Lavker, R. M. (2012). MicroRNA-31 targets FIH-1 to positively regulate corneal epithelial glycogen metabolism. *FASEB J, 26*(8), 3140-3147. doi: 10.1096/fj.11-198515

Peng, H., Kaplan, N., Hamanaka, R. B., Katsnelson, J., Blatt, H., Yang, W., . . . Lavker, R. M. (2012). microRNA-31/factor-inhibiting hypoxia-inducible factor 1 nexus regulates keratinocyte differentiation. *Proc Natl Acad Sci U S A, 109*(35), 14030-14034. doi: 10.1073/pnas.1111292109

Qi, H., Li, D. Q., Shine, H. D., Chen, Z., Yoon, K. C., Jones, D. B., & Pflugfelder, S. C. (2008). Nerve growth factor and its receptor TrkA serve as potential markers for human corneal epithelial progenitor cells. *Exp Eye Res, 86*(1), 34-40. doi: S0014-4835(07)00253-9 [pii]10.1016/j.exer.2007.09.003

Qi, H., Zheng, X., Yuan, X., Pflugfelder, S. C., & Li, D. Q. (2010). Potential localization of putative stem/progenitor cells in human bulbar conjunctival epithelium. *J Cell Physiol, 225*(1), 180-185. doi: 10.1002/jcp.22215

Qiu, C., Ma, Y., Wang, J., Peng, S., & Huang, Y. (2010). Lin28-mediated post-transcriptional regulation of Oct4 expression in human embryonic stem cells. *Nucleic Acids Res, 38*(4), 1240-1248. doi: gkp1071 [pii]10.1093/nar/gkp1071

Rama, P., Matuska, S., Paganoni, G., Spinelli, A., De Luca, M., & Pellegrini, G. (2010). Limbal stem-cell therapy and long-term corneal regeneration. *The New England journal of medicine, 363*(2), 147-155. doi: 10.1056/NEJMoa0905955

Reid, T. W., & Dushku, N. (2010). What a study of pterygia teaches us about the cornea? Molecular mechanisms of formation. *Eye Contact Lens, 36*(5), 290-295. doi: 10.1097/ICL.0b013e3181eea8fe

Reya, T., Morrison, S. J., Clarke, M. F., & Weissman, I. L. (2001). Stem cells, cancer, and cancer stem cells. *Nature, 414*(6859), 105-111. doi: 10.1038/35102167

Romano, R. A., Smalley, K., Magraw, C., Serna, V. A., Kurita, T., Raghavan, S., & Sinha, S. (2012). DeltaNp63 knockout mice reveal its indispensable role as a master regulator of epithelial development and differentiation. *Development, 139*(4), 772-782. doi: 10.1242/dev.071191

Ryan, D. G., Oliveira-Fernandes, M., & Lavker, R. M. (2006a). MicroRNAs of the mammalian eye display distinct and overlapping tissue specificity. *Molecular vision, 12*, 1175-1184.

Ryan, D. G., Oliveira-Fernandes, M., & Lavker, R. M. (2006b). MicroRNAs of the mammalian eye display distinct and overlapping tissue specificity. *Mol Vis, 12*, 1175-1184. doi: v12/a134 [pii]

Sachdeva, M., Zhu, S., Wu, F., Wu, H., Walia, V., Kumar, S., . . . Mo, Y. Y. (2009). p53 represses c-Myc through induction of the tumor suppressor miR-145. *Proc Natl Acad Sci U S A, 106*(9), 3207-3212. doi: 10.1073/pnas.0808042106

Saito, K., Ishizuka, A., Siomi, H., & Siomi, M. C. (2005). Processing of pre-microRNAs by the Dicer-1-Loquacious complex in Drosophila cells. *PLoS Biol, 3*(7), e235. doi: 05-PLBI-RA-0198R1 [pii]10.1371/journal.pbio.0030235

Sanuki, R., Onishi, A., Koike, C., Muramatsu, R., Watanabe, S., Muranishi, Y., . . . Furukawa, T. (2011). miR-124a is required for hippocampal axogenesis and retinal cone survival through Lhx2 suppression. *Nat Neurosci, 14*(9), 1125-1134. doi: 10.1038/nn.2897

Sathananthan, A. H., & Osianlis, T. (2010). Human embryo culture and assessment for the derivation of embryonic stem cells (ESC). *Methods Mol Biol, 584*, 1-20. doi: 10.1007/978-1-60761-369-5_1

Schermer, A., Galvin, S., & Sun, T. T. (1986). Differentiation-related expression of a major 64K corneal keratin in vivo and in culture suggests limbal location of corneal epithelial stem cells. *The Journal of cell biology, 103*(1), 49-62.

Schlotzer-Schrehardt, U., Dietrich, T., Saito, K., Sorokin, L., Sasaki, T., Paulsson, M., & Kruse, F. E. (2007). Characterization of extracellular matrix components in the limbal epithelial stem cell compartment. *Exp Eye Res, 85*(6), 845-860. doi: S0014-4835(07)00246-1 [pii]10.1016/j.exer.2007.08.020

Schlotzer-Schrehardt, U., & Kruse, F. E. (2005). Identification and characterization of limbal stem cells. *Exp Eye Res, 81*(3), 247-264. doi: S0014-4835(05)00080-1 [pii]10.1016/j.exer.2005.02.016

Schneider, B. G., John-Aryankalayil, M., Rowsey, J. J., Dushku, N., & Reid, T. W. (2006). Accumulation of p53 protein in pterygia is not accompanied by TP53 gene mutation. *Exp Eye Res, 82*(1), 91-98. doi: 10.1016/j.exer.2005.05.006

Sengupta, S., Nie, J., Wagner, R. J., Yang, C., Stewart, R., & Thomson, J. A. (2009). MicroRNA 92b controls the G1/S checkpoint gene p57 in human embryonic stem cells. *Stem Cells, 27*(7), 1524-1528. doi: 10.1002/stem.84

Shalom-Feuerstein, R., Serror, L., De La Forest Divonne, S., Petit, I., Aberdam, E., Camargo, L., . . . Aberdam, D. (2012). Pluripotent stem cell model reveals essential roles for miR-450b-5p and miR-184 in embryonic corneal lineage specification. *Stem Cells, 30*(5), 898-909. doi: 10.1002/stem.1068

Shen, W. W., Zeng, Z., Zhu, W. X., & Fu, G. H. (2013). MiR-142-3p functions as a tumor suppressor by targeting CD133, ABCG2, and Lgr5 in colon cancer cells. *J Mol Med (Berl)*. doi: 10.1007/s00109-013-1037-x

Skalsky, R. L., Samols, M. A., Plaisance, K. B., Boss, I. W., Riva, A., Lopez, M. C., . . . Renne, R. (2007). Kaposi's sarcoma-associated herpesvirus encodes an ortholog of miR-155. *Journal of virology, 81*(23), 12836-12845. doi: 10.1128/JVI.01804-07

Stadler, B., Ivanovska, I., Mehta, K., Song, S., Nelson, A., Tan, Y., . . . Ruohola-Baker, H. (2010). Characterization of microRNAs involved in embryonic stem cell states. *Stem Cells Dev, 19*(7), 935-950. doi: 10.1089/scd.2009.0426

Sun, L., Xie, H., Mori, M. A., Alexander, R., Yuan, B., Hattangadi, S. M., . . . Lodish, H. F. (2011). Mir193b-365 is essential for brown fat differentiation. *Nat Cell Biol, 13*(8), 958-965. doi: 10.1038/ncb2286ncb2286 [pii]

Sun, L., Yan, W., Wang, Y., Sun, G., Luo, H., Zhang, J., . . . Liu, N. (2011a). MicroRNA-10b induces glioma cell invasion by modulating MMP-14 and uPAR expression via HOXD10. *Brain research, 1389*, 9-18. doi: 10.1016/j.brainres.2011.03.013

Sun, L., Yan, W., Wang, Y., Sun, G., Luo, H., Zhang, J., . . . Liu, N. (2011b). MicroRNA-10b induces glioma cell invasion by modulating MMP-14 and uPAR expression via HOXD10. *Brain Res, 1389*, 9-18. doi: 10.1016/j.brainres.2011.03.013

Sun, T. T., Tseng, S. C., & Lavker, R. M. (2010). Location of corneal epithelial stem cells. *Nature, 463*(7284), E10-11; discussion E11. doi: nature08805 [pii]10.1038/nature08805

Sundermeier, T. R., & Palczewski, K. (2012). The physiological impact of microRNA gene regulation in the retina. *Cell Mol Life Sci, 69*(16), 2739-2750. doi: 10.1007/s00018-012-0976-7

Suzuki, H. I., Yamagata, K., Sugimoto, K., Iwamoto, T., Kato, S., & Miyazono, K. (2009). Modulation of microRNA processing by p53. *Nature, 460*(7254), 529-533. doi: 10.1038/nature08199

Takagi, T., Iio, A., Nakagawa, Y., Naoe, T., Tanigawa, N., & Akao, Y. (2009). Decreased expression of microRNA-143 and -145 in human gastric cancers. *Oncology, 77*(1), 12-21. doi: 000218166 [pii]10.1159/000218166

Takahashi, K., & Yamanaka, S. (2006). Induction of pluripotent stem cells from mouse embryonic and adult fibroblast cultures by defined factors. *Cell, 126*(4), 663-676. doi: 10.1016/j.cell.2006.07.024

Tang, X. L., Sun, J. F., Wang, X. Y., Du, L. L., & Liu, P. (2010). Blocking neuropilin-2 enhances corneal allograft survival by selectively inhibiting lymphangiogenesis on vascularized beds. *Mol Vis, 16*, 2354-2361.

Tay, Y., Zhang, J., Thomson, A. M., Lim, B., & Rigoutsos, I. (2008). MicroRNAs to Nanog, Oct4 and Sox2 coding regions modulate embryonic stem cell differentiation. *Nature, 455*(7216), 1124-1128. doi: nature07299 [pii]10.1038/nature07299

Thomson, T., & Lin, H. (2009). The biogenesis and function of PIWI proteins and piRNAs: progress and prospect. *Annu Rev Cell Dev Biol, 25*, 355-376. doi: 10.1146/annurev.cellbio.24.110707.175327

Touhami, A., Grueterich, M., & Tseng, S. C. (2002). The role of NGF signaling in human limbal epithelium expanded by amniotic membrane culture. *Invest Ophthalmol Vis Sci, 43*(4), 987-994.

Trinh, X. B., Tjalma, W. A., Vermeulen, P. B., Van den Eynden, G., Van der Auwera, I., Van Laere, S. J., . . . van Dam, P. A. (2009). The VEGF pathway and the AKT/mTOR/p70S6K1 signalling pathway in human epithelial ovarian cancer. *British journal of cancer, 100*(6), 971-978. doi: 10.1038/sj.bjc.6604921

Tsai, R. J., Li, L. M., & Chen, J. K. (2000). Reconstruction of damaged corneas by transplantation of autologous limbal epithelial cells. *The New England journal of medicine, 343*(2), 86-93. doi: 10.1056/NEJM200007133430202

Tsai, Y. Y., Chang, K. C., Lin, C. L., Lee, H., Tsai, F. J., Cheng, Y. W., & Tseng, S. H. (2005). p53 Expression in pterygium by immunohistochemical analysis: a series report of 127 cases and review of the literature. *Cornea, 24*(5), 583-586.

Tsai, Y. Y., Cheng, Y. W., Lee, H., Tsai, F. J., Tseng, S. H., & Chang, K. C. (2005). P53 gene mutation spectrum and the relationship between gene mutation and protein levels in pterygium. *Mol Vis, 11*, 50-55.

Tsai, Y. Y., Chiang, C. C., Yeh, K. T., Lee, H., & Cheng, Y. W. (2010). Effect of TIMP-1 and MMP in pterygium invasion. *Invest Ophthalmol Vis Sci, 51*(7), 3462-3467. doi: 10.1167/iovs.09-4921

Tseng, S. C. (2001). Amniotic membrane transplantation for ocular surface reconstruction. *Biosci Rep, 21*(4), 481-489.

Tseng, S. C., Kruse, F. E., Merritt, J., & Li, D. Q. (1996). Comparison between serum-free and fibroblast-cocultured single-cell clonal culture systems: evidence showing that epithelial anti-apoptotic activity is present in 3T3 fibroblast-conditioned media. *Curr Eye Res, 15*(9), 973-984.

Tsitsiou, E., & Lindsay, M. A. (2009). microRNAs and the immune response. *Current opinion in pharmacology, 9*(4), 514-520. doi: 10.1016/j.coph.2009.05.003

Turner, H. C., Budak, M. T., Akinci, M. A., & Wolosin, J. M. (2007). Comparative analysis of human conjunctival and corneal epithelial gene expression with oligonucleotide microarrays. *Investigative ophthalmology & visual science, 48*(5), 2050-2061. doi: 10.1167/iovs.06-0998

Umemoto, T., Yamato, M., Nishida, K., Kohno, C., Yang, J., Tano, Y., & Okano, T. (2005). Rat limbal epithelial side population cells exhibit a distinct expression of stem cell markers that are lacking in side population cells from the central cornea. *FEBS Lett, 579*(29), 6569-6574. doi: S0014-5793(05)01316-5 [pii]10.1016/j.febslet.2005.10.047

Walker, J. C., & Harland, R. M. (2009). microRNA-24a is required to repress apoptosis in the developing neural retina. *Genes Dev, 23*(9), 1046-1051. doi: gad.1777709 [pii]10.1101/gad.1777709

Walsh, M. F., Ampasala, D. R., Hatfield, J., Vander Heide, R., Suer, S., Rishi, A. K., & Basson, M. D. (2008). Transforming growth factor-beta stimulates intestinal epithelial focal adhesion kinase synthesis via Smad- and p38-dependent mechanisms. *The American journal of pathology, 173*(2), 385-399. doi: 10.2353/ajpath.2008.070729

Wan, Y. S., Wang, Z. Q., Voorhees, J., & Fisher, G. (2001). EGF receptor crosstalks with cytokine receptors leading to the activation of c-Jun kinase in response to UV irradiation in human keratinocytes. *Cell Signal, 13*(2), 139-144.

Wang, F. E., Zhang, C., Maminishkis, A., Dong, L., Zhi, C., Li, R., . . . Miller, S. S. (2010a). MicroRNA-204/211 alters epithelial physiology. *FASEB journal : official publication of the Federation of American Societies for Experimental Biology, 24*(5), 1552-1571. doi: 10.1096/fj.08-125856

Wang, F. E., Zhang, C., Maminishkis, A., Dong, L., Zhi, C., Li, R., . . . Miller, S. S. (2010b). MicroRNA-204/211 alters epithelial physiology. *FASEB J, 24*(5), 1552-1571. doi: fj.08-125856 [pii]10.1096/fj.08-125856

Wang, H. Q., Yu, X. D., Liu, Z. H., Cheng, X., Samartzis, D., Jia, L. T., . . . Luo, Z. J. (2011). Deregulated miR-155 promotes Fas-mediated apoptosis in human intervertebral disc degeneration by targeting FADD and caspase-3. *J Pathol, 225*(2), 232-242. doi: 10.1002/path.2931

Wang, S., Aurora, A. B., Johnson, B. A., Qi, X., McAnally, J., Hill, J. A., . . . Olson, E. N. (2008). The endothelial-specific microRNA miR-126 governs vascular integrity and angiogenesis. *Developmental cell, 15*(2), 261-271. doi: 10.1016/j.devcel.2008.07.002

Wang, S., Bian, C., Yang, Z., Bo, Y., Li, J., Zeng, L., . . . Zhao, R. C. (2009). miR-145 inhibits breast cancer cell growth through RTKN. *Int J Oncol, 34*(5), 1461-1466.

Wang, Y., Baskerville, S., Shenoy, A., Babiarz, J. E., Baehner, L., & Blelloch, R. (2008). Embryonic stem cell-specific microRNAs regulate the G1-S transition and promote rapid proliferation. *Nat Genet, 40*(12), 1478-1483. doi: ng.250 [pii]10.1038/ng.250

Wang, Y., & Blelloch, R. (2009). Cell cycle regulation by MicroRNAs in embryonic stem cells. *Cancer Res, 69*(10), 4093-4096. doi: 0008-5472.CAN-09-0309 [pii]10.1158/0008-5472.CAN-09-0309

Wang, Y., Medvid, R., Melton, C., Jaenisch, R., & Blelloch, R. (2007). DGCR8 is essential for microRNA biogenesis and silencing of embryonic stem cell self-renewal. *Nat Genet, 39*(3), 380-385. doi: ng1969 [pii]10.1038/ng1969

Werner, S., & Munz, B. (2000). Suppression of keratin 15 expression by transforming growth factor beta in vitro and by cutaneous injury in vivo. *Exp Cell Res, 254*(1), 80-90. doi: 10.1006/excr.1999.4726

Wilson, K. D., Venkatasubrahmanyam, S., Jia, F., Sun, N., Butte, A. J., & Wu, J. C. (2009). MicroRNA profiling of human-induced pluripotent stem cells. *Stem Cells Dev, 18*(5), 749-758. doi: 10.1089/scd.2008.0247

Xu, N., Papagiannakopoulos, T., Pan, G., Thomson, J. A., & Kosik, K. S. (2009). MicroRNA-145 regulates OCT4, SOX2, and KLF4 and represses pluripotency in human embryonic stem cells. *Cell, 137*(4), 647-658. doi: S0092-8674(09)00252-9 [pii]10.1016/j.cell.2009.02.038

Xu, S. (2009). microRNA expression in the eyes and their significance in relation to functions. *Prog Retin Eye Res, 28*(2), 87-116. doi: S1350-9462(08)00078-5 [pii]10.1016/j.preteyeres.2008.11.003

Xu, S., Witmer, P. D., Lumayag, S., Kovacs, B., & Valle, D. (2007). MicroRNA (miRNA) transcriptome of mouse retina and identification of a sensory organ-specific miRNA cluster. *J Biol Chem, 282*(34), 25053-25066. doi: M700501200 [pii]10.1074/jbc.M700501200

*Epigenetic codes in stem cells and cancer stem cells*, 2010/10/06 Sess. 177-199 (2010).

Yang, J. S., & Lai, E. C. (2010). Dicer-independent, Ago2-mediated microRNA biogenesis in vertebrates. *Cell Cycle, 9*(22), 4455-4460. doi: 13958 [pii]

Yang, M., Liu, R., Sheng, J., Liao, J., Wang, Y., Pan, E., . . . Yin, L. (2013). Differential expression profiles of microRNAs as potential biomarkers for the early diagnosis of esophageal squamous cell carcinoma. *Oncol Rep, 29*(1), 169-176. doi: 10.3892/or.2012.2105

Yang, S. F., Lin, C. Y., Yang, P. Y., Chao, S. C., Ye, Y. Z., & Hu, D. N. (2009). Increased expression of gelatinase (MMP-2 and MMP-9) in pterygia and pterygium fibroblasts with disease progression and activation of protein kinase C. *Invest Ophthalmol Vis Sci, 50*(10), 4588-4596. doi: 10.1167/iovs.08-3147

Ye, J., Song, Y. S., Kang, S. H., Yao, K., & Kim, J. C. (2004). Involvement of bone marrow-derived stem and progenitor cells in the pathogenesis of pterygium. *Eye (Lond), 18*(8), 839-843. doi: 10.1038/sj.eye.6701346

Yin, Q., Wang, X., McBride, J., Fewell, C., & Flemington, E. (2008). B-cell receptor activation induces BIC/miR-155 expression through a conserved AP-1 element. *The Journal of biological chemistry, 283*(5), 2654-2662. doi: 10.1074/jbc.M708218200

Yoo, H. J., Byun, H. J., Kim, B. R., Lee, K. H., Park, S. Y., & Rho, S. B. (2012). DAPk1 inhibits NF-kappaB activation through TNF-alpha and INF-gamma-induced apoptosis. *Cell Signal, 24*(7), 1471-1477. doi: 10.1016/j.cellsig.2012.03.010

Yu, J., Ryan, D. G., Getsios, S., Oliveira-Fernandes, M., Fatima, A., & Lavker, R. M. (2008a). MicroRNA-184 antagonizes microRNA-205 to maintain SHIP2 levels in epithelia. *Proceedings of the National Academy of Sciences of the United States of America, 105*(49), 19300-19305. doi: 10.1073/pnas.0803992105

Yu, J., Ryan, D. G., Getsios, S., Oliveira-Fernandes, M., Fatima, A., & Lavker, R. M. (2008b). MicroRNA-184 antagonizes microRNA-205 to maintain SHIP2 levels in epithelia. *Proc Natl Acad Sci U S A, 105*(49), 19300-19305. doi: 0803992105 [pii]10.1073/pnas.0803992105

Yu, J., Vodyanik, M. A., Smuga-Otto, K., Antosiewicz-Bourget, J., Frane, J. L., Tian, S., . . . Thomson, J. A. (2007). Induced pluripotent stem cell lines derived from human somatic cells. *Science, 318*(5858), 1917-1920. doi: 10.1126/science.1151526

Zeng, Y., & Cullen, B. R. (2004). Structural requirements for pre-microRNA binding and nuclear export by Exportin 5. *Nucleic Acids Res, 32*(16), 4776-4785. doi: 10.1093/nar/gkh82432/16/4776 [pii]

Zhang, Hong. (1999). Evaluation of four antibodies in detecting p53 protein for predicting clinicopathological and prognostic significance in colorectal adenocarcinoma. *Clin Cancer Res, 5*(12), 4126-4132.

Zhang, J., Sun, Q., Zhang, Z., Ge, S., Han, Z. G., & Chen, W. T. (2013). Loss of microRNA-143/145 disturbs cellular growth and apoptosis of human epithelial cancers by impairing the MDM2-p53 feedback loop. *Oncogene, 32*(1), 61-69. doi: 10.1038/onc.2012.28

Zhang, W., Xiao, J., Li, C., Wan, P., Liu, Y., Wu, Z., . . . Wang, Z. (2011). Rapidly Constructed Scaffold-free Corneal Epithelial Sheets for Ocular Surface Reconstruction. *Tissue Eng Part C Methods*. doi: 10.1089/ten.TEC.2010.0529

Zhang, X., & Zeng, Y. (2010). The terminal loop region controls microRNA processing by Drosha and Dicer. *Nucleic Acids Res, 38*(21), 7689-7697. doi: gkq645 [pii]10.1093/nar/gkq645

Zhong, X., Li, N., Liang, S., Huang, Q., Coukos, G., & Zhang, L. (2010). Identification of microRNAs regulating reprogramming factor LIN28 in embryonic stem cells and cancer cells. *J Biol Chem, 285*(53), 41961-41971. doi: M110.169607 [pii]10.1074/jbc.M110.169607

Zhou, M., Li, X. M., & Lavker, R. M. (2006). Transcriptional profiling of enriched populations of stem cells versus transient amplifying cells. A comparison of limbal and corneal epithelial basal cells. *J Biol Chem, 281*(28), 19600-19609. doi: M600777200 [pii]10.1074/jbc.M600777200

Zhou, Q., Gallagher, R., Ufret-Vincenty, R., Li, X., Olson, E. N., & Wang, S. (2011). Regulation of angiogenesis and choroidal neovascularization by members of microRNA-23~27~24 clusters. *Proceedings of the National Academy of Sciences of the United States of America, 108*(20), 8287-8292. doi: 10.1073/pnas.1105254108

Zhu, Q., Sun, W., Okano, K., Chen, Y., Zhang, N., Maeda, T., & Palczewski, K. (2011). Sponge transgenic mouse model reveals important roles for the microRNA-183 (miR-183)/96/182 cluster in postmitotic photoreceptors of the retina. *J Biol Chem, 286*(36), 31749-31760. doi: 10.1074/jbc.M111.259028

Zomer, A., Vendrig, T., Hopmans, E. S., van Eijndhoven, M., Middeldorp, J. M., & Pegtel, D. M. (2010). Exosomes: Fit to deliver small RNA. *Commun Integr Biol, 3*(5), 447-450. doi: 10.4161/cib.3.5.12339